

THE GEOCHEMISTRY OF Fe, Mn, Ni, Cu, Zn AND As IN THE WATER COLUMN,
SEDIMENTS AND POREWATERS IN A SEASONALLY ANOXIC LAKE

by

ALAN MARTIN

B.Sc., The University of British Columbia, 1991

A THESIS SUBMITTED IN PARTIAL FULFILLMENT OF
THE REQUIREMENTS FOR THE DEGREE OF MASTER OF SCIENCE

in

THE FACULTY OF GRADUATE STUDIES

(Department of Earth and Ocean Sciences)

We accept this thesis as conforming
to the required standard

THE UNIVERSITY OF BRITISH COLUMBIA

December 1996

© Alan Martin, 1996

In presenting this thesis in partial fulfilment of the requirements for an advanced degree at the University of British Columbia, I agree that the Library shall make it freely available for reference and study. I further agree that permission for extensive copying of this thesis for scholarly purposes may be granted by the head of my department or by his or her representatives. It is understood that copying or publication of this thesis for financial gain shall not be allowed without my written permission.

Department of Earth and Ocean Sciences

The University of British Columbia
Vancouver, Canada

Date JAN 7 / 97

ABSTRACT

The distributions of Fe, Mn, Ni, Cu, Zn and As in the water column, interstitial waters and associated solid phases in Balmer Lake, Ontario, were determined from samples collected in July and October of 1993, and March and May of 1994, in order to assess the seasonal biogeochemical controls governing trace metal behaviour and mobility. The basin has served as a repository for tailings pond effluents since 1967, and as a result, hosts elevated levels of contaminants in the sediments and lake waters.

During the ice-free periods of summer, fall and spring, the water column is characterized by fully oxygenated bottom waters and homogeneous distributions of all measured parameters. However, reducing conditions develop in deeper areas during the period of ice cover in response to the high biological demand of the organic-rich sediments coupled with restricted atmospheric exchange. Trace metal profiles collected during winter exhibit considerable lake-wide variation and appear to reflect variability in the duration and extent of bottom water anoxia, and the relative influence of metal-rich lateral inputs from the tailings circuits.

Solid-phase profiles indicate that the top decimetre of the sediment column has received variable contributions of both organic matter- and feldspar-rich natural detritus, and carbonate-, chlorite- and metal-rich tailings inputs. High resolution profiles of porewater NO_3^- , Fe, Mn and SO_4^{2-} illustrate that the sediments in Balmer Lake become anoxic within a few centimetres of the sediment-water interface during well-mixed periods. Evidence for the precipitation of a Cu-bearing sulphide phase in the lowermost winter bottom waters suggests that the sulphate redox-cline migrates above the sediment-water interface at some point during ice cover. The seasonal porewater distributions of

dissolved Ni, Cu and Zn exhibit pronounced consumption profiles at depths consistent with sulphate reduction zones, suggesting they are sequestered as metal-sulphide phases. Enrichments of dissolved Ni and Zn in the surficial sediments at most sites reflect the dissolution of labile particulates at the sediment-water interface. Diffusive influxes calculated for Zn, Ni and Cu suggest that diffusion mechanisms contribute insignificantly to the accumulation rates of these metals. Arsenic is remobilized at deeper sediment depths and appears to be largely governed by the redox geochemistry of Mn.

The data collectively demonstrate that trace metal mobility in the Balmer Lake water column/sediment system varies significantly over the course of the four seasons. With the exception of arsenic, however, dissolved metal fluxes indicate that the underlying contaminated sediments are providing a significant and permanent sink for dissolved metals.

TABLE OF CONTENTS

ABSTRACT	ii
TABLE OF CONTENTS	iv
LIST OF FIGURES	viii
LIST OF TABLES	xiv
ACKNOWLEDGEMENTS	xvi
I. INTRODUCTION	1
1.1 Trace Metal Geochemistry	1
1.2 Trace Metal Cycling in Lakes	3
1.2.1 Inputs of Trace Elements to Lacustrine Systems	4
1.2.2 Major Processes Governing Trace Metal Behaviour and Mobility	5
1.2.3 Transformations Across the Sediment-Water Interface	10
1.3 Contamination of Aquatic Systems From Metal Mining	13
1.3.1 Bioavailability and Toxicity	14
1.4 Research Objectives	15
II. STUDY SITE	18
2.1 Physiography, Physical and Chemical Limnology	18
2.2 History of Mine-Related Inputs	20
2.2.1 Campbell Mine	21

2.2.2 Arthur White Mine	22
2.3 Sampling Periods	23
2.4 Sampling Sites	24
III. SAMPLING AND METHODS	26
3.1 Sampling	26
3.1.1 Water Column	26
3.1.2 Physical Profiling.....	27
3.1.3 Porewaters	27
3.1.3.1 Peeper Description and Preparation.....	29
3.1.3.2 Peeper Deployment and Subsampling.....	32
3.1.4 Sediment Sampling	34
3.2 Instrumentation.....	35
3.2.1 ICP/MS	35
3.2.2 GFAAS.....	36
3.2.3 Ion Chromatography	36
3.2.4 X-ray Fluorescence.....	36
3.2.5 Coulometry	37
3.2.6 Carbon, Nitrogen and Sulphur	37
3.2.7 Spectrophotometry	37
3.2.8 Digestion of Polycarbonate Filters	38
IV. RESULTS	39
4.1 Water Column.....	39
4.1.1 Physical Profiling.....	39
4.1.2 Nitrate, Ammonium and Sulphate	42
4.1.3 Suspended Organics	53

4.1.4 Trace Metals	57
4.1.4.1 Dissolved Fraction	57
4.1.4.2 Particulate Fraction	64
4.2 Interstitial Waters.....	69
4.2.1 Peepers	69
4.2.1.1 Nutrients and Sulphate	69
4.2.1.2 Trace Metals	79
4.2.1.3 pH.....	95
4.2.2 Core Porewaters	97
4.2.2.1 Nutrients and Sulphate.....	97
4.2.2.2 Trace Metals	99
4.3 Sediments	101
 V. DISCUSSION	 109
5.1 Water Column	109
5.1.1 Physical Limnology	111
5.1.2 Sulphate.....	111
5.1.3 Ammonium and Nitrate	113
5.1.4 Suspended Particulates	117
5.1.5 Trace Metals	121
5.1.5.1 Iron	122
5.1.5.2 Manganese	124
5.1.5.3 Arsenic	126
5.1.5.4 Nickel.....	127
5.1.5.5 Copper	129
5.1.5.6 Zinc	130
5.1.6 Water Column Model	131

5.1.7 Comparison of Four Lake Zones	135
5.2 Sediment Geochemistry	142
5.3 Porewater Chemistry	147
5.3.1 Ammonium and Nitrate	149
5.3.2 Sulphate	153
5.3.3 Iron and Manganese.....	157
5.3.4 Nickel	169
5.3.5 Copper	174
5.3.6 Zinc	179
5.4 Factors Controlling the Diagenetic Behaviour of As	186
5.4.1 Experimental and Field Observations	186
5.4.2 The Behaviour of As in Balmer Lake Sediments.....	194
VI. SUMMARY AND CONCLUSIONS	202
VII. BIBLIOGRAPHY	205
VIII. APPENDICES	220
Appendix A. Typical ICP/MS operating conditions.....	220
Appendix B. Quality Assessment/Quality Control	221
Appendix C. Porewater Data	225
Appendix D. Sediment Data.....	235
Appendix E. Core Logs.....	237
Appendix F. Diffusive Fluxes.....	239
Appendix G. Accumulation Rates.....	243

LIST OF FIGURES

Fig. 2.1 Location map showing the sampling stations, lake bathymetry and tailings circuits of the adjacent mines. *pg. 19*

Figure 3.1. Schematic diagram of membrane dialysis sampler (peeper). *pg. 30*

Fig. 4.1 Summer water column profiles of temperature, dissolved oxygen and pH for stations 1, 2, 3 and 4 (A-D, respectively), Balmer Lake, June, 1993. The hatched line represents the sediment surface. *pg. 40*

Fig. 4.2 Fall water column profiles of temperature and dissolved oxygen for stations 1, 2, 3 and 4 (A-D, respectively), Balmer Lake, October, 1993. The hatched line represents the sediment surface. *pg. 41*

Fig. 4.3 Winter water column profiles of temperature and dissolved oxygen for stations 1, 2, 3 and 4 (A-D, respectively), Balmer Lake, March, 1994. The hatched line represents the sediment surface. *pg. 43*

Fig. 4.4 Spring water column profiles of temperature, dissolved oxygen and pH for stations 1, 2 and 4 (A-C, respectively), Balmer Lake, May, 1994. The hatched line represents the sediment surface. *pg. 44*

Fig. 4.5. Winter water column profiles of nitrate for stations 1, 2, 3 and 4 (A-D, respectively), Balmer Lake, March, 1994. Replicate samples are represented by double symbols at specific single depths. The hatched line represents the sediment surface. *pg. 50*

Fig. 4.6. Winter water column profiles of ammonium for stations 1, 2, 3 and 4 (A-D, respectively), Balmer Lake, March, 1994. Replicate samples are represented by double symbols at specific single depths. The hatched line represents the sediment surface. *pg. 51*

Fig. 4.7. Winter water column profiles of sulphate for stations 1, 2, 3 and 4 (A-D, respectively), Balmer Lake, March, 1994. Replicate samples are represented by double symbols at specific single depths. The hatched line represents the sediment surface. *pg. 52*

Fig. 4.8. Winter water column profiles of dissolved Fe, Mn, As, Ni, Cu and Zn (A-F, respectively) for station 1, Balmer Lake, March, 1994. Replicate samples are represented by double symbols at specific single depths. The hatched line represents the sediment surface.

pg. 59

Fig. 4.9. Winter water column profiles of dissolved Fe, Mn, As, Ni, Cu and Zn (A-F, respectively) for station 2, Balmer Lake, March, 1994. Replicate samples are represented by double symbols at specific single depths. The hatched line represents the sediment surface.

pg. 60

Fig. 4.10. Winter water column profiles of dissolved Fe, Mn, As, Ni, Cu and Zn (A-F, respectively) for station 3, Balmer Lake, March, 1994. Replicate samples are represented by double symbols at specific single depths. The hatched line represents the sediment surface.

pg. 61

Fig. 4.11. Winter water column profiles of dissolved Fe, Mn, As, Ni, Cu and Zn (A-F, respectively) for station 4, Balmer Lake, March, 1994. Replicate samples are represented by double symbols at specific single depths. The hatched line represents the sediment surface.

pg. 62

Fig. 4.12. Duplicate summer peeper profiles of dissolved NH_4^+ , NO_3^- and SO_4^{2-} for station 1 (A-C) and station 2 (D-F), Balmer Lake, June, 1993. Replicate samples are represented by double symbols at specific single depths.

pg. 70

Fig. 4.13. Fall peeper profiles of dissolved NH_4^+ , NO_3^- and SO_4^{2-} for stations 1 (A-C) and 5 (D-F), Balmer Lake, October, 1993. Replicate samples are represented by double symbols at specific single depths.

pg. 72

Fig. 4.14. Duplicate fall peeper profiles of dissolved NH_4^+ , NO_3^- and SO_4^{2-} (A-C, respectively) for station 2, Balmer Lake, October, 1993. Replicate samples are represented by double symbols at specific single depths.

pg. 73

Fig. 4.15 Winter peeper profiles of dissolved NH_4^+ , NO_3^- and SO_4^{2-} for stations 1 (A-C) and 2 (D-F), Balmer Lake, March, 1994. Replicate samples are represented by double symbols at specific single depths.

pg. 75

Fig. 4.16. Winter peeper profiles of dissolved NH_4^+ , NO_3^- and SO_4^{2-} for stations 4 (A-C) and 6 (D-F), Balmer Lake, March, 1994. Replicate samples are represented by double symbols at specific single depths. pg. 76

Fig. 4.17. Duplicate spring peeper profiles of dissolved NH_4^+ , NO_3^- and SO_4^{2-} (A-C, respectively) for station 1, Balmer Lake, May, 1994. Replicate samples are represented by double symbols at specific single depths. pg. 78

Fig. 4.18. Duplicate summer peeper profiles of dissolved Fe, Mn, As, Ni, Cu and Zn (A-F, respectively) for station 1, Balmer Lake, June, 1993. Replicate samples are represented by double symbols at specific single depths. pg. 80

Fig. 4.19. Duplicate summer peeper profiles of dissolved Fe, Mn, As, Ni, Cu and Zn (A-F, respectively) for station 2, Balmer Lake, June, 1993. Replicate samples are represented by double symbols at specific single depths. pg. 81

Fig. 4.20. Fall peeper profiles of dissolved Fe, Mn, As, Ni, Cu and Zn (A-F, respectively) for station 1, Balmer Lake, October, 1993. Replicate samples are represented by double symbols at specific single depths. pg. 83

Fig. 4.21. Duplicate fall peeper profiles of dissolved Fe, Mn, As, Ni, Cu and Zn (A-F, respectively) for station 2, Balmer Lake, October, 1993. Replicate samples are represented by double symbols at specific single depths. pg. 84

Fig. 4.22. Fall peeper profiles of dissolved Fe, Mn, As, Ni, Cu and Zn (A-F, respectively) for station 5, Balmer Lake, October, 1993. Replicate samples are represented by double symbols at specific single depths. pg. 85

Fig. 4.23. Winter peeper profiles of dissolved Fe, Mn, As, Ni, Cu and Zn (A-F, respectively) for station 1, Balmer Lake, March, 1994. Replicate samples are represented by double symbols at specific single depths. pg. 88

Fig. 4.24. Winter peeper profiles of dissolved Fe, Mn, As, Ni, Cu and Zn (A-F, respectively) for station 2, Balmer Lake, March, 1994. Replicate samples are represented by double symbols at specific single depths. pg. 89

Fig. 4.25. Winter peeper profiles of dissolved Fe, Mn, As, Ni, Cu and Zn (A-F, respectively) for station 4, Balmer Lake, March, 1994. Replicate samples are represented by double symbols at specific single depths. pg. 90

Fig. 4.26. Winter peeper profiles of dissolved Fe, Mn, As, Ni, Cu and Zn (A-F, respectively) for station 6, Balmer Lake, March, 1994. Replicate samples are represented by double symbols at specific single depths. pg. 91

Fig. 4.27. Duplicate spring peeper profiles of dissolved Fe, Mn, As, Ni, Cu and Zn (A-F, respectively) for station 1, Balmer Lake, May, 1994. Replicate samples are represented by double symbols at specific single depths. pg. 94

Fig. 4.28. Spring profile of porewater and bottom water pH measured from peeper 2, station 1, Balmer Lake, May, 1994. pg. 96

Fig. 4.29. Distributions of dissolved NO_3^- and SO_4^{2-} obtained from peeper (open circles) and core porewaters (diamonds) at station 1 (A-B) and station 6 (C-D), Balmer Lake, March, 1994. Replicate samples are represented by double symbols at specific single depths. pg. 98

Fig. 4.30. Dissolved distributions of dissolved Fe, Mn, As, Ni, Cu and Zn (A-F, respectively) obtained from peeper (open circles) and core porewaters (diamonds) at station 1, Balmer Lake, March, 1994. Replicate samples are represented by double symbols at specific single depths. pg. 100

Fig. 4.31. Dissolved distributions of dissolved Fe, Mn, As, Ni, Cu and Zn (A-F, respectively) obtained from peeper (open circles) and core porewaters (diamonds) at station 6, Balmer Lake, March, 1994. Replicate samples are represented by double symbols at specific single depths. pg. 102

Fig. 4.32. Sedimentary weight ratio profiles of Si/Al, Ti/Al, Mg/Al, K/Al, Na/Al and P/Al (A-F, respectively) for station 1 (duplicate cores 1a and 1b, open symbols) and station 6 (core 2, closed symbols), Balmer Lake, March, 1994. pg. 104

Fig. 4.33. Sedimentary weight ratio profiles of Zr/Al, Sr/Al and Rb/Al (A-C, respectively) for station 1 (duplicate cores 1a and 1b, open symbols) and station 6 (core 2, closed symbols), Balmer Lake, March, 1994. *pg. 105*

Fig. 4.34. Sedimentary concentrations of organic carbon, calcium carbonate, total nitrogen, values for organic carbon/nitrogen, total sulphur and iron/aluminum weight ratios (A-F, respectively), for station 1 (duplicate cores 1a and 1b, open symbols) and station 6 (core 2, closed symbols), Balmer Lake, March, 1994. *pg. 106*

Fig. 4.35. Sedimentary concentrations of manganese, nickel, zinc, copper, arsenic, and lead (A-F, respectively) for station 1 (duplicate cores 1a and 1b, open symbols) and station 6 (core 2, closed symbols), Balmer Lake, March, 1994. *pg. 107*

Fig. 5.1. Time series of progressive trace metal water column profiles (A-E) over the fall-winter transition in Balmer Lake: A) well-mixed water column, B) influence of remobilized bottom-water source, C) influence of interfacial sulphide sink, D) greater extent of sulphide removal, and E) influence of metal-rich lateral advective flow. Depth and concentration axes are in arbitrary units. *pg. 132*

Fig. 5.2. Seasonal peeper profiles of ammonium for stations 1 and 2 (A and B, respectively) in Balmer Lake. Replicate samples are represented by double symbols at specific single depths. *pg. 152*

Fig. 5.3. Seasonal peeper profiles of nitrate for stations 1 and 2 (A and B, respectively) in Balmer Lake. Replicate samples are represented by double symbols at specific single depths. *pg. 154*

Fig. 5.4. Seasonal peeper profiles of sulphate for stations 1 and 2 (A and B, respectively) in Balmer Lake. Replicate samples are represented by double symbols at specific single depths. *pg. 156*

Fig. 5.5. Seasonal peeper profiles of dissolved Fe for stations 1 and 2 (A and B, respectively) in Balmer Lake. Replicate samples are represented by double symbols at specific single depths. *pg. 160*

Fig. 5.6. Winter peeper profiles of dissolved Fe for stations 1, 2, 4 and 6 in Balmer Lake. Replicate samples are represented by double symbols at specific single depths. *pg. 161*

Fig. 5.7. Seasonal peeper profiles of dissolved Mn for stations 1 and 2 (A and B, respectively) in Balmer Lake. Replicate samples are represented by double symbols at specific single depths. *pg. 165*

Fig. 5.8. Time series of progressive bottom water and porewater profiles (A-D) over the fall-winter transition in Balmer Lake: A) fall profile, B) instantaneous input of Mn to bottom waters, C) profile after some time of equilibration, and D) late winter profile. Depth and concentration axes are in arbitrary units. *pg. 167*

Fig. 5.9. Seasonal peeper profiles of dissolved Ni for stations 1 and 2 (A and B, respectively) in Balmer Lake. Replicate samples are represented by double symbols at specific single depths. *pg. 173*

Fig. 5.10. Seasonal peeper profiles of dissolved Cu for stations 1 and 2 (A and B, respectively) in Balmer Lake. Replicate samples are represented by double symbols at specific single depths. *pg. 178*

Fig. 5.11. Seasonal peeper profiles of dissolved Zn for stations 1 and 2 (A and B, respectively) in Balmer Lake. Replicate samples are represented by double symbols at specific single depths. *pg. 181*

Fig. 5.12. Summer peeper profiles of dissolved Fe, Mn and As for station 2 in Balmer Lake. Replicate samples are represented by double symbols at specific single depths. *pg. 195*

Fig. 5.13. X-Y scatter plot illustrating the dependence of dissolved As on the distribution of dissolved Mn. The values (molar concentrations) represent a depth interval spanning from ~3 cm above the sediment surface to ~20 cm below. Coefficients of determination (r^2) from linear regression analyses for the respective stations are included. *pg. 197*

Fig. 5.14. Seasonal peeper profiles of dissolved As for stations 1 and 2 (A and B, respectively) in Balmer Lake. Replicate samples are represented by double symbols at specific single depths. *pg. 199*

LIST OF TABLES

Table 2.1. Estimated average yearly ranges of mine-related inputs from the Campbell Mine tailings system to Balmer Lake, Ontario, before and after chemical treatment. All values expressed in mg/L. Pg. 22

Table 2.2. Estimated average yearly concentrations of mine-related inputs from the Arthur White tailings system to Balmer Lake, Ontario. All values expressed in mg/L. Pg. 23

Table 2.3. Summer, fall, winter and spring sampling periods at Balmer Lake, Ontario, indicating stations of peeper deployment, coring and water column sampling. Pg. 25

Table 4.1. Summer water column distributions of dissolved Mn, Fe, Ni, Cu, Zn, As, Pb, NH_4^+ , NO_3^- , SO_4^{2-} and PO_4^{3-} for stations 1, 2, 3, and 4 in Balmer Lake, Ontario, June 1993. All values are expressed in $\mu\text{g/L}$ unless specified otherwise (BDL denotes below detection limit). Pg. 46

Table 4.2. Fall water column distributions of dissolved Mn, Fe, Ni, Cu, Zn, As, Pb, NH_4^+ , NO_3^- , SO_4^{2-} and PO_4^{3-} for stations 1, 2, 3, 4 and 5 in Balmer Lake, Ontario, October, 1993. All values are expressed in $\mu\text{g/L}$ unless specified otherwise (BDL denotes below detection limits). Pg. 47

Table 4.3. Winter water column distributions of dissolved Mn, Fe, Ni, Cu, Zn, As, Pb, NH_4^+ , NO_3^- , SO_4^{2-} and PO_4^{3-} for stations 1, 2, 3 and 4 in Balmer Lake, Ontario, March, 1993. All values are expressed in $\mu\text{g/L}$ unless specified otherwise (ND denotes not determined). Pg. 48

Table 4.4. Spring water column distributions of dissolved Mn, Fe, Ni, Cu, Zn, As, Pb, NH_4^+ , NO_3^- , SO_4^{2-} and PO_4^{3-} for stations 1, 2 and 4 in Balmer Lake, Ontario, May, 1993. All values are expressed in $\mu\text{g/L}$ unless specified otherwise (ND denotes not determined). Pg. 54

Table 4.5. Concentrations of total suspended solids (TSS), particulate organic carbon (SPOC), particulate organic nitrogen (SPON), C_{Org} :nitrogen ratio (C/N) and total particulate organic matter (POM) in the water column of Balmer Lake, Ontario, for the summer, fall, winter and spring field sessions. TSS values were determined from the particulate mass on pre-weighed 0.45 μm Nuclepore filters, while all organics were determined from glass fibre filters. *pg. 55*

Table 4.6. Particulate trace metal concentrations of Fe, Mn, Ni, Cu, Zn, As and Pb for the summer, fall, winter and spring water columns in Balmer Lake, Ontario. All values are expressed in $\mu\text{g}\cdot\text{L}^{-1}$. *pg. 65*

Table 4.7. Concentrations of trace metals ($\text{mg}\cdot\text{kg}^{-1}$), organic carbon (%) and organic nitrogen (%) in suspended particulates of the summer, fall, winter and spring water columns in Balmer Lake, Ontario. Trace metal values were determined from the particulate mass on pre-weighed 0.45 μm Nuclepore filters, while all SPOC and SPON values were determined from glass fibre filters. *pg. 67*

ACKNOWLEDGEMENTS

This project was jointly jointly funded by Placer Dome Inc. and Goldcorp Inc. Special thanks goes to Richard Janicki, Dave Hiller and Elias Dibb of Campbell Mine, Red Lake, who helped ensure the success of the fieldwork. We also thank Jim Robertson (PDI, Vancouver) for his interest and continued support.

I wish to thank Drs. Tom Pedersen, Steve Calvert, George Poling and Bill Cullen of my supervisory committee for their various degrees of input into my thesis. In particular, I deeply express my thanks to Tom Pedersen who is not the uncultured, useless, dirty, stinking heathen everyone says he is. I will always have fond memories of sitting in his office, Tom reclining back in his chair, hands clasped and brought to his mouth, his eyebrows progressively lowering over his piercing stare as I presented him with my latest views. "You have done a good job" he would say, as he passed you your crimsoned document, the pages weighted and thickened by the rigorous onslaught. I also extend my gratitude to Steve Calvert, whose insight and depth would intimidate the likes of Carl Sagan and Mr. Spock. As for Bill Cullen, I appreciate the fact that he left the country as I heard he can be quite intimidating at oral examinations.

Additional thanks goes to my fellow research group members, Rémy Chrétien, Darcy McDonald, Jay McNee, Raja Ganeshram, Robert Mugo, Brad Mckelvey, Maureen Soon and Bert "high sticking" Mueller, for making my graduate years (all four of them) a lot of fun. I will also never forget John "Leatherman" Ridley, whose mighty power aided in both the peeper deployments and his ability in snow wrestling. The boys (you know who you are) should also be praised for their efforts in getting me out of the house. I dedicate my thesis to my partner in crime, Debbie, who not only proofread this document, but ensured I received regular doses of mountain air throughout my degree.

I. INTRODUCTION

1.1 Trace Metal Geochemistry

The study of trace metal geochemistry is driven partly by curiosity, and as a result of the inherent toxicity of many metal species, partly by an obligation to the maintenance of human health and the well-being of the environment. The last decades have seen a large increase in the burden of trace metals in the environment, and as a consequence, enrichments now commonly exist in terrestrial and aquatic reservoirs (Ferguson and Gavis, 1972; Nriagu, 1989). Considerable attention has been given to the fates and effects of toxic metals. In recent times, the major research objectives on metal-polluted systems have progressed from initial surveys of sources and pathways toward more detailed investigations of the mechanisms controlling the distribution, mobility and bioavailability of different metal species.

Knowledge of the distribution and behaviour of trace elements in aquatic and marine systems has grown significantly over the past two decades, largely in part to advancements in sampling techniques and analytical methods. The development of clean collection techniques (Boyle and Edmond, 1977; Bruland *et al.*, 1979; Schaule and Patterson, 1981; Nriagu *et al.*, 1993) and sensitive analytical instrumentation has facilitated the reliable measurement of trace constituents; the use of clean methods has also exposed inaccuracies in previously reported data. As a result, well-defined vertical and horizontal variations in concentrations of dissolved components for the world's oceans now exist for the majority of trace elements. Prior to the implementation of clean techniques, the state of trace metal biogeochemistry of lacustrine systems suffered similar misrepresentation. Contamination artifacts introduced during the collection,

handling and analyses of samples severely compromised published data acquired in the absence of rigorous methods. The assumption that stringent, ultraclean laboratory methods are not required in "polluted" waters warrants close scrutiny following recent studies of the Great Lakes which report trace element concentrations comparable to, or even lower than, the levels commonly observed in the pelagic ocean (Nriagu, 1996; Flegal, 1988; Coale, 1989).

In the open ocean, dissolved trace element distributions are generally considered to be in steady state (Murray, 1987). Integrated, systematic studies have been used to determine the biogeochemical and physical processes governing the vertical and horizontal distributions of many trace elements (Bruland, 1980; McKelvey, 1994). Application of one-dimensional, vertical advection diffusion models fitted to oceanic profiles allow the extraction of chemical parameters such as production and scavenging rates (Morel and Hudson, 1985). In addition, oceanographic investigations have revealed the usefulness of many trace elements as effective markers of various marine processes.

The science of limnology has evolved greatly since the original pioneering works of Forel (1892, 1895, 1904), Mortimer (1941, 1942, 1951) and Hutchinson (1957). In spite of significant progress, chemical limnology has not yet reached the same state of sophistication as its marine counterpart. Essentially the same mechanisms act to control trace element distributions in lacustrine settings; however, trace metal distributions are driven by time-dependent processes which vary from days to seasons (Balistrieri and Murray, 1992). The variability induced by the transient nature of lake processes can make steady state assumptions invalid, and as a result, may inhibit the isolation of the variables controlling trace metal cycles (Murray, 1987). Furthermore, the dynamic nature of lakes hinders comparisons of different systems due to variations in factors

such as the surrounding geology and trophic status. Defined patterns of trace metal distributions in lakes are further hindered by the greater availability of competing scavenging phases (e.g., detrital particles, phytoplankton and authigenic precipitates) and compressed depth scales. Although the transient nature of lake processes adds extra complexities, time-dependent variations (e.g., oxic/anoxic cycles) can be taken advantage of to establish the dynamics of biogeochemical cycles (Balistrieri and Murray, 1992).

1.2 Trace Metal Cycling in Lakes

The intrinsic properties of a particular metal (e.g. crystal field stabilization energy, electronegativity, ionic radius, etc.) and the environmental conditions prevalent (e.g., types and concentrations of ligands present, available adsorptive surface areas, pH, p_e) are ultimately responsible for the distribution of particular species and their corresponding redox and coordination chemistries (Stumm and Morgan, 1981). Systematic studies of trace elements in lakes provide information on the physical, chemical and biological processes controlling their respective mobility and distribution. These processes include diffusion, advective transport, nutrient-like biological cycling, sorption by sediments or suspended particles, precipitation, atmospheric deposition, redox cycling, and fluxes across the sediment-water or air-water interface (Murray, 1987). The relative importance of these mechanisms depends on the prevalent abiotic and biotic environment as well as the element under consideration.

Spatial and temporal changes in the chemical environment of lacustrine systems can strongly influence biogeochemical pathways of various metal species. For example, lakes may possess chemical gradients with depth (e.g.,

dissolved O_2 , SO_4^{2-} , etc.) and exhibit significant seasonal differences in such major variables as pH and pe (Jenne, 1986). Furthermore, seasonal variations in productivity can foster corresponding shifts in pe and concentrations of organic products. Increases in autochthonous particles for instance, may provide additional complexation sites for trace metals, resulting in lower concentrations of dissolved metal species (Francois, 1990).

These multiple influences are briefly elaborated upon in the general review of trace element cycling in lake systems that is presented in the following sections. A brief introduction to the sources of trace metal inputs will be followed by more detailed descriptions delineating the processes governing metal behaviour and mobility in both the water column and underlying sediments and porewaters.

1.2.1 Inputs of Trace Elements to Lacustrine Systems

Trace metals are incorporated into lake systems primarily via tributary inflow, ground water inputs, coastal runoff, industrial and domestic effluent discharges and atmospheric fallout. Natural sources are primarily water or wind-borne soil particles, seasalt aerosols, volcanism, forest fires and biogenic particulate matter (Nriagu, 1989). Nriagu (1989) estimated that aerosols of biogenic origin dominate the natural fraction and can account for 30-50% of the global baseline emissions of trace metals in non-urban areas. Hydrothermal activity has also been shown to provide significant quantities of trace metals to specific fresh waters (Agett and O'Brien, 1985). Background metal levels in inland waters due to weathering processes are more difficult to establish than in the marine environment as a result of varying geology and fluctuations in water discharge (Baccini, 1984). In contrast, anthropogenically enriched levels of

metals are derived from domestic wastewater effluents, mining-related inputs, gasoline combustion, coal burning power plants, non-ferrous metal smelters, iron and steel plants and the dumping and incineration of sewage sludge (Nriagu, 1989).

1.2.2 Major Processes Governing Trace Metal Behaviour and Mobility

The distribution of trace metals between solution and particulate forms has widely been recognized as a major factor controlling the geochemical behaviour, transport and biological effects of metals in natural waters. Many trace metals (e.g. Cu, Pb, Hg, Cd, Zn, Ag) have been shown to be primarily associated with suspended and sedimentary particulates as opposed to dissolved phases (Davis and Leckie, 1978b; Nriagu *et al.*, 1981; Laxen, 1985; Tessier *et al.*, 1985). Particulates in natural waters consist predominantly of detrital particulate and colloidal organic matter, inorganic solids such as metal oxides and hydroxides (e.g., SiO₂, MnO₂, FeOOH, Al₂O₃), algal skeletal remains, carbonates and detrital aluminosilicates (e.g., clay minerals, feldspars) (Tessier *et al.*, 1985). In general, particulate organic matter (POM) often presents the major component of suspended material, accounting for up to 70% of the total particulate fraction (Nriagu *et al.*, 1982).

Settling particles, especially organic aggregates, can play a dominant role in the binding and transfer of heavy metals to lake sediments, thereby regulating the concentrations of dissolved species (Nriagu *et al.*, 1981; Sigg, 1985; Jackson and Bistricki, 1995). In general, inverse relationships between the residence times of particulate metals and the standing crops of suspended matter in the water column are evident for most lakes (Sigg, 1985). Variations in the residence times of various metals primarily reflect differences in their leachability from source

particulates and in the rates of biotal assimilation (Nriagu *et al.*, 1982). Sigg (1985) and more recently Morel and Hudson (1985) have extended the Redfield ratio concept (Redfield, 1958) to include trace elements, suggesting a stoichiometric formula of $C_{106}N_{16}P_1 (Fe, Zn, Mn)_{0.01} (Cu, Cd, Ni, Co)_{0.001}$. Sigg (1985) suggested that algal-metal associations could result in metal uptake with constant stoichiometric proportions. Although the concept of Redfield ratios may be applicable to the metal content of algae, the dynamic nature of lakes limits its usefulness because only under severely restricted conditions will the stoichiometry be reflected in dissolved metal concentrations (Reynolds and Hamilton-Taylor, 1992).

Cyclic variability in the composition of the total suspended matter is evident in many temperate lakes. In winter and early spring, isothermal conditions typically predominate and storm events can resuspend quantities of fine sedimentary matter (Baccini, 1984). This particulate fraction may have undergone considerable diagenetic alteration and be characterized by relatively low organic carbon and high mineral contents (e.g., clays). With the onset of large-scale vernal primary production, phytoplankton, zooplankton and the associated detrital material may dominate the particle pool. During periods of thermal stratification, the epilimnion is largely decoupled from the underlying colder waters of the hypolimnion resulting in unidirectional, downward transport of particulate matter. During the latter stages of stratification in the late summer and fall, the pH may be driven high enough by the production of organic matter to promote the precipitation of $CaCO_3$ in surface waters. Inorganically precipitated calcite has been shown to account for 20-90% of the particle pool in the Great Lakes during such periods (Eadie and Robbins, 1987).

The influence of biologically- and chemically-mediated redox reactions on the behaviour of trace elements has received considerable attention owing to the

pronounced effect such transformations have on the spatial and temporal distributions and on the speciation of such elements in solution, suspended particulates and sediments. The predominant mechanisms driving the redox cycling of elements in lakes are plankton growth in surface waters and the bacterially-mediated degradation of organic matter in sub-surface waters and sediments (Hamilton-Taylor and Davison, 1994). Redox-driven biogeochemical pathways of elements may involve direct redox transformations (e.g., As(V) → As(III)) in which the metal species itself undergoes a redox reaction (De Vitre *et al.*, 1991). Alternatively, metal species may be subject to indirect involvement, in which the distribution of the element is affected by redox-driven cycling, but apparently does not itself (e.g., Zn) undergo a redox transformation (Reynolds and Hamilton-Taylor, 1992).

The redox behaviour of iron and manganese in lakes has received considerable attention as a result of the central role that these abundant metals play in the geochemical cycling of trace elements (Sholkovitz, 1985; Leckie, 1986; Davison, 1993; Hamilton-Taylor and Davison, 1994). Both elements are common to natural waters in discrete mineral phases and in surface coatings on particulate material, usually occurring in oxic conditions as insoluble oxides at their higher oxidation states. Their reduced states, Fe²⁺ and Mn²⁺, are soluble and relatively uncomplexed (Davison *et al.*, 1982). Sedimentary iron and manganese oxyhydroxides exhibit high affinities for metal ions (e.g., As, Ni, Cu, Cd, Zn, and Pb) and have been repeatedly inferred to be sinks for trace metals (Crecelius, 1975; Nriagu *et al.*, 1981; Davison and Woof, 1984; Tessier *et al.*, 1985; Tessier *et al.*, 1996). The sorptive affinity of trace metals for oxide surfaces is strongly influenced by pH (Vuceta and Morgan, 1978), ionic strength (Stumm and Sulzberger, 1992), adsorbed ligands (Davis and Leckie, 1978a; Vuceta and Morgan, 1978) and humic substances (Tipping and Cooke, 1982). Theoretical and

experimental works on solid-solution interactions of trace metals with amorphous iron oxyhydroxide demonstrate the existence of a multiplicity of discrete binding sites with wide-ranging adsorptive characteristics (Davis and Leckie, 1978b; Benjamin and Leckie, 1981). The preferred adsorption sites for such trace elements as Cd, Zn, Cu, and Pb are apparently distinct from one another, which explains why competitive effects observed are weaker than one might otherwise expect. This heterogeneity of complexation sites has been explained in terms of the number and identity of nearest neighbours, proximity to various crystal defects, microcrystallinity, local electrical field strength, and physical constraints such as the size of pores leading to internal sites (Benjamin and Leckie, 1981).

Seasonal variations in the redox chemistry of iron and manganese in lakes can result in pronounced inter-annual variability in the distribution, behaviour and mobility of many trace elements. Non-steady state redox environments induced by productivity pulses and changes in local hydrography can significantly affect the distribution of their respective soluble and particulate phases (Tipping *et al.*, 1981). Meromictic lakes offer a range of redox conditions which vary spatially and temporally, and consequently, such basins are particular well suited to studying nuances of redox processes (Davison and Woof, 1984). Temperate lakes tend to exhibit seasonal stratification of the water column in the summer months which is induced by surface heating of a usually shallow mixed layer (Baccini, 1984). The redox boundary in a seasonally stratified lake may migrate from a horizon within the sediments under well-mixed conditions upwards into the water column during episodes of maximum stratification (Laxen, 1985). During unstratified conditions, oxygen may be present at the sediment-water interface, favouring the formation of Mn and Fe oxyhydroxides in the surficial sediments (Davison *et al.*, 1982). Upon burial of

the sediment, diagenetic respiration processes deplete oxygen and promote a reducing environment. The reductive dissolution of oxyhydroxides in reducing sediments promotes the mobilization of Fe(II) and Mn(II) and the concomitant mobilization of sorbed metals. In the absence of further chemical reactions, Fe(II), Mn(II) and the associated trace metals may diffuse upward along concentration gradients towards the sediment-water interface, where the predominant reactions are reprecipitation under oxic conditions, and release into the hypolimnion when anoxic conditions prevail (Agett and O'Brien, 1985; Aggett and Kriegman, 1988). In general, as the oxic zone of the sediments is compressed, retention of metals in the sediments primarily associated with metal oxides is decreased. Those elements with lower ionization potentials (i.e. decreased capability to take up electrons and thus a reduced tendency to form complexes) are more readily mobilized and thus enter solution at higher pe values (Stumm and Morgan, 1981). During the later stages of stratification, the hypolimnion may become sufficiently devoid of oxygen to enable the dissolved species to diffuse across the sediment-water interface where they may accumulate until overturn (Davison and Woof, 1984; Aggett and Kriegman, 1988). The duration of stratification and the volume of the hypolimnion strongly influence the fluctuations in the concentrations of dissolved trace metal species (Davison 1982). The misinterpretation of diagenetic metal enrichments as anthropogenically related features is, however, a potential problem in mildly reducing, Mn- and Fe-rich lake sediments.

1.2.3 Transformations Across the Sediment-Water Interface

Bottom sediments of lakes represent complex mixtures of diverse components that include: residues of weathering and erosion (e.g., aluminosilicates), inorganic and organic products of biological activity, and diagenetic products such as iron and manganese oxyhydroxides and sulphides (Tessier and Campbell, 1988). Trace metals may be scavenged from the water column and incorporated into the bottom sediments via several mechanisms including: sorption onto hydrous metal oxides, ion exchange with clay minerals, sorption on organically coated particulates, adsorption to or incorporation with detrital organic matter, and via diffusive influxes along concentration gradients. The particular physical and biogeochemical characters that dictate sediment geochemistry ultimately determine the nature of the various diagenetic (i.e., post depositional) reactions and resulting authigenic fractions. Authigenic phases encompass a wide spectrum of inorganically-derived precipitates which form in the water column or in the sediments after deposition. Organic matter constitutes a very important sedimentary component, as its diagenesis during decomposition provides the primary impetus behind the post-depositional reactions responsible for the formation of numerous hydrogenous components (Suess, 1979). Organic matter degradation has additional ramifications with respect to nutrient regeneration and benthic community structure (Emerson, 1976; Froelich *et al.*, 1979).

Studies of the microbially-mediated decomposition of organic matter have led to the development of a well-established model in which the distributions of oxidants, reductants, and metabolites with depth follow a predictable and universal sequence, given an elastic depth scale. Detailed accounts have been described by several authors (Sholkovitz, 1973; Froelich *et al.*, 1979;

Klinkhammer, 1980; Van der Weijden, 1992). Briefly, this degradation follows a thermodynamic order of sequential oxidation reactions which yield progressively lower free energy changes per mole of organic carbon oxidized. In practice, the reaction sequence is subject to oxidant availability and kinetic constraints, including the dominance of particular microbial populations. As previously stated, thermodynamics dictates that relative pore water distributions of metabolites will be consistent from site to site with the only variable being the depth scale over which these reactions occur. Organic-rich sediments, characterized by high diagenetic intensity and thus steep thermodynamic gradients, may, however, exhibit significant overlap in the sequence of oxidation reactions (Froelich *et al.*, 1979).

A recent evaluation of the redox zonation during the degradation of organic matter assessed the controls responsible for observations of the simultaneous reduction of Fe(III) and sulphate in several field studies (Postma and Jakobsen, 1996). They suggest that the sequential occurrence of these processes can be better explained by a partial equilibrium approach where initial fermentation determines the overall rate (i.e., the reactivity and amount of organic matter) while equilibrium is approached by the terminal electron accepting processes. They concluded that depending on the stability of the iron oxide and porewater pH, sulphate may be reduced simultaneously with, or even prior to Fe(III).

The flux of organic matter to the sediments exerts the primary control on diagenetic intensity and has a corresponding influence on metabolite distribution. In environments of rapid sediment accumulation and those with high input rates of organic matter, interstitial metabolite concentrations (e.g., HCO_3^- , HPO_4^{2-} , HS^-) may exceed the solubilities of certain inorganic equilibria

resulting in the formation of authigenic minerals and thus preferential removal of one or several of the dissolved constituents (Suess, 1979; Berner, 1984).

Thermodynamic calculations on the bulk solution of most freshwater and seawater typically show undersaturation with respect to known metal solid phases (Tessier *et al.* 1985). Even for interstitial waters of oxic sediments, in which trace metals have longer residence times than in the bulk solution and are thus more apt to approach a state of equilibrium with solid phases in the sediments, metals are usually undersaturated with respect to their least soluble compounds (Schindler, 1981). Trace metal adsorption to solid surfaces has been invoked to account for observed distributions. The trace metal-particulate association may include: sorption of metal ions at oxide surface sites, ion exchange within clay minerals, binding by organically-coated particulate matter or organic colloidal material, or adsorption of a metal-ligand complex. In particular, the important roles played by iron and manganese oxyhydroxides and humic materials in the adsorption of trace metals in soils and sediments have been strongly emphasized due to their high sorptive properties and ubiquitous presence in natural systems .

Thermodynamic modeling of interstitial waters is a useful technique for identifying possible controls on authigenic mineral formation. Experimentally derived ionic strengths, activity coefficients, and activities of various interstitial metabolites are often used to calculate the controlling mechanisms responsible for the distribution of various aqueous and solid fractions. Production and consumption rates of interstitial metabolites can be used to constrain further thermodynamic gradients and redox pathways. The availability of powerful mathematical tools which incorporate variables such as saturation indices, distribution coefficients and diffusive fluxes, aid in the development of conceptual models of sediment geochemistry. In more complex natural settings,

however, calculated values often deviate from the observed as complications arise from mixed mineral phases, adsorption and/or ion exchange equilibria (Matisoff *et al.*, 1980).

1.3 Contamination of Aquatic Systems From Metal Mining

While estimates of trace element emission rates to the environment differ (Lantzy and Mackenzie, 1979; Jaworowski *et al.*, 1981; Zoller, 1984; Nriagu, 1989), it is agreed that for most toxic metals emissions from industrial activities are larger than natural fluxes. Human operations have thus become the key agent in the global atmospheric cycle of trace metals and metalloids. For example, a comparison of world-wide median emission values from natural and anthropogenic sources suggests that industrial emissions of Pb, Cd and Zn exceed the flux from natural sources by factors of 18, 5 and 3, respectively (Nriagu 1989). Further, contributions from anthropogenic sources of As, Hg, Ni, Sb and V may exceed those from natural sources by 100-200% (Nriagu 1989).

The metal mining industry contributes significantly to the anthropogenic input of many trace elements to the Earth's atmospheric, terrestrial and aquatic systems (Nriagu, 1989). Impacts resulting from such activities can be highly localized, such as an acid-generating waste-rock pile, or can extend over hundreds of kilometres via emissions from the smelting of ore concentrates. In the case of sulphide-bearing ore deposits, the potential for loadings of acidity and metals to the environment presents the primary concern. In particular, smelter emissions, acidic drainages and the erosion of waste rock deposits can foster extensive and lasting environmental impact (Almer *et al.*, 1978; Salomons, 1995).

1.3.1 Bioavailability and Toxicity

The uptake of trace elements by biological systems is a speciation-sensitive process for which chemical specificity varies from one element to another (Turner, 1984; Campbell *et al.*, 1988). Bioavailable forms include free metal ions, organometallic species including organic complexes, and inorganic complexes including hydrolysis products (Turner 1984). Though much remains to be learned about the mechanisms of trace element uptake and nutrition in phytoplankton, the assimilation of trace metals appears to be in most cases a two stage process involving the binding of a relatively large pool of metal to the cell surface and transport through the cell membrane, presumably via metal-porter molecules (Morel and Hudson, 1985). The exact nature of either the surface binding groups or the porter molecules remains questionable. Seemingly, a significant fraction of the surface ligands must be complexed by a particular metal for that species to be taken up, the extent of binding being related to the intracellular assimilation (Turner 1984). Indiscriminate uptake of non-essential metal species appears to be related to the relatively low specificity of metal transport mechanisms and thus presents an important mode of toxicity (Harrison and Morel, 1983).

In addition to the major nutrient elements, many trace metals including Fe, Mn, Zn, Cu and Ni have been determined to be essential for life, and it has been argued that many major and trace elements, both essential and toxic, may be simultaneously controlling biological production in the oceans (Morel and Hudson 1985). These trace metals exhibit fairly narrow "concentration windows" that separate essential and toxic levels (Florence 1982). In the open ocean where concentrations are low, toxic effects are negligible; however, in coastal regions and lakes, metal inputs from weathering and anthropogenic processes result in

substantially higher metal concentrations that may exceed toxic thresholds (Elinder, 1984).

1.4 Research Objectives

Many trace elements exhibit toxic effects towards plant and animal species when present in sufficiently high concentrations. Particular attention has been given to the environmental significance of several heavy metals and metalloids (e.g., As, Hg, Pb, Ni, Zn, Cd, Cr) in view of their inherent toxicity and common occurrence (Elinder, 1984; Cullen and Reimer, 1989). Lake sediments represent the ultimate site of deposition for many trace elements introduced into the environment. Since an important fraction of the trace metals present in the aquatic environment is reversibly associated with the surficial sediments (Campbell *et al.*, 1988), the study of trace metal transformations and dynamics across the sediment-water interface is prerequisite to the understanding of their behaviour in whole aquatic systems.

The primary impetus behind this research was to investigate the poorly constrained biogeochemical cycling of metals within the water-sediment system in Balmer Lake. It is anticipated that the project will provide basic insight into the cycling of metals in shallow, boreal contaminated lakes as well as data which can be used to assess both the overall impact of the final discharge from Balmer Lake on the local water system, and prospects for mitigation of the contamination problem over the long term. More specifically, the research comprises three principal objectives: 1) To determine the biogeochemical processes governing the behaviour and mobility of trace metals in Balmer Lake sediments and assess the extent to which these metals are mobile; 2) To determine the direction and significance of benthic fluxes of trace metals; and 3)

To assess how the chemistry of the water column, underlying sediments and associated porewaters, change over the course of a full four-season cycle.

A seasonal study of Balmer Lake was essential in order to resolve the nature and extent of geochemical variations in response to seasonal changes in hydrography, oxygenation and plankton productivity. In particular, it was desired to link periods of seasonal anoxia and the influence of redox-related reactions on metal mobility and diagenetic chemistry. To meet these objectives, a two component research program was implemented: first, a seasonal assessment of the water column chemistry and second, a detailed seasonal investigation of the chemistry of the sediments and associated porewaters. The latter involved high resolution sampling of the interstitial waters and bottom waters. Balmer Lake provides an ideal *in situ* laboratory to address the nature of metal transfer mechanisms and partitioning across the sediment-water interface for two reasons: first, there is a large signal of metal contaminants; and second, the large benthic area to volume ratio makes the chemistry of the lake susceptible to influences from interfacial fluxes.

To determine accurately the nature of post-depositional reactivity, detailed analyses of both solid and dissolved phases are essential (Colley *et al.*, 1984; Carignan and Nriagu, 1985). Undetectable changes in the sediment fraction can significantly alter the chemical composition of the associated porewaters which can thus provide a sensitive indicator of the diagenetic reactions and equilibria between solid phases and dissolved species (Matisoff *et al.* 1980). In addition, the residence times of trace elements in the interstitial fraction are longer than in the overlying waters; porewaters are therefore more apt to approach a state of equilibrium with solid sediment phases (Schindler, 1981). Consequently, the composition of interstitial waters can be used to identify and quantify mineral equilibria and thus infer chemical mass transport (Matisoff *et al.*

1980). Porewater studies done in conjunction with investigations of the water column can provide a link between water column transport processes and sedimentary accumulation by showing evidence for the release of trace elements associated with the degradation of biogenic particulate matter (Shaw *et al.*, 1990).

II. STUDY SITE

2.1 Physiography, Physical and Chemical Limnology

Balmer Lake is a small, shallow, boreal lake situated in the Canadian Shield of northwestern Ontario (Fig. 2.1). The waterbody is 260 hectares in area, has an estimated mean depth of 2.4 m and a maximum basin depth of 4.0 m. Typical of shallow Precambrian shield lakes, Balmer Lake is productive and hosts organic-rich sediments (Conroy and Keller, 1976). The shallow water column maintains fairly well-mixed conditions during the ice-free periods of late spring, summer and fall. Periods of bottom water anoxia develop in the winter months in deeper areas (>2.5 m) of the ice-covered lake.

The waterbody has served as a repository of mining-related wastes for two underground gold mines since 1965 (Fig. 2.1). Both mines process high grade ores rich in Ni, Cu, Zn and As, and as a result, concentrations of these metals are significantly enriched in the lake waters and sediments. In addition, the lake hosts high inventories of other mining-related byproducts, including cyanide, ammonia, nitrate and sulphate. The water retention time in the lake is approximately 230 days, which aids the natural degradation and settling of cyanide and heavy metals before final discharge to the local water system. In the design of the tailings circuit, the lake was intended to receive only dissolved and colloidal loads. However, historical dam breaches of the surrounding tailings ponds have resulted in significant and episodic particulate loadings to areas of the lake. Over the period of mining activity, the lake has supported few fish and is not used recreationally. Since January of 1994, only the Arthur White Mine (Fig. 2.1) has been discharging effluents that have exceeded the recommended

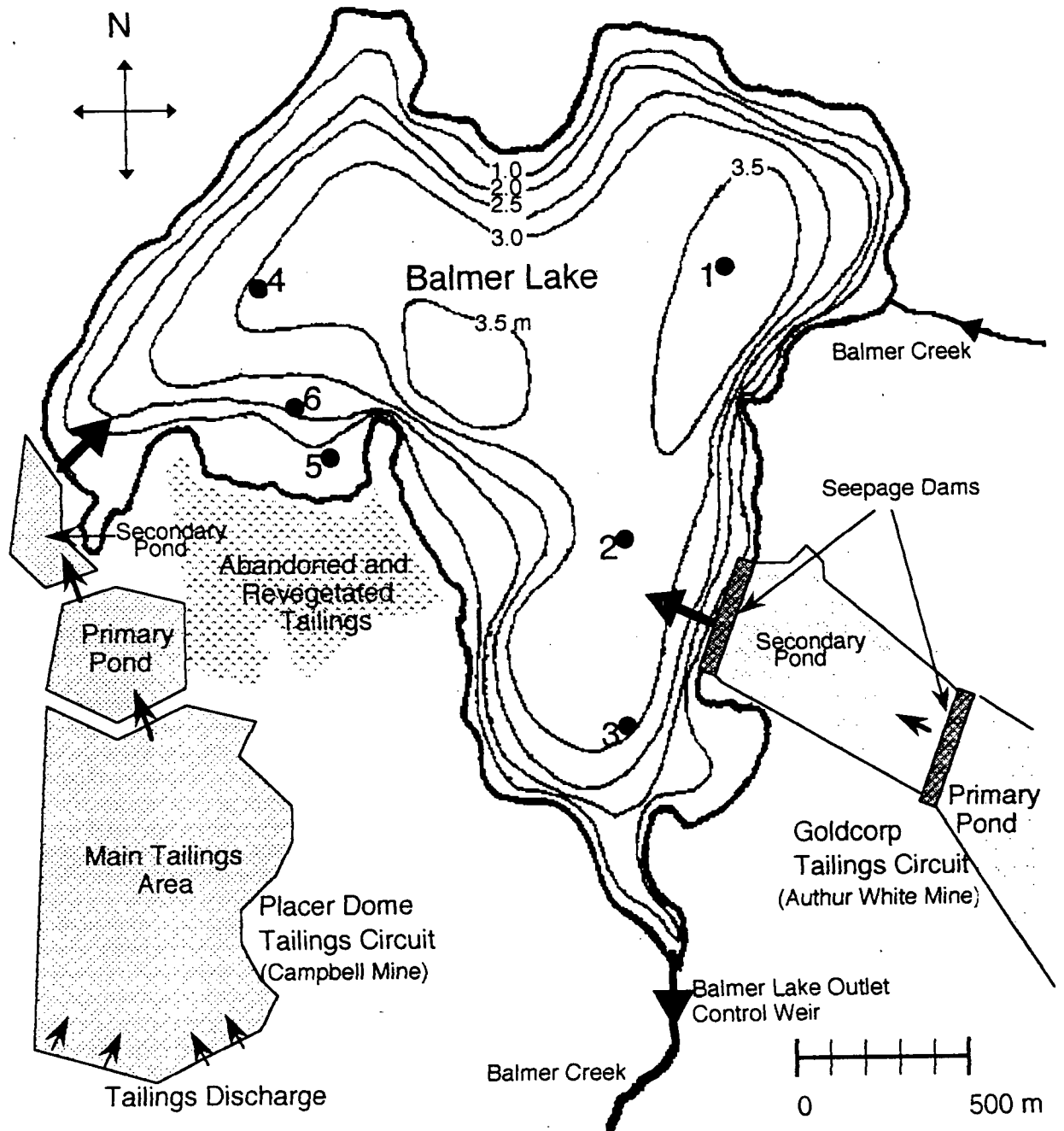


Fig. 2.1 Location map of Balmer Lake showing the sampling stations, lake bathymetry and tailings circuits of the adjacent mines.

COA (Certificate of Approval) limits with respect to total arsenic and heavy metals.

The general topography of the Balmer Lake region has been described as flat to rolling, with lowland coniferous and upland mixed forest cover. Examinations of the Quaternary geology show that the soil types are dominated by glacial deposits of bouldery to silty till one to several metres thick. The area is also characterized by scattered bedrock outcrops and glaciolacustrine deposits of clay and silt deposited in Lake Agassiz (Gulson *et al.*, 1993). Balmer Lake receives inputs from three main drainage basins, encompassing a total watershed area of 3,290 hectares (Masala, 1995). The natural drainage area comprises 2,550 ha and has been influenced to a moderate degree by road construction, timber harvesting and mining exploration, contributing to breaks in the natural forest cover. The remaining two drainage basins are represented by the Campbell and Dickenson mine sites which comprise active and revegetated tailings, clear water (polishing) ponds, and parts of the mines and townsite. Inputs from these drainages are predominantly mine-related with a small fraction being natural runoff (Masala, 1995a).

2.2 History of Mine-Related Inputs

The Archean greenstone belts in the Red Lake area of northwestern Ontario have been mined for their gold deposits since the gold rush to the district in 1926. Ore-grade gold mineralization in the area generally occurs in three specific associations: (i) massive ferroan-dolomite veins that contain gold + quartz + arsenopyrite in crosscutting veins; (ii) silicified patches with disseminated gold; and (iii) sulphide disseminations (arsenopyrite, pyrite, and lesser pyrrhotite) (Gulson *et al.*, 1993). More detailed summaries of the geology

of the Red Lake area can be found in Colvine *et al.* (1984), Corfu and Wallace (1986) and Corfu and Andrews (1987). Production mining in the area of the Balmer Lake began in 1948 upon operation of the Arthur White Mine. Balmer Lake, however, did not receive mining-related inputs until 1965, at which time, tailings were deposited along the basin of the south shore of the lake. A rock berm was subsequently constructed in 1967 to contain particulate mill effluents. Since this time, the waterbody has served as a tertiary polishing pond for mining wastes from both the Campbell (Placer Dome Inc.) and Arthur White (Goldcorp Inc.) mines.

2.2.1 Campbell Mine

The Campbell Mine is an underground gold mine which uses sub-level longhole and cut-and-fill ore extraction methods. Ore processing proceeds via cyanidation with carbon-in-pulp and Merrill-Crowe Gold Collection Processes. The coarse tails fraction (\approx 460 tons per day (TPD)) is combined with flyash and cement for underground backfilling while the fines (\approx 470 TPD) are sent to the tailings impoundment and settling ponds. Prior to January, 1993, decanted excess water from the main tailings pond proceeded through of a series of polishing ponds (including Balmer Lake) before final discharge to the environment at the Balmer Lake outlet (Fig. 2.1). However, this system was insufficient in reducing contaminant concentrations of Ni, Cu, Zn, As and CN^- to within COA limits on a consistent basis. Subsequently, Placer Dome Inc. commissioned the installation of a wastewater treatment plant which commenced operations in 1993. The chemical process utilizes INCO SO_2 technology (Devuyst *et al.*, 1982) and brought effluent parameters to within guideline specifications, thus effectively removing Balmer Lake from the

Campbell tailings circuit. A comparison of the effluent quality to Balmer Lake before and after chemical treatment is presented in Table 2.1.

Table 2.1. Estimated average yearly ranges of mine-related inputs from the Campbell Mine tailings system to Balmer Lake, Ontario, before and after chemical treatment. All values expressed in mg/L.

Year	Total Cyanide	Total Ni	Total Cu	Total Zn	Total As
Prior to treatment					
1992	0.5-30	2-6	1-7	0.3-1.5	0.2-0.5
1993	0.5-25	0.4-2.0	0.1-8	0.05-1.5	0.01-0.5
After treatment					
1994	0.4-1.5	0.05-0.3	0.05-0.2	0.02-0.06	0.01-0.03
1995	0.1-0.6	0.04-0.07	0.02-0.08	0.02-0.04	0.01-0.03

2.2.2 Arthur White Mine

The Arthur White Mine began production mining in 1948 and shares a similar mining protocol to its PDI counterpart. Ore production, rated at approximately 800 TPD, is achieved by shrinkage, horizontal hydraulic cut and fill, and long-hole stoping mining methods. Arthur White also possesses its own internal primary tailings disposal system, which consists of series of interconnected ponds (Fig. 2.1). Clarified effluent from the primary tailings area overflows the primary dam and drains into a secondary polishing pond. The drainage then proceeds through two rockfill seepage-dams before final discharge to the tertiary polishing pond (Balmer Lake). At the present time, no effluent

treatment facilities exist at the mine, and as a result, inputs from this system present the most significant contributor of heavy metals, sulphate and cyanide to Balmer Lake. Typical effluent concentrations of various parameters are presented in table 2.2.

Table 2.2. Estimated average yearly concentrations of mine-related inputs from the Arthur White tailings system to Balmer Lake, Ontario. All values expressed in mg/L.

Year	Total Cyanide	Total Ni	Total Cu	Total Zn	Total As
1983	9	0.9	1.0	0.7	0.4
1984	15	1.1	3.2	1.1	1.3
1985	7	0.2	0.4	0.1	0.5
1986	3	0.4	1.1	0.3	0.8
1987	5	0.6	1.0	0.3	0.4
1988	2	0.6	0.9	0.1	0.8
1989	4	0.9	2.1	0.2	1.3
1990	15	1.1	3.3	1.1	1.3
1991	8	0.9	1.1	0.7	1.1

2.3 Sampling Periods

Four sampling periods encompassing a summer-fall-winter-spring transition were carried out in order to represent accurately the full seasonal spectrum of the chemical environment in Balmer Lake. The summer sampling

period (Jun-Jul, 1993) was chosen to coincide with a potentially stratified water column, the condition being common to many temperate lakes in the summer months. The fall session (Oct-Nov, 1993) was planned to follow complete breakdown of stratification developed in the summer; sampling was performed just prior to freeze-up and after convective overturn of the shallow water column. In order to observe the maximal extent of sub-ice stratification established during the winter months, sampling was carried out just prior to ice-off in March-April of 1994. Gravity coring was also performed during this period to take advantage of the stable surface offered by the ice; this permitted slow and precise corer insertion. The spring sampling period was carried out two weeks subsequent to ice-off (May 1994) and was designed to capture a post-thaw episode of elevated heavy metal and cyanide levels previously observed during this time.

2.4 Sampling Sites

A survey of Balmer Lake in 1990 (PDI, 1990) established a suite of 45 permanent sampling sites, five of which were chosen as sampling stations for this project (Fig. 2.1). During the winter period, the ice extended to the bottom sediments at station 5 (~1 m deep), and consequently, sampling in that region of the lake required a move into deeper waters to station 6. It was originally anticipated to sample at stations 1 and 2 during every season. However, as a result of an improper insertion, peeper profiling in the winter session was restricted to station 1 only (see below).

To evaluate the precision of the porewater sampling method, two sets of tandem peepers (~ 10 m apart) were first deployed at stations 1 and 2 during the summer session. Subsequent results indicated good agreement among the

porewater profiles yielded by duplicate samplers. The fall period included deployments at stations 1 and 2, including a tandem arrangement at the latter. A fourth peeper was deployed at station 5 in order to assess the porewater chemistry in an area of the lake that has received substantial tailings inputs. This area, coined "Tailings Bay", is bordered by a tailings beach and occupies a significant portion of Balmer Lake (Fig. 2.1); the recent sediments are predominantly mine-related. Deployments at stations 1 and 2 were repeated in the winter session. In addition, peeper sampling was performed in a shallow area of the lake near the out-flow (station 3) and at another deeper site in Tailings Bay (station 6., Fig 2.1). Only three peepers were available for the spring field session, two of which were deployed in tandem at station 1. Upon retrieval of the third sampler positioned at station 2, it was concluded from sediment smears on the aluminum lander and stains on the polyethylene frit that the peeper had fallen on its side at or shortly after deployment. As a result, no data for station 2 were acquired. A summary of the peeper and water column sampling stations is presented in Table 2.3.

Table 2.3. Summer, fall, winter and spring sampling periods at Balmer Lake, Ontario, indicating stations of peeper deployment and water column sampling.

Sampling Period	Peeper Deployment	Water Column Sampling
Summer	Tandem peepers at stations 1 & 2	Stations 1, 2, 3, 4
Fall	Stations 1, 5; Tandem peepers at station 2	Stations 1, 2, 3, 4, 5
Winter	Stations 1, 2, 3, 6 Cores at station 1 and 6	Stations 1, 2, 3, 4
Spring	Tandem peepers at station 1	Stations 1, 2, 4, 6

III. SAMPLING AND METHODS

3.1 Sampling

3.1.1 Water Column

During ice-free conditions, all sampling of the lake water column and sediments, as well as peeper deployment, was carried out from a free-floating surface platform powered by a 9.9 Hp outboard. The deck provided approximately 12 m² working area, a sufficiently large area to accommodate a gas generator, winch, a peristaltic pump, a nitrogen gas cylinder, and permanent attachment of a nitrogen glove bag containment structure. Gravity cores, surface grabs and water column samples were drawn through a 3 m² hatch in the platform centre. Four 20 kg anchors maintained position at any given site. Winter sampling was carried out through 30 cm holes augered through the ice.

Water column samples were drawn from the lake using a "Masterflex" peristaltic pump (Cole-Palmer Instrument Co., Chicago, IL) and sampled directly in a nitrogen-filled glove-bag. Three litres were taken at each sampled depth, placed in a cooler, and taken immediately to the lab for filtration. One litre, to be analyzed for dissolved and particulate metal fractions, was filtered through an acid-cleaned, pre-weighted Nuclepore[®] 0.45 µm polycarbonate membrane filter using nitrogen overpressure, acidified to pH 2 with nitric acid (Seastar Chemicals), and stored in acid-cleaned polyethylene bottles. The remaining two litres were filtered through a 0.4 µm precombusted Glass Fibre filter using nitrogen overpressure for determinations of suspended particulate organic carbon (SPOC) and nitrogen (SPON). Ammonium concentrations were

determined from the filtrate spectrophotometrically on site; the remainder was frozen for subsequent analyses of nitrate, phosphate and sulphate.

3.1.2 Physical Profiling

Hydrographic profiling of temperature, dissolved oxygen and pH was performed using a Cole Palmer water analyser (model 5150). Profiles were collected by slowly lowering the probe to desired depths and allowing the electrodes and thermistor to equilibrate before proceeding to the next depth. During periods of stratification, higher resolution profiling was attained across the depth of the pycnocline. Profiles were obtained commensurate with water column sampling in order to be temporally consistent. For both ice-free and ice-covered sampling periods, all hydrographic profiling was performed at least 5 m away from the point of water column sampling to minimize potential contamination and water column disturbance in the vicinity of the sampler. The oxygen electrode was calibrated in the field on a daily basis while calibration of the pH sensor was performed in the lab.

3.1.3 Porewaters

The diagenetic cycling of metals in the sediments, and their exchange with the overlying water column was assessed by high resolution sampling of the interstitial and bottom waters using dialysis arrays. Diffusion sampling of sediment porewaters has become widely used since their initial application by Hesslein (1976) and Mayer (1976). Due to lower requirements of processing time and equipment, dialysis methods offer a suitable alternative to squeezing and

centrifuging techniques. Samplers typically consist of plastic sheets machined with compartments down their length which are filled with DDW and covered with a semi-permeable membrane; upon insertion into the sediments, the samplers are allowed to approach diffusive equilibrium with the adjacent porewaters. *In situ* dialysis has been shown to be particularly well suited to the study of trace constituents in sedimentary porewaters under field conditions (Carignan *et al.*, 1985) and has been successfully implemented in studies of Canadian Shield Lakes (Carignan and Nriagu, 1985; Carignan and Tessier, 1985a; Gaillard *et al.*, 1986).

Potential artifacts are inherent to the spectrum of interstitial water sampling techniques. Methods such as squeezing and centrifugation followed by filtration, for example, are prone to effects resulting from sample oxidation and temperature variations (Bischoff *et al.*, 1970). Diffusion techniques share a similar susceptibility to potential sources of error including the type of membrane used, construction material, dialyzer design, equilibration time and sampler preparation (Carignan, 1984; Carignan *et al.*, 1985; Brandl and Hanselmann, 1991; Carignan *et al.*, 1994).

Knowledge of the permeability characteristics of each membrane type, its sorptive properties for chemical compounds and microorganisms, and its resistance to microbial degradation are essential to the application of diffusion samplers and determination of optimal incubation times. A review by Brandl and Hanselmann (1991) determined from a study of 13 different membranes that cellulose-based dialysis membranes were the best choice in lake sediments at low temperatures. The cellulose membranes tested, however, exhibited marked weight losses due to microbial degradation when incubated at elevated temperatures (~28 °C). Martens and Klump (1980) also observed some physical breakdown of cellulose-based membranes. A digestible membrane polymer

could easily produce false porewater compositions due to a weakening of membrane stability, changes in membrane permeability or blockage of membrane pores. In consideration of warm water conditions ($>20\text{ }^{\circ}\text{C}$) characteristic of Balmer Lake in the summer and fall, such membranes were excluded from this study. In its place, a Gelman (HT-450) polysulfone membrane was chosen for its mechanical stability and resistance to microbial attack. The suitability of such a dialysis system has been validated in several examinations of lake porewaters (Carignan, 1984; Carignan *et al.*, 1985; Gaillard *et al.*, 1986; Carignan *et al.*, 1994).

In some peeper preparations, a thin Nuclepore polycarbonate membrane ($0.2\text{ }\mu\text{m}$) was used in conjunction with the Gelman membrane to provide a better seal. Most samplers, however, were prepared solely with a $0.45\text{ }\mu\text{m}$ Gelman polysulfone sheet. For measurements of porewater constituents, Carignan *et al.* (1985) showed that profiles obtained with a dual $0.45\text{ }\mu\text{m}$ (polysulfone) + $0.03\text{ }\mu\text{m}$ (polycarbonate) membrane system were not significantly different from those obtained with a $0.45\text{ }\mu\text{m}$ membrane alone. This result suggests that the Brownian diffusion of colloidal metal species through relatively large pores of $0.45\text{ }\mu\text{m}$ is unlikely

3.1.3.1 Peeper Description and Preparation

The dialyzers implemented in this study are similar in design to that of Hesslein (1976) and consist of $120 \times 20 \times 2.3\text{ cm}$ Plexiglas plates with two rows of chambers, each $6.5 \times 0.7 \times 0.7\text{ cm}$, machined in at 1.25 cm intervals, centre to centre (Fig. 3-1). This scheme is interrupted by a 20 cm section containing 31 chambers, each $3.5 \times 0.7 \times 0.7$, spaced at 0.625 cm intervals. This zone is intended to coincide with the sediment-water interface upon deployment and provides

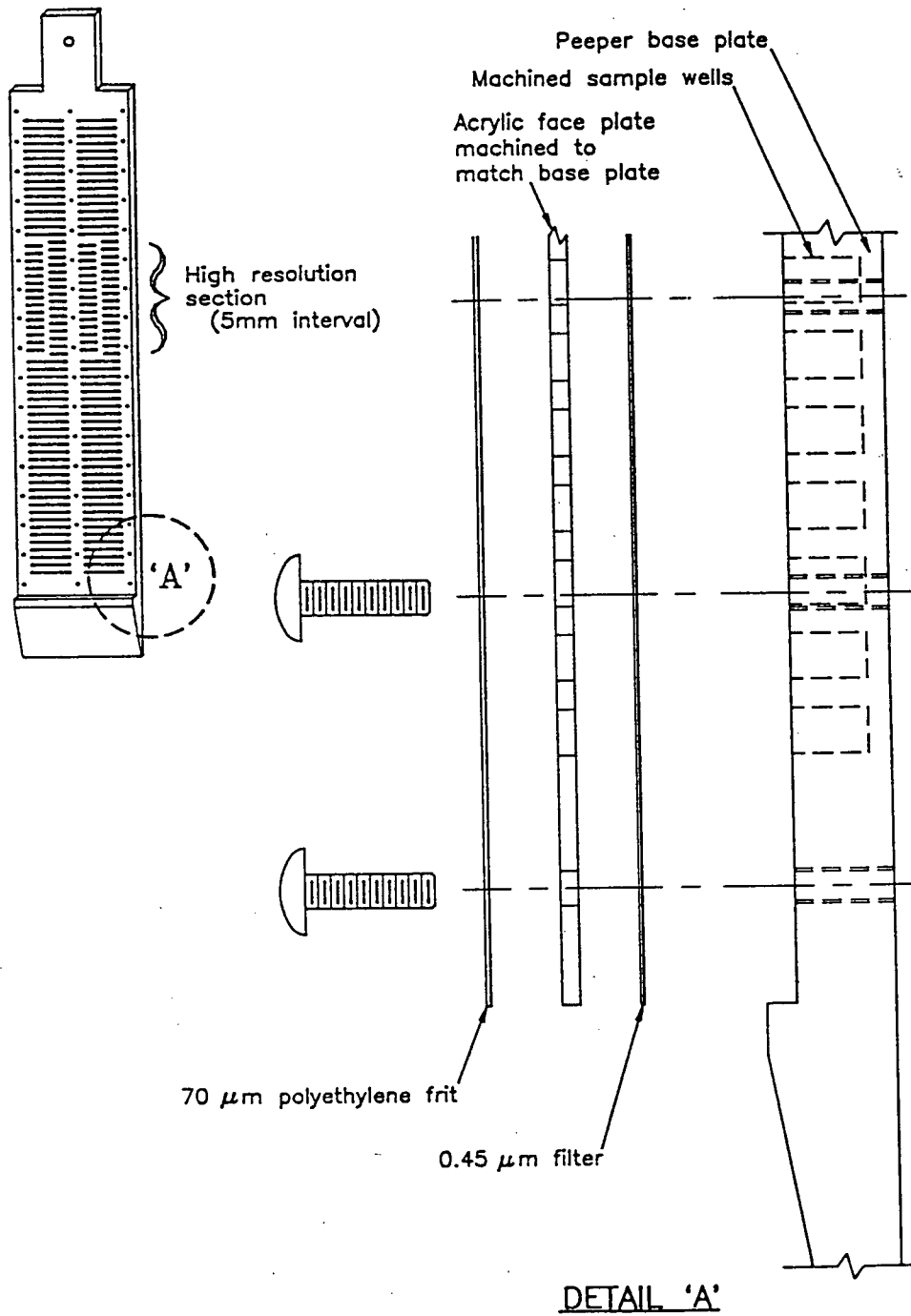


Figure 3.1. Schematic diagram of membrane dialysis sampler (peeper).

greater resolution in the surficial sediments and bottom waters. The peeper design affords high resolution pore water and bottom water profiles of the dissolved constituents from 40 cm above the sediment-water interface to a sediment depth of 50 cm. A membrane filter arrangement positioned between the chamber and face plates was implemented to facilitate dialysis and preclude the entrance of particulates (Fig. 3.1). In addition, the exterior surface of the face plate was fitted with a polyethylene frit to provide a coarse filtering screen, facilitate easier insertion and thus minimize sediment disturbance. Three rows of nylon screws positioned at 4.5 cm spacing down the peeper securely fastened the frit, face plate and filters to the chamber plate.

Peeper preparation and assembly was performed at U.B.C. prior to shipment to the study site. The peepers and their Plexiglas cases were first washed in a mild detergent (Isoclean, ISOLAB Inc, Akron Ohio) followed by several rinses in DDW. The components were then soaked in dilute ultrapure HNO₃ (Seastar Chemicals) followed by several 24 h soaks in DDW to remove any residual contaminants and acid. Other than serving as nitrogen flushing sleeves, the plexiglass cases served as sturdy transport containers and provided a sterile transport environment. The Nuclepore and Gelman membranes received a dilute soak in ultrapure HNO₃ and several rinses in DDW.

Peeper assembly was carried out in a laminar flow hood (class 100) in a shallow plexiglass tank of deoxygenated, distilled, deionized water (DDDW). The chamber plate was first submersed, and then using a clean pipette tip, all bubbles on the acrylic surface were dislodged. Two peeper membrane configurations were utilized. The first consisted of a twin membrane arrangement of a Nuclepore filter (polycarbonate, 0.2 μm poresize) overlain by a Gelman HT-450 filter (polysulfone, 0.45 μm poresize). The second arrangement consisted of only a 0.45 μm Gelman filter membrane. Upon placement of the

filter membrane(s) on the chamber plate, the acrylic face plate and polyethylene frit (70 μm pore size) were placed appropriately and securely fastened with 51 nylon screws. The assembled peepers were stored in sealed acrylic cases containing DDDW bubbled with nitrogen until deployment. All peeper flushing cases were purged with nitrogen for approximately 48 hours before transport and for a further 24 hours prior to deployment.

Carignan *et al.* (1994) have recently brought attention to potential effects of free oxygen liberated from acrylic samplers. The presence of such oxygen traces could introduce an artifact by reacting with ferrous iron which may diffuse into peeper cells after deployment and perhaps precipitate as $\text{Fe}(\text{OH})_3$. Carignan observed that acrylic (Plexiglas) in equilibrium with the atmosphere can absorb 1.6% (vol/vol) O_2 that is lost slowly (half-time ~ 5.7 d) once the material is exposed to anoxic conditions. This translated into significant differences in the observed porewater distributions of total Fe, Fe^{2+} , dissolved reactive P, and SO_4^{2-} between those samplers conditioned by a 30-d exposure to N_2 before deployment and those that received an 18-h bubbling in N_2 (Carignan *et al.*, 1994). This phenomenon was originally described by Carignan (1984), who observed an orange discolouration on peepers deployed in anoxic sediments. The peeper preparation in this study included flushing periods greater than 72 h and suggests the potential for post-deployment releases of oxygen is minimal.

3.1.3.2 Peeper Deployment and Subsampling

Each sampling session involved the deployment of four peepers at various sites within the lake. Peeper deployment for the first sampling period was achieved via diver insertion; peepers were pushed vertically into the sediments to a specified depth marked on the acrylic surface. Each sampler was marked via

a 6 m slack line from the peeper to a 20 kg anchor and a line from the anchor to a surface float. Subsequent peeper deployments and retrievals during ice-free periods were performed using weighted aluminum "landers". These cube-shaped support structures (1 m x 1 m x 0.8 m) remained *in situ* during the equilibration period with the peeper attached and ensured vertical insertion to a specific sediment depth. During the winter sampling period, peepers were fixed to 5 m long teflon-coated pipes and pushed vertically into the sediments through augered holes in the ice surface. A 1 m long peg attached horizontally to the pipe and placed flush with the ice ensured a correct insertion depth and maintained the position of the pole over the deployment period.

All peepers were allowed to equilibrate for at least 14 days. The most important factors determining the equilibration time are the diffusion coefficient of the constituent, its sorptive properties, and the temperature and porosity of the sediments (Carignan, 1984). Carignan determined that for the porosities observed in recent lake sediments, equilibration periods of 15 days for warm (20°–25° C) and 20 days for cold (4°–6° C) appear to provide sufficient incubation.

Peeper removal and subsampling occurred on a daily basis, with one peeper being removed per day. Upon retrieval, each peeper was brought to just below the lake surface, briefly agitated to dislodge adhering particulates, transferred to the boat and immediately placed in a nitrogen-purged sleeve for transport to the lab. The former procedures took less than 2 minutes. Peepers were subsequently processed in a nitrogen-filled glove bag and involved the careful removal of nylon screws, frit and face-plate, followed by the removal of the 0.45 µm Gelman filter (when used in tandem with the 0.2 µm polycarbonate membrane). Each peeper was then subsampled by direct puncturing of the filter membrane with an Eppendorf pipettor and acid-washed pipette tips. The dual

row chamber arrangement of the peepers allowed one row to be subsampled for metals while the other for nutrients and sulphate. Direct probe insertion into chambers at selected depths allowed for measurements of porewater pH. Samples to be analyzed for dissolved metals, nutrients and sulphate were treated as described above for the water column protocol. Sample extraction and partitioning was accomplished within 2 hours of peeper retrieval.

3.1.4 Sediment Sampling

Coring was performed during the winter survey as it was hoped that the stable ice platform would facilitate the acquisition of high quality cores. Three such cores with well-defined sediment-water interfaces were collected through augered holes in the ice by lowering a light-weight gravity corer (Pedersen *et al.*, 1985) suspended from a metre-block and tripod. Cores were carried by hand to the lab and immediately processed.

Cores were first logged and then firmly attached to the underside of an extrusion table fitted with a nitrogen-filled glove-bag. The core was extruded through a hole in the center of the table and carefully sectioned; core slices were placed in acid-washed 250 mL high-density polyethylene (HDPE) centrifuge bottles and spun at ~1,200 gravities for 20 minutes at which point they were transferred to an additional nitrogen-filled glove bag for decantation of the interstitial waters and filtration. Supernatant water from the centrifuged sample was decanted into an acid-washed 50 mL disposal polypropylene syringe fitted with an acid-washed Syfril 0.45 μm mixed cellulose acetate disposable filter. An acid-washed polyethylene piston was utilized to express the interstitial solution through the filter and into an acid-washed HDPE sample bottle. The remaining

filtrate was passed through a 0.1 µm disposable filter and acidified to pH 2 with ultra-pure nitric acid (Seastar Chemicals). Sediment samples were bagged and frozen until analysis.

3.2 Instrumentation

3.2.1 ICP/MS

A VG "PQ Turbo Plus" inductively-coupled plasma mass spectrophotometer (ICP/MS) (VG Elemental, Surrey, UK) was used for the determination of the concentrations of Mn, Ni, Cu, Zn, As and Pb. Data analyses were handled by a Dell 486 computer equipped with PQ vision 4.1.1 software. Pure (99.998 %) ICP-grade argon (Medigas, Vancouver, B.C.) was used as the plasma and carrier gas. A Rheodyne 6 port flow injection system (Mandel Scientific, Guelph, Ont.), positioned between the peristaltic pump and the nebulizer, was used to facilitate small sample volumes.

Operating conditions of the ICP/MS were optimized daily to obtain maximum sensitivity. Resolution and peak shape were optimized using a solution containing 10 ppb Co, In, Pb and Bi. Sample analyses were performed using pneumatic nebulization (de Gallen v-grove glass nebulizer). The instrument was run in a multichannel peak jump mode with a 10 milli-second dwell time, one point per peak and a 20 second acquisition time. The concentrations of the respective metals were calculated using a linear calibration curve derived from certified metal standards. A 10 ppb In internal standard was applied to all samples, standards and blanks to correct for sensitivity variations during analyses. Typical operating conditions are outlined in Appendix A.

3.2.2 GFAAS

Graphite furnace atomic adsorption spectroscopy (GFAAS) was performed using a Varian Spectra AA300 with a Zeeman background correction to determine Fe concentrations in the water column and porewaters. All determinations were conducted using L'Vov platforms. Concentrations were calculated from linear calibrations derived from certified metal standards using instrumental parameters suggested by the manufacturer.

3.2.3 Ion Chromatography

Determinations of porewater and water column concentrations of nitrate and sulphate were performed using a DIONEX DX-100 ion chromatograph. The system provided efficient isocratic separation of the respective inorganic anions using a 1.8mM Na₂CO₃/ 1.7 mM NaHCO₃ eluent in conjunction with an IonPac[®] AS12A anion exchange column and a ASRS-1 anion self-regenerating suppressor.

3.2.4 X-ray Fluorescence

An aliquot of each freeze-dried sediment sample was ground in a tungsten carbide disc mill prior to preparation for X-ray fluorescence, C-N-S and coulometric analyses. Metal concentrations were determined in the solid phase by X-ray fluorescence spectrometry using pressed powders and glass discs for minor and major elements, respectively. Calibration procedures and precision estimates for most elements were very similar to those reported by Calvert *et al.* (1985) with the exception that the calibration range for As was extended by

making artificial standards spiked with known weights of As_2O_3 . A linear calibration was obtained for As up to a maximum concentration of 5000 ppm. Accuracy of the elemental analyses was monitored by including aliquots of the standard sediment powders MESS-1, BCSS-1, PACS-1 with each batch of samples.

3.2.5 Coulometry

Carbonate carbon was determined photometrically in a Coulometrics Inc. 5010 coulometer. Precision, as the relative standard deviation, was $\pm 3.7\%$. Reagent-grade CaCO_3 was used to assess routinely the accuracy of the coulometer.

3.2.6 Carbon, Nitrogen and Sulphur

Total C, N and S of sediments and suspended particulates were determined by combustion/gas chromatography using a Carlo-Erba (NA-1500) elemental analyser. Precisions were ± 0.6 , 3.5 and 3.5 % (1 σ rsd), respectively. Organic carbon was obtained from the difference between the total and carbonate carbon values (combined 1 σ rsd = 1.9 %).

3.2.7 Spectrophotometry

Water column and porewater ammonium concentrations were determined spectrophotometrically similar to the alternative method outlined by Parsons *et al.* (1984). Ammonia reacts with phenol in an alkaline citrate medium with

sodium nirtoprusside added as a catalyst and forms blue indophenol. The absorbance is then measured at 640 nm.

3.2.8 Digestion of Polycarbonate Filters

Polycarbonate membranes were placed in pre-weighed 5 mL teflon vials and oxidized at 80°C with 1 mL of ammonia (Seastar Chemicals). After being dried down (80°C), 0.5 mL each of HCl, HF and HNO₃ (Seastar Chemicals) were added and microwave-digested for 45 minutes at 60 PSI. After being dried down once again, the digest was brought up in 250 µL HNO₃ and diluted to approximately 4 mL. ICP-MS was used to determine the concentrations of Mn, Ni, Cu, Zn, As and Pb. Total Fe concentrations were determined via GFAAS.

IV. RESULTS

Results for the water column, interstitial waters and sediment components of the Balmer Lake survey are presented in this chapter. The quality assurance and quality control (QA/QC) for all measured parameters was excellent (Appendix B). Values obtained for field blanks, field replicates, laboratory blanks, laboratory replicates and reference materials all met acceptable criteria.

4.1 Water Column

4.1.1 Physical Profiling

Hydrographic data of temperature and dissolved oxygen suggest that the water column of Balmer Lake maintains fairly well-mixed conditions during ice-free periods. The first sampling period in the summer of 1993 was chosen to coincide with a stratified water column, since stratification is common to many temperate lakes in the summer months. Basic hydrographic data, however, revealed fully oxygenated bottom waters and invariant temperature and pH profiles (Fig. 4.1). Temperatures ranged from 16-18 °C while dissolved oxygen concentrations ranged from 7-9 mg/L. Profiling of pH revealed a slightly acidic to slightly basic water column with values ranging from 6.2 to 7.8 pH units. The overall homogeneity was probably a result of the common windy conditions and the resultant mixing of the shallow water column (~4 m deep). Fall sampling took place subsequent to convective overturn and was also characterized by a well-mixed water column. Cooler water temperatures (~2-3°C) and higher dissolved oxygen concentrations (10-12 mg/L) were evident (Fig. 4.2). A pH

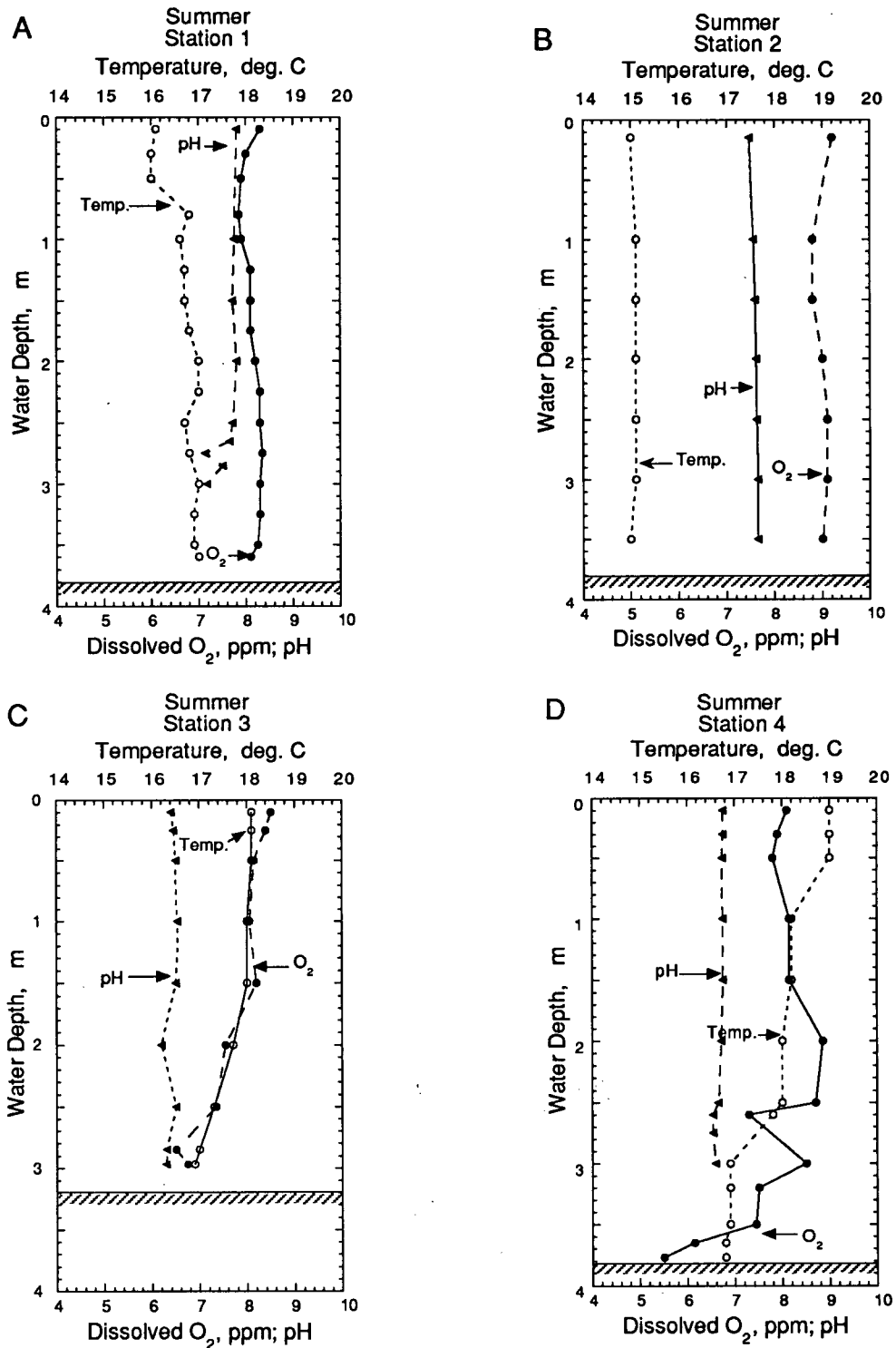


Fig. 4.1 Summer water column profiles of temperature, dissolved oxygen and pH for stations 1, 2, 3 and 4 (A-D, respectively), Balmer Lake, June, 1993. The hatched line represents the sediment surface.

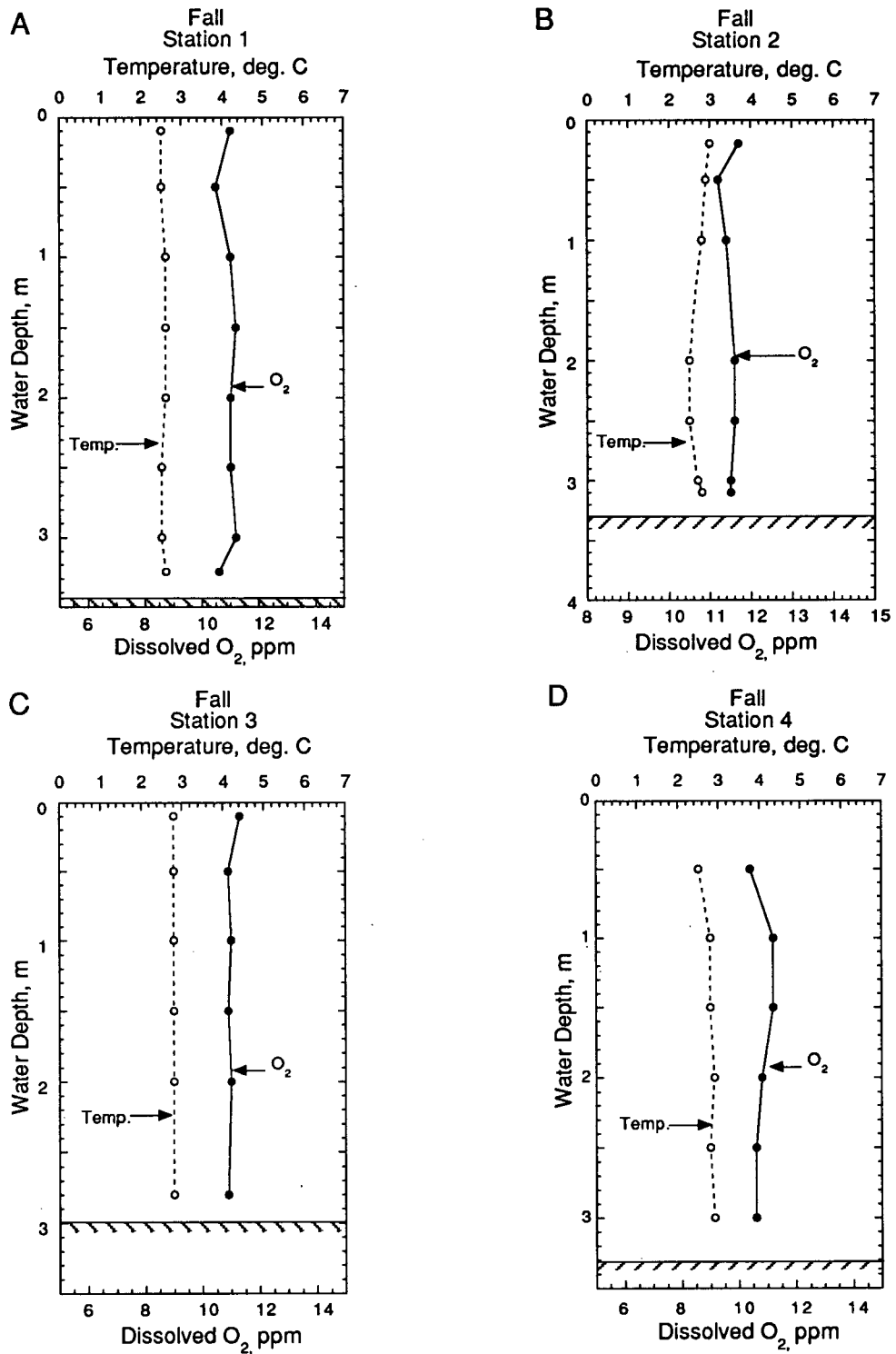


Fig. 4.2 Fall water column profiles of temperature and dissolved oxygen for stations 1, 2, 3 and 4 (A-D, respectively), Balmer Lake, October, 1993. The hatched line represents the sediment surface.

meter was unavailable for the fall and winter field sessions, and as a result, such data are absent.

Winter profiling near the end of the ice-over period indicated a moderately stratified water column at the stations sampled (Fig. 4.3). Temperatures increased gradually from 0 °C immediately below the ice (~1 m thick) to 3-4 °C in the bottom waters. Conversely, dissolved oxygen levels decreased quickly in the lowermost half metre from approximately 5-7 mg/L to below detection limits 10-30 cm above the sediment surface (Fig. 4.3). However, at the shallowest station (station 3, 2.6 m depth) only a slight basal oxygen depletion was observed during this period (Fig. 4.3). The early-spring sampling, conducted less than two weeks after ice-off, revealed the reoccurrence of a well-mixed water column (Fig. 4.4). Constant profiles of temperature (9.5-10.5 °C) and dissolved oxygen (8-9 mg/L) were evident. Profiling of pH revealed a neutral to slightly basic water column with values ranging from 7.0-7.7 pH units.

4.1.2 Nitrate, Ammonium and Sulphate

Variations in lake-wide average concentrations of nitrate, ammonium and sulphate closely parallel one another throughout the seasonal sampling periods. For all three ions, the seasonal hierarchy of mean concentrations follows the order winter > spring > summer ≥ fall. The well-mixed water column and well-oxygenated bottom waters characteristic of the summer and fall field sessions, are consistent with the uniform profiles of dissolved constituents measured during these periods. Stations sampled during the summer period exhibited constant depth profiles of nitrate and sulphate with lake-wide values averaging

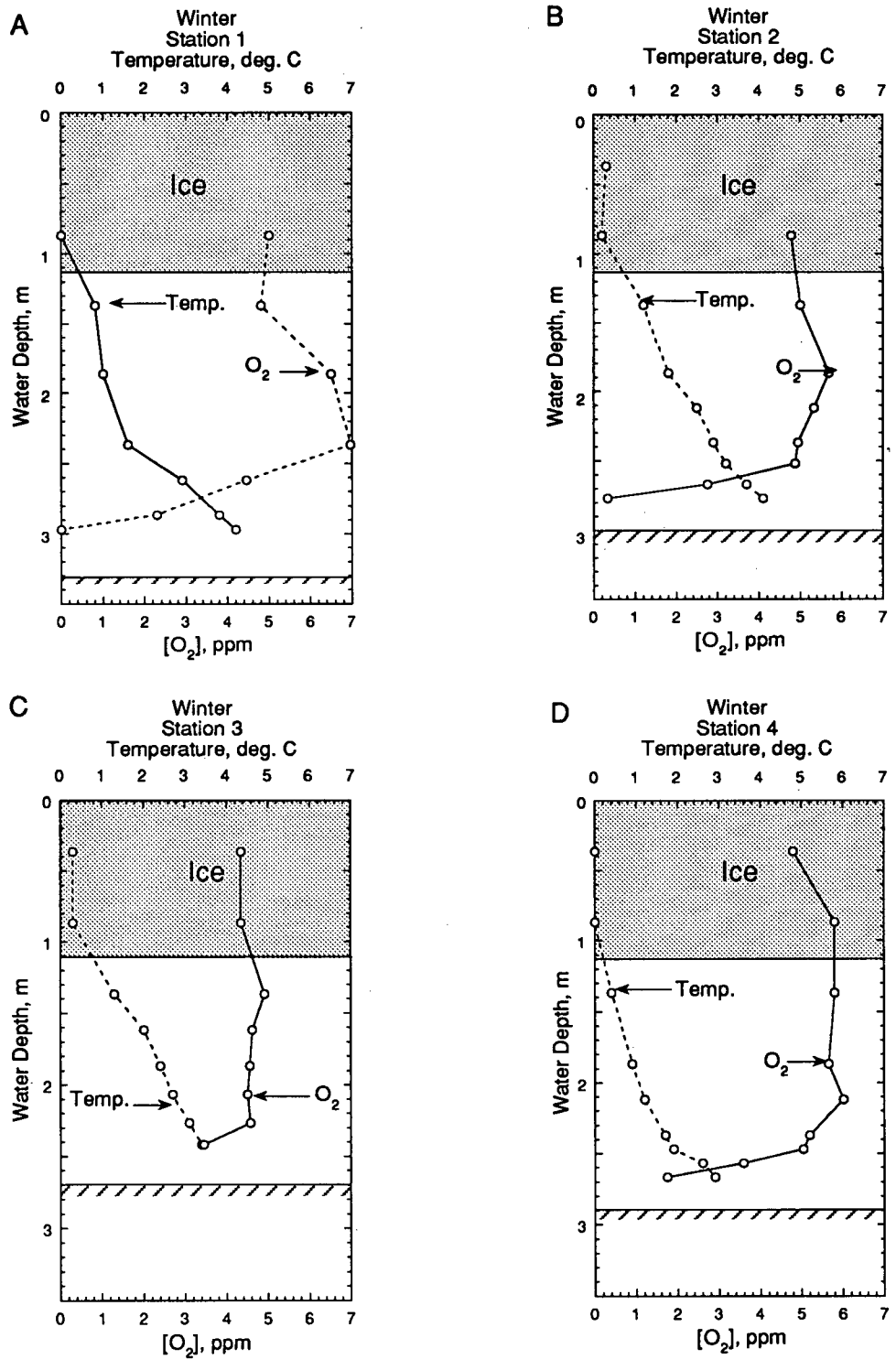


Fig. 4.3 Winter water column profiles of temperature and dissolved oxygen for stations 1, 2, 3 and 4 (A-D, respectively), Balmer Lake, March, 1994. The hatched line represents the sediment surface.

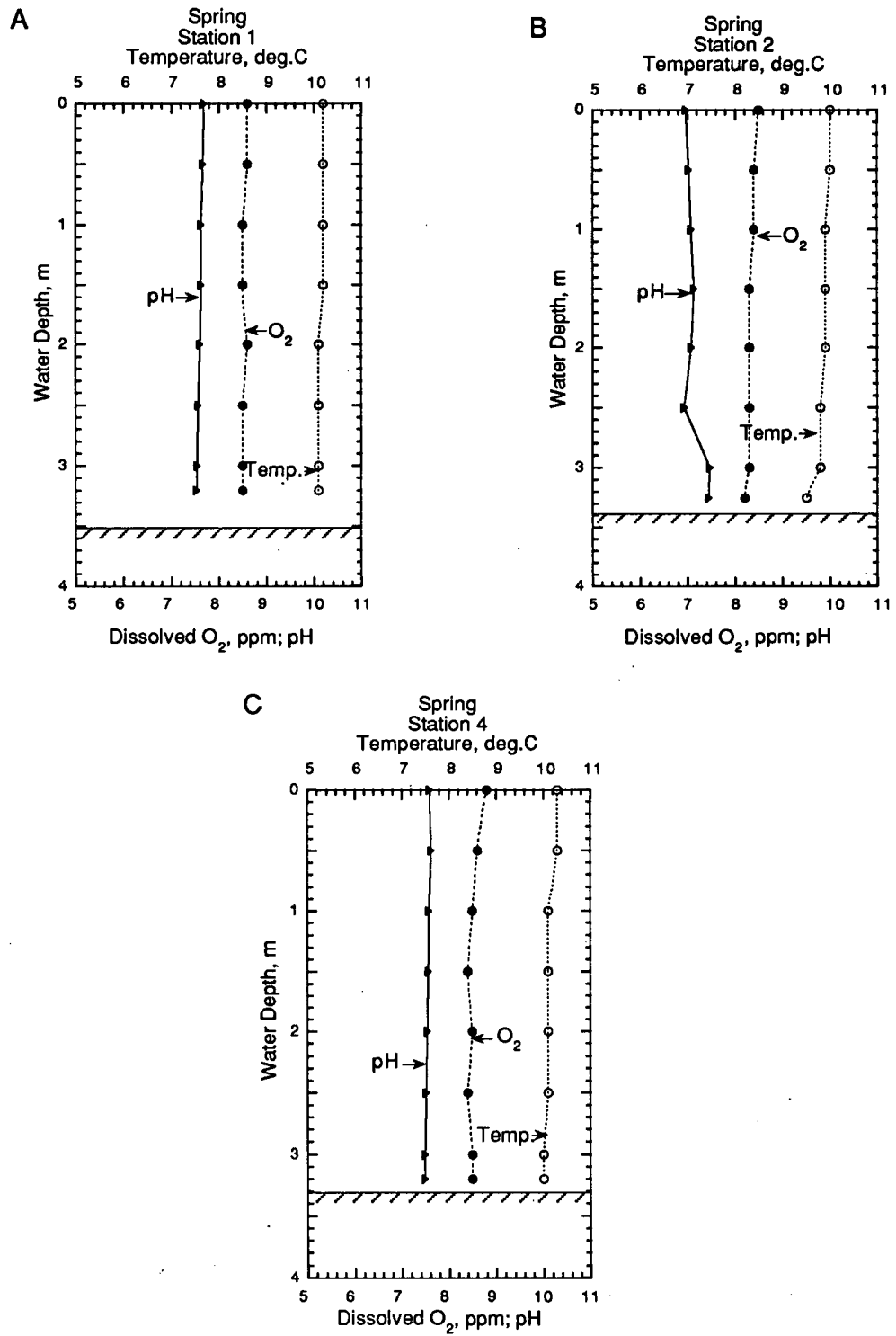


Fig. 4.4 Spring water column profiles of temperature, dissolved oxygen and pH for stations 1, 2 and 4 (A-C, respectively), Balmer Lake, May, 1994. The hatched line represents the sediment surface.

330 $\mu\text{mol/L}$ (274-342) and 3.30 mmol/L (2.69-3.45), respectively (Table 4.1). Ammonium was fairly uniformly distributed in the surface waters, with values ranging from 86-123 $\mu\text{mol/L}$ (Table 4.1). Depletions of ammonium with depth were evident for stations 2 and 3, where bottom water concentrations were approximately 60 % of their respective surface values (Table 4.1). At all sites and depths, phosphate concentrations remained below detection limits (~ 1 $\mu\text{mol/L}$). Significant decreases in average ammonium concentrations were evident over the summer-fall transition with average lake values falling from 94 to 50 $\mu\text{mol/L}$ (Table 4.2). Water column nitrate and sulphate contents during the fall period remained consistent with the summer season and averaged 312 $\mu\text{mol/L}$ (292-346) and 3.41 mmol/L (3.32-3.69), respectively (Table 4.2). As seen for the summer period, phosphate concentrations were not detectable throughout the water column.

The major ion distributions observed during the winter period show distinct relationships to the stratification indicated by the temperature and oxygen data (Table 4.3; Figs. 4.5 -4.7). Nitrate removal in the suboxic to anoxic bottom waters, and/or in shallow sediments, results in pronounced depletions at all stations 40-60 cm above the sediment-water interface (Table 4.3; Fig. 4.5). Sub-ice nitrate values averaging 415 $\mu\text{mol/L}$ (372-435) decline to minima of 16 to 80 $\mu\text{mol/L}$ in the bottom waters. Less significant reductions in nitrate concentrations are observed in the 'deep' waters at shallow station 3, where values decrease to ~ 175 $\mu\text{mol/L}$ (Fig. 4.5C). A large increase in the inventory of ammonium was evident during the winter sampling period (Fig. 4.6); contents in bottom waters at all locales except station 4, ranged from 260 to over 500 $\mu\text{mol/L}$. Ammonium values were not obtained below 2.6 m at station 4, and as a result, the presence or absence of a bottom water increase was not determined.

Table 4.1. Summer water column distributions of dissolved Mn, Fe, Ni, Cu, Zn, As, Pb, NH₄⁺, NO₃⁻, SO₄²⁻ and PO₄³⁻ for stations 1, 2, 3, and 4 in Balmer Lake, Ontario, June 1993. All values are expressed in µg/L unless specified otherwise (BDL denotes below detection limits).

Station	Depth, m	Mn	Fe	Ni	Cu	Zn	As	Pb	NH ₄ mM	NO ₃ mM	SO ₄ mM	PO ₄ mM
1	0.5	271	35	387	164	46	282	0.4	128	327	3.32	BDL
	2	287	41	405	170	49	288	0.4	128	329	3.19	BDL
	2	285	43	409	168	50	286	0.3	130	326	3.28	BDL
	3.5	282	39	399	171	59	286	0.3	128	327	3.26	BDL
2	0.1	281	38	406	172	45	276	0.4	86	362	3.38	BDL
	1	277	43	403	173	48	277	0.6	70	331	3.39	BDL
	2	274	46	409	172	48	286	0.6	77	274	2.69	BDL
	2	275	51	411	175	50	283	0.4	75	294	2.87	BDL
	3	300	50	437	181	56	293	0.7	77	337	3.44	BDL
	3.6	289	39	420	179	60	290	0.4	55	313	3.15	BDL
3	0.5	282	47	423	172	46	285	0.4	99	335	3.35	BDL
	2	280	35	400	175	48	287	0.3	68	341	3.38	BDL
	2	282	35	405	179	48	289	0.4	70	342	3.42	BDL
	2.8	292	58	411	169	52	288	0.4	59	337	3.25	BDL
4	0.5	287	35	407	175	45	290	0.5	103	338	3.45	BDL
	0.5	289	32	410	175	46	288	0.5	105	342	3.43	BDL
	2	289	39	411	169	48	292	1	103	332	3.32	BDL
	3.5	286	44	418	173	52	289	0.4	91	337	3.34	BDL
	3.5	284	39	421	175	54	290	0.4	91	332	3.31	BDL

Table 4.2. Fall water column distributions of dissolved Mn, Fe, Ni, Cu, Zn, As, Pb, NH₄⁺, NO₃⁻, SO₄²⁻ and PO₄³⁻ for stations 1, 2, 3, 4 and 5 in Balmer Lake, Ontario, October, 1993. All values are expressed in µg/L unless specified otherwise (BDL denotes below detection limits).

Station	Depth, m	Mn	Fe	Ni	Cu	Zn	As	Pb	NH ₄ µM	NO ₃ µM	SO ₄ mM	PO ₄ µM
1	0.5	161	94	262	114	63	203	0.4	45	302	3.33	BDL
	2	165	95	262	112	59	207	0.5	51	309	3.38	BDL
	2	170	92	260	110	60	208	0.4		299	3.32	BDL
	3	171	88	265	114	55	210	0.3	56	307	3.42	BDL
2	0.5	171	89	278	121	48	214	0.3	51	346	3.44	BDL
	1.5	158	93	273	121	63	208	0.3	49	310	3.41	BDL
	3	166	101	269	119	47	211	0.4	48	311	3.36	BDL
3	0.5	186	79	281	121	63	203	0.5	55	317	3.47	BDL
	0.5	180	90	283	124	58	203	0.5		306	3.46	BDL
	1.5	185	84	283	123	59	207	0.6	55	313	3.42	BDL
	1.8	196	99	288	126	55	210	0.5	56	292	3.42	BDL
4	0.5	181	94	279	124	40	214	0.3	46	307	3.38	BDL
	0.5	182	89	282	118	45	219	0.2	48	316	3.52	BDL
	1.5	183	97	284	122	65	217	0.4	45	316	3.45	BDL
	1.5	182	90	280	125	62	215	0.4		338	3.40	BDL
	3	180	88	275	112	56	210	0.4		307		BDL
5	0.1	227	98	312	130	124	242	0.3		300	3.62	BDL
	0.1	203	88	300	101	59	235	0.3		304	3.69	BDL

Table 4.3. Winter water column distributions of dissolved Mn, Fe, Ni, Cu, Zn, As, Pb, NH₄⁺, NO₃⁻, SO₄²⁻ and PO₄³⁻ for stations 1, 2, 3 and 4 in Balmer Lake, Ontario, March, 1993. All values are expressed in µg/L unless specified otherwise (ND denotes not determined). Note that replicate samples were collected at a number of depths at all stations.

Station	Depth, m	Mn	Fe	Ni	Cu	Zn	As	Pb	NH ₄ µM	NO ₃ µM	SO ₄ mM	PO ₄ µM
1	1.0	404	170	455	294	83	337	0.6		372	4.94	ND
	1.0	396		438	285	84	343	0.6				
	2.0	285	158	432	274	68	384	0.5	121	409	5.19	ND
	2.3	299	147	473	331	63	358	0.2	133	415	5.17	ND
	2.3		151									
	2.5	306	141	474	301	67	338	0.1	125	418	5.31	ND
	2.8								245			
	2.8	504	73	502	177	130	199	0.3	251	288	8.09	ND
	3.0	926	76	532	52	149	260	0.1	446	174	13.79	ND
	3.0									173		
	3.2	972	48	554	46	158	283	0.2	502	16	12.04	ND
	3.2	1043	52	578	46	161	289	0.4				
	2	1.0	312	131	523	450	68	386	0.1	211	395	5.02
1.8		311	139	512	444	63	365	0.1	208	390	4.97	ND
1.8			133						211			
2.3		307	129	503	438	77	392	0.4	213	388	5.00	ND
2.5		275	134	425	289	64	346	0.3	190	379	5.09	ND
2.5		300		467	314	65	345	0.3				
2.7		312	115	407	216	63	270	0.2	214	282	4.92	ND
2.8		662	73	493	100	121	209	0.2	248	185	8.66	ND
2.9		978	119	503	58	178	282	0.6	406	82	11.63	ND
2.9		1015	133	532	59	180	298	0.4				
3	1.0	347	177	468	314	67	353	1.1	160	411	5.16	ND
	1.5	325	170	445	302	66	337	1.1	162	414	5.26	ND
	1.8	348	175	471	307	74	354	0.3	158	420	5.32	ND
	1.8	334	173	457	287	61	324	0.9				
	2.0	358	167	487	310	67	349	0.9	160	385	5.20	ND
	2.0								162			
	2.2	362	165	525	328	65	349	0.4	170	407	5.18	ND
	2.2	369		539	320	64	345	0.3				
	2.4	342	160	524	388	67	381	0.3	198	394	5.13	ND
	2.6	667	152	451	382	135	410	0.4	263	175	4.93	ND

Station	Depth, m	Mn	Fe	Ni	Cu	Zn	As	Pb	NH ₄	NO ₃	SO ₄	PO ₄
4	1.0	322	154	466	235	73	331	0.1	94	379	4.95	ND
	1.0	291		427	221	71	319	0.3				ND
	1.5	295	150	416	208	75	317	0.3				
	1.5		158									
	2.0								89			
	2.0								89			
	2.5	315	140	461	240	73	324	0.2	91	425	5.27	ND
	2.6	326	148	494	320	87	357	0.4	118	436	5.38	ND
	2.7	362	156	528	346	87	367	0.2				
	2.7	341		500	310	79	333	0.2				
	2.8	674	129	429	149	132	310	0.4		48	6.55	ND

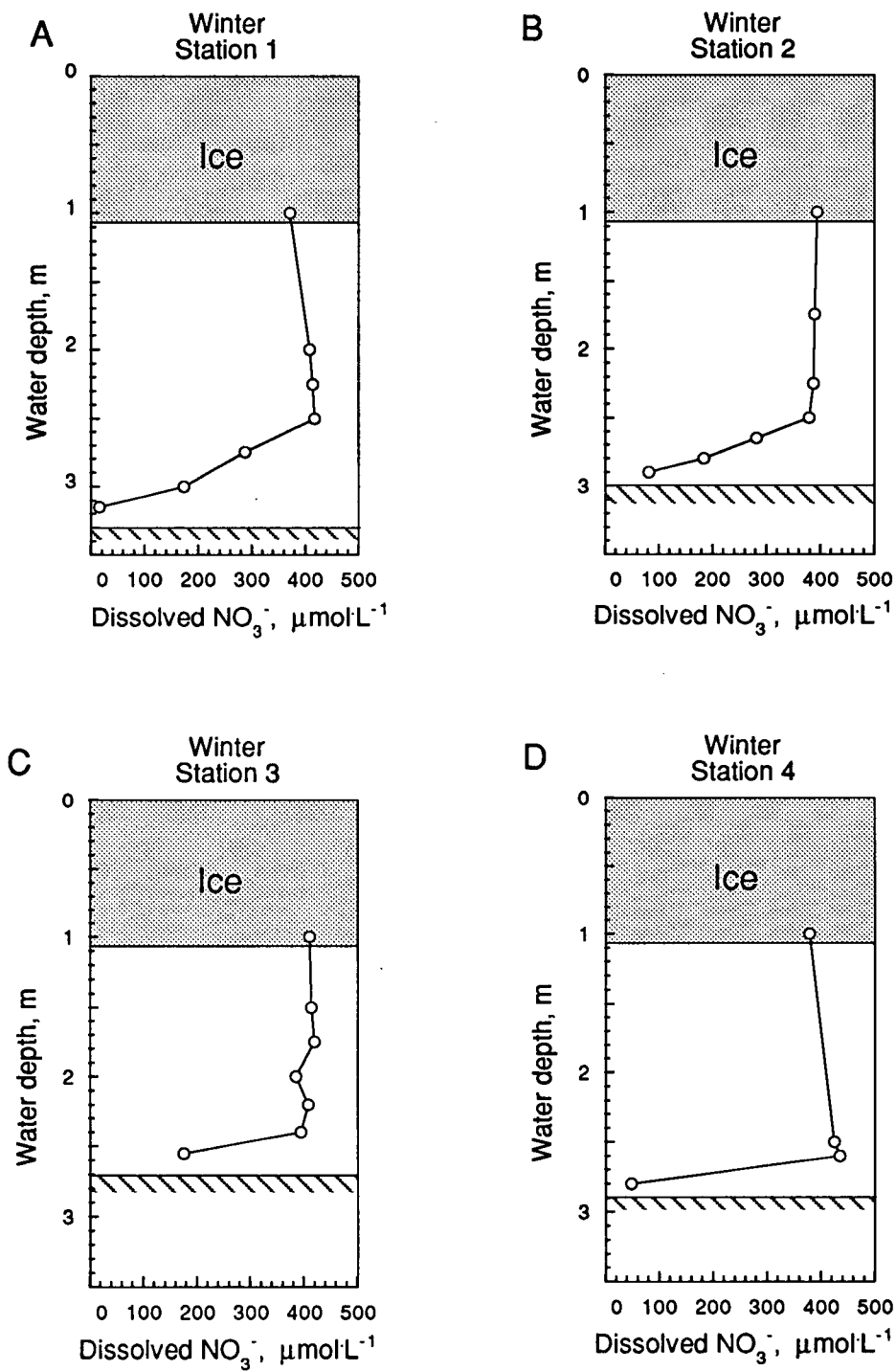


Fig. 4.5. Winter water column profiles of nitrate for stations 1, 2, 3 and 4 (A-D, respectively), Balmer Lake, March, 1994. Replicate samples are represented by double symbols at specific single depths. The hatched line represents the sediment surface.

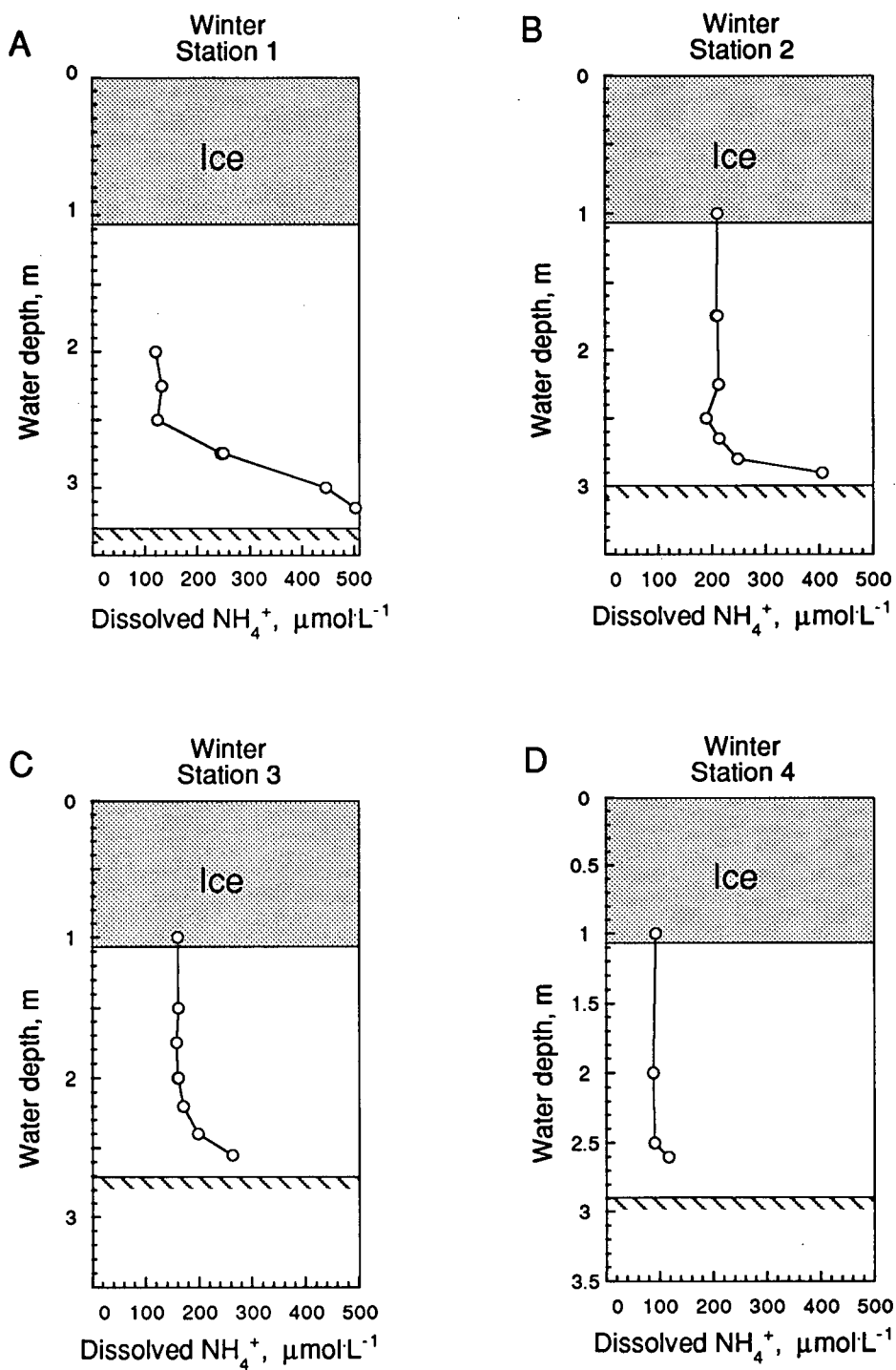


Fig. 4.6. Winter water column profiles of ammonium for stations 1, 2, 3 and 4 (A-D, respectively), Balmer Lake, March, 1994. Replicate samples are represented by double symbols at specific single depths. The hatched line represents the sediment surface.

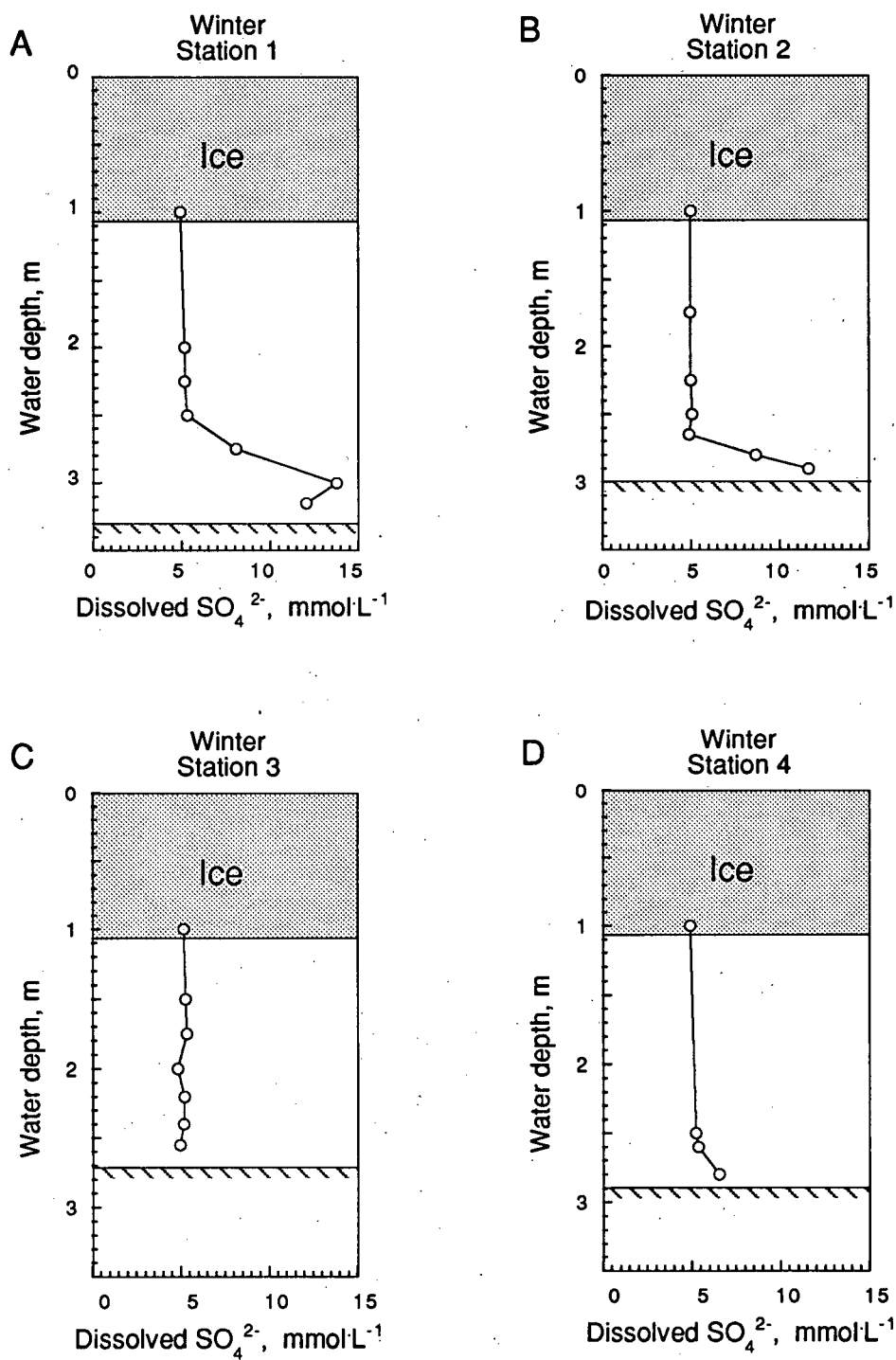


Fig. 4.7. Winter water column profiles of sulphate for stations 1, 2, 3 and 4 (A-D, respectively), Balmer Lake, March, 1994. Replicate samples are represented by double symbols at specific single depths. The hatched line represents the sediment surface.

The winter water column was also characterized by a significantly greater burden of sulphate, with values averaging 5.2 mmol/L immediately below the ice surface (Table 4.3; Fig. 4.7) . Pronounced bottom water enrichments of sulphate were observed at or below depths of 2.8 m throughout the lake (Fig. 4.7). In the deeper lake areas (stations 1 and 2), sulphate values increase to near 14 mmol/L at water depths greater than 2.9 m (Fig 4.7A-B).

During spring sampling, the concentrations of the major ions exhibited little lake-wide variation throughout the water column with values averaging 145 $\mu\text{mol/L}$ for NH_4^+ , 268 $\mu\text{mol/L}$ for NO_3^- and 3.47 mmol/L for SO_4^{2-} (Table 4.4). Due to analytical difficulties, phosphate concentrations were not determined for the winter and fall periods.

4.1.3 Suspended Organics

The seasonal water column concentrations of total suspended material (TSM), organic-C (SPOC), organic-N (SPON) and total particulate organic matter (POM) are shown in Table 4.5. A crude estimate of the particulate organic matter (POM) content was obtained from the relationship, $[\text{POM}] = 1.8 \times [\text{POC}]$ (Nriagu *et al.*, 1981). The TSM content of the water column exhibited negligible variability over the summer-fall-winter transition with values averaging 3.2-4.4 mg/L (Table 4.5). However, the winter water column was characterized by bottom water enrichments of total suspended solids at stations 1 and 4. Significant increases in the concentrations of suspended material were observed in the spring, during which values averaged 11 mg/L (Table 4.5). The fraction of suspended particulates represented by POM over the summer, fall, winter and spring varied considerably, with contributions averaging 47, 24, 26 and 14 %, respectively (Table 4.5). During the well-mixed periods of the summer, fall and

Table 4.4. Spring water column distributions of dissolved Mn, Fe, Ni, Cu, Zn, As, Pb, NH₄⁺, NO₃⁻, SO₄²⁻ and PO₄³⁻ for stations 1, 2 and 4 in Balmer Lake, Ontario, May, 1993. All values are expressed in µg/L unless specified otherwise (ND denotes not determined).

Station	Depth, m	Mn	Fe	Ni	Cu	Zn	As	Pb	NH ₄ µM	NO ₃ µM	SO ₄ mM	PO ₄ µM
1	1	301	86	428	220	59	224	1.1	136	252	3.25	ND
	2	284	86	403	210	87	223	0.9	141	268	3.47	ND
	3	299	85	428	223	57	225	1.3	142	275	3.46	ND
2	1	250	82	350	190	57	216	1.1	139	259	3.34	ND
	2	257	91	380	202	57	217	1.7	144	265	3.36	ND
	2	257	81	384	201	55	219	1.7	144	270	3.42	ND
	3	244	92	358	191	60	229	1.4	144	273	3.45	ND
	3					60	226	1.6				ND
4	1	267	80	377	184	65	230	0.9	148	269	3.63	ND
	1	262	78	361	180	65	244	1.3	152			ND
	2	265	76	363	180	64	250	1.6	152	269	3.62	ND
	3.2	251	75	343	171	59	230	1.7	156	275	3.71	ND

Table 4.5. Concentrations of total suspended solids (TSS), particulate organic carbon (SPOC), particulate organic nitrogen (SPON), C_{Org}:N weight ratio (C/N) and total particulate organic matter (POM) in the water column of Balmer Lake, Ontario, for the summer, fall, winter and spring field sessions. TSS values were determined from the particulate mass on pre-weighed 0.45 µm Nuclepore filters, while all organics were determined from glass fibre filters. ND deontes not determined.

Season	Station	Depth, m	TSS mg·L ⁻¹	SPOC µg·L ⁻¹	SPON µg·L ⁻¹	C/N Wt. Ratio	POM µg·L ⁻¹
Summer	1	0.5	3.7	988	135	7.32	1778
		2.0	3.3	876	119	7.36	1577
		2.0	4.0				
		3.5	3.3	920	122	7.54	1656
Summer	2	0.1	3.7	772	103	7.50	1390
		1.0	4.2	883	116	7.61	1589
		1.0	4.2				
		2.0	3.9	893	118	7.57	1607
		3.0	4.7	762	110	6.93	1372
		3.6	3.6	1191	171	6.96	2144
Summer	3	0.5	3.2	1017	128	7.95	1831
		2.0	2.1				
		2.8	4.0	1308	165	7.93	2354
Summer	4	0.5	3.8	923	114	8.10	1661
		2.0	2.4	856	107	8.00	1541
		3.5	5.5	1033	130	7.95	1859
		3.5	4.7	ND	ND	ND	ND
Fall	1	0.5	3.9	540	81	6.67	972
		2.0	4.4	521	77	6.77	938
		3.0	4.2	552	82	6.73	994
Fall	2	0.5	4.5	ND	ND	ND	ND
		1.5	5.5	ND	ND	ND	ND
		1.5	4.4	ND	ND	ND	ND
		3.0	4.6	ND	ND	ND	ND
Fall	3	0.5	4.0	ND	ND	ND	ND
		1.5	4.0	ND	ND	ND	ND
		1.8	4.1	ND	ND	ND	ND
Fall	4	0.5	3.3	515	76	6.78	927
		1.5	4.0	508	74	6.86	914
		2.8	6.2	ND	ND	ND	ND

Season	Station	Depth, m	TSS	SPOC	SPON	C/N	POM
Winter	1	1.0	3.0	376	82	4.59	677
		2.0	2.4	336	79	4.25	605
		2.25	2.6	ND	ND	ND	ND
		2.5	2.3	ND	ND	ND	ND
		2.75	2.6	332	77	4.31	598
		3.0	4.1	416	69	6.03	749
		3.15	6.3	754	138	5.46	1357
Winter	2	1.0	4.0	577	137	4.21	1039
		1.75	3.1	498	131	3.80	896
		1.75	2.7	498	131	3.80	896
		2.25	3.2	ND	ND	ND	ND
		2.5	3.1	530	149	3.56	954
		2.65	3.5	ND	ND	ND	ND
		2.8	2.7	376	112	3.36	677
2.9	4.4	ND	ND	ND	ND		
Winter	3	1.0		360	80	4.50	648
		1.5	3.0	ND	ND	ND	ND
		1.75	3.2	ND	ND	ND	ND
		2.0	2.2	372	84	4.43	670
		2.2	2.7	ND	ND	ND	ND
		2.4	3.1	ND	ND	ND	ND
		2.55	ND	945	157	6.02	1701
Winter	4	1.0	2.6	300	63	4.76	540
		1.5	3.2	ND	ND	ND	ND
		2.0	2.5	333	67	4.97	599
		2.5	2.6	310	65	4.77	558
		2.6	2.0	404	83	4.87	727
		2.7	3.5	ND	ND	ND	ND
		2.8	5.6	722	110	6.56	1300
Spring	1	1.0	8.2	798	142	5.62	1436
		2.0	7.9	731	135	5.41	1316
		3.0	9.3	743	139	5.35	1337
Spring	2	1.0	ND	749	137	5.47	ND
		2.0	ND	706	135	5.23	ND
		2.0	ND	700	134	5.22	ND
		3.0	ND	739	137	5.39	ND
Spring	4	1.0	10.8	816	138	5.91	1469
		1.0	11.9	ND	ND	ND	ND
		2.0	12.1	834	144	5.79	1501
		3.2	12.7	823	142	5.80	1481
Spring	5	0.5	11.2	913	151	6.05	1643
		0.5	10.9	867	148	5.86	1561

spring, concentrations of suspended POC and PON varied only slightly with depth. Values for SPOC over these seasons averaged 960 $\mu\text{gC/L}$ (762-1308), 530 $\mu\text{gC/L}$ (508-552) and 815 $\mu\text{gC/L}$ (731-913), respectively (Table 4.5). Furthermore, concentrations of SPON over the summer, fall and spring periods averaged respectively 125 $\mu\text{gN/L}$ (103-171), 78 $\mu\text{gN/L}$ (74-82) and 142 $\mu\text{gN/L}$ (135-151) (Table 4.5). The discrepancy in the ranking of magnitudes in the SPOC and SPON values over these periods can be explained by seasonal differences in their respective particulate C/N ratios (Table 4.5). With the exception of station 2, all sampling sites during the winter period exhibited bottom water enrichments of SPOC and SPON (Table 4.5). The bottom waters of stations 1, 3, and 4 were characterized by higher C/N ratios and SPOC/SPON concentrations over two times greater than their respective near-surface values.

4.1.4 Trace Metals

4.1.4.1 Dissolved Fraction

The well-mixed conditions of the summer, fall and spring water columns, revealed by physical profiling of temperature and dissolved oxygen, are in good agreement with the constant vertical distributions of dissolved trace metals observed during such periods. Concentrations of dissolved species during the summer period averaged 286 $\mu\text{g/L}$ for Mn, 40 $\mu\text{g/L}$ for Fe, 411 $\mu\text{g/L}$ for Ni, 173 $\mu\text{g/L}$ for Cu, 51 $\mu\text{g/L}$ for Zn and 287 $\mu\text{g/L}$ for As (Table 4.1). During all seasons and at all depths, concentrations of dissolved Pb hovered at or below its detection limit of approximately 0.5 $\mu\text{g/L}$. The fall sampling period was characterized by generally lower dissolved metal inventories with values

averaging 175 $\mu\text{g/L}$ for Mn, 91 $\mu\text{g/L}$ for Fe, 275 $\mu\text{g/L}$ for Ni, 119 $\mu\text{g/L}$ for Cu, 56 $\mu\text{g/L}$ for Zn and 210 $\mu\text{g/L}$ for As (Table 4.2).

The winter period exhibits marked differences in water column structure with respect to dissolved trace metals. In general, concentration profiles relate to the observed stratification (Table 4.3, Figs. 4.8-4.11). At depths shallower than the oxycline (approximately 2.5 m), dissolved metal concentrations are significantly greater than those observed during other seasons with values averaging 323 $\mu\text{g/L}$ for Mn, 152 $\mu\text{g/L}$ for Fe, 468 $\mu\text{g/L}$ for Ni, 307 $\mu\text{g/L}$ for Cu, 70 $\mu\text{g/L}$ for Zn and 348 $\mu\text{g/L}$ for As (Table 4.3; Figs. 4.8-4.11).

Dissolved trace metal profiles in the sub- or anoxic bottom waters of Balmer Lake contrast greatly with those seen during other periods. At all stations, dissolved Mn and Zn are characterized by bottom water enrichments up to 3.2 and 2.7 times their respective near-surface concentrations (Table 4.3; Figs. 4.8-4.11). Conversely, dissolved Cu profiles suggest removal for this element in the bottom waters at all locales except at the shallowest site, station 3 (Table 4.3). Depletions of dissolved copper were more pronounced in the deeper sites (stations 1 and 2; Figs. 4-8 and 4-9), where bottom concentrations represent 16 and 13 % of their respective near-surface levels. The bottom water gradients evident for Mn and Zn occur across the corresponding interval for dissolved oxygen depletion (see Fig. 4.3); similarly, zones of decreasing Cu concentrations are consistent with that of dissolved oxygen.

The water column distributions for As and Ni are more complex. At the two deepest stations (stations 1 and 2, Figs. 4.8 and 4.9, respectively) concentrations of dissolved As begin to decrease between 2-2.5 m, reaching minima at approximately 2.7-2.8 m depth. At slightly greater depths, arsenic levels increase sharply to values in bottom waters approximately 100 $\mu\text{g/L}$ greater than their respective minima (Figs 4.8 and 4.9). At the shallowest site

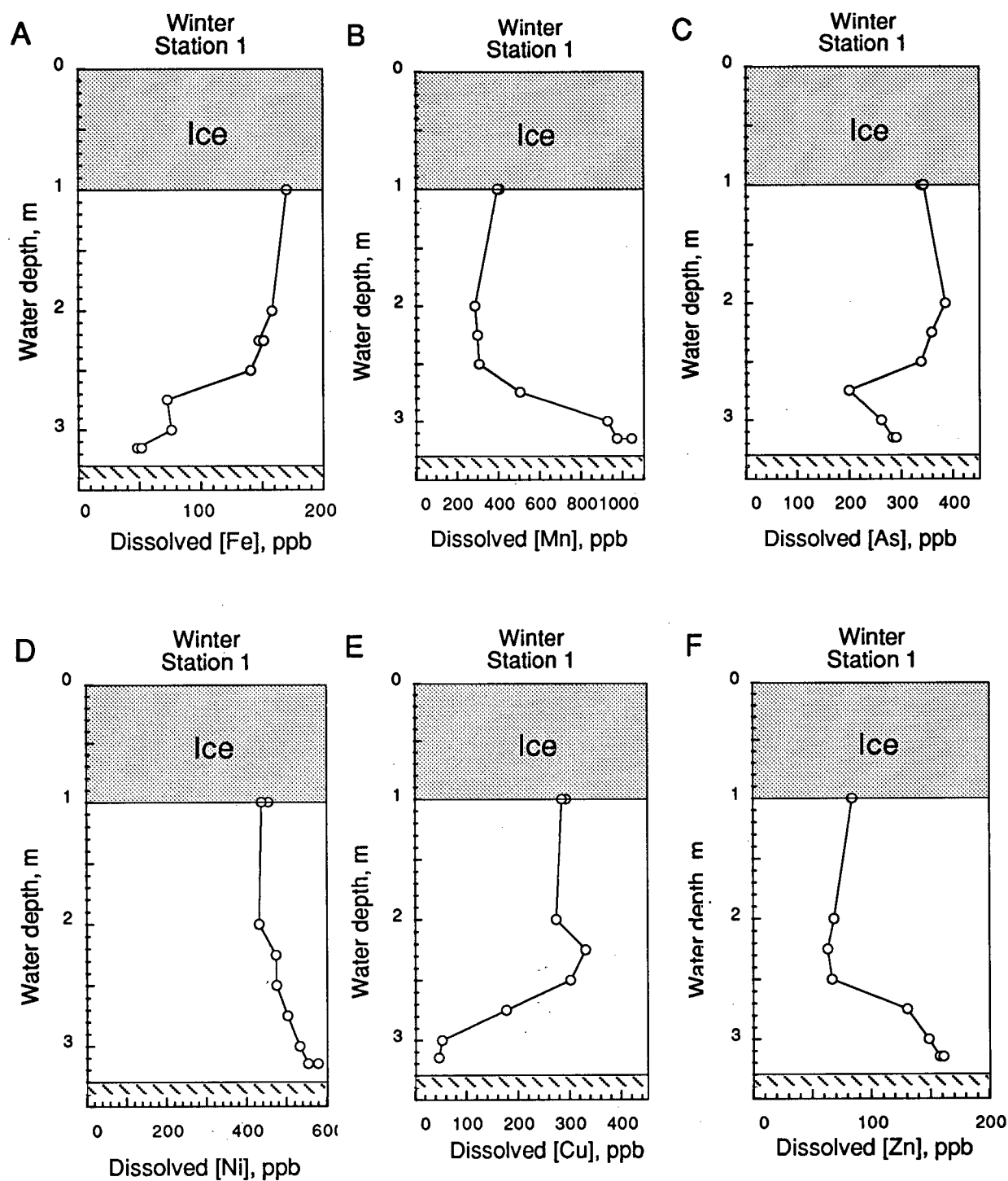


Fig. 4.8. Winter water column profiles of dissolved Fe, Mn, As, Ni, Cu and Zn (A-F, respectively) for station 1, Balmer Lake, March, 1994. Replicate samples are represented by double symbols at specific single depths. The hatched line represents the sediment surface.

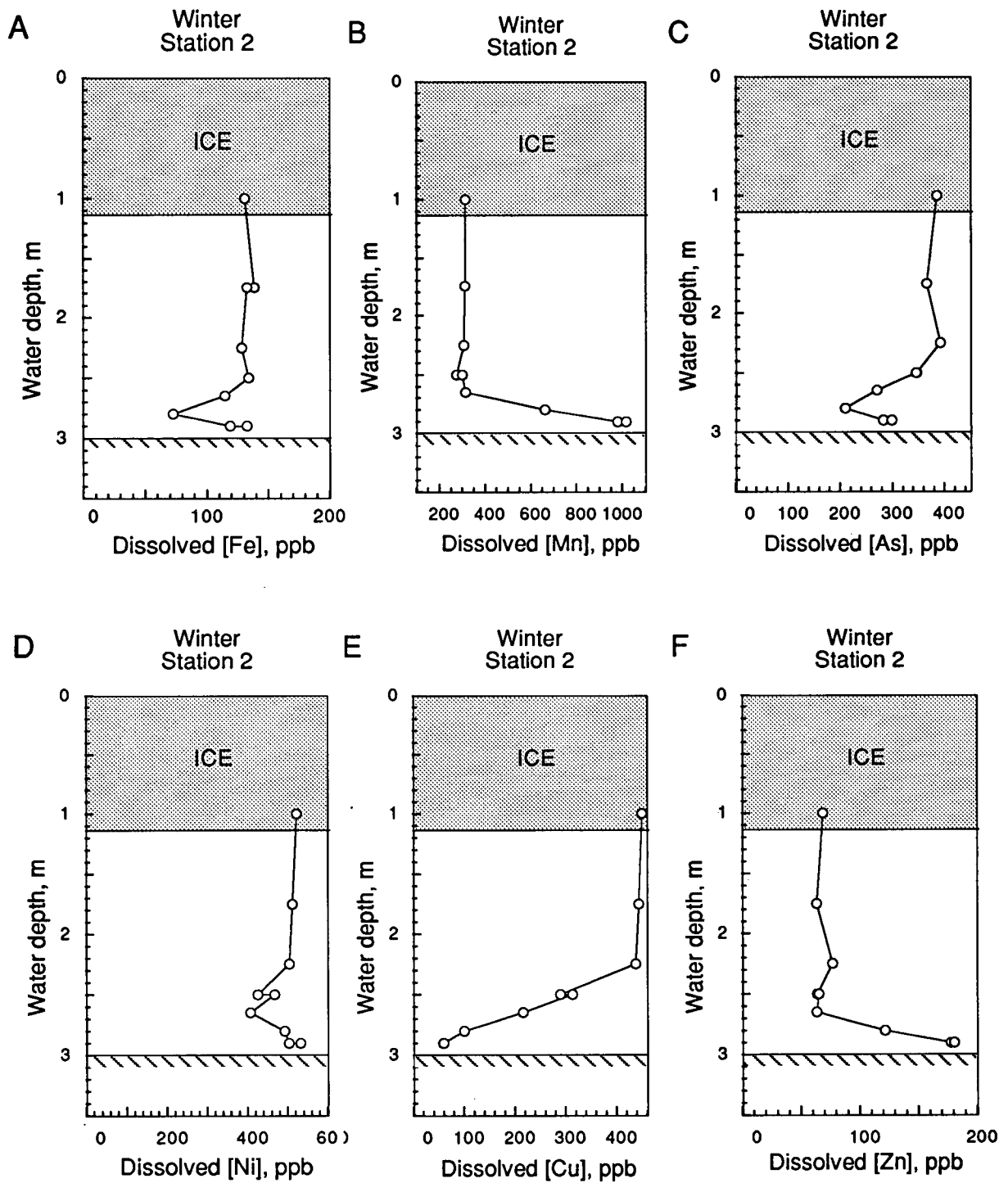


Fig. 4.9. Winter water column profiles of dissolved Fe, Mn, As, Ni, Cu and Zn (A-F, respectively) for station 2, Balmer Lake, March, 1994. Replicate samples are represented by double symbols at specific single depths. The hatched line represents the sediment surface.

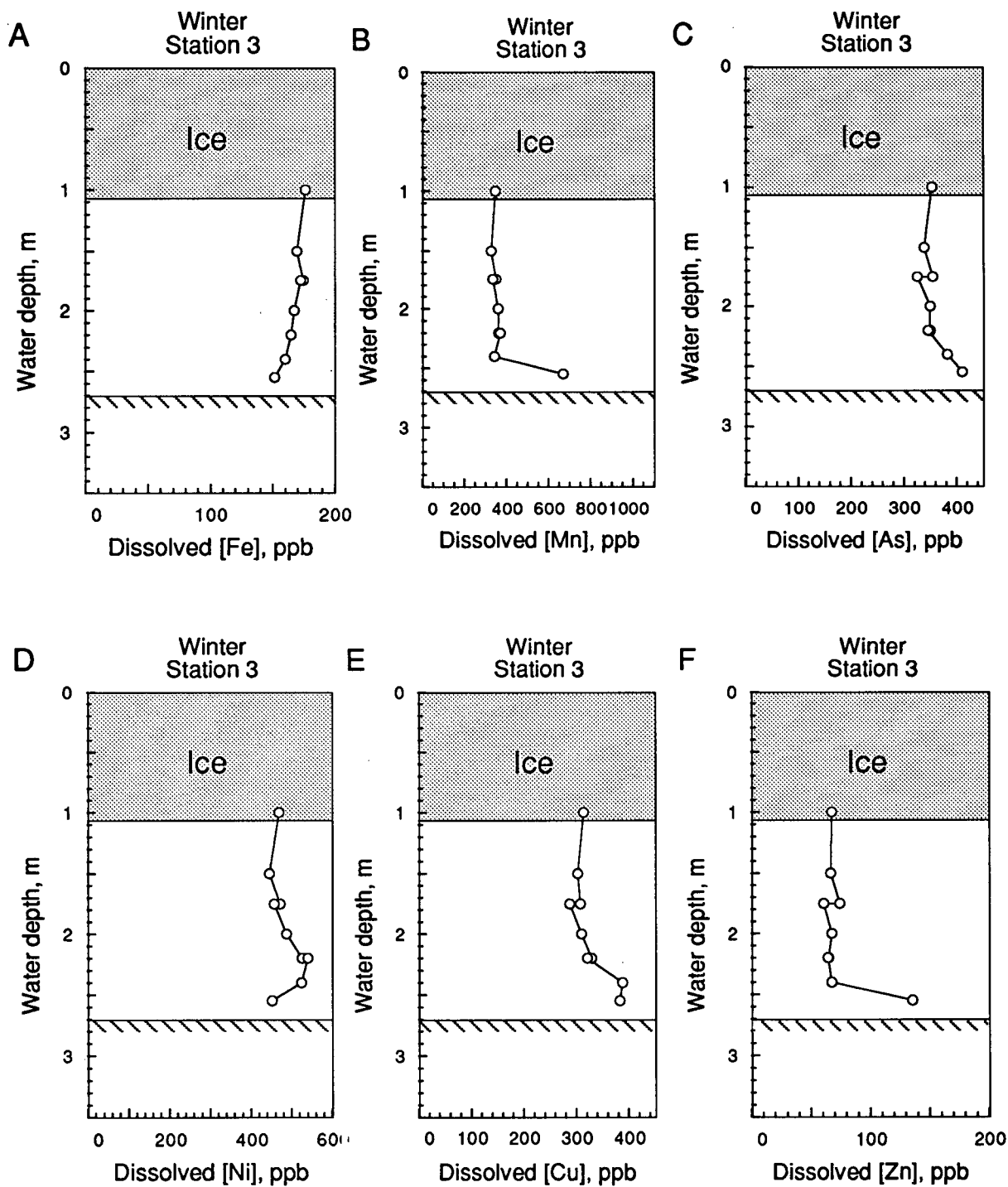


Fig. 4.10. Winter water column profiles of dissolved Fe, Mn, As, Ni, Cu and Zn (A-F, respectively) for station 3, Balmer Lake, March, 1994. Replicate samples are represented by double symbols at specific single depths. The hatched line represents the sediment surface.

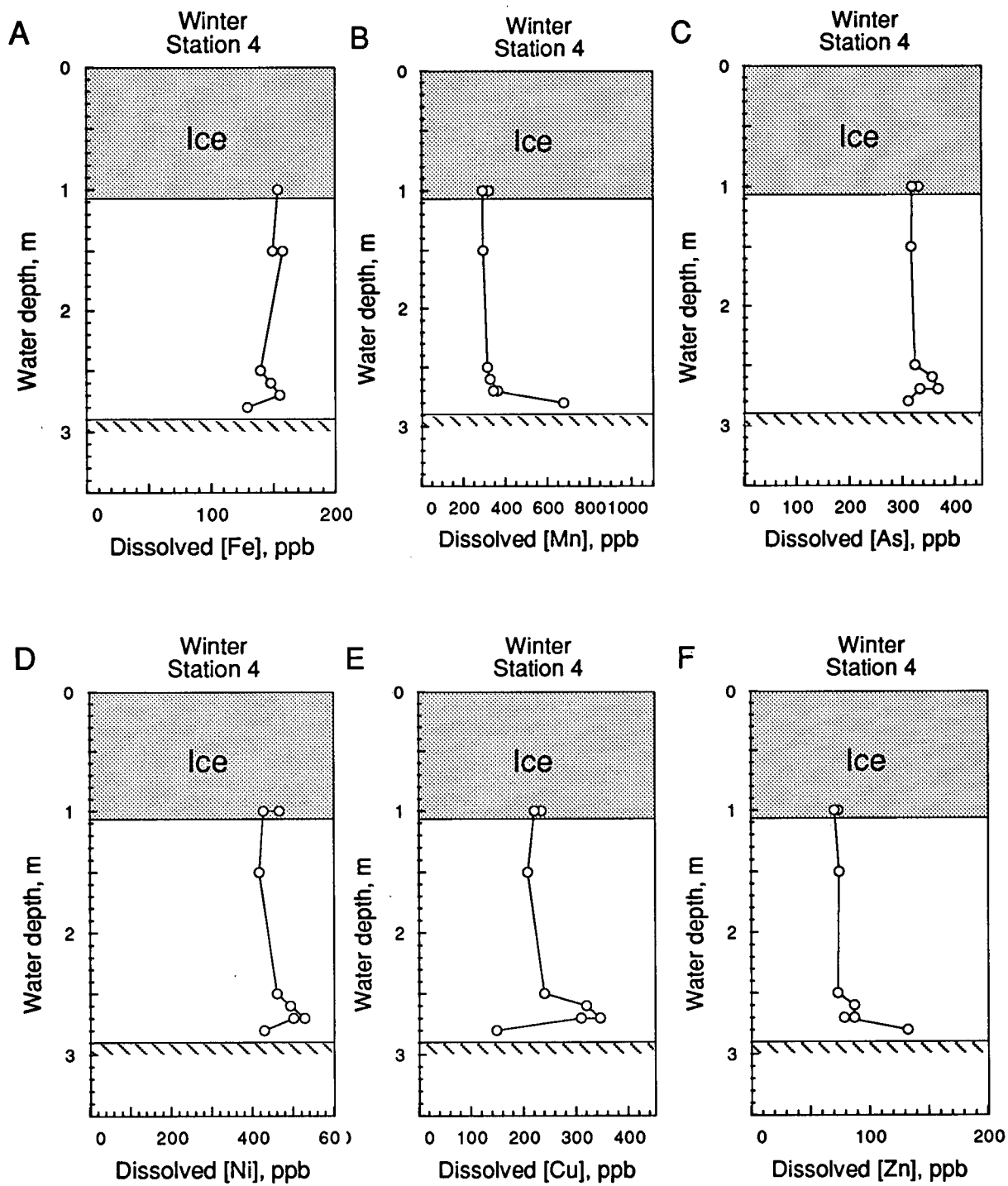


Fig. 4.11. Winter water column profiles of dissolved Fe, Mn, As, Ni, Cu and Zn (A-F, respectively) for station 4, Balmer Lake, March, 1994. Replicate samples are represented by double symbols at specific single depths. The hatched line represents the sediment surface.

(station 3, Fig. 4.10), profiles of dissolved As lack a defined minimum, although values increase slightly below 2.2 m. Conversely, the water column at station 4 is characterized by a near-bottom maximum of dissolved As at ~2.7 m, below which concentrations decrease (Fig. 4.11). Bottom water maxima are also evident for dissolved Fe, Ni, Cu and to a lesser degree Zn, at the same horizon at this site (Fig. 4.11).

Dissolved Ni distributions during the winter period differ markedly between sampling sites. Stations 1, 3 and 4 all exhibit some increase with depth (Figs. 4.8, 4.10 and 4.11); values at stations 3 and 4, however, fall back to near-surface levels below deep maxima (Figs. 4.10 and 4.11). Concentrations of dissolved Ni remain fairly constant at station 2, except for a minimum evident between 2.5 and 2.8 m (Fig. 4.9).

Distributions of Fe share similar inconsistencies to those seen for dissolved nickel. The steady drop in dissolved Fe below 2.5 m at station 1 occurs across the same interval observed for decreases in dissolved As and Cu (Fig. 4.8). The iron profile is characterized by a bottom water minimum at station 2 coincident with the As minimum observed at this site (Fig. 4.9). In contrast, stations 3 and 4 exhibit fairly uniform profiles of dissolved Fe (Figs. 4.10 and 4.11).

During the well-mixed conditions of the spring sampling period, concentrations of dissolved metal species varied little throughout the water column with values averaging 265 $\mu\text{g/L}$ for Mn, 80 $\mu\text{g/L}$ for Fe, 372 $\mu\text{g/L}$ for Ni, 196 $\mu\text{g/L}$ for Cu, 61 $\mu\text{g/L}$ for Zn and 224 $\mu\text{g/L}$ for As (Table 4.4). In general, the magnitudes fall within the ranges observed for the summer session.

4.1.4.2 Particulate Fraction

The seasonal concentrations of particulate trace metals in the water column of Balmer Lake have been expressed in terms of both mass of metal per unit volume (Table 4.6) and mass of metal per unit mass of total particulate matter (Table 4.7). The well-mixed periods of summer, fall and spring, are characterized by considerably more intra-site variability in comparison to associated dissolved trace metal distributions. In general, the particulate fraction for most metals (except Fe) contributes a small percentage of the total pool of metals in the water column during all seasons.

The water column concentrations of particulate Fe, Mn, Ni, Cu, Zn and As during the summer period averaged 107, 3, 5, 13, 27 and 7 $\mu\text{g}\cdot\text{L}^{-1}$, respectively, and represented 71, 1, 1, 7, 30 and 2% of the respective totals (Table 4.6). These lake-wide averages translate into mass ratios of 29,600 $\text{mg}\cdot\text{kg}^{-1}$ for Fe, 850 $\text{mg}\cdot\text{kg}^{-1}$ for Mn, 1,330 $\text{mg}\cdot\text{kg}^{-1}$ for Ni, 3,250 $\text{mg}\cdot\text{kg}^{-1}$ for Cu, 7900 $\text{mg}\cdot\text{kg}^{-1}$ for Zn and 1760 $\text{mg}\cdot\text{kg}^{-1}$ for Pb (Table 4.7). The autumn particulate data contrast little from the summer values; concentrations of particulate Fe, Mn, Ni, Cu, Zn and As averaged 205, 4, 5, 15, 16 and 9 $\mu\text{g}\cdot\text{L}^{-1}$, respectively (Table 4.6). The fall proportions of the dissolved and solid-phase fractions show additional inter-season similarity with the particulates averaging 69, 2, 2, 11, 21 and 4 % of the respective totals of Fe, Mn, Ni, Cu, Zn and As.

The influence of ice cover on the chemical and physical environment during the winter months can be further realized upon observation of the vertical distributions of particulate metal species (Tables 4.6 and 4.7). Slight decreases in dissolved Fe with depth are mirrored by significant increases in concentrations of Fe-bearing particulates which surpass 400 $\mu\text{g}\cdot\text{L}^{-1}$ at some sites (Table 4.6). Conversely, Mn, Ni, Cu and Zn particulates exhibit minimal variation with

Table 4.6. Particulate trace metal concentrations of Fe, Mn, Ni, Cu, Zn, As and Pb for the summer, fall, winter and spring water columns in Balmer Lake, Ontario. All values are expressed in $\mu\text{g}\cdot\text{L}^{-1}$.

Season	Station	Water depth, m	Fe	Mn	Ni	Cu	Zn	As	Pb
Summer	1	0.5	105.2	1.5	3.1	6.8	56.4	3.8	0.1
		2.0	108.1	2.3	3.8	9.1	26.3	3.9	0.2
		2.0	126.6	2.8	4.5	11.9	3.0	5.1	0.3
		3.5	102.2	2.0	3.2	8.9	28.1	4.0	0.3
Summer	2	0.1	99.3	2.5	5.3	11.6	93.9	6.3	0.2
		1.0	118.0						
		1.0	95.9	2.8	4.7	11.1	9.0	6.1	0.1
		2.0	138.0	3.8	6.2	15.8	5.1	8.0	0.2
		3.0		16.3	22.2	50.1	43.9	35.8	1.8
		3.6	122.9	3.5	4.9	11.8	4.5	6.6	0.2
Summer	3	0.5	88.7	1.5	2.5	7.1	28.2	3.2	0.2
		2.0	68.1	1.4	2.3	6.0	25.9	2.5	0.2
Summer	4	0.5	101.5	2.0	3.7	9.9	33.0	4.1	0.4
		2.0	70.5	1.6	2.6	6.7	17.1	2.8	0.2
		3.5	147.0	2.9	4.3	11.3	7.3	4.5	0.3
Fall	1	0.5	182.0	3.2	4.2	12.5	14.6	7.3	0.9
		2.0	212.6	3.6	4.8	14.5	43.1	8.8	1.1
		3.0	203.7	3.4	4.5	12.8	20.8	8.0	0.9
Fall	2	0.5	182.3	3.3	4.7	14.8	6.9	7.6	0.9
		1.5	214.3	3.9	5.5	17.7	10.8	9.5	1.3
		1.5	195.2	3.4	4.9	15.5	8.7	8.1	1.0
		3.0	219.8	3.7	5.3	16.9	7.4	9.2	1.1
Fall	3	0.5	213.6	4.1	5.7	17.5	9.0	10.2	1.2
		1.5	193.4	3.4	4.8	14.6	7.3	8.4	1.1
		1.8	192.0	3.4	4.8	14.5	6.6	8.4	1.0
Fall	4	0.5	171.0	2.8	3.8	11.7	16.5	7.2	0.9
		1.5	189.1	3.3	4.5	13.2	14.9	8.3	1.0
		2.8	283.2	4.5	5.3	14.8	38.4	9.4	1.1

Season	Station	Depth	Fe	Mn	Ni	Cu	Zn	As	Pb
Winter	1	1.0	130.8	1.6	5.6	32.1	6.3	11.6	0.8
		2.0	156.3	2.0	7.7	36.0	13.5	9.5	0.9
		2.25	157.0	2.6	9.6	50.8	8.6	11.4	0.7
		2.5	160.5	2.6	8.9	42.6	7.0	11.7	0.7
		2.75	149.4	2.4	6.5	51.2	5.6	11.7	0.5
		3.0	388.3	3.0	6.4	22.6	6.9	121.4	0.6
		3.15	366.2	6.2	14.8	38.0	16.3	42.3	0.7
Winter	2	1.0	205.5	2.0	11.7	109.6	15.5	6.4	0.2
		1.75	148.7						
		2.25	193.6	2.5	13.4	115.2	14.9	16.0	1.3
		2.5	223.9	2.6	15.4	97.4	18.2	14.0	1.3
		2.65	222.3	2.7	15.6	81.6	18.8	14.0	1.3
		2.8	175.3	2.4	12.6	59.5	19.1	10.7	0.8
		2.9	424.4	3.4	13.1	53.3	19.4	110.9	1.4
Winter	3	1.5	161.5	2.2	7.8	45.5	31.7	12.3	0.9
		1.75	153.3	2.1	7.7	45.4	50.1	12.9	0.8
Winter	4	1.0	163.9	2.6	7.2	29.1	8.7	11.4	0.8
		1.5	176.0	2.8	7.6	31.3	11.8	12.2	1.0
		2.0	151.1	2.2	6.1	25.2	3.9	10.0	0.7
		2.5	143.3	2.0	6.0	27.6	16.3	8.8	0.8
		2.6	130.1	1.8	5.5	32.8	11.3	8.4	0.7
		2.7	190.2	2.5	8.6	54.5	16.7	13.5	1.1
		2.8	479.9	4.5	11.2	49.7	73.9	116.1	2.3
Spring	1	1.0	445.5	5.7	7.5	70.7	22.6	49.2	0.8
		2.0	566.0	7.2	9.4	88.5	29.9	70.8	1.2
		3.0	569.6	7.5	10.2	90.8	27.5	69.0	1.0
Spring	4	1.0	733.0	10.2	11.2	101.1	30.6	73.4	1.4
		1.0	739.3	11.3	12.5	105.9	31.3	75.8	1.4
		2.0	744.5	11.1	12.1	105.2	33.7	78.3	4.7
		3.2	742.3	11.4	11.6	96.8	27.3	69.1	1.3

Table 4.7. Concentrations of trace metals ($\text{mg}\cdot\text{kg}^{-1}$), organic carbon (%) and organic nitrogen (%) in suspended particulates of the summer, fall, winter and spring water columns in Balmer Lake, Ontario. Trace metal values were determined from the particulate mass on pre-weighed $0.45\ \mu\text{m}$ Nuclepore filters, while all SPOC and SPON values were determined from glass fibre filters.

Season	Station	Water depth, m	Fe	Mn	Ni	Cu	Zn	As	Pb	SPOC	SPON
Summer	1	0.5	28,510	410	840	1850	15380	1030	27	26.8	3.7
		2.0	32,560	690	1130	2730	8010	1160	70	26.4	3.6
		2.0	31,320	700	1100	2940	830	1270	65		
		3.5	31,290	620	970	2730	8700	1230	77	28.2	3.7
Summer	2	0.1	26,770	690	1420	3120	25410	1690	60	20.8	2.8
		1.0	28,190							21.1	2.8
		1.0	22,590	670	1100	2610	2180	1440	26		
		2.0	35,790	980	1610	4100	1390	2070	50	23.2	3.1
		3.0		3480	4750	10710	9450	7670	380	16.3	2.4
		3.6	34,020	970	1350	3270	1320	1840	52	33.0	4.7
Summer	3	0.5	27,780	460	790	2230	8930	1020	66	31.8	4.0
		2.0	33,060	680	1140	2900	12720	1220	110		
										32.9	4.1
Summer	4	0.5	26,940	520	990	2620	8840	1100	95	24.5	3.0
		2.0	29,300	670	1100	2790	7210	1150	67	35.6	4.4
		3.5	26,600	520	780	2050	1380	810	54	18.7	2.4
Fall	1	0.5	46,590	810	1060	3190	3870	1870	220	13.8	2.1
		2.0	47,940	810	1080	3270	9830	1970	260	11.7	1.7
		3.0	48,040	790	1060	3010	5030	1890	210	13.0	1.9
Fall	2	0.5	40,760	740	1060	3310	1650	1710	210		
		1.5	38,750	710	990	3200	2040	1710	230		
		1.5	44,110	770	1100	3510	2080	1830	230		
		3.0	47,540	810	1140	3660	1710	1980	240		
Fall	3	0.5	53,940	1030	1440	4410	2400	2590	310		
		1.5	48,730	850	1210	3680	1970	2120	270		
		1.8	46,650	810	1180	3530	1720	2040	240		
Fall	4	0.5	52,450	870	1170	3580	5220	2220	260	15.8	2.3
		1.5	47,790	840	1130	3350	3890	2100	260	12.8	1.9
		2.8	45,620	720	860	2380	6260	1520	170		

Season	Station	Depth	Fe	Mn	Ni	Cu	Zn	As	Pb	SPOC	SPON
Winter	1	1.0	42,960	520	1850	10540	3340	3800	260	12.4	2.7
		2.0	64,660	810	3170	14880	7200	3950	360	13.9	3.3
		2.25	59,280	970	3620	19190	4730	4300	260		
		2.5	71,220	1140	3970	18920	4840	5190	300		
		2.75	56,490	900	2480	19370	3600	4410	190	12.6	2.9
		3.0	95,010	740	1580	5540	2650	29700	140	10.2	1.7
		3.15	58,520	990	2360	6080	3220	6760	120	12.0	2.2
Winter	2	1.0	51,750	510	2960	27600	4890	1600	40	14.5	3.4
		1.75	54,380							16.0	4.2
		1.75								18.2	4.8
		2.25	60,960	800	4210	36290	5920	5030	400		
		2.5	71,120	830	4890	30920	7020	4460	410	16.8	4.7
		2.65	64,240	780	4510	23570	6560	4050	380		
		2.8	66,020	920	4760	22410	8650	4020	320	14.2	4.2
		2.9	96,040	770	2960	12070	5270	25100	310		
Winter	3	1.5	54,730	730	2640	15400	12080	4170	300		
		1.75	47,430	660	2380	14050	16720	4000	250		
		2								17.3	3.9
Winter	4	1.0	64,220	1020	2840	11400	4920	4480	330	11.8	2.5
		1.5	55,520	890	2390	9880	4940	3840	300		
		2.0	61,120	910	2480	10180	3150	4030	290	13.5	2.7
		2.5	54,790	780	2280	10570	7730	3350	320	11.9	2.5
		2.6	65,370	890	2740	16490	7630	4220	370	20.3	4.2
		2.7	54,690	720	2480	15680	5940	3870	330		
		2.8	85,830	800	2010	8880	13920	20770	420	12.9	2.0
Spring	1	1.0	54,650	700	930	8670	3000	6030	100	9.8	1.7
		2.0	71,280	900	1180	11150	4000	8910	150	9.2	1.7
		3.0	61,080	800	1090	9740	3160	7400	110	8.0	1.5
Spring	4	1.0	67,680	940	1040	9340	3000	6780	130	7.5	1.3
		1.0	61,990	950	1050	8880	2780	6360	120		
		2.0	61,500	920	1000	8690	2940	6470	390	6.9	1.2
		3.2	58,450	890	910	7620	2300	5440	100	6.5	1.1

depth (Table 4.6). Profiles of particulate As species are characterized by large bottom water spikes which range from 111-120 $\mu\text{g}\cdot\text{L}^{-1}$ (Table 4.6).

The spring period exhibited the greatest concentrations of metal-bearing particulate phases, with values for Fe, Mn, Ni, Cu, Zn and As averaging 649, 9, 11, 94, 29 and 69 $\mu\text{g}\cdot\text{L}^{-1}$. In addition, the total burdens of these metals in the water column received relatively greater contributions from their respective particulate phases; percentages for Fe, Mn, Ni, Cu, Zn and As averaged, respectively, 89, 3, 3, 33, 31 and 23 % (Tables 4.6 and 4.7).

4.2 Interstitial Waters

4.2.1 Peepers

4.2.1.1 Nutrients and Sulphate

Two pairs of tandem peepers, set approximately 15 m apart in Balmer Lake, were emplaced at stations 1 and 2 for the first deployment during the summer session. The use of two peepers at each site was designed to assess the reproducibility of the dialysis arrays, as well as the homogeneity of the sediments over short lateral distances. A coarse examination of the porewater profiles indicated that the samples collected by the arrays provided consistent representations of the porewater constituents (Fig. 4.12). The porewater results of all parameters are presented in Appendix C.

Examination of the duplicate profiles acquired 15 m apart at each site during the summer period reveals marked similarity in the distributions of nitrate, ammonium and sulphate. Values for these constituents in the peeper-sampled bottom waters remain fairly uniform above the sediment-water

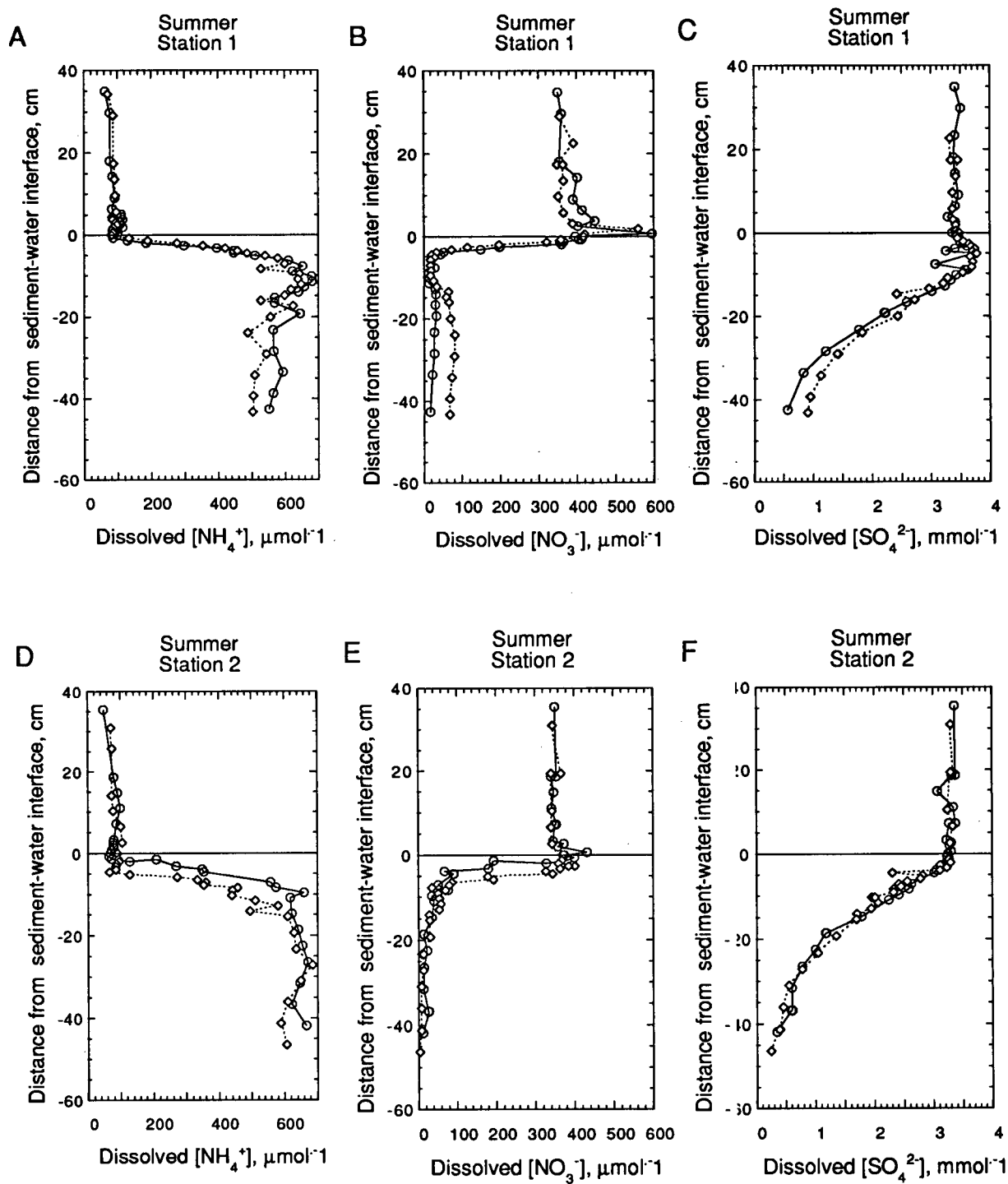


Fig. 4.12. Duplicate summer peeper profiles of dissolved NH_4^+ , NO_3^- and SO_4^{2-} for station 1 (A-C) and station 2 (D-F), Balmer Lake, June, 1993. Replicate samples are represented by double symbols at specific single depths.

interface (Fig. 4.12) and closely match those concentrations measured from pumped samples drawn independently during the peeper deployment period (compare Table 4.1 with Appendix C). At both stations, steep porewater ammonium gradients are evident immediately below the sediment-water interface where they approach maxima of 600-700 $\mu\text{mol}\cdot\text{L}^{-1}$ at ~ 10 cm (Fig. 4.12). Nitrate profiles show sharp spikes at, or just above the interface, below which values decrease precipitously to low levels at shallow sediment depths (Fig. 4.12). Larger interfacial increases and steeper porewater gradients characterize the distribution at station 1. As for nitrate, sulphate concentrations decrease with depth, although less abruptly; levels fall gradually throughout the sampled sediment column, the profiles being concave-downward (Fig. 4.12).

The peeper samples collected in the fall yield nitrate, ammonium and sulphate profiles similar to those observed during the summer period. The duplicate peeper arrangement repeated at station 2 again demonstrates the good consistency between profiles 15 m apart (Fig. 4.14). At all three sites sampled (stations 1, 2 and 5), porewater nitrate values plummet dramatically at shallow sediment depths, reaching very low concentrations at ~ 5 cm (Figs. 4.13 and 4.14). Sulphate distributions for stations 1 and 2 exhibit good agreement; concave-down profiles decrease gradually throughout the sampled sediment column from ~ 3.6 to ~ 0.5 $\text{mmol}\cdot\text{L}^{-1}$. Peeper data for the shallow site in "Tailings Bay" (station 5), however, show evidence for a bottom water sulphate enrichment before sharply decreasing at, or slightly above, the sediment-water interface to a minimum of ~ 2 $\text{mmol}\cdot\text{L}^{-1}$. The ammonium profile obtained for this site relates closely to that observed for sulphate; concentrations are enriched in the lowermost bottom waters and are depleted at, or below, the sediment surface (Fig. 4.13D). Concentrations of ammonium do, however, increase in the porewaters below ~ 10 cm depth at this site. Stations 1 and 2 show similar

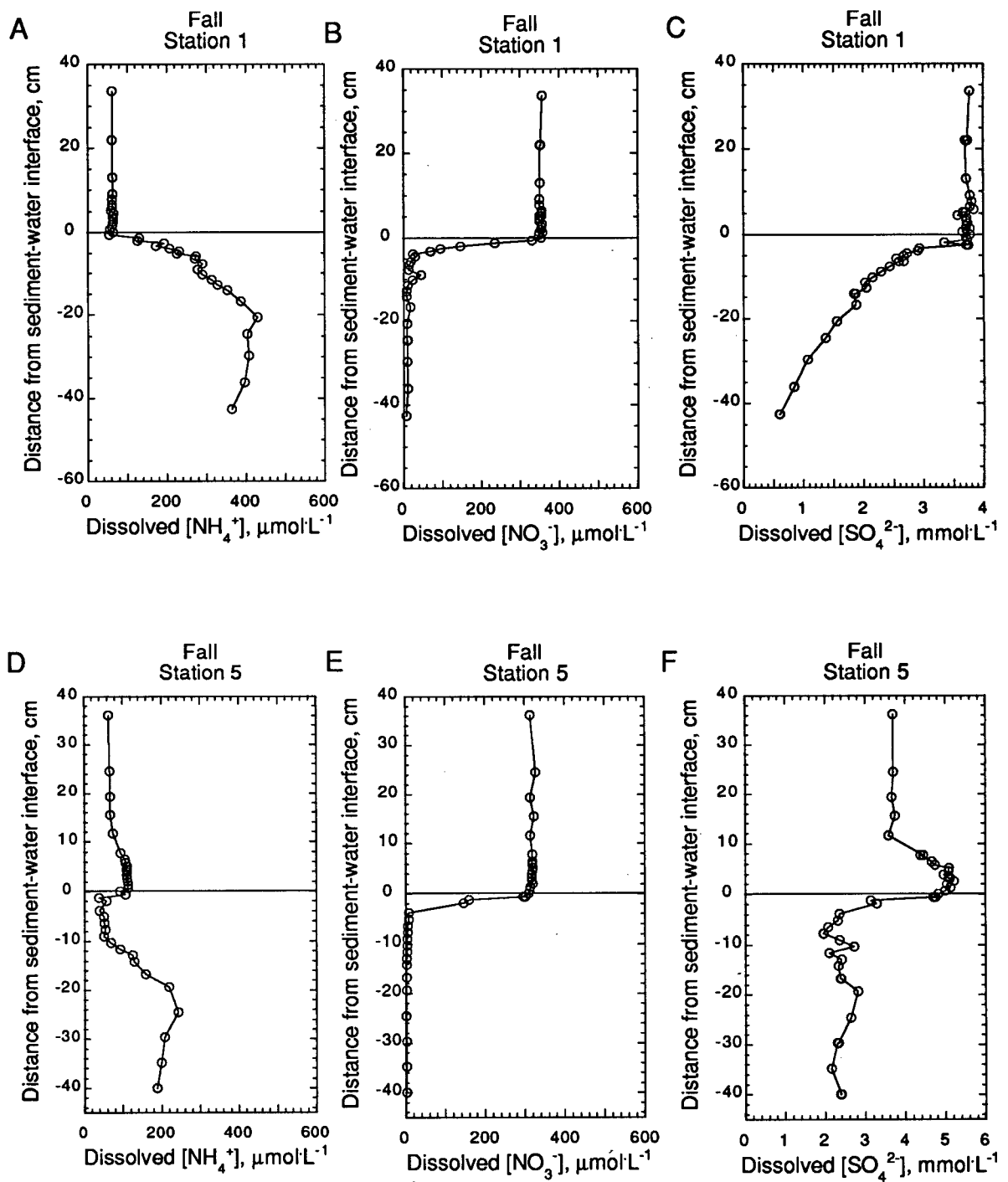


Fig. 4.13. Fall peeper profiles of dissolved NH_4^+ , NO_3^- and SO_4^{2-} for stations 1 (A-C) and 5 (D-F), Balmer Lake, October, 1993. Replicate samples are represented by double symbols at specific single depths.

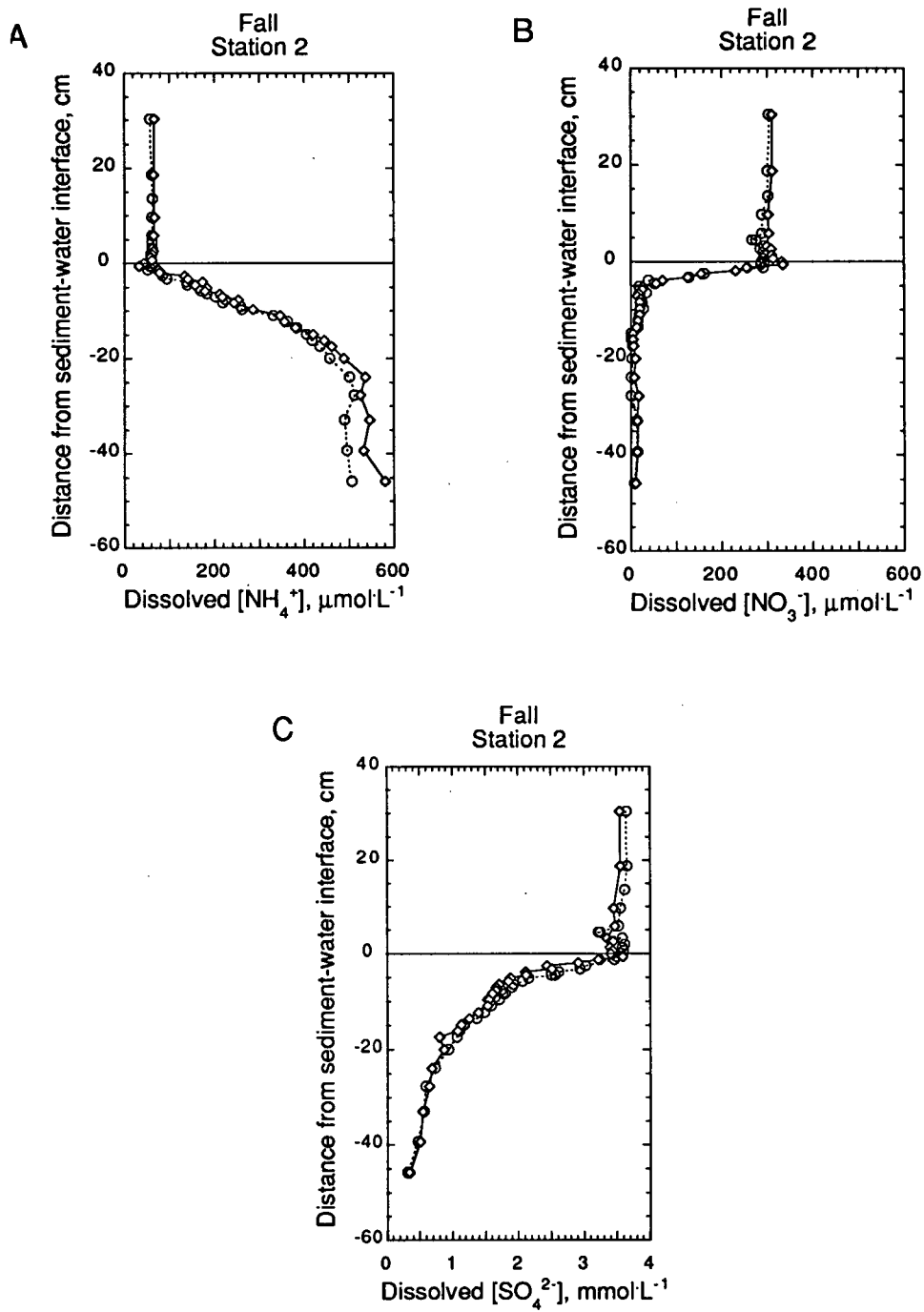


Fig. 4.14. Duplicate fall peeper profiles of dissolved NH_4^+ , NO_3^- and SO_4^{2-} (A-C, respectively) for station 2, Balmer Lake, October, 1993. Replicate samples are represented by double symbols at specific single depths.

consistency with respect to ammonium distributions. Steep porewater ammonium gradients are evident immediately below the sediment-water interface where they approach maxima of 400-600 $\mu\text{mol}\cdot\text{L}^{-1}$ (Figs. 4.13A and 4.14A). Peeper values for nitrate, sulphate and ammonium in the fall bottom waters closely match those concentrations measured from pumped samples drawn independently during the peeper deployment period (compare Table 4.2 with Appendix C).

The bottom water distributions for nitrate, sulphate and ammonium determined from peeper sampling during the winter period (Figs. 4.15 and 4.16) accentuate nicely the values measured from independently drawn water column samples. At the deeper locales (stations 1, 2 and 4), nitrate profiles exhibit negligible inter-site variation, with values decreasing sharply in the lower bottom waters to minima 5-10 cm above the sediment surface (Figs. 4.15 and 4.16). At the shallow site in "Tailings Bay" (station 6, 2 m depth), nitrate levels decrease immediately below the interface; concentrations of the ion approach zero below 20 cm depth (Figs. 4.15 and 4.16).

The deeper stations (stations 1, 2 and 4) exhibit marked similarity with respect to winter distribution of sulphate. Stations 1 and 2 show pronounced bottom water maxima of $\sim 11\text{-}14 \text{ mmol}\cdot\text{L}^{-1}$ 5-10 cm above the sediment surface, below which their concave-down profiles decrease progressively to $< 0.5 \text{ mmol}\cdot\text{L}^{-1}$ in the lowest sampled horizons (Fig. 4.15). Station 4 is marked by a less intense bottom water enrichment and occurs in vicinity of the interface. Sulphate concentrations in the lower three decimetres of the shallow water column at station 6 vary insignificantly. Levels initially decrease at the sediment-water interface and continue to decline to a depth of 20 cm where values approach a minimum of $\sim 2 \text{ mmol}\cdot\text{L}^{-1}$ (Fig. 4.16).

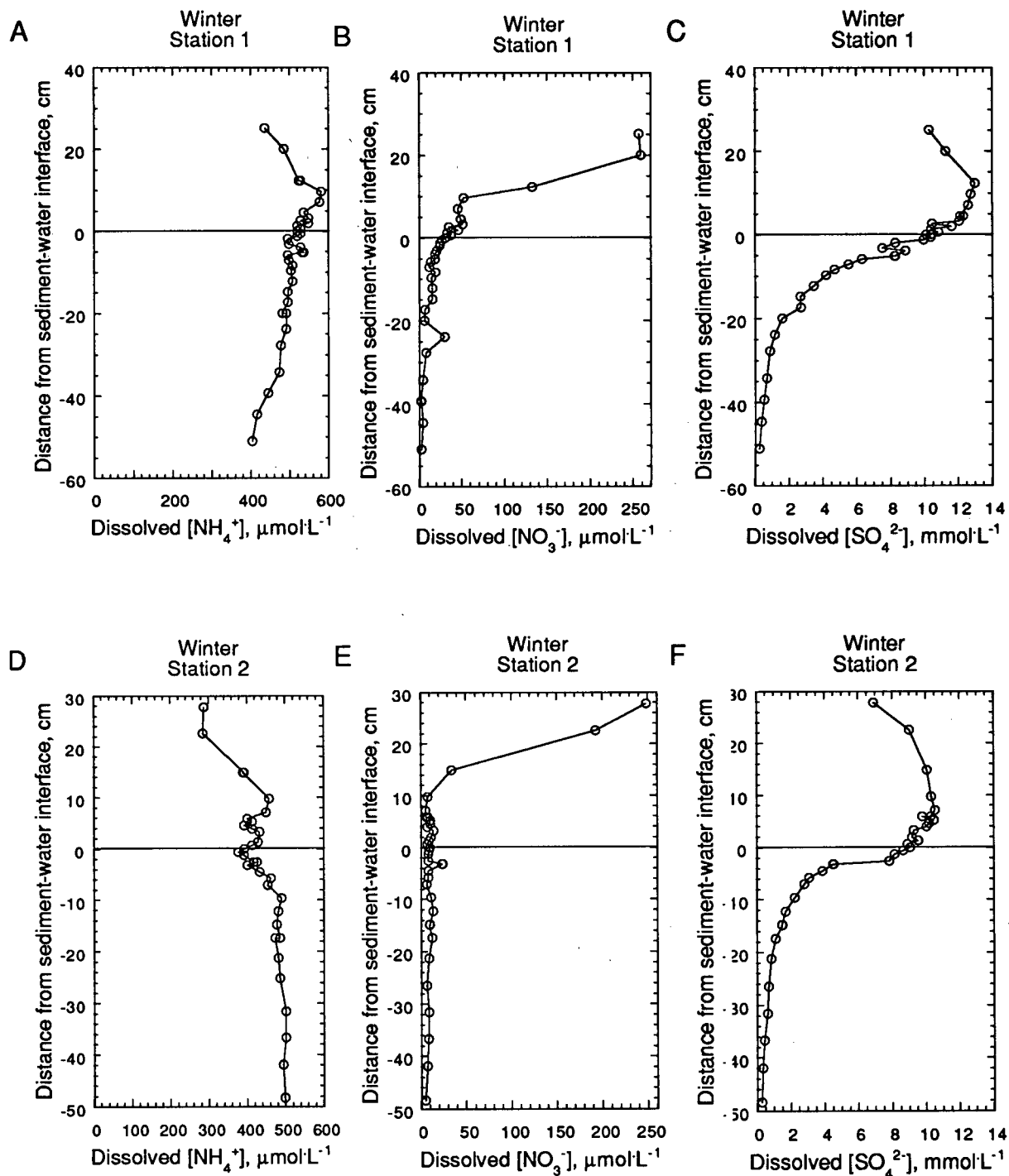


Fig. 4.15 Winter peeper profiles of dissolved NH_4^+ , NO_3^- and SO_4^{2-} for stations 1 (A-C) and 2 (D-F), Balmer Lake, March, 1994. Replicate samples are represented by double symbols at specific single depths.

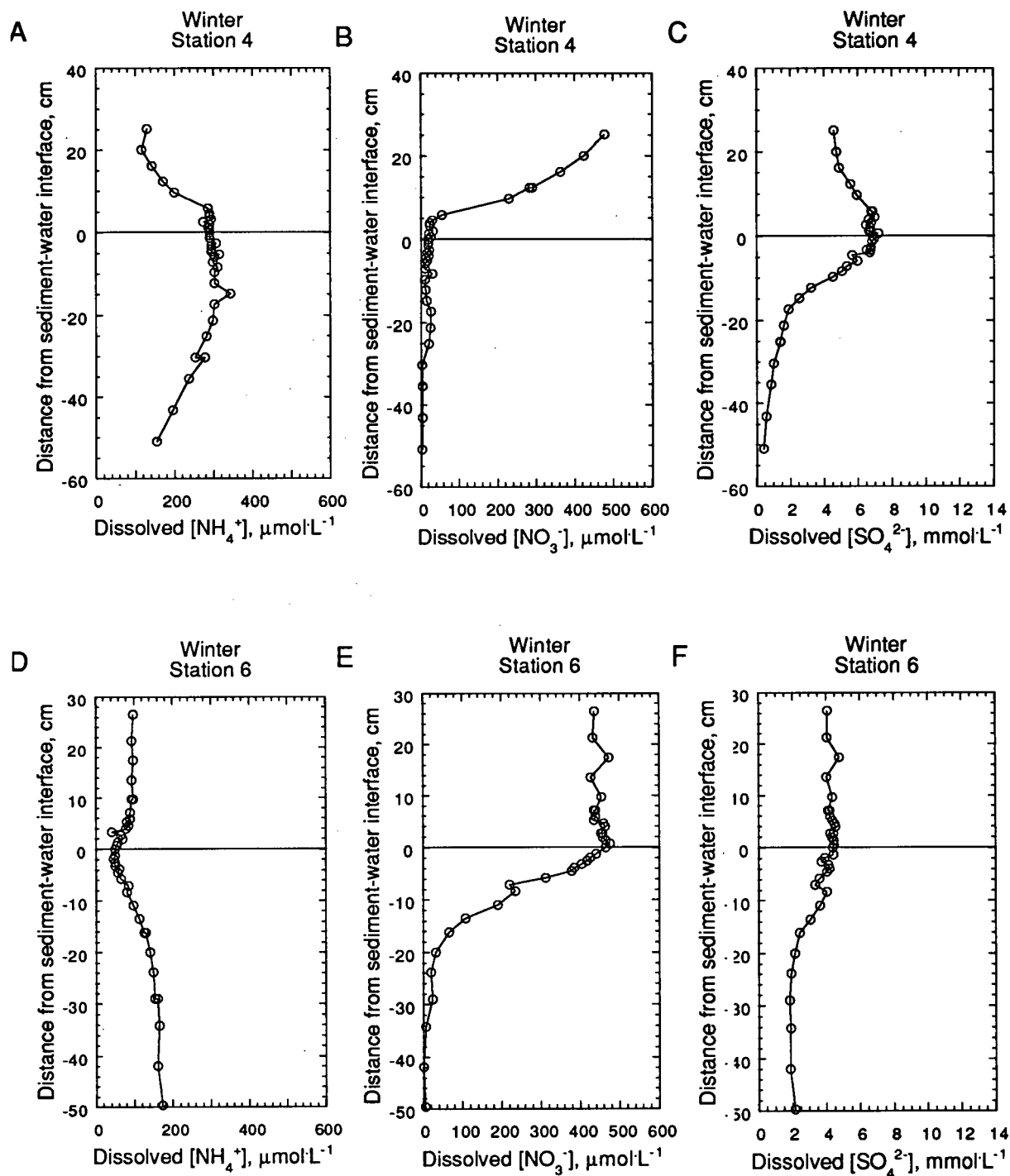


Fig. 4.16. Winter peeper profiles of dissolved NH_4^+ , NO_3^- and SO_4^{2-} for stations 4 (A-C) and 6 (D-F), Balmer Lake, March, 1994. Replicate samples are represented by double symbols at specific single depths.

The winter bottom water and porewater ammonium profiles at stations 1, 2 and 4 are quite similar. Concentrations at all three stations increase substantially in the lower bottom waters to values ranging from ~ 300-580 $\text{mmol}\cdot\text{L}^{-1}$ (Figs. 4.15 and 4.16). Stations 1 and 2 are characterized by bottom water maxima ~10 cm above the sediment-water interface. Ammonium concentrations at station 1 steadily decrease below this depth, while those at station 2 are variable near the interface; below the interface at station 2 levels increase gradually through the top decimetre (Figs. 4.15 and 4.16). Below the bottom water maximum at station 4, the ammonium content is invariant to ~15 cm in the sediments, and steadily declines to the base of the profile. Conversely, the ammonium distribution at station 6 is characterized by a pronounced bottom water depletion in the top decimetre above the sediment surface. Concentrations decrease gradually to shallow sediment depths, below which levels increase in a concave-down profile (Fig. 4.16).

The duplicate peepers deployed at station 1 during the spring period yielded good precision with respect to dissolved nutrients and sulphate. The nitrate profiles are similar to those observed at this locale during the summer and fall; uniform bottom water values decline precipitously in the top 10 cm to minima of < 10 $\mu\text{mol}\cdot\text{L}^{-1}$ (Fig. 4.17). Ammonium distributions are also similar to those seen during ice-free periods (Fig. 4.17). However, sulphate profiles differ greatly from those seen during other seasons. Concentrations increase sharply from uniform bottom water values of ~3.5 $\text{mmol}\cdot\text{L}^{-1}$ to subsurface maxima of ~6 $\text{mmol}\cdot\text{L}^{-1}$ at 5-10 cm depth, and decrease rapidly below this horizon to values that approach 1 $\text{mmol}\cdot\text{L}^{-1}$ (Fig. 4.17).

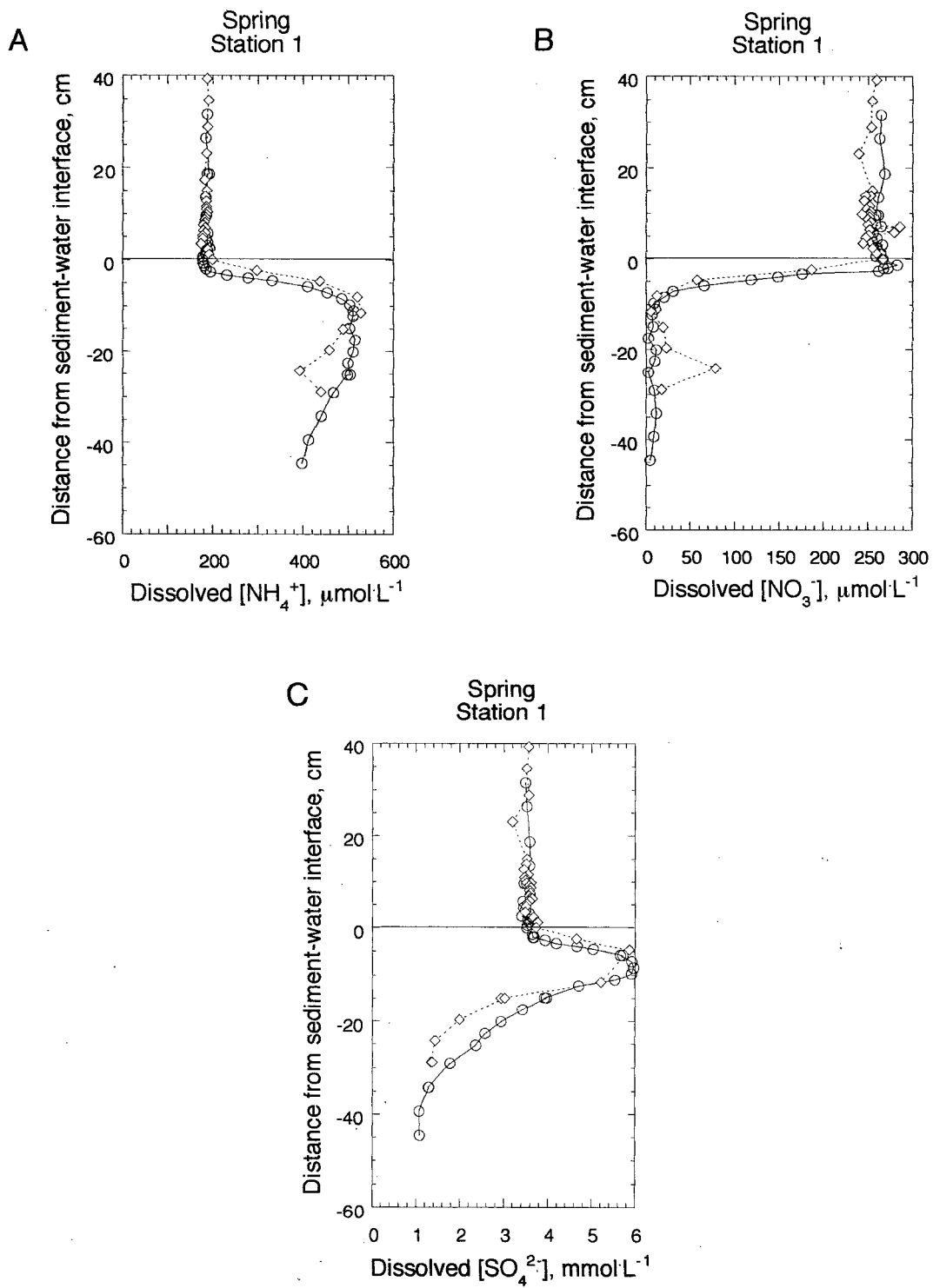


Fig. 4.17. Duplicate spring peeper profiles of dissolved NH_4^+ , NO_3^- and SO_4^{2-} (A-C, respectively) for station 1, Balmer Lake, May, 1994. Replicate samples are represented by double symbols at specific single depths.

4.2.1.2 Trace Metals

Porewaters were analyzed for a suite of dissolved trace metals including Mn, Fe, Ni, Cu, Zn, As and Pb. Throughout the seasons and at all depths sampled, dissolved Pb concentrations generally hovered at or below its detection limit of $\sim 0.5 \mu\text{g}\cdot\text{L}^{-1}$. Consequently, plots of porewater Pb distributions are not presented; measured values, however, are reported in Appendix C. Examination of the respective trace metal profiles suggest that some discrete samples may have been contaminated. Contamination could have resulted from the addition of small amounts of tailings to the porewater samples during peeper subsampling; the subsequent addition of acid would then have dissolved such metal-rich particles, yielding high dissolved metal concentrations. Given that diffusion acts to reduce concentration differences relatively quickly over short spatial scales, the principal criterion used here to define suspected contamination of samples is an obvious lack of consistency of the high concentrations with lower values measured in adjacent horizons. Such single-sample "spikes" are rejected from subsequent interpretation.

Trace metal distributions observed during the summer period at stations 1 and 2 are very similar (Figs. 4.18 and 4.19); reasonable agreement also exists between the intra-site measurements. Profiles are generally characterized by uniform distributions above the sediment-water interface and sharp sub-surface concentration gradients in the shallow porewaters. Dissolved Mn concentrations increase sharply below the sediment-water interface to concentrations as high as $\sim 800\text{-}1100 \mu\text{g}\cdot\text{L}^{-1}$ between 10-15 cm depth (Figs. 4.18 and 4.19). Below depths of 10 cm, Mn levels remain fairly constant. Dissolved As closely tracks Mn at both stations. Concomitant increases in As levels result in large sub-surface maxima of $2\text{-}5 \text{mg}\cdot\text{L}^{-1}$ within 10 cm of the sediment-water interface (Figs. 4.18 and 4.19).

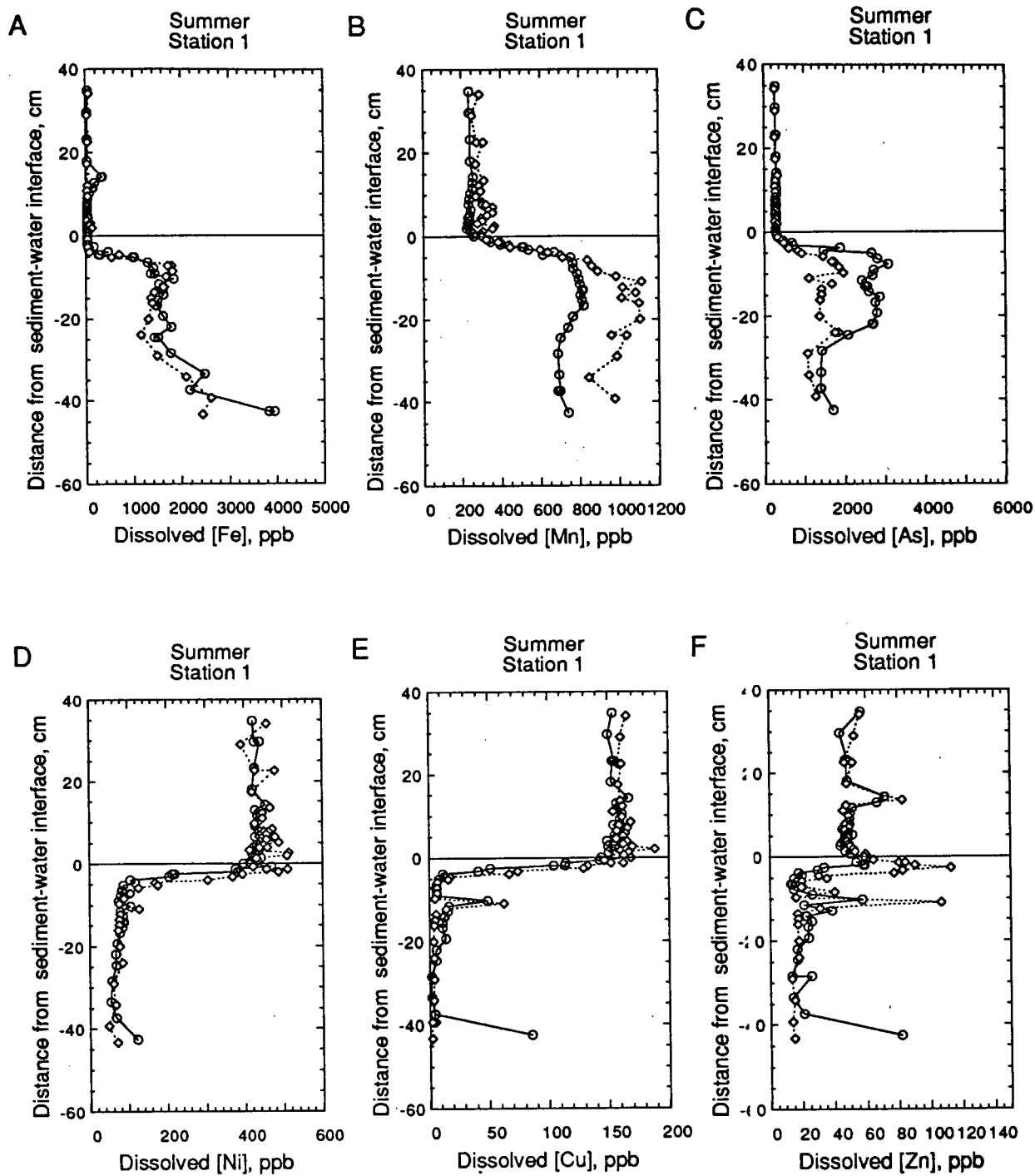


Fig. 4.18. Duplicate summer peeper profiles of dissolved Fe, Mn, As, Ni, Cu and Zn (A-F, respectively) for station 1, Balmer Lake, June, 1993. Replicate samples are represented by double symbols at specific single depths.

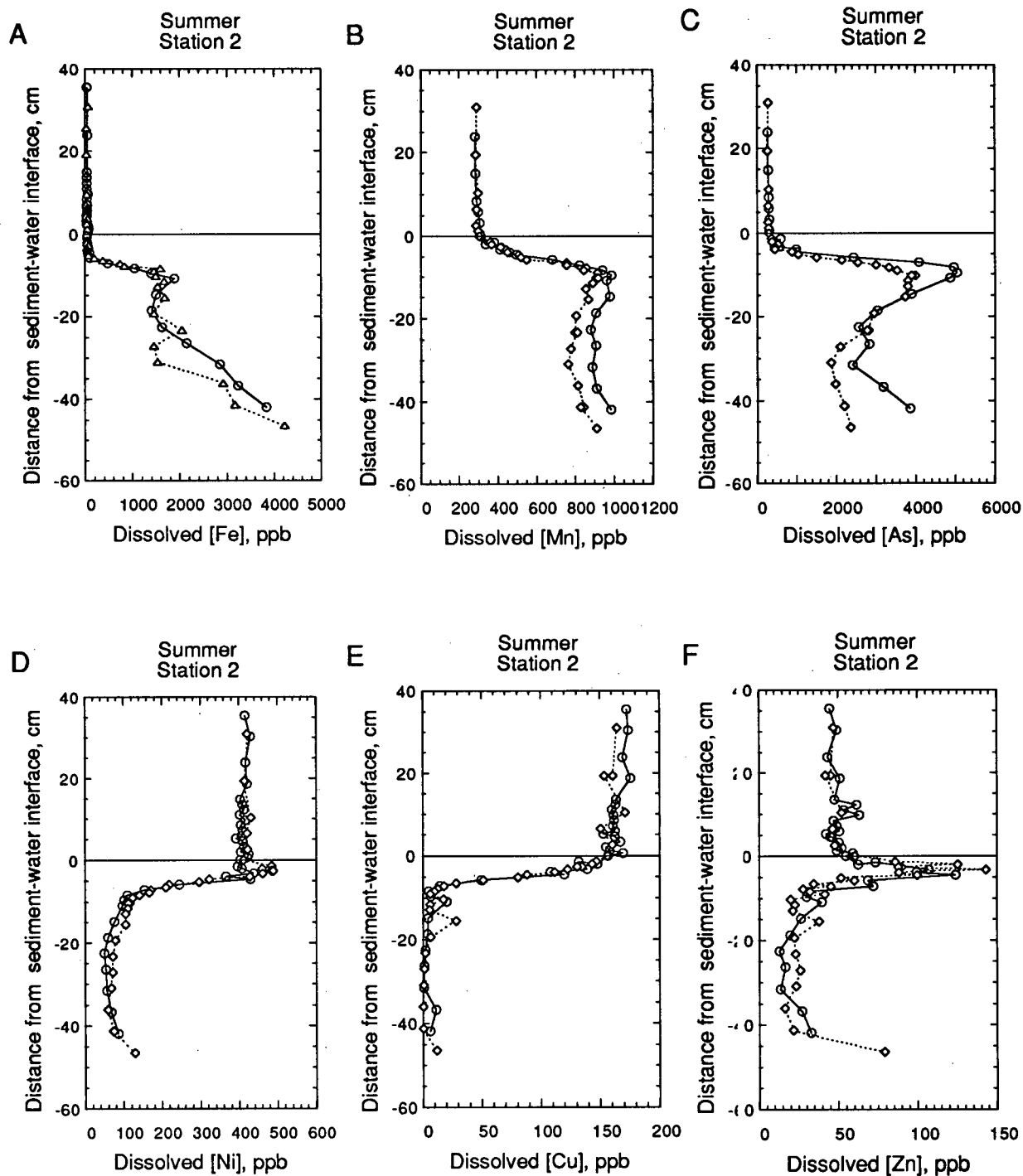


Fig. 4.19. Duplicate summer peeper profiles of dissolved Fe, Mn, As, Ni, Cu and Zn (A-F, respectively) for station 2, Balmer Lake, June, 1993. Replicate samples are represented by double symbols at specific single depths.

As profiles also show evidence of depletion at greater depths. Note that at station 1 (Fig. 4.18), the magnitudes of the subsurface maxima differ significantly.

Significant enrichments of dissolved Fe appear below those observed for manganese. At both stations, concentrations increase rapidly between 5-10 cm, below which gradual increases result in peeper bottom values up to $4 \text{ mg}\cdot\text{L}^{-1}$ (Figs. 4.18 and 4.19). Dissolved Zn profiles exhibit variable sub-surface enrichments in the top 5 cm ranging from $60\text{-}150 \text{ }\mu\text{g}\cdot\text{L}^{-1}$, which immediately fall off to concentrations less than half of the observed water column values. Dissolved Cu and Ni profiles exhibit marked similarity at the two sampled stations (Figs. 4.18 and 4.19). With two exceptions, the concentrations of both elements decrease sharply immediately below the sediment-water interface and remain generally constant below minima of $\sim 5 \text{ }\mu\text{g}\cdot\text{L}^{-1}$ for Cu and $\sim 60 \text{ }\mu\text{g}\cdot\text{L}^{-1}$ for Ni. The exceptions are two dissolved Ni profiles, one at each site, which show evidence of slight subsurface enrichments in the first few centimetres below the interface (Figs. 4.18 and 4.19). Results from the summer period exhibited excellent agreement between bottom water values obtained from peepers and those from concurrently drawn pumped samples (compare Figs. 4.18 and 4.19 with Table 4-1).

The trace metal porewater data for the fall period are comparable to the summer results (Figs. 4.20-4.22). The tandem peepers at station 2 yielded consistent profiles for all constituents (Fig. 4.21). Dissolved Mn and As porewater distributions are nearly parallel. Stations 1 and 2 are characterized by initially steep Mn gradients in the top 5 cm, below which concentrations gradually increase to values ranging from $\sim 700\text{-}1000 \text{ }\mu\text{g}\cdot\text{L}^{-1}$ in the deepest horizons (Figs 4.20 and 4.21). Mn levels in the porewaters of "Tailings Bay" (station 5) steadily increase from $\sim 200 \text{ }\mu\text{g}\cdot\text{L}^{-1}$ at the interface to $1800 \text{ }\mu\text{g}\cdot\text{L}^{-1}$ between 20 and 30 cm. Below this maximum, concentrations drop to $\sim 700 \text{ }\mu\text{g}\cdot\text{L}^{-1}$

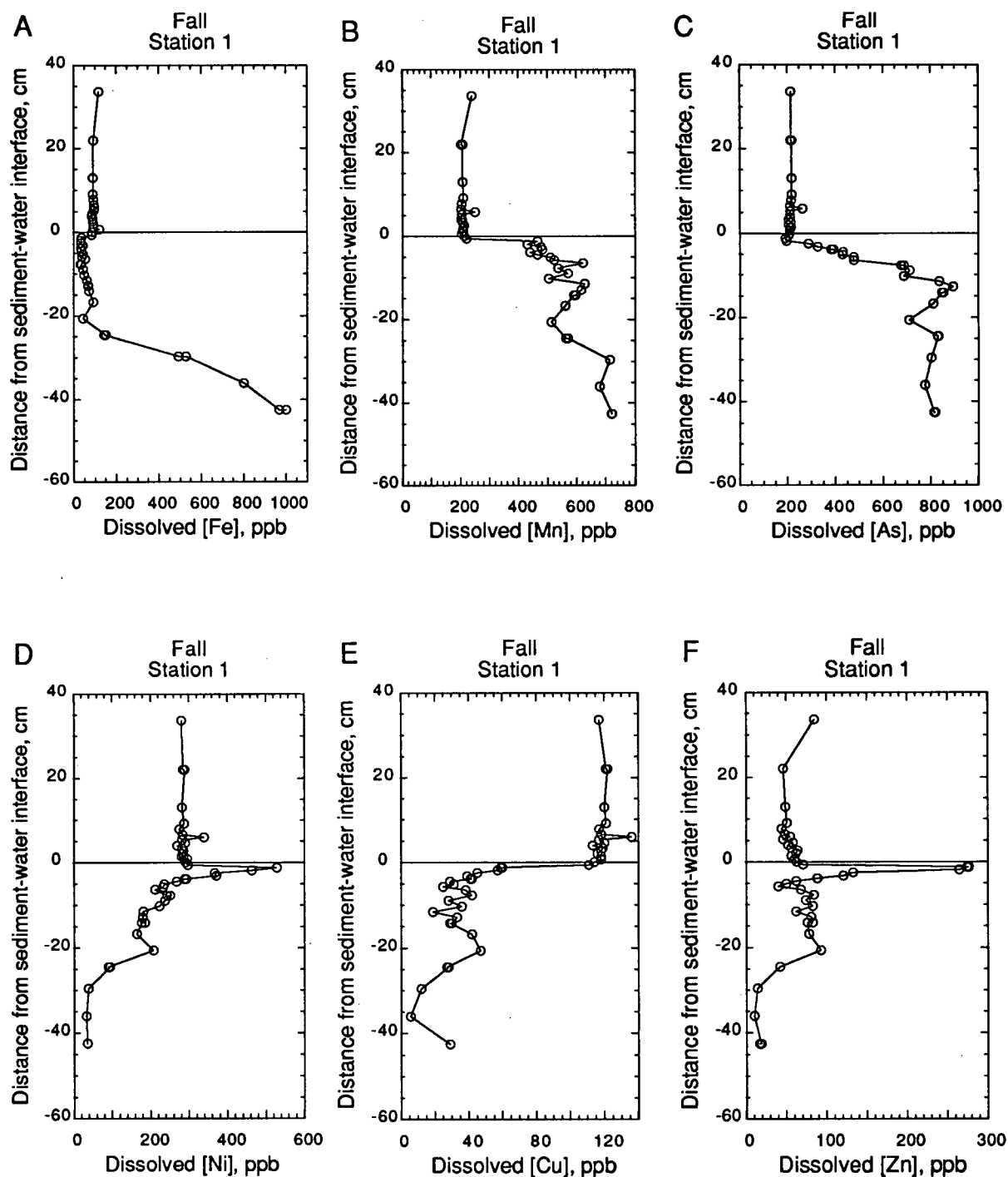


Fig. 4.20. Fall peeper profiles of dissolved Fe, Mn, As, Ni, Cu and Zn (A-F, respectively) for station 1, Balmer Lake, October, 1993. Replicate samples are represented by double symbols at specific single depths.

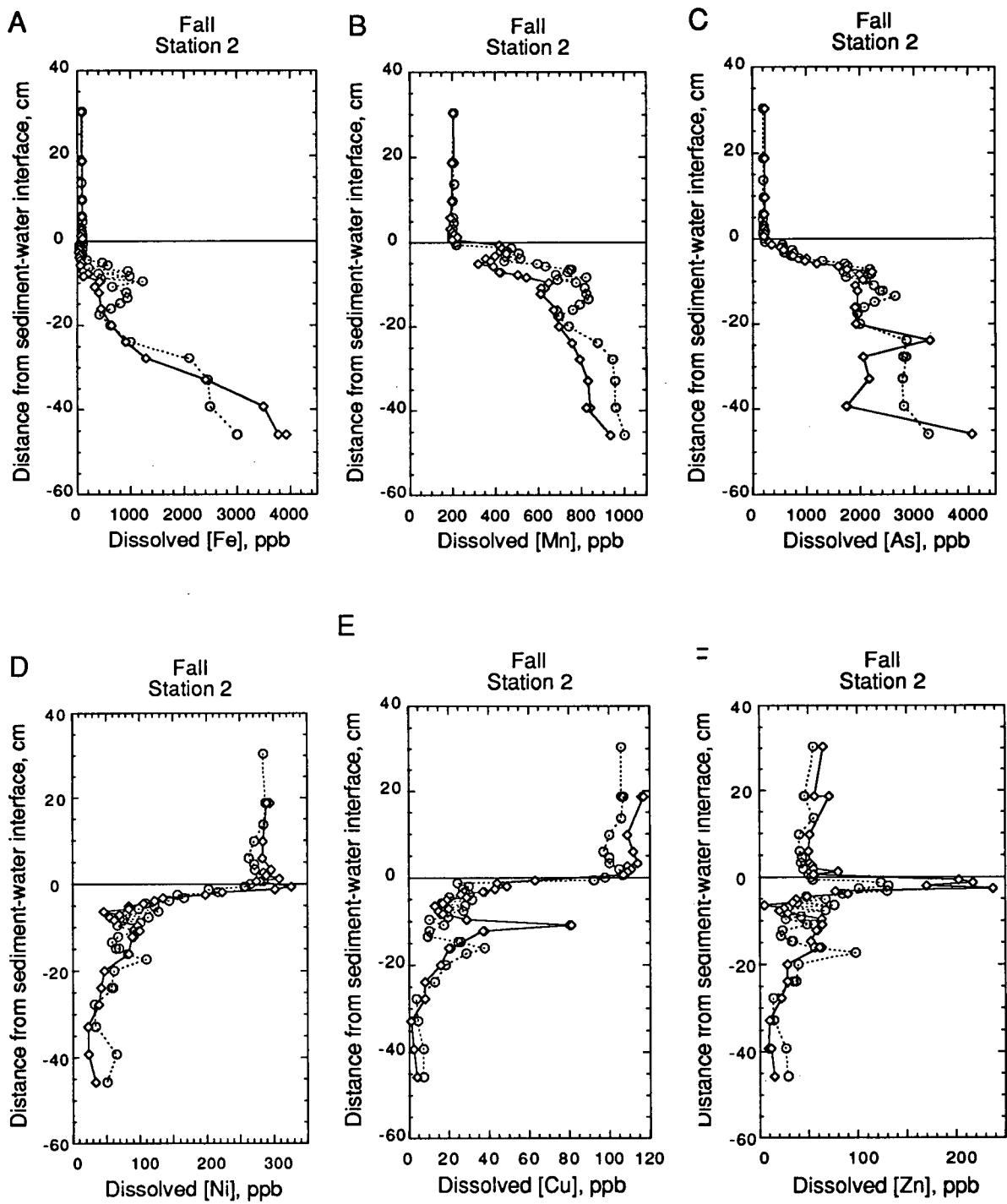


Fig. 4.21. Duplicate fall peeper profiles of dissolved Fe, Mn, As, Ni, Cu and Zn (A-F, respectively) for station 2, Balmer Lake, October, 1993. Replicate samples are represented by double symbols at specific single depths.

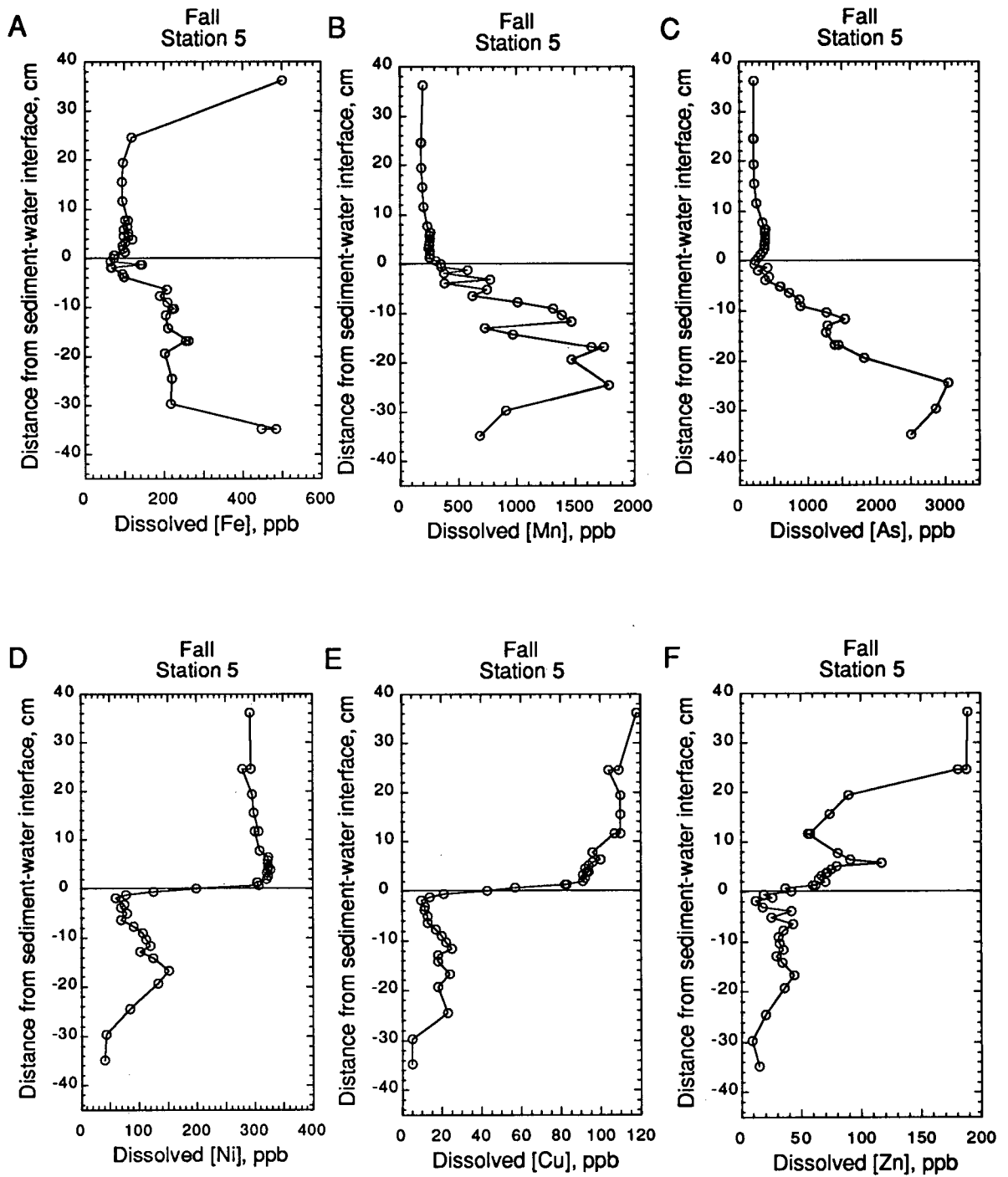


Fig. 4.22. Fall peeper profiles of dissolved Fe, Mn, As, Ni, Cu and Zn (A-F, respectively) for station 5, Balmer Lake, October, 1993. Replicate samples are represented by double symbols at specific single depths.

in the deepest samples (Fig. 4.22). At all stations, dissolved As concentrations begin to rise at shallow sediment depths, reaching maxima between ~900 and 3000 $\mu\text{g}\cdot\text{L}^{-1}$ (Figs. 4.20-4.22).

Dissolved Fe increases in concentration with depth at all sites during the fall period; however, the depths and magnitudes of the enrichments vary. Levels at station 1 remain essentially uniform to a depth of 20 cm whereupon concentrations increase gradually to a maximum of ~1000 $\mu\text{g}\cdot\text{L}^{-1}$ at the base of the profile (Fig. 4.20). Iron distributions seen at stations 2 and 5 are characterized by variable increases starting at 5-10 cm depth (Fig. 4.21 and 4.22), with concentrations rising to values as high as ~3-4 $\text{mg}\cdot\text{L}^{-1}$ in the deepest samples at station 2, but only to 400-500 $\mu\text{g}\cdot\text{L}^{-1}$ at station 5.

Dissolved Zn profiles from the fall at stations 1 and 2 exhibit pronounced, shallow sub-surface enrichments ranging from ~130-300 $\mu\text{g}\cdot\text{L}^{-1}$ (Figs. 4.20 and 4.21). Below these maxima, concentrations decline dramatically to values less than their respective bottom water levels. In contrast to the other sites, dissolved Zn concentrations at station 5 generally decrease from the uppermost sampled bottom waters to shallow sediment depths (Fig. 4.22). Below a few centimetres in the sediment column at this site, dissolved Zn levels decrease marginally (Fig. 4.22).

The bottom water and porewater distributions of dissolved Cu and Ni from the autumn sampling are similar to those seen in the summer, exhibiting minimal lake-wide variability. At stations 1 and 2 (Figs. 4.20 and 4.21), Cu concentrations decline precipitously at shallow sediment depths, approaching minima of <20 $\mu\text{g}\cdot\text{L}^{-1}$ ~5 cm below the interface. Station 5 is characterized by a similar gradient; decreases, however, begin at or slightly above the sediment surface (Fig. 4.22). Steep sub-surface gradients are also evident for dissolved Ni distributions at all stations sampled. Nickel profiles at station 1, and to a lesser

extent at station 2, show distinct subsurface enrichments, before levels dramatically decline immediately below their respective maxima (Figs. 4.20 and 4.21). As seen for Ni, dissolved Cu concentrations at station 5 begin a steep decline at or above the sediment surface (Fig 4.22).

The winter distributions of the various dissolved constituents demonstrate that a dramatic shift in the chemical environment of the bottom waters and porewaters occurs during periods of ice-cover (Figs. 4.23-4.26). The bottom water enrichments of dissolved Mn that were clearly depicted at all sampled stations from water column profiling are similarly represented in their respective peeper profiles. Stations 1, 2 and 4 are characterized by increasing dissolved Mn concentrations throughout the lowermost bottom waters to the interfacial porewaters (Figs. 4.23-4.25). Profiles at stations 1 and 2 continue to increase below the sediment surface, reaching maxima between 1200-1400 $\mu\text{g}\cdot\text{L}^{-1}$ at depths of ~15 and 5 cm, respectively (Figs. 4.23-4.24). At greater depths at these sites, and below the interfacial maximum at station 4, dissolved Mn concentrations decrease to ~600-700 $\mu\text{g}\cdot\text{L}^{-1}$ and remain constant to peeper-bottom (Figs. 4.23-4.25). The bottom waters in "Tailings Bay" (station 6) show no evidence of a near-interface dissolved Mn enrichment; concentrations remain essentially constant to a sediment depth of ~ 10 cm then fall steeply to levels that approach 20-30 $\mu\text{g}\cdot\text{L}^{-1}$ (Fig. 4.26).

Dissolved Fe distributions in the bottom waters and interstitial fractions observed during the winter period exhibit considerable lake-wide variability. Station 1 is characterized by relatively uniform levels of dissolved Fe to a sediment depth of ~5 cm, below which values increase erratically to ~2100 $\mu\text{g}\cdot\text{L}^{-1}$ in the lowest horizons (Fig. 4.23). Concentrations at station 4 remain < 200 $\mu\text{g}\cdot\text{L}^{-1}$ in the bottom waters and porewaters to a sediment depth of ~40 cm, but increase to ~600 $\mu\text{g}\cdot\text{L}^{-1}$ at greater depths (Fig. 4.25). In contrast, the bottom waters

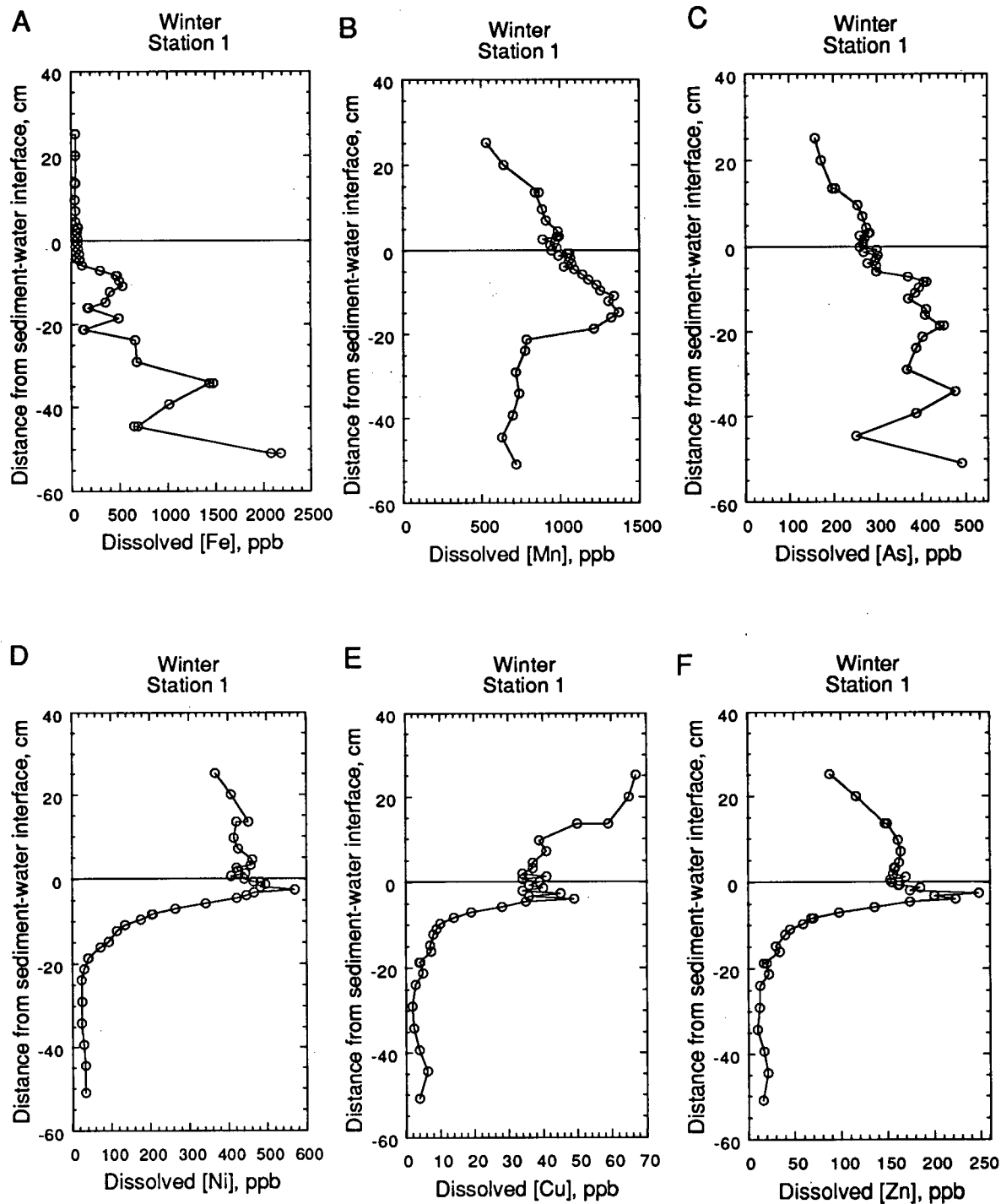


Fig. 4.23. Winter peeper profiles of dissolved Fe, Mn, As, Ni, Cu and Zn (A-F, respectively) for station 1, Balmer Lake, March, 1994. Replicate samples are represented by double symbols at specific single depths.

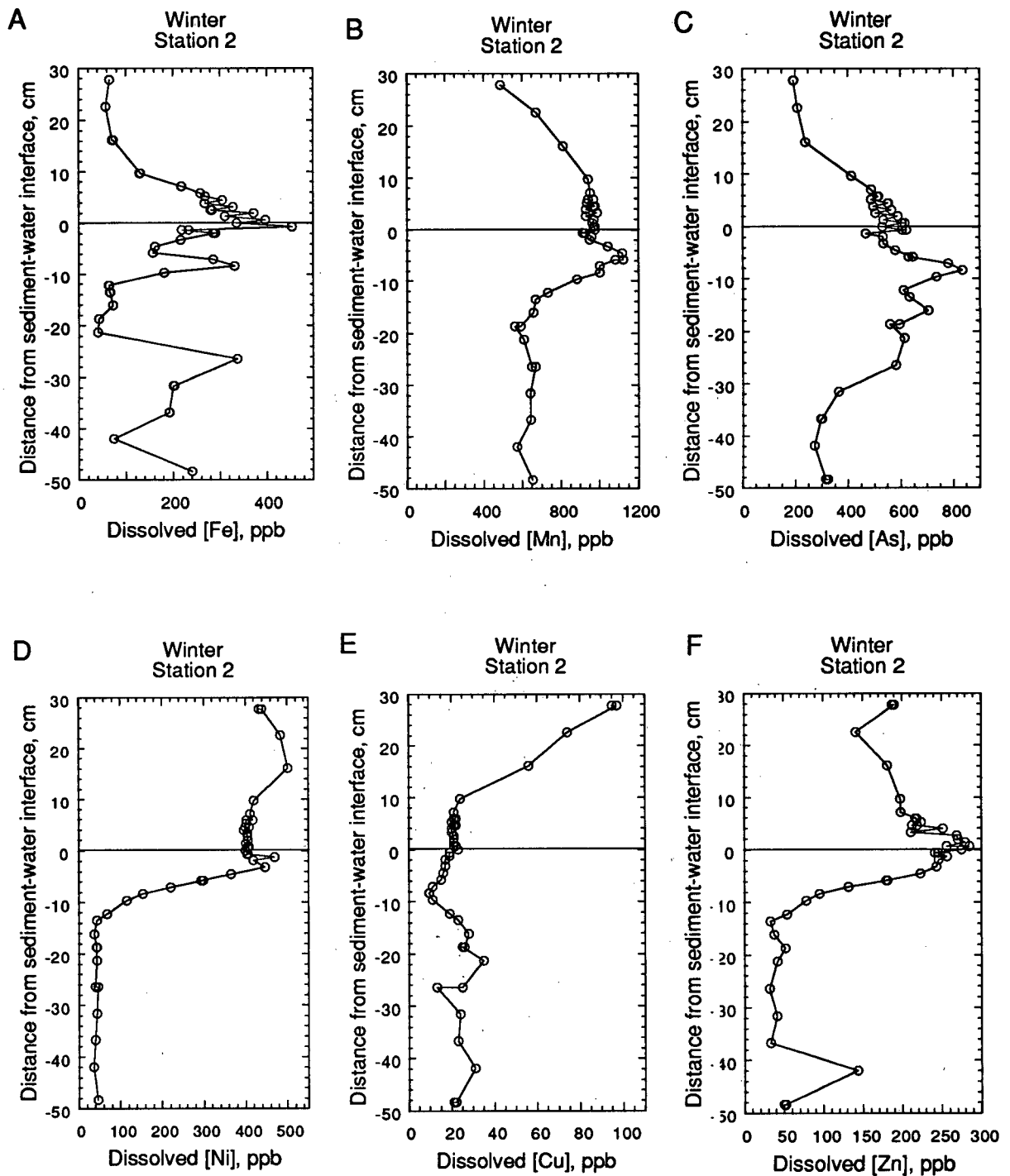


Fig. 4.24. Winter peeper profiles of dissolved Fe, Mn, As, Ni, Cu and Zn (A-F, respectively) for station 2, Balmer Lake, March, 1994. Replicate samples are represented by double symbols at specific single depths.

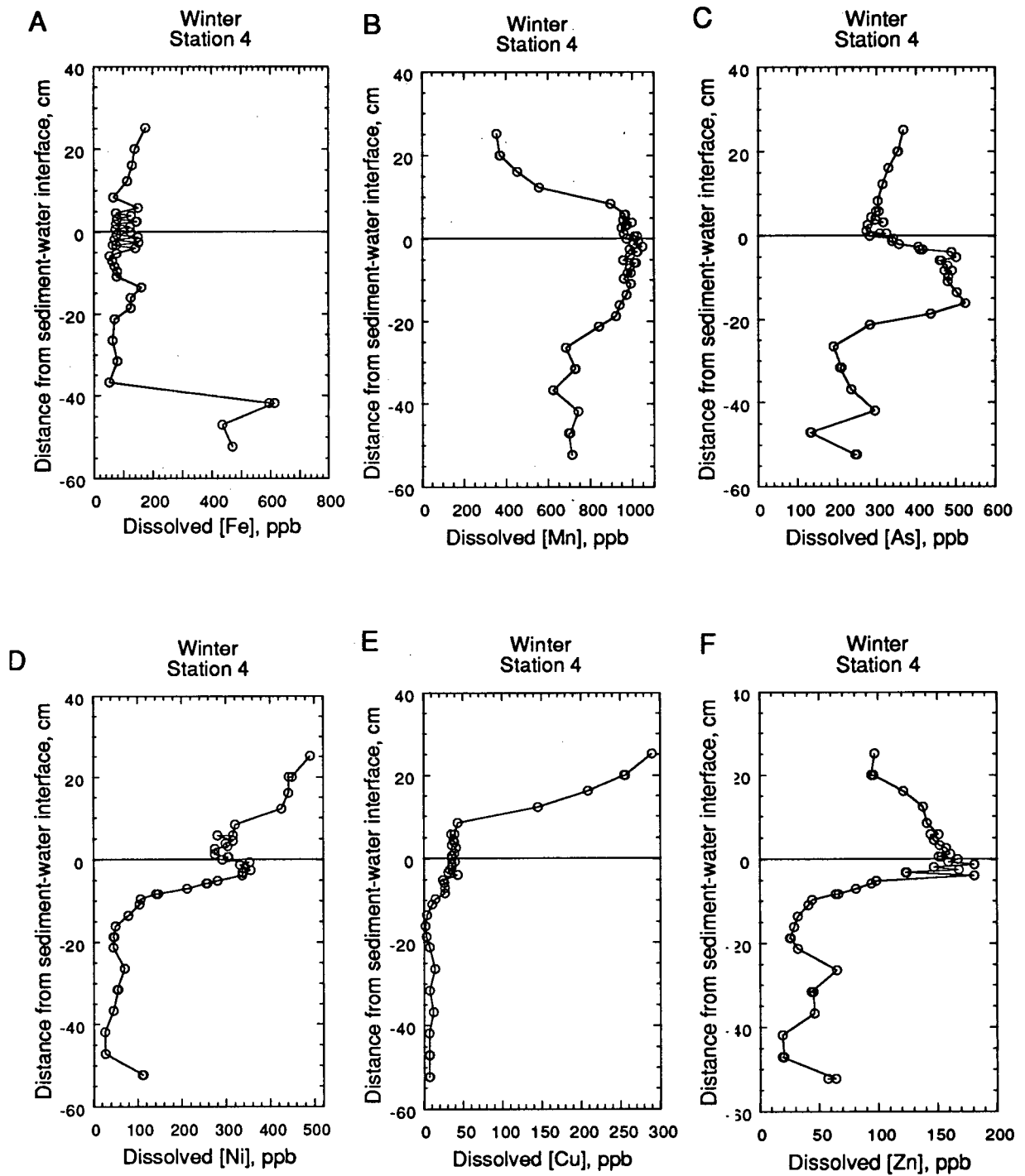


Fig. 4.25. Winter peeper profiles of dissolved Fe, Mn, As, Ni, Cu and Zn (A-F, respectively) for station 4, Balmer Lake, March, 1994. Replicate samples are represented by double symbols at specific single depths.

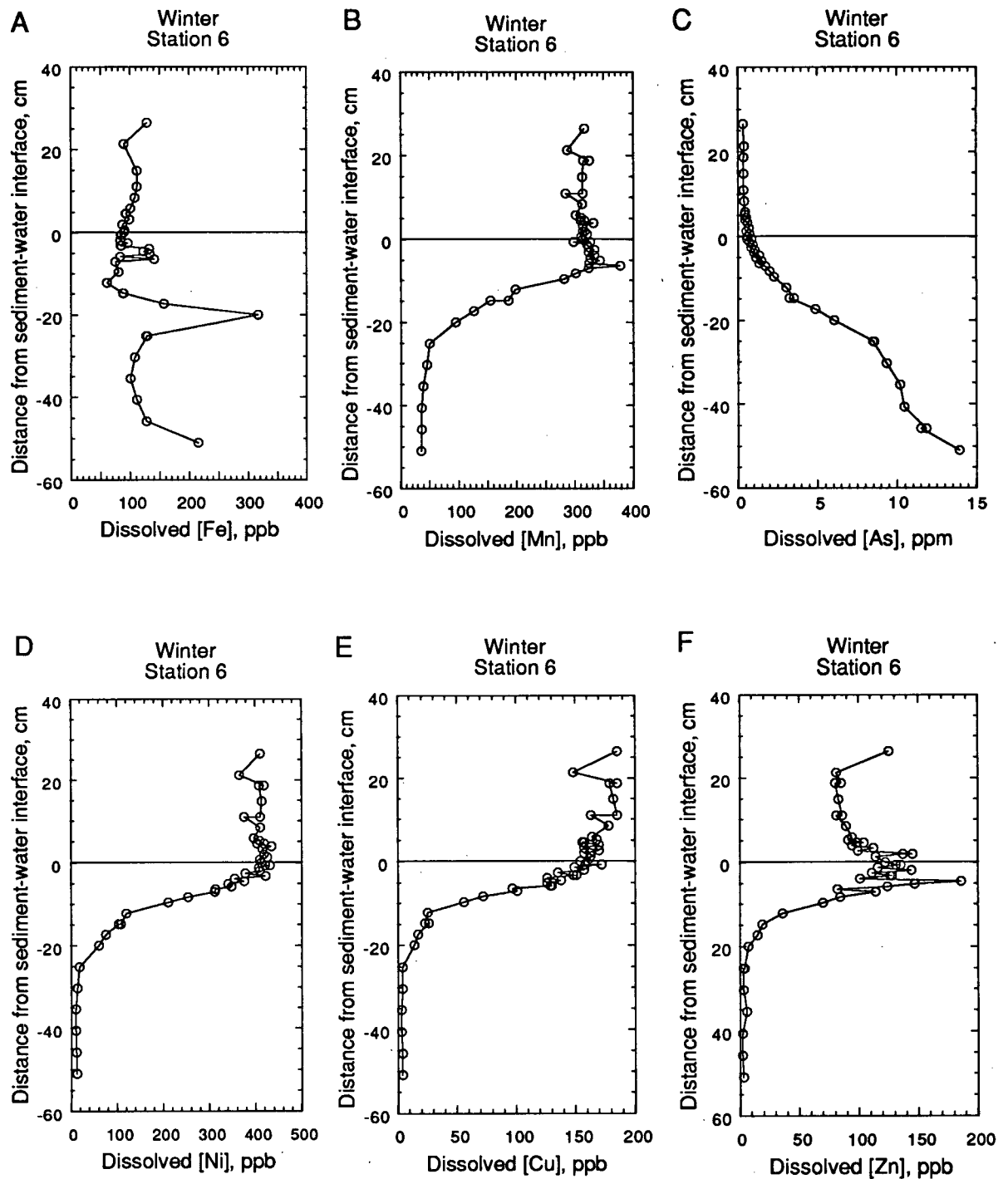


Fig. 4.26. Winter peeper profiles of dissolved Fe, Mn, As, Ni, Cu and Zn (A-F, respectively) for station 6, Balmer Lake, March, 1994. Replicate samples are represented by double symbols at specific single depths.

immediately above the sediment surface at station 2 are enriched in dissolved Fe. Below the interface, concentrations fluctuate significantly throughout the sediment column (Fig. 4.24).

The strong similarities between the distributions of dissolved As and Mn observed for the summer and fall periods are not clearly obvious during the winter session. The As profiles at stations 1 and 2 are characterized by zones of generally increasing concentration, extending from the bottom waters, across the sediment-water interface, to depths of ~20 and 10 cm, respectively (Figs 4.23 and 4.24). Dissolved As profiles at stations 4 and 6 exhibit uniform bottom water values and increased levels at shallow sediment depths (Figs. 4.25 and 4.26). A zone of relatively high As concentrations between ~5 and 15 cm depth at station 4, overlies porewaters that contain variably lower concentrations (Fig. 4.25). Dissolved As at station 6 increases essentially monotonically throughout the sampled sediment column (Fig. 4.26).

Dissolved zinc distributions during the winter period are similar to those observed for other seasons; profiles are characterized by variable increases near the interface at each site, below which levels decline sharply to minima in the top two decimetres (Figs. 4.23-4.26). The well-defined bottom water enrichment of dissolved Zn seen at station 1, corroborates that observed in the water-column sample set (Fig. 4.23). Similar maxima at stations 2 and 4, although evident from water column profiling, are not as clearly defined by the peeper data (Figs. 4.24 and 4.25).

The winter distributions of dissolved Ni demonstrate significant lake-wide consistency and resemble profiles observed during other seasons (Figs. 4.23-4.26). Gradients in bottom waters are not distinct in the peeper profiles except perhaps at station 4, where the concentration decrease accords with the respective water column profile (see Fig. 4.11D). At all stations, dissolved Ni concentrations

diminish abruptly from values of 300-450 $\mu\text{g}\cdot\text{L}^{-1}$ in bottom waters to minima of < 40 $\mu\text{g}\cdot\text{L}^{-1}$ in the first two decimetres (Figs. 4.23-4.26). Slight sub-surface maxima can be seen at stations 1, 2 and 4 (Figs. 4.23-4.25).

The gradients of dissolved Cu in winter bottom waters seen in the water column sample set (Figs. 4.8-4.11) are verified by corresponding peeper data (Figs. 4.23-4.26). Profiles at stations 1, 2 and 4 clearly illustrate the zone of decreasing dissolved Cu concentrations above the interface (Figs. 4.23-4.25). Below this horizon, values continue to decline at stations 1 and 4 to concentrations < 10 $\mu\text{g}\cdot\text{L}^{-1}$ (Figs. 4.23 and 4.25). Station 6 is characterized by a more intense sub-surface gradient where levels decrease from over 400 to < 20 $\mu\text{g}\cdot\text{L}^{-1}$ in the top 20 cm (Fig. 4.26).

Sampling conducted in the spring following ice break-up yielded bottom water and porewater distributions of dissolved trace metals comparable to those seen during the well-mixed periods of summer and fall. Logistic and sampling problems restricted the deployment of only two peepers which were emplaced 20 m apart at station 1. Concentrations for all constituents exhibit uniform profiles in the bottom waters and agree well with independently measured water column values (compare Fig. 4.27 with Table 4.4). Reproducibility between the profiles was fair for dissolved Cu and Ni, but limited for Fe, Zn and As.

Dissolved Mn contents in the spring porewaters at station 1 sharply increase at shallow sediment depths to maxima ranging from ~820-1100 $\mu\text{g}\cdot\text{L}^{-1}$ (Fig. 4.27). Below these peaks, concentrations steadily decline to values of ~500-700 $\mu\text{g}\cdot\text{L}^{-1}$ at ~40 cm depth. The dissolved Fe profiles are characterized by dissimilar sub-surface enrichments. Concentrations obtained from peeper 1 remain constant to a depth of ~20 cm, at which point levels increase rapidly to ~1 $\text{mg}\cdot\text{L}^{-1}$ in the deepest horizons (Fig. 4.27). Conversely, the profile of peeper 2 shows only slight enrichments up to ~400 $\mu\text{g}\cdot\text{L}^{-1}$ between depths of 10 and 20 cm.

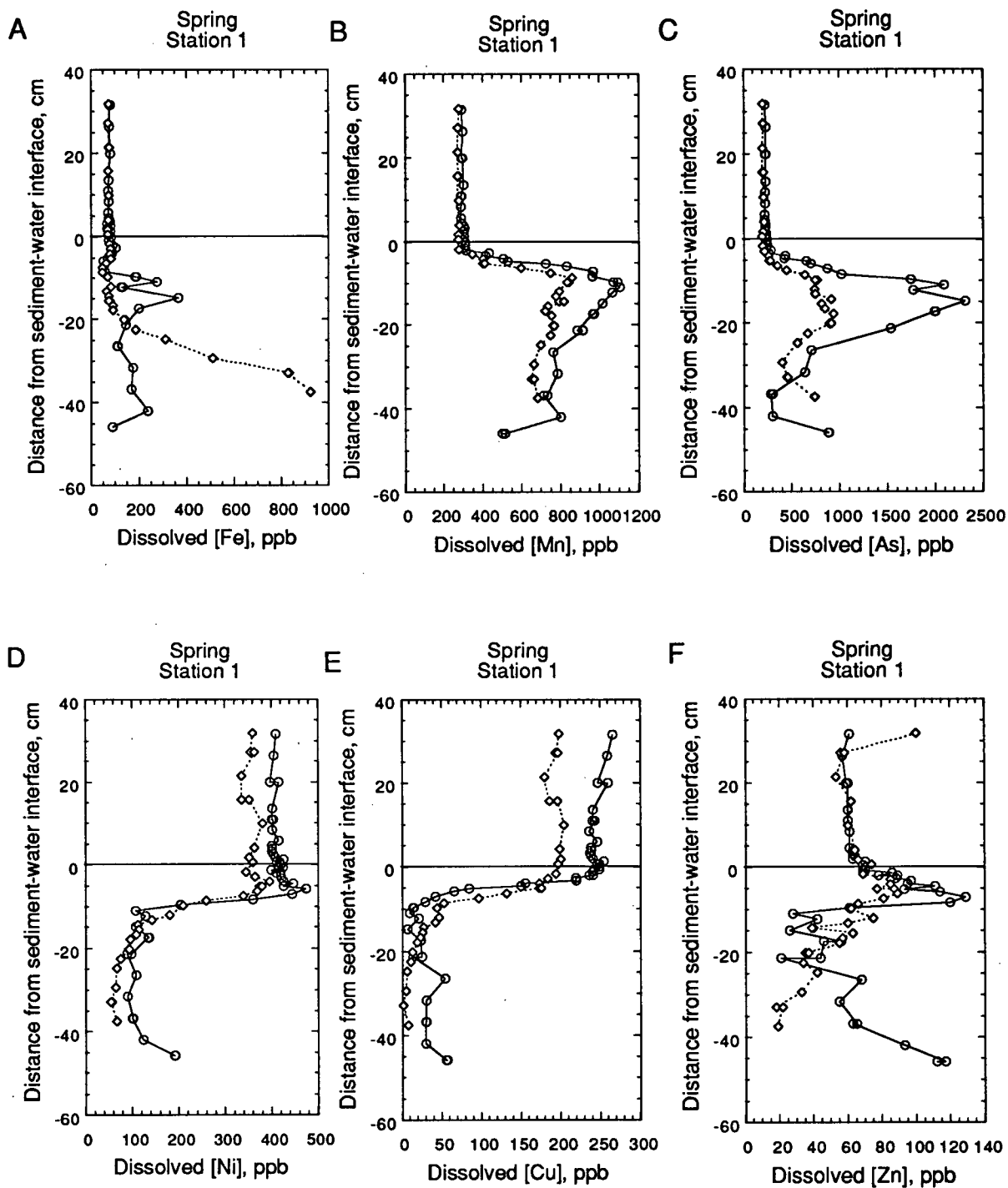


Fig. 4.27. Duplicate spring peeper profiles of dissolved Fe, Mn, As, Ni, Cu and Zn (A-F, respectively) for station 1, Balmer Lake, May, 1994. Replicate samples are represented by double symbols at specific single depths.

The distributions of dissolved As and Zn are both characterized by sub-surface enrichments in the shallow porewaters at station 1. Variable As maxima occur between depths of 10-20 cm; concentrations below these enriched horizons generally decrease to peeper bottom (Fig. 4.27). Profiles of dissolved Zn also exhibit broad maxima of variable magnitude between the sediment surface and depths of ~10 cm (Fig. 4.27). Concentrations in one profile steadily decline at greater depths, while in the other (peeper 2), they increase again below a minimum confined between 10 and 20 cm depth.

Although bottom water concentrations of dissolved Ni and Cu obtained from peeper 1 are significantly lower than those from peeper 2 (Fig. 4.27), their profiles match well at shallow sediment depths. Sharp decreases are evident for both elements in close proximity to the sediment surface, and minima are approached in the first decimetre. Dissolved Ni profiles exhibit subtle sub-surface maxima at depths of 5 cm.

4.2.1.3 pH

In the spring sampling period, selected cells down the length of one peeper at station 1 were measured for pH by direct insertion of the probe into each chamber. The pH profile is fairly uniform, with values ranging from 7.32-8.02 (Fig. 4.28). A slight increase in the vicinity of the interface contrasts with a subtle decrease towards deeper horizons.

Spring Station 1

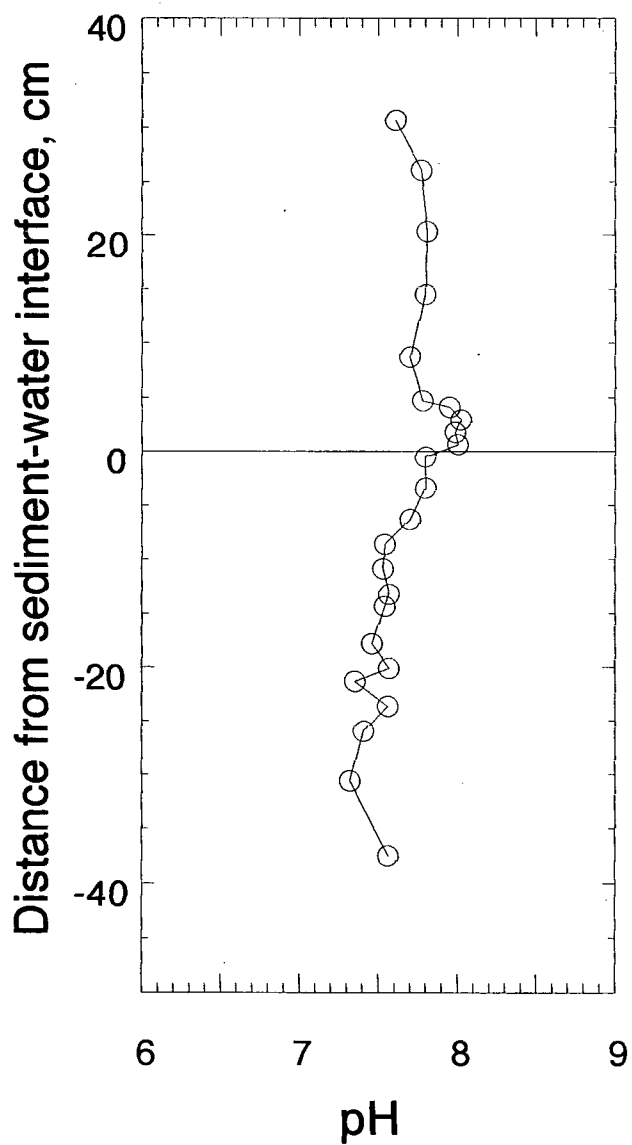


Fig. 4.28. Spring profile of porewater and bottom water pH measured from peeper 2, station 1, Balmer Lake, May, 1994.

4.2.2 Core Porewaters

4.2.2.1 Nutrients and Sulphate

Analytical results obtained from centrifuged core samples have been plotted against peeper-derived profiles in order to compare the two methods. Core porewaters were not analyzed for ammonium; consequently, peeper/core comparisons are limited to nitrate and sulphate concentrations. The interstitial nitrate and sulphate fractions from duplicate cores at station 1 demonstrate excellent inter-core coherence and agree well with peeper values (Fig. 4.29). Concentrations determined from the core supernatant, however, disagree with lowermost bottom water measurements acquired from peeper sampling. It appears the composition of the core-top waters are similar to values measured 20-30 cm above the sediment surface. Examination of the data revealed that the disparity is not due to any analytical difficulty, but instead reflects a design limitation of the corer. The upper portion of the sleeve valve of the corer has two large ports which allow upward-flowing water to escape during instrument descent. However, the flow is not free, in that the total cross-sectional area of the ports is less than that of the mouth of the core barrel. The resistance to the flow of water through the instrument ports during lowering causes some water inside the barrel to be carried down with the corer, for probably not more than 1-2 metres. In regions of fine-scale stratification, there is the potential for the supernatant water to consist of a mixture of waters from distinct layers. In addition, the top corer ports sit 30-50 cm above the sediment surface, a distance greater than the thickness of the compositionally distinct strata observed in the bottom waters. Since the core-top waters most likely represent an integrated sample of the lower bottom waters, data from these samples have been plotted 20

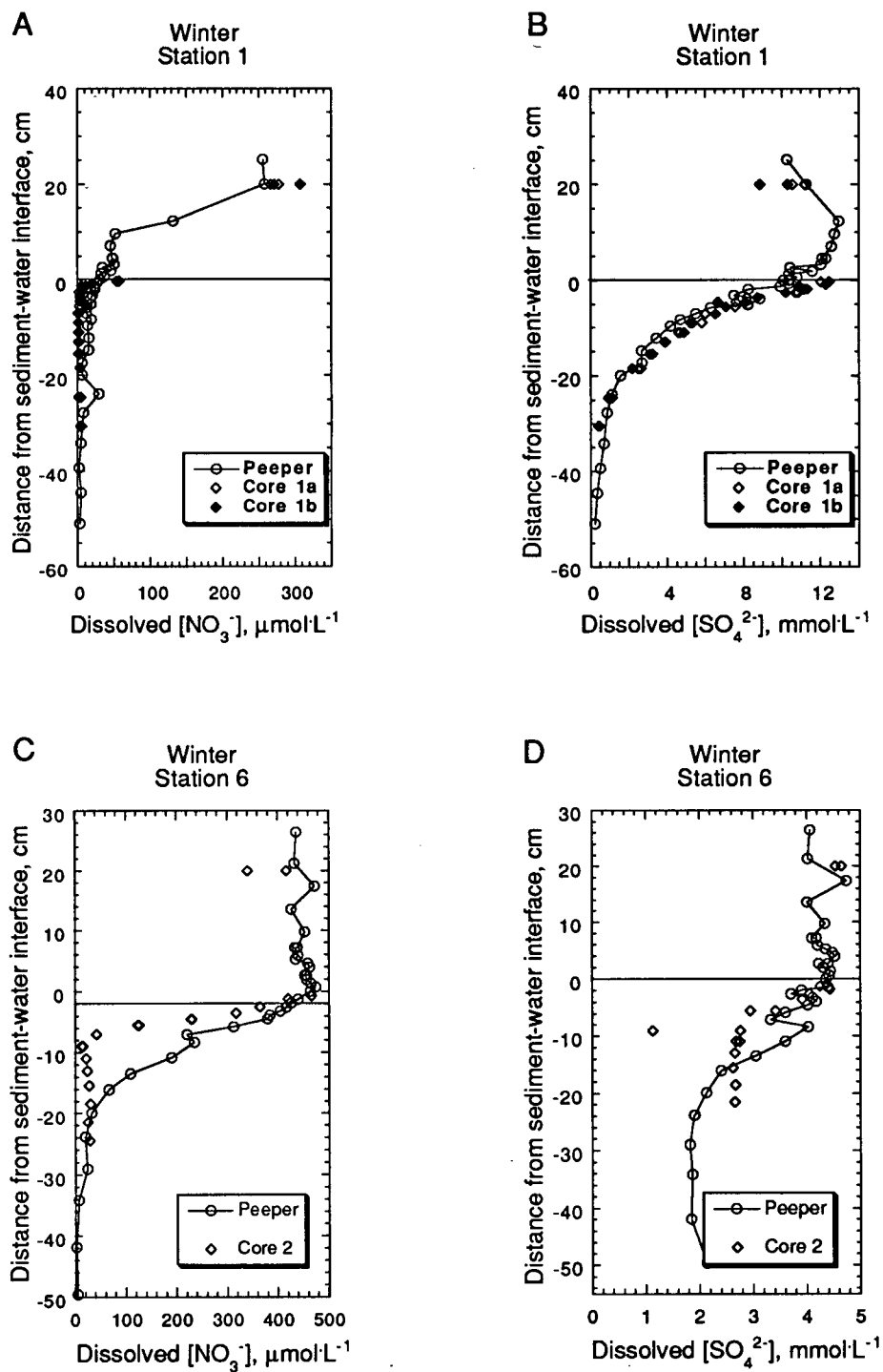


Fig. 4.29. Distributions of dissolved NO_3^- and SO_4^{2-} obtained from peeper (open circles) and core porewaters (diamonds) at station 1 (A-B) and station 6 (C-D), Balmer Lake, March, 1994. Replicate samples are represented by double symbols at specific single depths.

cm above the sediment-water interface. In the following discussion, however, only peeper-derived bottom water values will be used in comparisons with shallow porewaters.

The core-derived nitrate profile in the sediments in "Tailings Bay" (station 6) exhibits a steeper sub-surface gradient than the analogous peeper profile; core values approach minima at a sediment depth of 10 cm as opposed to 20 cm (Fig. 4.29). Excluding one presumably contaminated core sample, the corresponding sulphate distributions parallel one another reasonably well.

4.2.2.2 Trace Metals

The duplicate trace metal distributions obtained from core samples at station 1 are generally similar in form but exhibit variable congruence with the respective peeper profiles. Dissolved Fe concentrations at station 1 increase at depth, with core-derived profiles exhibiting steeper gradients (Fig. 4.30). The magnitudes of sub-surface dissolved Mn maxima differ markedly in the two cores; core 1b is comparable to the maximum in the peeper profile, albeit shallower, while the corresponding peak in core 1a is $\sim 400 \mu\text{g}\cdot\text{L}^{-1}$ less. Fundamental differences are evident in comparisons of dissolved As distributions. Core-derived duplicate profiles show dramatic sub-surface enrichments in excess of $1200 \mu\text{g}\cdot\text{L}^{-1}$ at 5 cm depth; such increases are not observed in the peeper profile (Fig. 4.30). Distributions for dissolved Ni, Cu and Zn at station 1 exhibit better agreement between their respective core and peeper profiles; decreases in their concentrations occur abruptly at shallow sediment depths. The core-derived sub-surface gradients for all three elements, however, are steeper than those seen in the peeper profiles (Fig. 4.30).

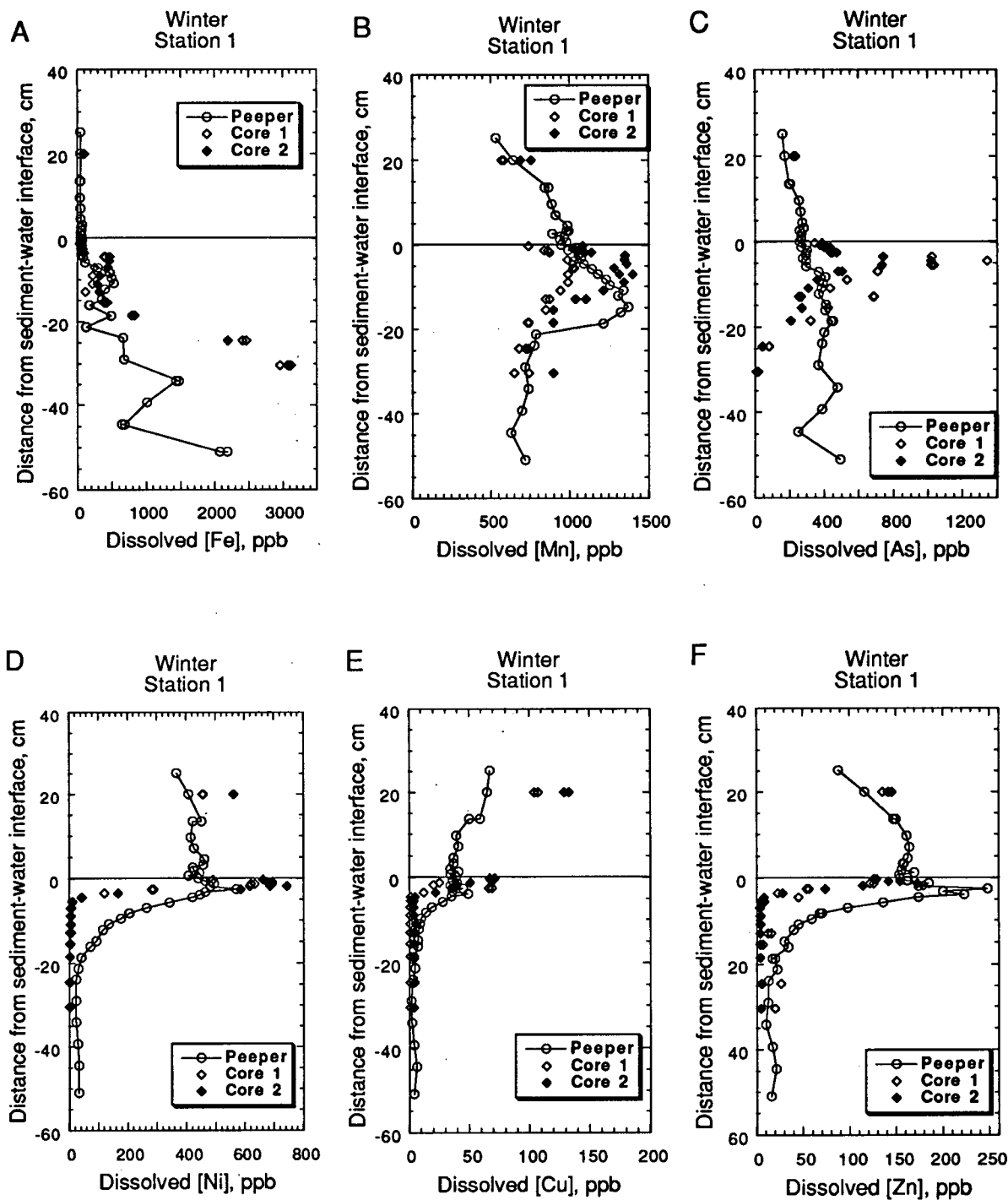


Fig. 4.30. Dissolved distributions of dissolved Fe, Mn, As, Ni, Cu and Zn (A-F, respectively) obtained from peeper (open circles) and core porewaters (diamonds) at station 1, Balmer Lake, March, 1994. Replicate samples are represented by double symbols at specific single depths.

The differences in peeper- and core-derived trace metal profiles at station 6 are similar to those at station 1 (Fig. 4.31). For most elements, gradients in the core porewaters are steeper. For example, decreases in dissolved Mn, Ni, Cu and Zn in core 2 occur over a sediment depth one-half that of decreases of similar magnitude in the peeper profile. Similarly, porewater As increases more rapidly with depth in the core porewaters (Fig. 4.31)

4.3 Sediments

Three high quality cores were obtained using the lightweight gravity corer described by Pedersen *et al.* (1985). Duplicate cores 1a and 1b were collected approximately 3 m apart in the more "natural" sediments at station 1, while core 2 was taken from a predominantly tailings region in "Tailings Bay" (station 6). Core logs are presented in Appendix D.

Duplicate cores 1a and 1b were visually and compositionally identical. Both cores were veneered by a 2 to 3 mm thick cap of brown noncohesive very fine-grained sediment. The top two centimetres were additionally characterized by alternating light/dark millimetre-scale laminations. These surface horizons were underlain by ~2 cm of gray, homogenous, less-cohesive ooze which graded into a black layer occupying a depth from 4 to 8 cm. Small bubbles, presumably methane, were evident in the latter. Below the 10 cm horizon, a homogeneous gray/chocolate brown ooze comprised the remainder of the core. Core 2, collected from station 6 in "Tailings Bay" was very different from the duplicate cores obtained at station 1. Most of the core comprised homogeneous, very fine grained, light-gray, silty tailings material; intermittent thin amber bands (~1 mm thick) occurred in the top 3 cm.

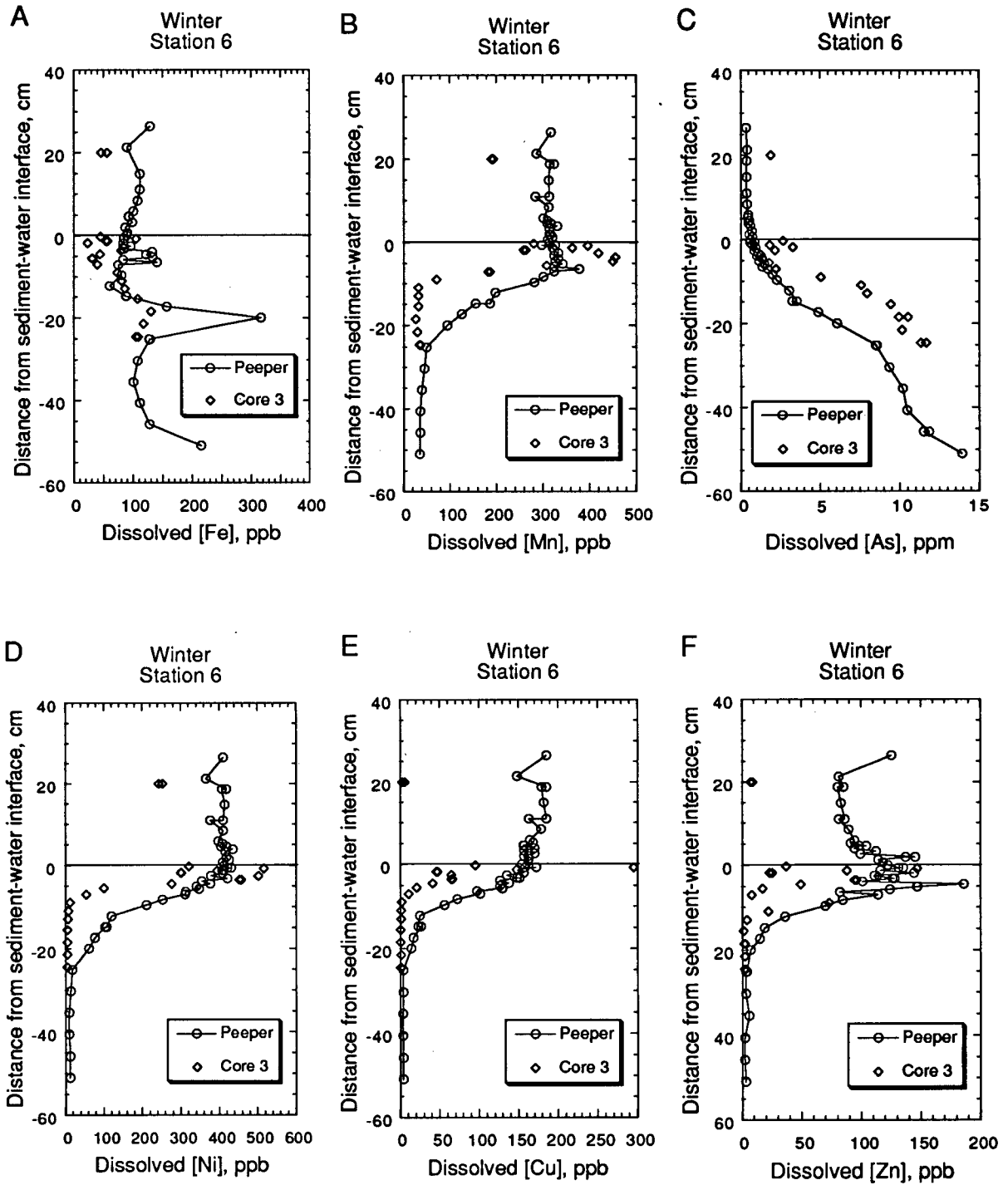


Fig. 4.31. Dissolved distributions of dissolved Fe, Mn, As, Ni, Cu and Zn (A-F, respectively) obtained from peeper (open circles) and core porewaters (diamonds) at station 6, Balmer Lake, March, 1994. Replicate samples are represented by double symbols at specific single depths.

The "natural" sediments at station 1 and the tailings deposits at station 6 are compositionally distinct, particularly below 10 cm depth, as shown by the solid-phase ratio data (Figs. 4.32-4.33). Below the 10 cm horizon, the distributions of most parameters remain essentially constant at both sites. The upper decimetre at station 1 has clearly received a significant input of anthropogenic material.

XRD analyses indicate that the "natural" Balmer Lake sediments and the tailings material represent two distinct mineralogical assemblages; the major and minor elemental compositions of the three cores are reported in Appendix E. The natural deposits contain variable mixtures of quartz and feldspar (mainly plagioclase). These contrast with the tailings deposits, which are relatively feldspar-poor and replete with quartz, abundant clay minerals and halite. The clay fraction is composed primarily of chlorite, with minor contributions from montmorillonite and micaceous minerals (illite and biotite). Both natural sediment and tailings signatures are evident in the top horizons.

Cores 1a and b consist of essentially tailings-free, organic-rich sediments below ~10 cm depth, as shown by the C_{org} , nitrogen, P, Ni, Cu, Zn and As distributions (Figs. 4.34-4.35). Extraordinarily high metal concentrations in the top several centimetres of both cores, reaching up to ~0.5 wt. % Ni, 1.8 wt. % Cu, 0.6 wt. % Zn and 0.5 wt. % As (Fig. 4.35), demonstrate that the upper stratum is composed of a mixture of tailings material and natural deposits, which is capped by a 0.5 to 1 cm thick surface veneer of more natural sediments. The opposing $CaCO_3$ and organic carbon distributions in the upper 7 cm reflect dilution of natural sediments by relatively carbonate-enriched tailings (Fig. 4.34). The data in Figures 4.34E and 4.35A imply that S and Mn are also enriched in the tailings component at station 1.

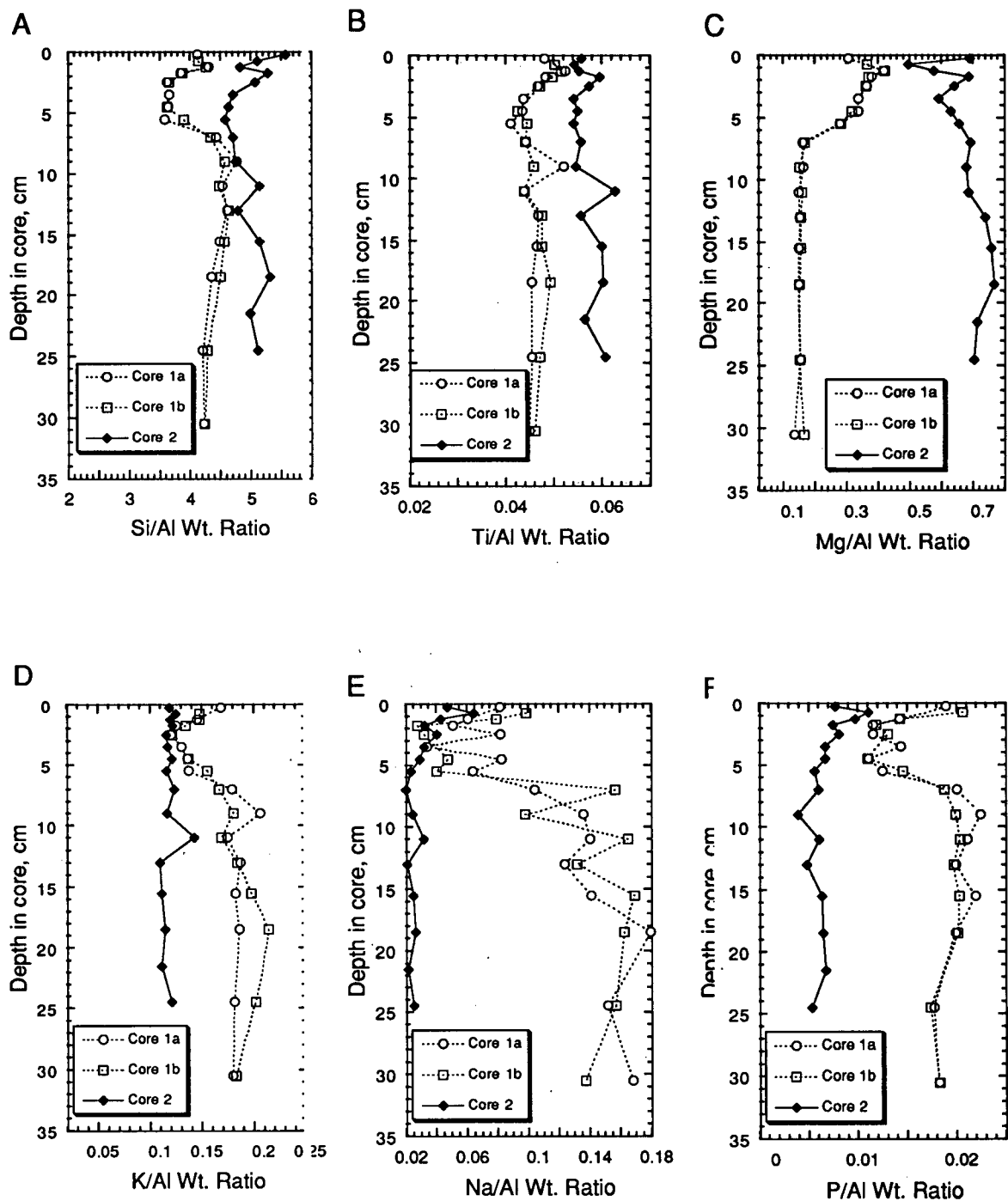


Fig. 4.32. Sedimentary weight ratio profiles of Si/Al, Ti/Al, Mg/Al, K/Al, Na/Al and P/Al (A-F, respectively) for station 1 (duplicate cores 1a and 1b, open symbols) and station 6 (core 2, closed symbols), Balmer Lake, March, 1994.

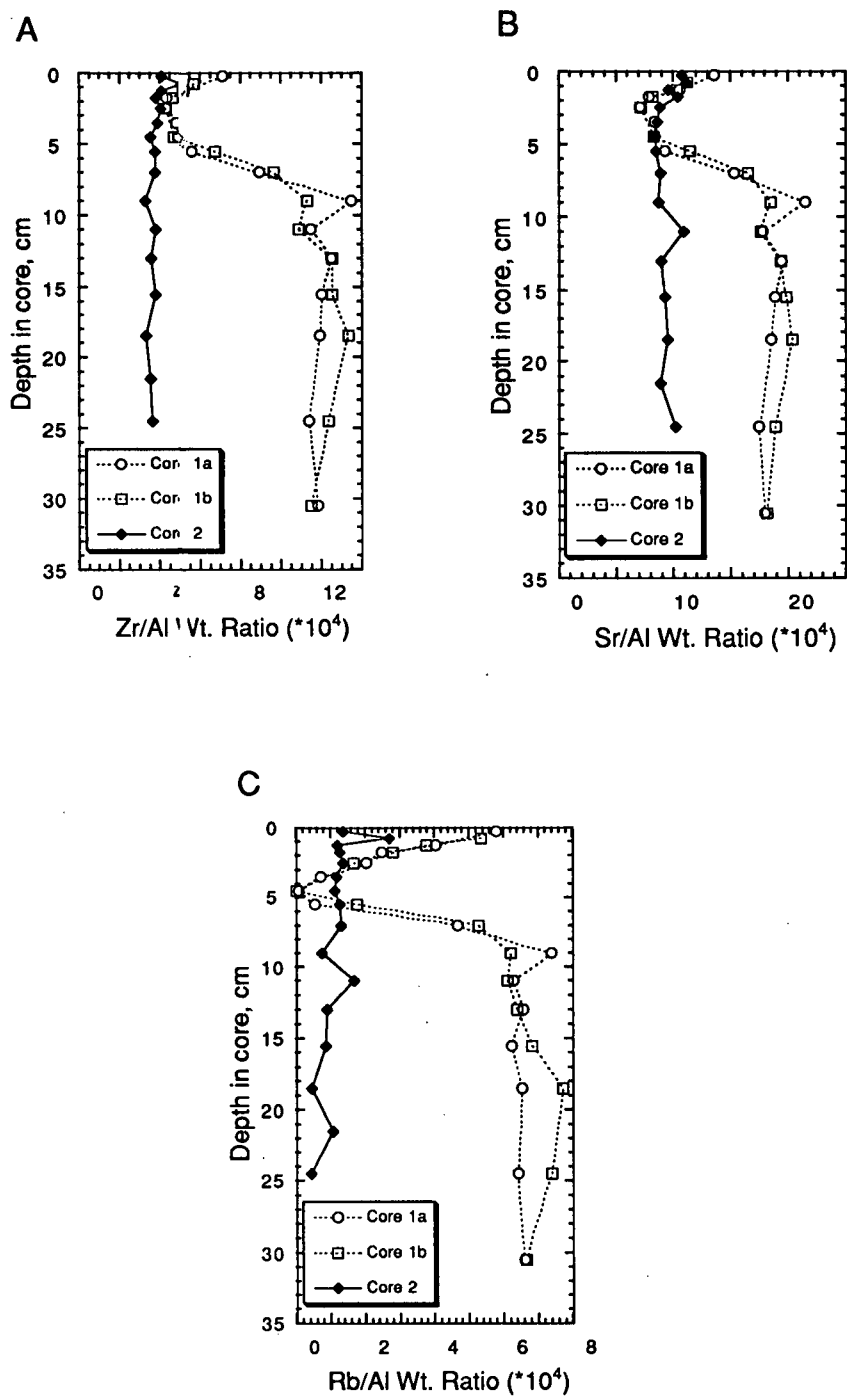


Fig. 4.33. Sedimentary weight ratio profiles of Zr/Al, Sr/Al and Rb/Al (A-C, respectively) for station 1 (duplicate cores 1a and 1b, open symbols) and station 6 (core 2, closed symbols), Balmer Lake, March, 1994.

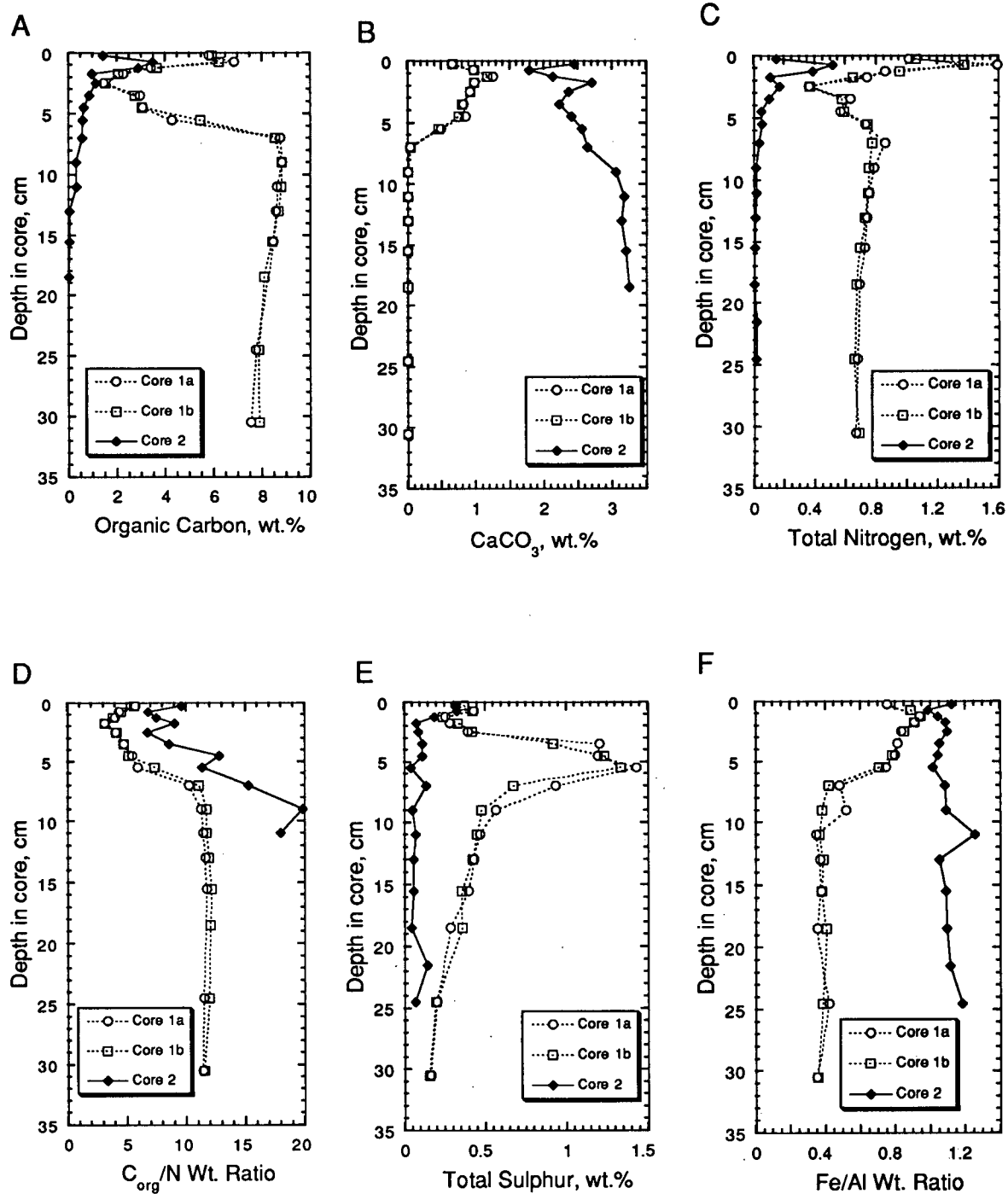


Fig. 4.34. Sedimentary concentrations of organic carbon, calcium carbonate, total nitrogen, values for organic carbon/nitrogen, total sulphur and iron/aluminum weight ratios (A-F, respectively), for station 1 (duplicate cores 1a and 1b, open symbols) and station 6 (core 2, closed symbols), Balmer Lake, March, 1994.

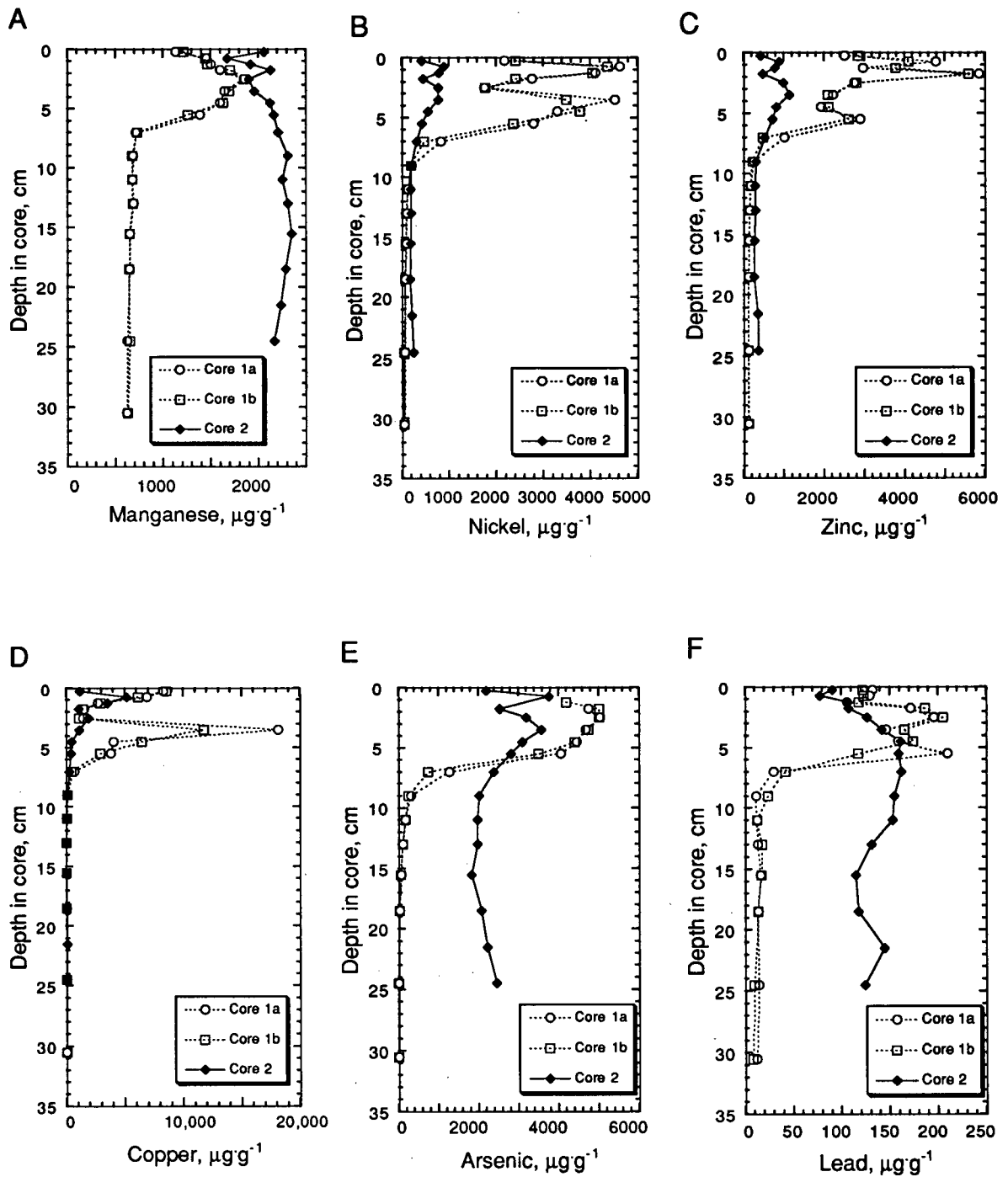


Fig. 4.35. Sedimentary concentrations of manganese, nickel, zinc, copper, arsenic, and lead (A-F, respectively) for station 1 (duplicate cores 1a and 1b, open symbols) and station 6 (core 2, closed symbols), Balmer Lake, March, 1994.

In contrast to the "natural" sediments site, "Tailings Bay" sediments (core 2) are characterized by higher carbonate contents, low overall organic C, total S, and total N and P contents, and higher Fe/Al weight ratios (Fig. 4.34). Paradoxically, the concentrations of total sulphur and trace elements (e.g., Ni, Cu, Zn and As) are significantly depressed at shallow sediment depths relative to maximum values observed at station 1 (Fig. 4.34 and 4.35). Profiles for Mn, Ni, Zn, Cu, As, total S, and Fe/Al are essentially invariant throughout the sampled sediment column, with the exception of slight surficial enrichments in Cu and As.

The compositional contrasts between the two lake sites can be further assessed by means of element/Al ratios. Variations in such ratios can be interpreted in terms of the texture and mineralogy of sediments (Calvert, 1976). The ratio profiles in Figs. 4.32 and 4.33 show that there is some compositional similarity in the top horizons, but at depths greater than a few centimetres, there are major differences in mineralogy between the two locations.

V. DISCUSSION

5.1 Water Column

Balmer Lake is a highly dynamic system which exhibits pronounced seasonal variability, both physically and chemically. The non-steady state nature largely results from the geographic position of this inland, boreal waterbody, and from variable loadings and dynamics of mining-related inputs. The annual freeze-thaw cycle of the terrestrial and aquatic regimes fosters significant seasonal signatures. For example, the formation of ice in early winter essentially cuts off atmospheric interactions for several months; subsequent reactions in such shallow "closed systems" can greatly affect water column chemistry. The freeze-up period is also characterized by reduced circulation, allowing the development of fine-scale stratification. In addition, the associated seasonal temperature swings of up to 20°C undoubtedly influence the kinetics of abiotic and microbially mediated reactions in the water column and sediments. Pronounced seasonal pulses of fresh water and associated allochthonous inputs to Balmer Lake are evident in the spring. Spring-melt at these latitudes is rapid, and the combined inputs of terrestrial run-off and the melting of 1 m of surface ice, may lead to a 30 % increase in liquid-water volume. Furthermore, vigorous stream activity can result in increased particulate loads in spring.

The nature of the tailings circuit design, in combination with the annual freeze/thaw cycle in Balmer Lake, results in a pronounced seasonal signal with respect to heavy metals and cyanide. Dramatic increases in the concentrations of these parameters are consistently observed at the Balmer Lake outlet (Fig. 2.1) in the spring, and have been shown to be strongly correlated with ice deterioration

(EIG, 1986). Moreover, the total inventory of heavy metals also increases at this time.

Four independent controls are believed to account for the observed annual cyclicity. First, the absence of wind turbulence under the ice allows the denser, metal-rich effluents to collect in the bottom waters over the winter months. Prior to whole-lake turnover in the spring, the outfall drains the less contaminated surface waters. However, upon ice break-up and subsequent wind-mixing, the accumulated inventory of mine-effluents is dispersed throughout the water column; this can contribute to higher metal levels at the outfall. The total increased metal burden in Balmer Lake at ice-out can also be attributed to freeze/thaw processes. As will be mentioned in section 5.1.4 below, the resuspension of a non-cohesive flocculant layer (built up over the winter months) has been suggested to account for lake-wide increases in springtime metal levels (EAG, 1986). Greater dissolved loads at this time may also stem from the dissolution of cyanide compounds. Metal-cyanide complexes, such as ferricyanide $[\text{Fe}(\text{CN})_6]^{-4}$, can form insoluble double-metal cyanide precipitates such as copper ferrocyanide $[\text{Cu}_2\text{Fe}(\text{CN})_6]$ (Higgs, 1979). Such complexes are stable in the absence of UV radiation and may potentially accumulate on the lake bottom over the winter months. Upon ice break-up, however, their dissolution may foster significant releases of CN^- and associated metals into the water column. Finally, the processes described above also occur in the tailings ponds; however, similar increases in heavy metal concentrations and cyanide precede those in Balmer Lake due to the earlier thaw. Thus, seasonally elevated inputs from the tailings circuits also contribute episodically to the lake burden.

5.1.1 Physical Limnology

The shallow water column of Balmer Lake is fairly well-mixed for the approximately 7-month ice-free period. During this time, the solubility of dissolved oxygen is temperature dependent. The generally windy conditions during the summer field session obviate detectable thermal stratification (Fig. 4.1). The high biological oxygen demand of the organic-rich sediments in the lake, (6-10 % organic carbon) in combination with restricted atmospheric exchange, fosters a gradual depletion of dissolved oxygen in the deeper lake areas over the duration of ice coverage (~ 5 months) (Fig. 4.3). Spring sampling, conducted less than 2 weeks after ice-off, revealed no traces of the previous stratification (Fig. 4.4). The rapid breakdown of chemical gradients and the pronounced warming of the water column over a short time period in the spring, suggest that wind and solar influences play a significant seasonal role.

5.1.2 Sulphate

The oxidation of sulphide-bearing ore in the milling circuit liberates large quantities of SO_4^{2-} which are delivered with the tailings to the clearwater ponds. Dissolved SO_4^{2-} loads entering Balmer Lake average over 20 mmol/L. This has resulted in a lake-wide yearly average dissolved sulphate concentration of > 3 mmol/L, greatly exceeding natural concentrations in non-perturbed Canadian Shield lakes (Nriagu *et al.*, 1982). Due to the scale of this input, month-to-month variations in the sulphate loadings from the two mines should ultimately determine any seasonal variability.

While SO_4^{2-} distributions remain essentially constant through the spring, summer and fall, winter profiling revealed large bottom water enrichments in the deeper lake areas (Fig 4.7). Peeper profiles of bottom water and porewater sulphate, however, indicate that the sediments were not releasing sulphate during this period; interfacial gradients in fact suggest pronounced sedimentary SO_4^{2-} consumption (Figs. 4.15-4.16; porewater sulphate profiles will be discussed in greater detail in section 5.3.2). The bottom water sulphate increases (which are seen only at depths > 2.5 m) must therefore represent a lateral advective flow of dense, sulphate-rich water moving out across the deeper lake basin. Indeed, profiling conducted to 2.6 m at the shallowest water column site (station 3), and at the shallow peeper site (station 6) did not reveal any evidence of such enrichments (Fig. 4.7C and 4.16F, respectively); only a marginal signal was observed at the 3 m depth at station 4 (4.7D).

Although the exact source and timing of such events cannot be determined accurately, the respective inputs from the Dickenson and Campbell tailings ponds represent two obvious potential sources of the high density discharge. During the winter sampling period in March, 1994, the Campbell mine was not discharging to Balmer Lake; complete cessation of discharge was in effect from Dec. 10/'93 to May 2/'94 (PDI, pers. comm.). However, waste inputs from Dickenson persisted throughout the winter months. The effluents potentially contributing to the observed chemical stratification averaged approximately 25 mmol/L SO_4^{2-} , 1.5 mmol/L NH_4^+ , 10.2 mg·L⁻¹ CN, 2.5 mg·L⁻¹ Cu, 1.5 mg·L⁻¹ Ni, 1.0 mg·L⁻¹ Zn, and 2.0 mg·L⁻¹ As (Goldcorp, pers. comm.). The high dissolved salts content of the tailings effluents, reflecting largely the high sulphate concentrations, would impart considerably higher densities than associated lake waters. An episode of slumping and oxidation of sulphide-rich

tailings material from somewhere within the lake represents a less likely, indeed implausible, explanation for the bottom water SO_4^{2-} increases.

During the fall sampling period, a bottom water sulphate enrichment was also evident at the site most proximal to the Campbell Mine effluent discharge (Fig. 4.13F). In light of the typical windy conditions, it is reasonable to assume that during ice-free periods such profiles would only be manifested within a short distance from the input point.

The winter water column distributions of dissolved Fe, As and Cu suggest that sulphide precipitation occurs in the seasonally reducing bottom waters of Balmer Lake (Figs. 4.8-4.11). Due to the large excess of SO_4^{2-} , however, direct evidence for sulphate reduction in the water column profiles is probably obscured. Bottom water SO_4^{2-} distributions seen in peeper profiles at stations 1 and 2, and to a lesser extent at station 4, suggest a mechanism for sulphate removal near the sediment-water interface at these sites (Figs. 4.15 and 4.16). Considering the trace metal profiles, the abundance of reducible sulphate and the reducing conditions prevalent in the winter, the seasonal precipitation of authigenic mineral sulphides in the water column is a tenable hypothesis that will be further assessed in the trace metal sections below.

5.1.3 Ammonium and Nitrate

The burdens of ammonia and nitrate in the water column of Balmer Lake greatly exceed concentrations observed in non-contaminated fresh water bodies. The observed enrichments can be partially attributed to mining-related by-products delivered to the lake via drainages from lake-side clearwater polishing ponds. More specifically, excess levels of NH_4^+ and NO_3^- appear to be derived from the breakdown of cyanide compounds.

The addition of sodium cyanide in the tailings circuit facilitates the removal of gold, and other metals, in carbon-in-pulp milling operations. The long-term use of such concentration techniques has resulted in significant additions of cyanide to the waters of Balmer Lake, with levels in the past sometimes exceeding 5 mg/L. Historically, mitigation of cyanide inputs has entailed degradation that occurs naturally in tailings ponds. In such systems, the volatilization of HCN to the atmosphere has been shown to be primarily responsible for cyanide removal (IEC, 1979). More sophisticated treatments emerged with stricter environmental standards in the late 1970's, at which time hydrogen peroxide (Vickell *et al.*, 1989) and Inco-SO₂ (Devuyst *et al.*, 1982) methods became more widespread.

The large ammonium burdens in Balmer Lake are partly attributable to the hydrolysis of cyanate (CNO⁻) and cyanide (CN⁻) compounds. Cyanate is generated in the milling processes due to reaction of free cyanide and cupric ions. It may additionally stem from the treatment of cyanide-bearing wastes upon oxidation with hydrogen peroxide or hypochlorite (Higgs, 1993). Cyanate can hydrolyze in basic mill effluents to produce ammonia via:



At pH's < 9.3 (i.e., Balmer Lake), however, NH₄⁺ is the thermodynamically favoured product of cyanate hydrolysis (Stumm and Morgan, 1981). Cyanide will also hydrolyze in neutral waters to form ammonium via:

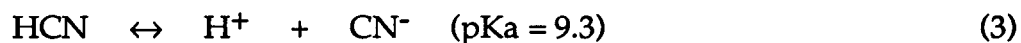


The large bottom water ammonium enrichments in the winter water column in Balmer Lake are believed to be derived from both sediment sources and from mining-related lateral advective flows. Ammonium is generated by heterotrophic bacteria as a primary end-product of organic matter decomposition, either directly from proteins or from other nitrogenous organic compounds (Van der Weijden, 1992). The remineralization of organic matter in Balmer Lake sediments, and the concomitant release of NH_4^+ to the porewaters, results in steep gradients at shallow sediment depths. Ammonium released during aerobic respiration into oxic horizons will be oxidized by nitrifying bacteria (nitrification) to nitrate (Sholkovitz, 1973). Similarly, the same fate holds true for upward diffusing NH_4^+ that migrates into oxic sediments. However, the complete consumption of oxygen, and the reductive dissolution of Mn oxyhydroxide phases in the reducing winter bottom waters, effectively remove these potential oxidants from interfacial horizons. In this environment, remineralized NH_4^+ is allowed to diffuse from permanently reducing horizons and accumulate in the anoxic bottom waters. Such effluxes have been described elsewhere: Stadelmann (1971) and Wetzel (1975), for example, report the presence of $>500 \mu\text{mol L}^{-1} \text{NH}_4^+$ in temperate, productive lakes in Michigan and Switzerland, respectively. This topic will be discussed in greater detail in section 5.3.1.

The large NH_4^+ concentrations reported in the effluents discharged to Balmer Lake indicate that the winter bottom water enrichments can also be partially attributed to a lateral transport mechanism, as suggested for sulphate. Support for this argument can be seen in the fall bottom water and porewater NH_4^+ distribution (Fig. 4.13D) in "Tailings Bay" (station 5). The ammonium profile is characterized by a well-defined bottom water enrichment, comparable to that observed for SO_4^{2-} . Like sulphate at this site, ammonium concentrations

decrease dramatically at shallow sediment depths demonstrating that the sediments are not releasing NH_4^+ , but are serving as a diffusive sink.

Ice formation in Balmer Lake may also indirectly contribute to the large winter NH_4^+ inventories. Free cyanides exist in solution as cyanide (CN^-) and hydrocyanic acid (HCN) in the equilibrium (Stumm and Morgan, 1981):



At the neutral pH of Balmer Lake, 95% of free cyanide exists as molecular HCN. As a result of its relatively high vapour pressure, HCN tends to volatilize to the atmosphere, even in stagnant solutions (Higgs, 1993); the presence of an ice cap during the winter months, however, prevents HCN release. Thus, the increased residence time of cyanide compounds during the winter months, and their subsequent breakdown, may contribute to the increased winter NH_4^+ concentrations in Balmer Lake.

During the well-mixed periods of the spring, summer and fall, nitrate concentrations remain fairly constant (Tables 4.1, 4.2 and 4.4). Pronounced decreases beginning 10-20 cm below the top of the oxycline at all sites in the winter, however, suggest that denitrification is occurring in the bottom waters during this period below depths of 2.4-2.7 m (Fig. 4.5). Denitrification becomes important at low O_2 concentrations ($<6 \mu\text{mol/L}$) and involves the bacterially-mediated reduction of one or both ionic nitrogen oxides (nitrate or nitrite) to their gaseous oxides and eventually to N_2 (Froelich *et al.*, 1979). Peeper bottom-water profiles at stations 1, 2 and 4 suggest that nitrate consumption (i.e., defined where $d^2[\text{NO}_3^-]/dz^2 > 0$) begins in winter at depths approximately 10, 15 and 5 cm above the sediment-water interface, respectively (Figs. 4.15B, E and 4.16B); peeper data were not obtained from station 3. Similar profiles demonstrate that

denitrification does not occur in the shallow waters (~1 m) at station 6 in winter (Fig. 4.16E).

Nitrate is produced in most lake systems primarily by the fixation of molecular N_2 by cyanobacteria and via the bacterial-mediated oxidation of ammonium diffusing upwards into oxygenated horizons in the sediments or water column (Wetzel, 1975). The abundance of oxidizable NH_4^+ suggests that nitrification is responsible for a high proportion of the NO_3^- burden in Balmer Lake. In general, the ratio of NO_3^- -N to NH_4^+ -N is a highly variable function of lake trophic status, hydrogeology, and natural and pollution-derived sources (Wetzel, 1975). Well-buffered, oligotrophic lakes receiving drainages from calcareous landforms, for example, can have NO_3^- -N: NH_4^+ -N ratios of greater than 25:1. Conversely, in permanently anoxic, eutrophic lakes, ratios of 1:10 are common (Wetzel, 1975). The values of NO_3^- -N: NH_4^+ -N in Balmer Lake progressively increase over the winter, spring, summer and fall, with ratios averaging <1, 1.8, 3.5 and 6.2, respectively. This hierarchy largely reflects a decrease in NH_4^+ concentrations from the maximum observed during the winter period. The relative removal of NH_4^+ can be attributed to biological nitrification, phytoplankton uptake and sorption to clay minerals.

5.1.4 Suspended Particulates

The considerable intra-station variability of particulate trace metal concentrations in the well-mixed water column of Balmer Lake warrants consideration of potential sampling and analytical errors (Tables 4.6 and 4.7). Inaccuracies in the data set may have arisen from two sources. First, the over-pressure filtration units, on occasion, leaked. In such circumstances, the total volume of water filtered could not be accurately determined, and as a result,

errors would be manifested where the total mass of particulate metal per unit volume is computed. Such error should not be introduced, however, into the determinations of total mass of metal per gram of suspended material. Yet, the coarsely paralleled variability of mass: mass calculations with those of mass: volume, suggest that some degree of particulate heterogeneity is evident in the water column. Additional error may have been introduced into the mass:mass values since the absolute particulate fraction, determined by subtracting the pre-filtered from post-filtered weights, was very small.

A third source of error, with respect to Zn concentrations, appears to have originated from contamination either during cleaning of the polycarbonate filters or during the filtration procedure. Values determined from filtration blanks ranged from 0.3-4.8 ppb (Appendix B). Such levels exceed some of the low-end water column particulate values. In order to obtain the most representative estimates, averages of the respective filter blanks for each sampling session were subtracted from the total. It should be noted that filters taken out of their wrappers and processed (i.e., not acid-cleaned) exhibited negligible levels of all metals (Appendix B). Zn enrichments most likely arose from water contact with zinc-rich rubber fittings in the filter apparatus, despite the O-rings and stoppers being wrapped in teflon tape prior to use.

Concentrations of total suspended solids in the water column of Balmer Lake are high, and are fairly typical of levels encountered in productive, nearshore lake zones characterized by higher rates of sediment resuspension (Nriagu *et al.*, 1981). The particulate trace metal levels greatly exceed values reported for other non-perturbed inland waters (Table 4.6). In general, values in Table 4.6 are high in comparison to suspended metal concentrations observed in lacustrine and estuarine waters receiving pollutant metal inputs (Kubota *et al.*, 1974; Jackson, 1978; Sholkovitz, 1979; Nriagu *et al.*, 1982; Jackson and Bistricki,

1995). Moreover, the lake-wide averages for the observed concentrations in suspended particulates of approximately 5 wt.% Fe, 850 mg·kg⁻¹ Mn, 1500 mg·kg⁻¹ Ni, 7000 mg·kg⁻¹ Cu, 5000 mg·kg⁻¹ Zn and 4000 mg·kg⁻¹ As also surpass reported values of other polluted systems (see Nriagu *et al.*, 1982). The relatively large magnitudes of the particulate values demonstrate that the settling of suspended material may present an important transport mechanism of metals to bottom sediments.

Aquatic microorganisms exert controls on the geochemical cycles of many trace elements via active and indiscriminant associations (Morel and Hudson, 1985). The interactions of organic particles with metal ions and other reactive elements can occur via two mechanisms: metal ions can become coordinated to particulate surfaces of cells and/or fecal material in accordance with surface coordination or sorption equilibria, or alternatively, they can be incorporated into living cells and physiologically assimilated (Sigg, 1985). The high affinity of metal ions for biological surfaces suggests that biogenic particles may play a prominent role in the binding and transfer of metals to bottom sediments (Nriagu *et al.*, 1981; Sigg, 1985; Morfett *et al.*, 1988; Reynolds and Hamilton-Taylor, 1992). Particulate organic matter is abundant in the water column of Balmer Lake and constitutes a large percentage of the total suspended solids (Tables 4.5 and 4.7); concentrations are similar to levels measured in other Ontario lakes (e.g., Nriagu *et al.*, 1981, Nriagu *et al.*, 1982). Several studies have indeed shown that concentrations of particulate trace metals are strongly influenced by the production of POC (Sigg, 1985; Nriagu *et al.*, 1981 and 1982). They attributed more efficient scavenging of trace elements to larger productivities and higher particle sedimentation rates. Except for Zn, however, particulate metal levels in Balmer Lake do not exhibit a clear correlative relationship with concentrations of POM.

Other than associations with organic matter, variable fractions of the particulate trace metal burden are likely to be associated with metal oxyhydroxide precipitates (e.g., Fe, Mn and Al) and clay minerals in the lake waters. The relative distribution of trace metals between these fractions is unknown. However, some inferences can be made based on seasonal comparisons of POM, TSS, metal per volume and metal per gram particulate. For example, the highest particulate metal concentrations evident in the spring water column coincided with the highest levels of total suspended solids (Tables 4.5 and 4.6). The relatively lower organic content of these particulates, however, implies that large fractions of the trace metals are associated with inorganic matter. Furthermore, the winter water column was characterized by less than half the average POM content of the summer, but contained comparable or greater concentrations of all trace elements (Tables 4.5 and 4.6).

From the above discussion, it is evident that POM does not exert the principal control on particulate metal levels in the water column of Balmer Lake. However, given the abundance of particulate iron in lake waters, control by Fe-oxide phases may be important. Indeed, existing reports on trace metal scavenging by Fe and Mn oxyhydroxides in lakes polluted with mine and smelter wastes illustrate the importance of such metal-particulate associations (Jackson and Bistricki, 1995). Seasonal concentrations of particulate Fe species in Balmer Lake range from 107-649 $\mu\text{g}\cdot\text{L}^{-1}$ which correspond to 3 to 6 wt.% of suspended material (Tables 4.6 and 4.7). The average seasonal concentrations of particulate Ni, Cu and As track mean suspended iron concentrations; for all four elements (including Fe) the seasonal hierarchy follows the order: spring > winter \geq summer and fall (Table 4.6). Variations in iron-trace metal relationships may be influenced by the relative proportion of less reactive Fe species, such as those in the lattices of resuspended clay minerals. Inorganic particulate fractions may

also be present as CaCO_3 , quartz, chlorite, illite and feldspars; these minerals are also capable of sorbing both organic substances and metal ions, but they have relatively small specific surface areas and thus relatively little capacity for metal ion binding (Sigg, 1985).

A basic mass balance analysis conducted during a period of elevated metal concentrations in Balmer Lake in the spring of 1986, suggests that an increase in the discharges from the adjacent tailings ponds could not alone account for the total increased metal levels (Masala, 1995). The latter point, in conjunction with observations of greater particulate metal fractions during this period, leads to the conclusion that wind-suspension of fine-particulate material were contributing to such loadings. More specifically, it was proposed that in the quiet waters under the ice in winter, finer particulates settle out gradually and form a non-cohesive flocculant layer susceptible to resuspension upon ice break-up (PDI, 1986). This argument is consistent with the high TSS and particulate metal levels observed in Balmer Lake observed during the study period.

5.1.5 Trace Metals

The dynamic nature of Balmer Lake is marked by considerable variability in the seasonal distributions of the measured trace elements. Two principal mechanisms are invoked to account for the observed variability: seasonal shifts in the redox geochemistry of the sediments and bottom waters, and the effect of mining-related discharges. It will be demonstrated below that an understanding of the timing and relative influence of such mechanisms is critical in the evaluation of the spatial variability observed in the winter water column.

To constrain fully the mechanisms controlling the behaviour of trace metals in the water column of Balmer Lake, both interfacial and porewater distributions must be examined. A detailed assessment of the seasonal porewater chemistry is presented in section 5.3, and an interpretation of trace metals in the water column is offered immediately below. The latter is divided into three sections: 1) descriptions of the respective trace element geochemistries; 2) presentation of a water column model; and 3) application of the model to four zones in Balmer Lake.

5.1.5.1 Iron

The transport of Fe and Mn in water bodies and sediments has received a great deal of attention because of the central role that these abundant metals play in the geochemical cycling of other elements. The surface properties of Fe oxyhydroxides and associated trace metal sorption mechanisms, in particular, have been well studied (Davis and Leckie, 1978a; Davis and Leckie, 1978b; Vuceta and Morgan, 1978; Benjamin and Leckie, 1982; Tessier *et al.*, 1996). The redox geochemistry of Fe has been repeatedly stressed as a principal mechanism governing the distribution of many trace elements in lacustrine systems (Laxen, 1985; Tessier *et al.*, 1985; Belzile and Tessier, 1990; Davison, 1993; Hamilton-Taylor and Davison, 1994; Jackson and Bistricki, 1995).

Iron (II) and iron (III), represent the two oxidation states of importance to the aquatic geochemistry of Fe. Ferrous iron is stable in anoxic water, exists predominantly as a simple hydrated aquo ion, and is soluble with respect to most inorganic ions; however, in some environments, the solubility products of siderite (FeCO_3), amorphous iron sulphide (FeS) and vivianite [$\text{Fe}_3(\text{PO}_4)_2$] may be exceeded (Davison, 1993). In well oxygenated waters, Fe(III) is the stable

oxidation state. This acidic cation occurs as completely hydrolyzed oxides at neutral pH, with its solubility being controlled by amorphous iron hydroxide (Stumm and Morgan, 1981).

Numerous field and experimental works have been carried out to characterize iron and manganese oxide phases in lacustrine waters and sediments (Davis and Leckie, 1978b; Laxen and Chandler, 1983; Davison *et al.*, 1992). For the most part, the nature of iron oxide particles in natural waters is not completely understood. Although variations in particle size, composition and structure have been observed, general similarities exist. In oxygenated lake waters, ferric iron has been predominantly found as amorphous particles and colloids, which are negatively charged due to adsorption of humic substances (Tipping, 1981). The spherical or ellipsoidal particles are presumed to be poorly crystalline ferrihydrite with mean diameters typically in the range of 0.05-0.5 μm . The general presence of these particles as amorphous phases makes them readily susceptible to dissolution under anoxic conditions. Tipping *et al.* (1981) used electron microscopy to examine iron-rich particles in Esthwaite Water surface sediments. The particles contained 30-40 % Fe (by weight), with P, N, Mn, Si, S, Ca and Mg accounting for up to 8 wt. %. Organic matter constituted up to 36 wt. % with one third of this being represented by humic substances.

The data in Table 4.6 clearly illustrate that particulate Fe fractions dominate the total iron inventory in the waters of Balmer Lake. The ratio of particulate to filterable species exhibits considerable seasonal consistency with particulates comprising 60-89 % of the total Fe inventory. The Fe-particulates are believed to comprise variable mixtures of iron oxides and clay mineral fractions derived from resuspended sources. It should be noted that dissolved Fe species become more important during the winter months.

5.1.5.2 Manganese

As for iron, the biogeochemical cycling of Mn has been shown to govern the behaviour and mobility of redox sensitive elements in freshwater environments (Davison and Woof, 1984; Agett and O'Brien, 1985; Sigg *et al.*, 1991; Young and Harvey, 1992; Davison, 1993). Of the three naturally occurring oxidation states, Mn(II) is stable in anoxic waters, where the predominant species are simple hydrated aquo ions. Manganese (II) is very soluble with respect to most inorganic ions, although in certain environments, such as interstitial waters, it is possible to exceed the solubility product of rhodochrosite (MnCO_3) (Carignan and Nriagu, 1985). Conversely, in well-oxygenated waters, MnO_2 (Mn IV) is the thermodynamically stable form. In practice, a range of metastable oxidation products exist in natural waters due to kinetic limitations (Stumm and Morgan, 1981); Mn(III) is only stable in a lattice of mixed oxidation state (Davison *et al.*, 1993).

Numerous works have attempted to describe manganese oxidation products and characterize them using electron microscopy and X-ray diffraction (De Vitre and Davison, 1993). However, the basic chemistry of both the Mn(IV) and Mn(III)-bearing phases are not well understood. Natural manganese particles are difficult to identify because of their extreme microcrystallinity which renders them X-ray amorphous. In addition, due to their tendency to coexist and coat many other minerals and organic material, sometimes only electron microscopy can provide identification (Chiswell and Mokhtar, 1986). The most common forms of Mn oxides identifiable in oxic lake sediments are $\gamma\text{-MnOOH}$ and birnessite (MnO_2). The structure of the latter can be complex. Birnessite is thought to contain Mn(III) and possibly Mn(II) or other divalent metal cations (e.g., Pb, Cu, Zn) in addition to predominant tetravalent Mn species. The humic

content of these phases is low (~1 %), but bacteria and/ or algae may contribute 20-30 % by weight (Davison,1993).

In well-oxygenated, neutral waters (pH 6-8), the half-life of Mn(II) is typically on the order of days to months; by contrast, Fe(II) has a typical half-life of ~4 h under the same conditions (Stumm and Morgan, 1981). The variable reaction rates of Mn have been attributed to bacterial-mediated oxidation kinetics; various strands of evidence have been introduced to support the importance of microbial interactions (Davison,1993). The differing oxidation kinetics have corresponding consequences with respect to the distribution of soluble and particulate species.

Examination of the partitioning of Mn in the water column of Balmer Lake indicates that particulate phases are insignificant relative to the dissolved fraction (Tables 4.6 and 4.7). During all sampling periods, dissolved manganese counted for at least 95 % of the total inventory. These results agree well with a recent study of Mn speciation in a Precambrian Shield lake, where predominantly non-particulate forms were also observed (LaZerte and Burling, 1990). As for Fe, the term "dissolved" must be used with caution, as colloidal phases have been shown to contribute significantly to filterable fractions (De Vitre *et al.*, 1988; LaZerte and Burling, 1990).

In natural systems, the proportion of Mn in particulate form may vary considerably. For example, Laxen *et al.* (1984) showed that in various British rivers and streams the particulate fraction varied from 0 to 100%. The wide range has been attributed to the relative contributions of Mn from two distinct sources: 1) weathering of Mn-bearing minerals which yields suspended particles; and 2) inputs of soluble manganous species from oxygen-deficient sediments and ground waters (Davison, 1993). The relative influences of these sources, and therefore the particulate proportion in a particular lake or stream, depends on the

local hydrogeology. It will be shown below that the dominance of filterable species in the Balmer Lake water column can be attributed to the direct input of dissolved manganese.

5.1.5.3 Arsenic

The inherent toxicity of many As compounds and their transformations in biogeochemical cycles has stimulated considerable interest in As speciation in the environment (Ferguson and Gavis, 1972; Sanders, 1983; Reimer and Thompson, 1988; Cullen and Reimer, 1989; Anderson and Bruland, 1991; Bowell, 1994). Although total dissolved As was measured in Balmer Lake, predictions of speciation can be made using relevant thermodynamic constraints and results of previous studies. Dissolved As can occur in natural waters in both inorganic and organic forms. In oxygenated waters at neutral pH, the anionic arsenate species (H_2AsO_4^- at $3.6 < \text{pH} < 7.3$) is the thermodynamically stable form of As. Conversely, neutrally charged arsenite ($\text{As}(\text{OH})_3^0$) is the predicted form in reducing environments (Cullen and Reimer, 1989). The large predicted As(V)/As(III) ratio of 10^{15} - 10^{26} suggests that As(III) should contribute a negligible fraction of total inventories in neutral waters. However, the observation of significant amounts As(III) in oxygenated waters, and the presence of As(V) in reducing regimes, suggests that the two are rarely in thermodynamic equilibrium.

Arsenic is also host to a suite of organic compounds, of which monomethylarsonic acid (MMAA) and dimethylarsinic acid (DMAA) contribute significantly (~10%) to total As concentrations in freshwaters (Andreae, 1979; Anderson and Bruland, 1991). Because arsenate and phosphate are chemical analogues there is little discrimination between the two species during biological

uptake. This has led to the suggestion that organisms have developed mechanisms to isolate and detoxify As by producing organoarsenicals (Wood, 1974). However, the processes that promote biological methylation of As are still poorly understood. Factors including high As:PO₄²⁻ ratios in ambient waters, and the nature of biotal communities, have been invoked to explain greater abundances of methylated compounds (Anderson and Bruland, 1991).

Arsenic concentrations in the water column of Balmer Lake greatly exceed natural baseline values observed in non-perturbed Canadian Shield lakes. The abundance of arsenopyrite in the milled ore suggests that the oxidation of this phase during the milling process is responsible for the large inventory. Arsenic is largely dominated by filterable fractions throughout the sampled seasons, contributing over 95% of the total burden (Table 4.6). Large bottom-water particulate spikes observed during the winter season (27-32% of the total inventory) represent the only deviations from the typically low suspended particulate As values. Considering that Balmer Lake is productive and hosts excess As with respect to phosphate, there is a high probability that concentrations of methylated species are substantial. In all likelihood, however, these species probably represent an insignificant fraction of the total arsenic in the lake waters. Arsenic species in the water column of Balmer Lake are most likely dominated by arsenate and arsenite, with their respective contributions fluctuating in accordance with seasonal oxic/anoxic cycles.

5.1.5.4 Nickel

Nickel exhibits a nutrient-type distribution in the oceans and is characterized by both shallow and a deep water regeneration. Vertical profiles in the top 800 m appear similar to phosphate, while below this depth nickel exhibits a deep maximum similar to silicate (Bruland, 1983). Concentrations of dissolved nickel increase from $\sim 2 \text{ nmol}\cdot\text{L}^{-1}$ in surface central gyre waters of the North Pacific to a deep maximum of $11 \text{ nmol}\cdot\text{L}^{-1}$ (Sclater *et al.*, 1976; Bruland, 1980). Similarly shaped profiles determined for the North Atlantic exhibit maxima one half the magnitude of those observed in the deep North Pacific (Bruland and Franks, 1983).

The non-steady-state nature of lacustrine systems combined with the relative dearth of appropriate data make generalizations of nickel distributions in lakes difficult. The micronutrient-like behaviour observed for Ni in marine systems, for example, has not been clearly demonstrated for freshwaters. Available evidence suggests that vertical variability is largely dictated by the redox transformations of Fe, Mn and S. Concentrations of dissolved nickel in the hypolimnion of Lake Sammamish, for example, were shown to increase in response to bottom water anoxia (Balistrieri and Murray, 1992); the supply of dissolved Ni to the bottom waters was attributed to the dissolution of nickel-bearing Mn-oxide phases. Indeed, Fe and Mn oxides have been repeatedly inferred to control the distribution of Ni in lake waters, sediments and porewaters (Green *et al.*, 1989; Tessier *et al.*, 1996). Conversely, the removal of nickel from reducing bottom waters (Green *et al.*, 1989) and porewaters (Carignan and Nriagu, 1985) has been largely attributed to the precipitation of authigenic Ni-sulphides.

Nickel concentrations in Balmer Lake greatly exceed those in non-perturbed Canadian Shield lakes. Loadings from the tailings circuit, which average over $1 \text{ mg}\cdot\text{L}^{-1}$, contribute to the high values. The nickel inventory in the water column is dominated by dissolved species throughout the sampled seasons, which is consistent with measurements of nickel partitioning in other lake systems (Nriagu *et al.*, 1981; Balistrieri and Murray, 1992). Speciation calculations of freshwaters suggest that nickel exists largely as the free aquo ion Ni^{2+} and as carbonate complexes during well-mixed periods in Balmer Lake (Florence, 1982; Carignan and Nriagu, 1985).

5.1.5.5 Copper

In the oceans, copper exhibits a distribution intermediate between that of nutrient-type elements and that of scavenged elements such as Pb. The vertical distribution of Cu in the Pacific, for example, is characterized by an approximately linear increase with depth (Bruland, 1980). The deviation from a nutrient-type element (e.g., cadmium) is due to *in situ* scavenging by particulates in the intermediate and deep waters. The remineralization of Cu-bearing phases at the sediment-water interface, however, results in a major portion of the total benthic Cu-flux being recycled back into the bottom waters (Bruland, 1980). Deep water concentrations in the Atlantic (Bruland and Franks, 1983) are one-half to two-thirds of deep Pacific waters due to the progressive addition of dissolved Cu during deep water migration.

The compressed depth scales and dynamic nature of lacustrine systems prevent generalizations of the vertical distributions of copper in lakes. However, the available data suggest that redox transformations and particle scavenging represent two important controls. The dissolution of sinking Mn and Fe oxides,

for example, can yield peaks of dissolved Cu at oxic/anoxic boundaries (Green *et al.*, 1989). Conversely, hypolimnetic depletions can result from the precipitation of copper-bearing sulphide phases in reducing bottom waters (Green *et al.*, 1989; Balistrieri *et al.*, 1992) and porewaters (e.g., Carignan and Nriagu, 1985). Direct evidence linking Cu distributions with biological cycles is rare, although algal decomposition has been invoked to account for Cu enrichments at the sediment-water interface in a British lake (Morfett *et al.*, 1988).

Filterable copper species dominate the Balmer Lake water column throughout the sampled seasons, comprising between 65 and 90% of the total pool. Speciation calculations suggest copper exists predominantly as CuOH^+ and CuCO_3 in aerobic freshwaters (Stumm and Morgan, 1981), with a significant portion of the dissolved fraction potentially bound to organic ligands. Inorganic and organic colloids have also been shown to contribute significantly to total copper burdens in freshwaters (Dai *et al.*, 1995).

5.1.5.6 Zinc

Zinc is a group IIb element which has well-established associations with biological cycles in both marine and lacustrine environments. In the oceans, zinc exhibits a nutrient-type distribution similar to that of silicic acid; dissolved concentrations in the central North Pacific increase from $\sim 0.2 \text{ nmol}\cdot\text{L}^{-1}$ in the surface mixed layer to $\sim 8 \text{ nmol}\cdot\text{L}^{-1}$ in the intermediate and deep waters (Bruland *et al.*, 1994). Although biologically-mediated Zn-nutrient associations are often obscured by other processes in lakes, two convincing data sets clearly illustrate a biological control. In productive Lake Windemere, for example, dissolved zinc, phosphate and silicate were positively correlated throughout the water column during a rapid growth phase of a spring diatom bloom (Reynolds and Hamilton-

Taylor, 1992). Similarly, acid-soluble zinc concentrations were shown to correlate with silicate distributions during summer stratification in Lake Sammamish, Washington (Balistrieri et al., 1992).

Although there is little doubt that Fe and Mn oxides also act as carriers for Zn in lacustrine systems, observations indicate that redox related phenomena have a relatively small effect on the vertical distribution of dissolved Zn in lakes. Conversely, numerous examinations of the early diagenesis of zinc in oxic lake sediments have demonstrated the importance of Fe and Mn oxide phases with respect to zinc mobility (Carignan and Tessier, 1985b; Tessier *et al.*, 1989; Young and Harvey, 1992; Tessier *et al.*, 1996). In reducing sediments, dissolved zinc is commonly removed from pore-solution via the precipitation of sphalerite (ZnS) and/or mixed Fe-sulphide phases (Carignan and Tessier, 1985b; Pedersen *et al.*, 1993).

The zinc concentrations in the water column of Balmer Lake greatly exceed those in unpolluted freshwater systems. Although dissolved fractions dominate the zinc burden, a considerable portion is present in suspended particulates. The filterable zinc species are predicted to exist predominantly as Zn^{2+} and $ZnCO_3$, with inorganic and organic colloids potentially hosting a significant portion (Florence, 1982).

5.1.6 Water Column Model

The following section presents a model to explain the water column profiles of trace elements over the fall-winter-spring transition. The scheme, presented in Fig. 5.1, represents a time series, and encompasses the broad range of profiles observed in Balmer Lake.

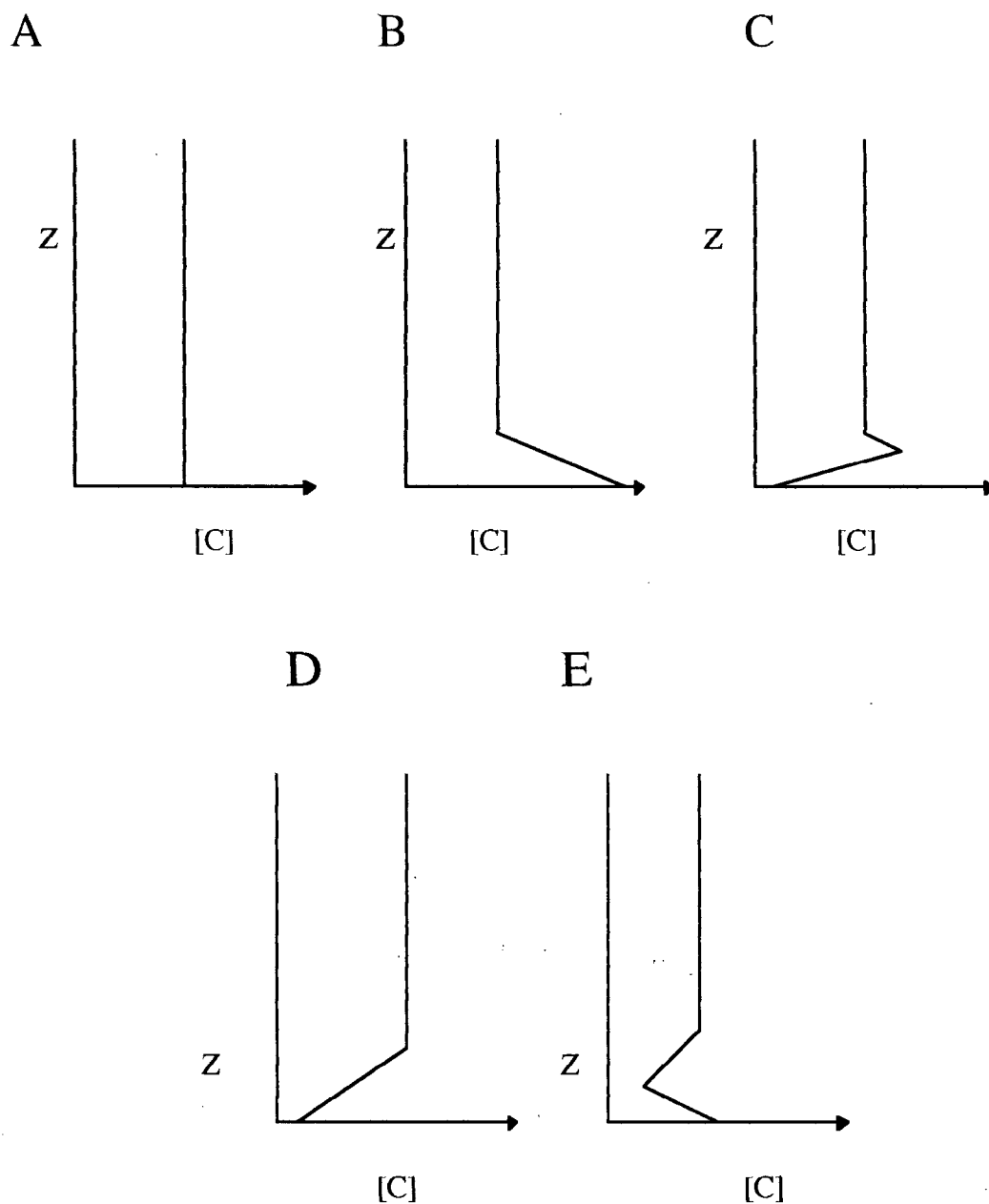


Fig. 5.1. Time series of progressive trace metal water column profiles (A-E) over the fall-winter transition in Balmer Lake: A) well-mixed water column, B) influence of remobilized bottom-water source, C) influence of interfacial sulphide sink, D) greater extent of sulphide removal, and E) influence of metal-rich lateral advective flow. Depth and concentration axes are in arbitrary units.

As described in section 1.2.3, the degradation of organic matter is mostly an oxidative process, for which electron acceptors must be present. Remineralization follows a sequence of oxidation reactions in which the redox couple that liberates the highest free energy yield acts before the next most efficient couple. Bacterial assemblages, specialized in using the energy released in each of these redox reactions, obey this sequence (Froelich *et al.*, 1979). The thermodynamic sequence of oxidant depletion follows the order: O₂, NO₃⁻ and Mn(III,IV)-oxides, Fe (III)-oxides, SO₄²⁻ and finally CO₂. Deviations of this sequence are possible, however, and relate to such factors as porewater pH and the stability of the iron oxide (Postma and Jakobsen, 1996).

During the well-mixed, oxygenated periods of the spring, summer and fall in Balmer Lake, the anoxic-oxic redox boundary (as defined by the depth where SO₄²⁻ reduction commences) lies below the sediment-water interface. The formation of ice in early winter, however, creates the conditions necessary to promote the gradual consumption of the oxidant pool, and the evolution of bottom water anoxia. The SO₄²⁻ redox boundary is predicted to migrate upwards towards the sediment surface over the duration of ice cover, and in some areas, cross the interface into the bottom waters. Examination of the water column and interfacial metal distributions measured in late winter suggests that extensive sulphide precipitation had already occurred earlier that season in the deeper lake areas. Authigenic sulphide formation has been suggested to present a significant control on trace element distributions during anoxic periods in other dimictic lakes (Morfett *et al.*, 1988).

Discharges to Balmer Lake from the adjacent tailings circuits present another important consideration. Measurements made on tailings pond effluents suggest that significant burdens of trace metals, sulphate, cyanide and ammonia are associated with these discharges. The influence of mining-related effluents in

the lake appears to be related to water depth, and to the proximity to the point of discharge. Due to its large signal in mine discharge waters, sulphate is considered to be the most appropriate tracer of these inputs.

During well-mixed periods, homogenous conditions resulting from extensive wind-mixing of a shallow water column produce uniform depth profiles of dissolved constituents as was shown in Chapter 4, which are summarized schematically in Fig. 5.1A. The formation of ice in early winter removes any atmospheric influences and permits the development of water column stratification. As anoxia develops over the course of ice-cover, the predicted reducing swing in the redox environment at the sediment-water interface promotes the reductive dissolution of labile Mn-bearing solid phases. Significant input to bottom waters subsequently yields the generalized profile shown in Fig. 5.1B.

After the consumption of NO_3^- and Mn-oxides, the oxidation of organic matter proceeds via Fe(III) reduction. The most reactive phases are those with the highest solubility, i.e., amorphous and poorly crystalline Fe-oxyhydroxides (Van der Weijden, 1992). Dissolved Fe distributions during such periods resemble the profile shown in Fig. 5.1B. The remobilization of Fe and Mn oxyhydroxide phases is often associated with the concomitant release of sorbed trace elements which may yield similar enrichment patterns of such elements in bottom waters (e.g., Green *et al.*, 1989; Aggett and Kriegman, 1988).

As conditions become more reducing at the sediment-water interface, and reactive Fe(III)- and Mn(IV)-bearing solid phases have become exhausted, sulphate reduction is expected to become important (Froelich *et al.*, 1979). The introduction of an interfacial metal-sulphide sink to the situation shown in Fig. 5.1B, may yield a profile similar to that shown in Fig 5.1C. More extensive sulphide precipitation, in conjunction with diffusional processes, may remove

any evidence of prior metal release (Fig. 5.1D). The final profile in the model sequence results if a dense, metal-rich lateral flow displaces or mixes into metal depleted bottom waters (Fig. 5.1E). This five-step order of events is used below to assess the intra-lake variability during the winter sampling period.

5.1.7 Comparison of Four Lake Zones

To reiterate, the trace metal distributions observed during the spring, summer and fall sampling periods exhibited little variability with depth; windy conditions prevented the development of any thermal stratification and, in effect, inhibited the detection of bottom water gradients associated with sediment consumption or release. The relatively stagnant conditions during winter sampling, however, permitted the development of chemical stratification. The fact that Balmer Lake has a large surface area to volume ratio enables benthic exchanges to be more easily manifested in the water column structure. The following discussion attempts to resolve the winter variability of trace metal distributions with respect to four lake areas (stations 1-4, Fig. 2.1).

Evidence for interfacial sulphide precipitation throughout Balmer Lake implies that the reductive dissolution of labile sedimentary Mn- and Fe-oxides, and associated metal releases, had occurred some time prior to sampling. It should be noted that at any time during the development of reducing conditions, the redox intensity at the sediment-water interface may exhibit significant lake-wide variation; differential rates can be attributed to such major variables as water depth and the concentration of organic matter. This point will become relevant in the following interpretations of water column profiles.

Steep porewater manganese gradients evident during the other seasons imply that the upward diffusion of remobilized Mn(II) species across the

interface is at least partially responsible for enrichments in the reducing winter bottom waters. The fact that stations 3 and 4 exhibit minimal or negligible signatures from pollutant effluents (i.e., insignificant SO_4^{2-} signal) and are still characterized by bottom water Mn maxima, supports this premise (Figs. 4.7, 4.10 and 4.11).

The decoupling of the soluble and particulate Mn fractions seen in Balmer Lake results from the relatively slow oxidation kinetics of its reduced form; this results in greater stability and thus longer residence time of reduced Mn species in oxygenated waters. However, in aquatic systems where Mn oxidation is substantially accelerated by bacterial processes, or where residence times are long (i.e., some lakes), the interconversion of the two forms may be an important process. Indeed, the pronounced decrease in the dissolved Mn content, which occurred over the four week sampling hiatus between the winter and spring sessions, implies a removal mechanism from the water column. The oxidation of Mn^{2+} and subsequent precipitation as MnO_2 provides a probable mechanism.

Bottom water concentrations of Mn exceed 1 mg/L in some zones of Balmer Lake. The release is predicted to be predominantly present as reduced Mn(II) hydrated aquo ions, since speciation studies suggest that inorganic and organic complexes represent insignificant fractions (Chiswell and Mokhtar, 1986; LaZerte and Burling, 1990). Manganese enrichments in the anoxic hypolimnia of lakes in excess of $1 \text{ mg}\cdot\text{L}^{-1}$ have been reported by many authors (Davison *et al.*, 1982; Sigg, 1985; Cornwell, 1986; Agett and Kriegman, 1988; Morfett *et al.*, 1988; Anderson and Bruland, 1991). The seasonal anoxia in these studies, however, occurs in the summer, and results from the development of thermal stratification in combination with enhanced organic transport to the hypolimnion.

Sulphate reduction in the bottom waters also implies that the reductive dissolution of reactive Fe phases had occurred prior to winter sampling.

Interfacial enrichments of dissolved Fe derived from remobilized sediment sources have been reported in several studies of seasonally anoxic lakes (e.g., Davison *et al.*, 1982; Cornwell, 1986; Anderson and Bruland, 1991; Sigg, 1985; Agett and Kriegman, 1988).

The extremely high metal levels in Balmer Lake, and thus their increased ability to compete for surface sorption sites, may suggest that Fe and Mn amorphous phases in the top few centimetres host significant burdens of exchangeable metals. Therefore, the reductive dissolution of Fe and Mn oxides may promote a pronounced release of sorbed constituents (Belzile and Morris, 1995). Moreover, trace metals associated with conspicuous porewater maxima (i.e., Fe, Mn, As, Zn and to a lesser extent Ni) could diffuse into the bottom waters in the absence of an interfacial oxide trap.

In addition to Mn(II), Fe(II), and associated trace elements remobilized from reducing sediments, the reductive dissolution of sinking oxide particles in reducing horizons has also been invoked to support enrichments of metals in the bottom waters of stratified lakes (Green *et al.*, 1989; Anderson and Bruland, 1991; Balistreri and Murray, 1992). This pattern of supply to the surface waters and remobilization at depth, may lead to maxima in the concentration of soluble constituents towards the end of seasonal stratification (Davison, 1993). The abundance of metal particulates in the winter water column of Balmer Lake, suggests that trace metals remobilized from sinking particles may present an important input to the bottom waters. Because the lower stratified zone in Balmer Lake is < 1m thick the residence times of particulates in this zone are predicted to be brief, suggesting that remobilization occurs predominantly at the sediment-water interface.

In general, considerable difficulty arises when trying to distinguish between diffusion across the sediment water interface and dissolution of settling

oxide particles as the source of increased concentrations. In an earlier review, Sholkovitz (1985) demonstrated that enhanced redox-related effluxes were accountable for increased bottom water concentrations of Na, K, Mg, Ca, Ba, Fe, Mn, P, Si and NH₃ in some seasonally anoxic lakes. However, evidence showing similar effects with other elements is scarce.

Visible dissolved trace metal gradients associated with bottom water sources have also been attributed to the remineralization of organic matter (Morfett *et al.*, 1988; Hamilton-Taylor and Willis, 1990; Reynolds and Hamilton-Taylor, 1992). In the oceans, many trace elements (e.g., Cu, Zn, Ni, Cd) display vertical concentration distributions strongly correlated with those of the major nutrients; they are depleted in the eutrophic zone by incorporation onto or into planktonic material, carried out of the surface waters by settling, and partly regenerated at depth through decomposition of the organic particles (Bruland, 1980). However, distinct correlations evident between concentrations of P and Si and several trace elements that have been observed in the oceans are rare for lake systems (Balistrieri, 1992). The absence of such correlations may reflect the contrasting environments of marine and freshwater systems, but may also reflect a lack of appropriate lacustrine data (Reynolds and Hamilton-Taylor, 1992). Metal inputs to terrestrial receiving waters are typically greater than loadings to seawater, and given the relative shallowness of lakes, little vertical segregation may develop between the biological scavenging of metals in near surface waters and their partial release at depth during respiration (Sigg 1985).

Sigg (1985) and Morel and Hudson (1985) have suggested that algae incorporate trace elements stoichiometrically, resulting in the approximate formula C₁₀₆N₁₆P₁ (Fe, Zn, Mn)_{0.01} (Cu, Cd, Ni, Co, etc.)_{0.001}. Although this concept of Redfield ratios may be applicable to the metal content of algae, the dynamic nature of lakes limits its usefulness because only under severely

restricted conditions will the stoichiometry be reflected in dissolved metal concentrations (Reynolds and Hamilton-Taylor, 1992). Furthermore, the scheme proposed here remains hypothetical, as some elements that have shown correlations with nutrients have no clear biological role.

The mechanisms described above (i.e., trace element remobilization from sedimentary and settling particulate oxide phases, and organic matter remineralization) are proposed to account for the Ni, Cu, As and Zn enrichments observed in the winter bottom waters at station 3 (Fig. 4.10). The relative partitioning of these elements will be discussed in the porewater sections below. Station 3 has the shallowest water column (2.8 m deep), and appears to lie above the depth of influence of dense mining-related effluents (Fig. 4.7C). Several of the dissolved trace metal profiles at this site show evidence of a bottom water source and generally resemble Fig. 5.1B. The slight contrasts among bottom water gradients of dissolved Mn, Ni, As and Zn, may reflect kinetic variability with respect to the oxidation and precipitation of upward diffusing species (Fig. 4.10). Although corresponding peeper data were not collected from this site, sulphide precipitation appears to be a less significant control on trace metal distributions. Indeed, the less pronounced nitrate removal with depth suggests that reducing conditions are in a less advanced stage of development as compared to deeper lake areas (Fig. 4.5C).

The removal of trace metals as authigenic sulphides in anoxic lake systems has been reported for several elements, including Fe, As, Cd, Cu, Ni, Pb and Zn (Davison *et al.*, 1982; Morfett *et al.*, 1988; Green *et al.*, 1989; Davison *et al.*, 1992; Balistrieri, *et al.*, 1992). Evidence for metal precipitation stems largely from calculated ion activity products using measured values of dissolved constituents in the water column and porewaters. Although sulphide was neither measured nor observed (by smell) in Balmer Lake, the abundant reducible sulphate in the

anoxic winter bottom waters, and the observed trace metal distributions, suggest that sulphide removal presents a principal control on trace element distributions in the deeper lake sites.

In a more reducing area of Balmer Lake (station 4), sulphide precipitation mechanisms become more relevant. This site (3 m deep) is slightly deeper than station 3, and appears to be only marginally affected by mining-related advective flows (Fig. 4.7D). The reduced influence of such discharges is thought to be a result of the shallow depth and its relatively large distance from effluent inputs (Fig. 2.1). Profiles of dissolved Fe, As, Ni and Cu at this site exhibit pronounced decreases below deep water column maxima (Fig. 4.11) and, with two exceptions (Mn and Zn), generally resemble Fig. 5.1C. The removal zones for Ni and Cu appear to be up to 5-10 cm above the sediment surface (Figs. 4.25D and E). The insignificant decreases in dissolved Fe over these horizons in comparison to other trace elements suggest that co-precipitation with FeS is not significant; rather, precipitation as their respective sulphides (i.e., As_2S_3 , NiS and CuS,) presents a more likely mechanism. Prior to the onset of sulphate reduction, the near-bottom distributions of dissolved Fe, As, Ni and Cu may have been similar at this site. However, it is suggested that sulphide removal has since consumed part of the excess of remobilized dissolved trace metals to produce the observed profiles. The fact that diffusional processes have not eroded the prominent dissolved maxima indicates that a steady input of dissolved species (presumably remobilized from sinking particulates) is being supplied to these horizons. Similar water column profiles of various dissolved constituents in permanently stratified Lake Vanda, Antarctica (60 m deep), were attributable to such processes (Green *et al.*, 1989). However, due to the extreme compression of depth scales in Balmer Lake, and the relatively shallow depth of the bottom stratified

layer, particulate metal distributions analogous to those in Lake Vanda are not observed.

Throughout the lake during the winter period, dissolved Mn concentrations exhibit no evidence for sulphide removal, as expected given the high solubility of MnS (Emerson, 1976). Indeed, the Mn distributions suggest a continual supply of dissolved species, which are presumably remobilized from sediments and settling particulates.

Although dissolved Zn profiles exhibit pronounced lake-wide removal at shallow sediment depths (Figs. 4.23-4.25), authigenic sulphide precipitation above the sediment-water interface does not appear to be relevant. Strong associations with organic matter have been suggested previously to explain the decoupling of Zn from the redox cycling of Mn and Fe in a seasonally anoxic lake (Morfett *et al.*, 1988). The apparently strong associations of POM with Zn in Balmer Lake (section 5.1.4; Tables 4.5 and 4.7) may suggest that organic matter remineralization is contributing to the persistent bottom water enrichments. The reductive dissolution of zinc-bearing Mn oxides may also serve as an input mechanism of dissolved Zn (Sigg *et al.*, 1987).

Examinations of the deeper sites (stations 1 and 2) illustrate the greater extent of sulphide reduction in the bottom waters as well as the local importance of deep lateral advection. At station 1, dissolved Fe, As and Cu gradients begin at the 2.5 m depth horizon (Fig. 4.8). The general similarity of this trio of profiles suggests similar controls on the distributions of the three elements in the near-bottom waters. Peeper profiles imply that Cu removal begins 10-15 cm above the sediment-water interface (Fig. 4.23E). While Cu and Fe concentrations continue to decrease to the sediment surface (Fig. 4.8, summarized in Fig. 5.1D), As shows an opposite distribution below 2.8 m (Fig. 4.23C). Such an increase, as well as those for Fe, As, Ni at station 2, can be perhaps attributed to the influence of

relatively metal-rich advective flows (Figs. 4.23 and 4.24; see Fig. 5.1E). At both stations 1 and 2, bottom water SO_4^{2-} increases to values over 12 mmol L^{-1} below depths of 2.7 m (Fig. 4.7). Further evidence for lateral flows lies in the observation that sulphide precipitation alone could not account for the water column minima; i.e., sulphide removal acting near the sediment-water interface could not produce a minimum 40-70 cm above the sediment surface. Furthermore, if the bottom sediments were providing a metal source, and the water column minima were the result of trace metal scavenging at an oxic front, one should see evidence of metal release from the porewaters. However, near-interface trace metal profiles for Fe, As and Ni at station 2, and As at station 1, offer little support for diffusive effluxes fostered by sub-interface release (Fig. 4.24 and 4.23). In addition, profiles of the respective dissolved and particulate metal fractions do not support the removal of upward diffusing species by incorporation into Fe- or Mn-oxide precipitates (Tables 4.6 and 4.7).

5.2 Sediment Geochemistry

The sediments in Balmer Lake represent complex mixtures of lithogenic, biogenic and authigenic phases which vary in time and space. For example, the composition of settling particulate matter varies over the course of a year due to seasonal fluctuations in primary productivity, ice coverage and terrestrial runoff. In addition, significant heterogeneity has been introduced via episodic events of lake-wide tailings deposition. Organic matter in the deposits stems both from *in situ* lake production of phytoplankton and macrophytes, and from external inputs via streams and wind-borne transport which vary with the extent of runoff. Prior to the onset of mining activity, allochthonous inputs from Balmer Creek (Fig. 2.1) represented the only significant lithogenous contributions to the

lake. However, since the commencement of mining, tailings have become the major detrital input.

Profiles of several compositional parameters illustrate that below approximately 10 cm, the sediments at stations 1 (cores 1a and 1b) and station 6 (core 2) represent two discrete assemblages and can be clearly seen in the weight ratios of Mg/Al (Fig. 4.32C), Na/Al (Fig. 4.32E), Rb/Al (4.33B) and Zr/Al (4.33C). Those deposits in the lower horizons at station 1 consist of pre-industrial natural deposits, while sediments in core 2 are predominantly mining-derived tailings material throughout. Above the 10 cm transition horizon, the deposits at both locations appear to have received variable contributions from both anthropogenic and natural sources.

The organic carbon content in Balmer Lake sediments of 8-9 wt.% (Fig. 4.34A), agrees with previously measured values and fall within the ranges observed in other productive Canadian Shield lakes (Conroy and Keller, 1976; Semkin and Kramer, 1976; Carignan and Tessier, 1988). Biological activity in Precambrian Shield Lakes has been shown to be influenced by morphology (surface area/volume), lithology (surficial and bedrock geology) and atmospheric loadings (Conroy and Keller, 1976). Water bodies such as Balmer Lake, with high surface area to volume ratios and situated in calcareous terrain, tend to exhibit higher productivity. Lower production characterizes acid lakes (pH<5.5) that have been impacted by acid rain, are poorly buffered, and have high volume: surface area ratios.

Total nitrogen is enriched in the surface sediments of both stations 1 and 6 (Fig. 4.34C) and is illustrated in the depth distributions of the respective $C_{Org}:N$ wt. ratios (Fig. 4.34D). Lower C_{Org}/N values in the upper horizons are most likely the result of increased inputs of inorganic-N compounds and not the result of variations in the C:N ratio of introduced organic matter. Increased inputs of

terrigenous organics, which are commonly associated with lake-side industry (e.g., forest clearing, etc.), would have resulted in a higher C:N signal. The observed distribution of N can be explained by a combination of two relatively recent inputs. First, the hydrolysis of cyanide introduced by the adjacent ore processing operations has increased the abundance of nitrate and ammonium in the lake. Second, accidental dam breaches have supplied significant loadings of fine-grained, chlorite-rich material to the inherently clay-deficient natural deposits (PDI, personal communication). The exchange capacity of chlorite for cations such as NH_4^+ , Cs^+ , Rb^+ and K^+ is comparable to that of illite (Grim, 1953). Therefore, the mineralogical shift induced by the addition of chlorite could have contributed to the relative abundance of particulate nitrogen in the upper decimetre of the Balmer Lake deposits.

The presence of clay-rich deposits in the upper of horizons was established by semi-quantitative X-ray diffraction and examinations of element/Al wt. ratios. XRD peak-height ratios suggest that the quartz content in the upper stratum at station 1 is higher than at depths below 10 cm at this site. However, an increased quartz content cannot represent the sole mineralogic contrast in the upper decimetre because Si/Al wt. ratios decrease in this stratum (Fig. 4.32A). The recent addition of a relatively Al-rich mineral phase to station 1 presents the only plausible explanation that can account for the lower Si:Al ratios. XRD analyses indeed confirm the presence of abundant clay minerals, notably chlorite, in the upper horizons. The data collectively imply that the deposition of detrital chlorite ($\text{Si:Al} \cong 1.3$) has overwhelmed the input of quartz. The high Mg content in chlorite and the higher Mg:Al wt. ratios in the upper stratum at station 1 (Fig. 4.32C) provide further support for a chlorite input. In contrast to station 1, Si:Al ratios in the upper horizons at station 6 imply a

relatively higher quartz content. This is supported by the XRD data: quartz/clay peak height ratios in deposits at station 6 are higher than those at station 1.

The locations of historic tailings discharges with respect to the coring locations could be expected to have exerted significant control on the composition of mining-derived material that reached the respective locales. Station 6 is situated tens of metres from the major points of tailings discharge while station 1 sits over 1 km away. Deposits immediately proximal to such outputs would be expected to be relatively coarser-grained than those more distal. Such textural influences could contribute to the mineralogical differences in the tailings-containing deposits in the two lake areas.

Below depths of 10 cm at station 1, sediment concentrations of all trace metals are low, and are comparable to values typical of Canadian Shield lakes (Semkin and Kramer, 1976). In contrast, the lowest concentrations of Ni, Zn, Cu, As and Pb observed in the tailings deposits are still 4, 2, 2, 20 and 10 x greater, respectively, than the natural contents (Fig. 4.35). The upper horizons at both locales, which are characterized by overall increased metal inventories, are punctuated by dramatic metal spikes; however, those at station 1 (i.e., most distal from the tailings discharge) are an order of magnitude greater than comparable enrichments at station 6. This implies that higher metal contents are associated with the more widely dispersable "slimes" fraction of the tailings.

Pedersen and others (1993) proposed a textural argument to account for metal distributions observed in Anderson Lake, Manitoba, into which tailings have been deposited since 1979. In their study, a coring site over 1 km distant from the tailings discharge was characterized by bands of metal-rich sediments in the upper facies that had Zn, Cu and Pb concentrations an order of magnitude greater than those observed in pure bulk tailings deposits. These horizons hosted ~2 wt.% Cu, ~12 wt.% Zn and ~15 wt.% S, and were marked by high

Fe/Al ratios (~4:1), suggesting metal-pyrite and metal-sulphide associations. The sulphur distribution at station 1 in Balmer Lake sediments is not clearly matched with the observed metal spikes (Fig. 4.34E). A broad S enrichment of 1.5 wt.% between 3 and 8 cm, and a minor surficial increase do correlate coarsely with Ni, Zn, Cu and As profiles. Assuming sulphide stoichiometries of Cu_2S , ZnS , NiS and As_2S_3 , the sulphur inventory present is more than needed to account for the metal enrichments if they occur as their respective sulphides. Fe/Al profiles at station 1, although characterized by general increases in the top stratum, correlate poorly with the observed metal spikes (Fig. 4.34F). However, the large Fe signal contributed by the clay fraction of the tailings input would potentially overwhelm any contribution of Fe associated with the observed metal spikes.

A coarse calculation comparing the S accumulation rate and the downward diffusive flux of sulphate was performed in order to test whether the observed distribution could possibly represent an authigenic sulphide precipitate (Appendix E). The lake-wide averaged diffusive influx of sulphate-S was calculated to be within an order of magnitude of the S accumulation rate, suggesting that *in situ* sulphide precipitation may partially account for the observed S distribution at station 1.

Carignan and Tessier (1988) also observed sedimentary S maxima between 2 and 8 cm below the interface in eight sulphate-enriched Canadian Shield lakes. Such values, which ranged from 0.2-3.4 wt.%, were attributed to diagenetic enrichments arising from the downward diffusion of SO_4^{2-} followed by its fixation as various S species. Reduced inorganic (e.g., Fe-mono sulphides, pyrite, and elemental S), rather than organic sulphur compounds constituted the major proportion of the total S in these sediments. Organic forms of S were also

shown to be insignificant in polluted lakes near Sudbury, Ontario (Nriagu and Soon, 1985).

Seasonal profiles of porewater Mn distributions (Section 5.3) indicate that considerable diagenetic cycling occurs in the near-surface sediments of Balmer Lake. Manganous ions remobilized in the reducing porewaters migrate upwards where they may precipitate as manganese oxide in aerobic sediments. At steady-state, the reducing horizon will migrate upward at the rate of linear sediment accumulation. Under such conditions, the cycle of dissolution and precipitation results in progressive solid-phase Mn enrichment above the Mn oxide redox boundary (Klinkhammer, 1980). In the organic-rich, highly reducing sediments in Balmer Lake, however, the thin veneer of oxic sediments limits the extent to which Mn can accumulate. For this reason, the broad, deep, solid-phase Mn maximum observed at station 1 does not likely represent a diagenetic profile. The Mn enrichment probably stems from the addition of a tailings-derived carbonate or sulphide phase. The sedimentary geochemistry of Mn will be discussed in greater detail in section 5.3.3.

5.3 Porewater Chemistry

Examination of trace metal porewater distributions (Appendix C), in conjunction with the various metabolite profiles associated with the degradation of organic matter, provides an effective way to study metal behaviour and mobility in sediments. The dialysis-array samplers used in the Balmer Lake project yielded high resolution profiles of dissolved constituents across the sediment-water interface, and these are usually sufficient to allow reasonably accurate determinations of the direction and extent of diffusive trace metal fluxes. Furthermore, the high-resolution information provides good support for

the interpretation of post-depositional processes of trace metal consumption and remobilization.

Various tools can be employed to assist interpretations of porewater profiles. Saturation indices, for example, are often used to elucidate solution/precipitation chemistry in marine and lacustrine sediments (e.g., Carignan and Nriagu, 1985; Balistrieri et al., 1992). However, caution must be exercised when comparing the measured ion activity product with the solubility product to deduce the tendency of a solid phase to form, as the kinetics of solid phase formation are often slow, and the measurement of soluble species (e.g., by filtration) may include colloidal forms (Davison, 1993). Furthermore, metal complexation with ligands in solution or those associated with particle surfaces can also promote deviations from predicted equilibria.

Due to the lack of reliable thermodynamic data, most studies consider simple mineral phases in solubility calculations. This can result in further misinterpretation, as the formation of mixed phases has been proposed to control the concentration of numerous species (Suess, 1979). Various programs, including MINEQL, and HYDRAQL (Papelis *et al.*, 1988), are often used to constrain chemical speciation and equilibrium in such solubility calculations.

Examination of the dissolved trace metal and metabolite porewater profiles in Balmer Lake sediments demonstrate that dramatic changes in the chemical environment occur across the sediment-water interface. Sharp gradients for most constituents appear at or shortly below the sediment surface throughout the lake during all seasons.

The shapes and depths of trace metal and metabolite profiles, in combination with solid phase distributions, are used below in the interpretation of the porewater chemistry in Balmer Lake. In particular, zones of non-linear concentration gradients delineate the depths of trace metal consumption and

remobilization. The absence of porewater HS^- , PO_4^{2-} and HCO_3^- measurements prevented calculation of the solubility of various authigenic trace metal precipitates. However, due to the high spatial resolution of the profiles and the well-constrained thermodynamic transitions defined by NO_3^- , Mn(II) , Fe(II) and SO_4^{2-} data, a reasonable degree of confidence can be drawn in the predictions of trace metal behaviour.

Diffusive fluxes, and hence estimates of reaction rates, were calculated from linear concentration gradients (Appendix F) using Fick's First Law:

$$J_z = \frac{D_j^o}{F} \phi \frac{dc}{dz}$$

where J_z = flux; D_j^o = *in situ* diffusion coefficient in $\text{cm}^2\cdot\text{sec}^{-1}$ (Li and Gregory, 1974); F = formation factor $\cong 1.4$ for silty clay (Manheim, 1970); this takes into account the tortuous diffusion path of an ion in wet sediments; ϕ = porosity $\cong 0.87$, calculated using the measured water content and an average particle density of $2.65 \text{ g}\cdot\text{cm}^{-3}$; and dc/dz = concentration gradient in $\text{g}\cdot\text{cm}^{-4}$. It is assumed that porosity and diffusion coefficients are invariant with depth. Diffusion coefficients were not corrected for any random transport mechanisms such as biodiffusion, gas ebullition or wave mixing.

5.3.1 Ammonium and Nitrate

The cycles of the essential elements, C, N, and P, are coupled because they are incorporated into the living biomass of primary producers in relatively constant ratios. The complete mineralization of this biomass must therefore lead to the regeneration of the nutrients, HCO_3^- , NH_4^+ and HPO_4^{2-} in a similar stoichiometric proportion (Redfield, 1958). The generally concave-downward

profiles in Balmer Lake sediments suggest that NH_4^+ is actively being liberated throughout the sampled sediment column (Figs. 4.12-4.14; 4.17). The large porewater NH_4^+ gradients evident during the spring, summer and fall, support upward diffusive fluxes towards the sediment water interface. Efflux estimates over these periods range from $0.2\text{-}1.2 \text{ mmol m}^{-2} \text{ d}^{-1}$ (Appendix F). The bottom water mining-derived enrichment in the shallow waters of "Tailings Bay" (station 5) in the fall, however, fosters a downward influx of NH_4^+ into the sediments (Fig. 4.13D). The combination of a deeper remineralized sediment source at this site results in bi-directional diffusion toward the interface.

The nitrification of upward diffusing NH_4^+ at oxygenated horizons during the spring, summer and fall, represents the principal NH_4^+ sink in the interfacial sediments and bottom waters (Froelich *et al.*, 1979). Oxidation is usually considered to proceed via the reduction of molecular O_2 and Mn(IV) by nitrifying bacteria (Van der Weijden, 1992). From NH_4^+ profiles, it is generally assumed that NH_4^+ is not oxidized, directly or indirectly, by Fe(III) oxide (Froelich *et al.*, 1979). Lower C:N ratios in the upper sediment stratum, however, suggest a portion of the remobilized NH_4^+ sorbs to the abundant clay fractions or other phases in these horizons (see section 5.2).

Over the fall-winter transition, considerable shifts occur with respect to the distribution of porewater and bottom water NH_4^+ (see section 5.1.3). When the lake becomes ice-covered and anoxia develops at depth, NH_4^+ is predicted to diffuse across the sediment-water interface into the bottom waters. Diffusive effluxes are expected to be greatest in the earliest stages of anoxia, and to wane as diffusive equilibrium develops between interstitial and bottom waters. At the time of sampling in late winter, development of such an equilibrium was anticipated to be in an advanced stage. If the largest diffusive NH_4^+ flux calculated above of $1.2 \text{ mmol m}^{-2} \text{ d}^{-1}$ remained constant over time, it would take

approximately 170 days to produce a $200 \mu\text{mol L}^{-1}$ enrichment in the lowermost metre of the water column. Although this calculation represents a maximum, it suggests that diffusive processes significantly affect bottom water concentrations during the seasonally anoxic period.

The relatively minor influences of mining inputs at station 4 make this site the most suitable to assess winter benthic exchanges due to natural processes (Fig. 4.16A). Gradients normally observed in the sediments migrate above the sediment surface during the winter at this site; the NH_4^+ profile reflects diffusive equilibrium across the interface. The concave-upward profile between 5 and 20 cm above the sediment surface implies oxidative removal of NH_4^+ in this zone. Similarly, a concave-upward profile for NO_3^- mirrors that of NH_4^+ , suggesting active nitrification (4.16B).

The seasonal NH_4^+ distributions at stations 1 and 2 have been plotted together to illustrate the variability over the course of a full year (Fig. 5.2). Note that spring profiles were not obtained for station 2. The spring, summer and fall profiles clearly illustrate ammonia production below the interface; these contrast strongly with the generally invariant NH_4^+ distribution in the winter. The zone of oxidative removal migrates above the sediment surface in winter, and is characterized by a dramatic decrease in the concentration gradient. An unusual winter maximum above the sediment-water interface is proposed to reflect a non-steady-state input associated with mining-related discharges. Closer inspection of the winter NH_4^+ distributions at stations 1 and 2 (Figs. 4.15A and D) illustrates the interfacial variation at these sites. It is suggested that variations with respect to the timing, frequency and magnitude of mine-related inputs can account for such variability. The fact that the NH_4^+ concentrations are slightly higher in bottom waters at station 1 in winter implies that a minor ammonium influx to the sediments exists temporarily under the ice at this location.

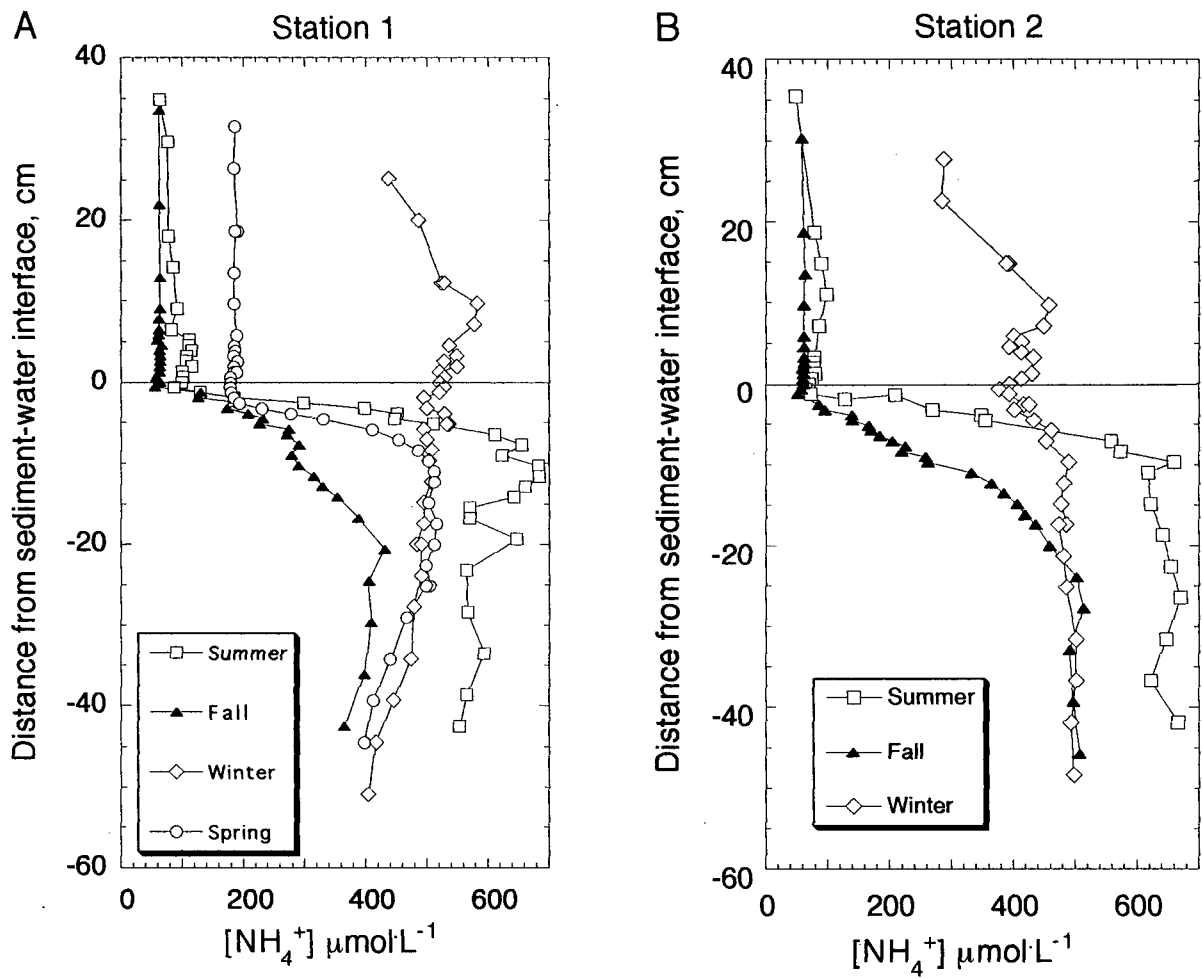


Fig. 5.2. Seasonal peeper profiles of ammonium for stations 1 and 2 (A and B, respectively) in Balmer Lake. Replicate samples are represented by double symbols at specific single depths.

Nitrate profiles during the spring, summer and fall exhibit remarkable inter-season and inter-site consistency (Fig. 5.3). Vigorous nitrate reduction begins 2-5 cm below the sediment-water interface, resulting in downward fluxes ranging from 0.3-1.3 mmol N·m⁻²·d⁻¹ during the well-mixed periods (Appendix F). Such implied denitrification rates are similar to those observed in organic-rich sediments of other temperate lakes (Rudd *et al.*, 1986), and lie intermediate to denitrification rates observed in aerobic deep-sea sediments (3-10 μmol N·m⁻²·d⁻¹) and eutrophic coastal marine systems (7 mmol N·m⁻²·d⁻¹) (Jenkins and Kemp, 1984).

The oxidation of upward diffusing NH₄⁺ appears to account for the interfacial NO₃⁻ spikes seen particularly in summer at sites 1 and 2 (Fig. 5.3). Coastal marine sediments commonly have a sharp NO₃⁻ peak close to the sediment surface, from which NO₃⁻ is lost to the bottom waters via upward diffusion (Emerson, 1976). In this case, the peaks apparently occur at or immediately above the interface, implying that the sediment surface is the site of extremely active nitrification in summer.

The winter data indicate that NO₃⁻ reduction begins 7-15 cm above the sediment-surface at stations 1, 2 and 4 (Figs. 4.15 and 4.16; see section 4.1.3). The near-bottom anoxia implied by these profiles is not illustrated by the nitrate profiles at the shallow (2m) station 6 (Fig. 4.16E), indicating that anoxia is restricted to deeper lake areas.

5.3.2 Sulphate

After aerobic respiration, SO₄²⁻ reduction is, on a global scale, the most important process in the diagenesis of organic matter in marine systems. However in lakes, sulphate reduction is relatively insignificant given the dearth

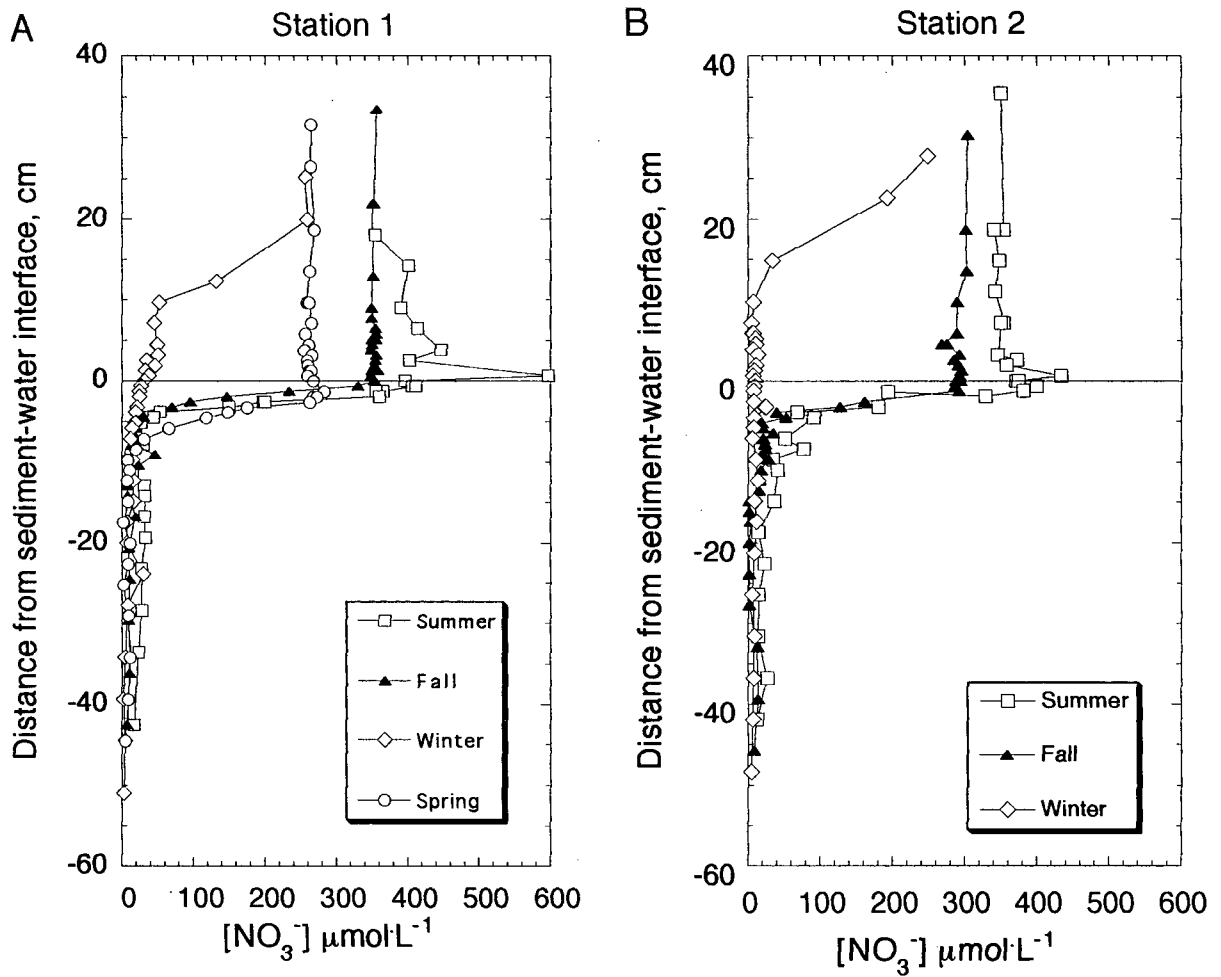


Fig. 5.3. Seasonal peeper profiles of nitrate for stations 1 and 2 (A and B, respectively) in Balmer Lake. Replicate samples are represented by double symbols at specific single depths.

of dissolved SO_4^{2-} (usually $< 100 \mu\text{mol}\cdot\text{L}^{-1}$). This generalization does not apply to Balmer Lake, however, where relatively recent anthropogenic additions of SO_4^{2-} have undoubtedly shifted the respective proportions of organic matter oxidized by O_2 and SO_4^{2-} . This becomes particularly relevant during periods of bottom water anoxia, during which the absence of other oxidants at the sediment-water interface implies that organic matter remineralization proceeds via SO_4^{2-} reduction alone for possibly several months per year.

The dialysis-array data nicely depict the temporal mechanisms that govern the seasonal distribution of SO_4^{2-} . In winter, large external SO_4^{2-} inputs impart a diffusive influx of SO_4^{2-} into the sediments; the topmost porewaters host in excess of $8 \text{ mmol}\cdot\text{L}^{-1}$ during such periods (Figs 4.15 and 4.16). In spring, average water column values are greatly reduced (to $\sim 3.5 \text{ mmol}\cdot\text{L}^{-1}$) as a result of water column mixing and an increase in lake volume. The subsurface maximum in spring represents the remnant of the interfacial SO_4^{2-} excess seen in the late winter (Fig. 5.4). The reduction of SO_4^{2-} in the porewaters, combined with diffusional transport, indicate that the sub-surface peak is in a state of progressive decay. Indeed, early summer profiles at station 1 exhibit a highly attenuated SO_4^{2-} maximum (Fig. 4.12C), and no evidence of the peak remains by fall (Fig. 4.13C).

Diffusive influxes of sulphate over the course of the sampling year ranged from $0.5\text{-}2.4 \text{ mmol}\cdot\text{m}^{-2}\cdot\text{d}^{-1}$ (Appendix F). The lower end of this range agrees well with Rudd *et al.* (1986), who reported reduction rates ranging from $0.1\text{-}0.4 \text{ mmol}\cdot\text{m}^{-2}\cdot\text{d}^{-1}$ in organic-rich sediments in several temperate lakes. The upper limit in Balmer Lake sediments represents enhanced transport across the interface due to the large gradients imposed by sulphate-rich effluents. The depth where sulphate reduction commences in the Balmer Lake deposits, defined where $d^2[\text{SO}_4^{2-}]/dz^2 > 0$, varies seasonally. The reduction horizon appears to

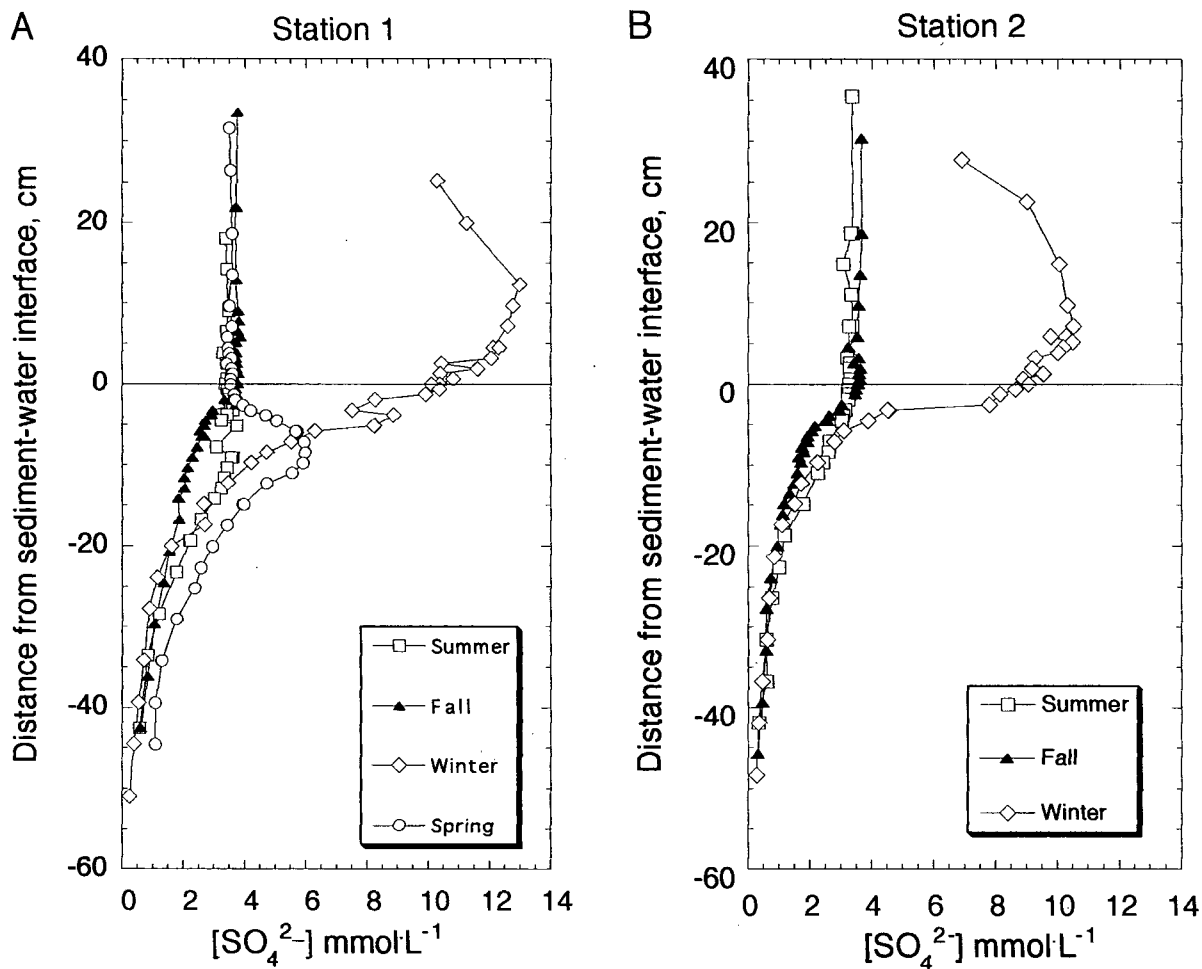


Fig. 5.4. Seasonal peeper profiles of sulphate for stations 1 and 2 (A and B, respectively) in Balmer Lake. Replicate samples are represented by double symbols at specific single depths.

migrate towards the interface through the summer-fall-winter transition, indicating that SO_4^{2-} is being consumed at progressively shallower depths. The presence of abundant electron acceptors other than SO_4^{2-} (e.g., reactive Fe(III) and Mn(IV)) may sustain microbial processes in the upper sediments during the early summer. However, enhanced production and build-up of organic matter over the summer would cause labile Fe and Mn species to become progressively depleted, thus favouring the consumption of SO_4^{2-} at shallower sediment depths. Although dissolved Cu profiles suggest SO_4^{2-} is being reduced several centimetres above the sediment-water interface in winter (Fig. 4.23-4.25), non-linear SO_4^{2-} concentration gradients only become obvious below the sediment surface (Fig. 5.4). The SO_4^{2-} -rich advective inputs most likely overwhelm consumption signatures in the hypolimnion in this season. The SO_4^{2-} reduction horizon deepens again in the spring as Mn and Fe oxides precipitate at and just below the reoxygenated interface.

In addition to the reduction of sulphate, sulphide is also introduced to porewaters by the hydrolysis of proteins in organic detritus; fresh plankton has an organic-S content ranging from 1-2 wt.% (Jorgensen, 1977). Although dissolved trace metal profiles point to the precipitation of solid-phase sulphides as a sink for H_2S , the respective organic and inorganic contributions to the overall accumulation of sulphur remain unclear (see section 5.2).

5.3.3 Iron and Manganese

Diagenetic Fe and Mn enrichments are commonly observed at, or near the surface of oxic lake sediments. Such accumulations normally result from the upward diffusion of porewater Fe(II) and Mn(II) in anoxic sediments, followed by precipitation as their oxyhydroxides in surficial oxidized horizons (Carignan

and Tessier, 1988). In neutral lake waters, the oxidation of Fe is believed to proceed chemically, although its removal below the oxycline indicates that other oxidants in addition to O_2 , such as NO_3^- and Mn(II), may be involved. The extent of diagenetic iron oxyhydroxide enrichments in Balmer Lake can not be determined from the solid-phase data due to the large mining-derived signals of Fe and Mn in the top 10 cm of the sediment column (see section 5.2; Figs. 4.34F and 4.35A). However, the respective remobilization depths of porewater Fe and Mn during oxygenated periods provide an indication of the thickness of surficial oxide enrichments and hence help assess the sorptive capacity for trace metals.

Dissolved Mn distributions in porewaters during the spring, summer and fall periods suggest that Mn oxyhydroxides are remobilized at depths ranging from ~2 to 8 cm (Figs. 4.18-4.27). The shallower depths evident in the fall suggest the Mn reduction horizon migrates upwards throughout the summer months, as alluded to in Section 5.3.2. The addition of dissolved Fe to the summer porewaters is thermodynamically consistent with the Mn distribution; significant gradients are evident 2-3 cm below comparable increases for Mn (Figs. 4.18 and 4.19). Assuming that the Fe oxyhydroxide dissolution front migrates in accordance with Mn, it can be proposed that the sorptive capacity of the surficial sediments for trace elements decreases through the summer, fall and winter, and increases again in the spring.

Although dissolved iron distributions in Balmer Lake sediments exhibit considerable inter-site and inter-season (i.e., non-steady-state) variability, the available evidence indicates that authigenic sulphide precipitation presents a significant control on the distribution of Fe and other trace elements. During the summer period, concavity in the Fe profiles between ~8 and 20 cm depth at Stations 1 and 2 implies removal from pore solution (Figs. 4.18A and 4.19A). Since these zones lie immediately below the nitrate-zero boundary, sulphide

precipitation is implicated as a likely Fe sink. Sulphide precipitation was proposed to account for similarly shaped profiles in a Canadian Shield lake (Carignan, 1984; Carignan and Nriagu, 1985). The non-steady-state effects on the porewater sulphate distributions in Balmer Lake limit the use of the sulphate profiles in precisely defining dissolved sulphide production zones. In general, however, the sulphate distributions are thermodynamically consistent with the respective sulphate reduction horizons (Figs. 4.12C and F).

The migration of the SO_4^{2-} reduction horizon towards the interface over the summer implies that authigenic sulphides precipitate at shallower sediment depths in the fall. The relative absence of Fe above 20 cm at station 1 in the fall (Fig. 5.5) can be attributed to two factors: (i) the reducible iron oxide inventory in the upper sediment column in spring is exhausted by late autumn; and (ii) sulphide precipitation removes iron from porewaters in the upper two decimetres as conditions become more reducing through the late summer. Deep sources of dissolved Fe can also be seen in profiles from stations 1 and 2 (Fig 5.5). Such increases at depth may represent the historical addition of dissolved iron to porewaters prior to the mining operations, when the natural dissolved sulphate concentration in the watershed was very low. Under such conditions, limited production of dissolved sulphide during diagenesis allows high Fe^{2+} concentrations to persist in porewaters.

Winter Fe profiles exhibit considerable inter-site variability (Fig. 5.6). The distribution at station 1 is fairly consistent with the summer and fall profiles at this site. The high concentrations of dissolved Fe observed in the deep porewaters at station 2 during the summer and fall ($3\text{-}4\text{ mgL}^{-1}$) are absent in winter (Fig. 5.6). At stations 4 and 6, dissolved Fe levels generally remain $< 500\text{ }\mu\text{gL}^{-1}$. Whether such seasonal disparity at station 2 represents a sampling artifact, or a combination of diffusion and consumption mechanisms, remains

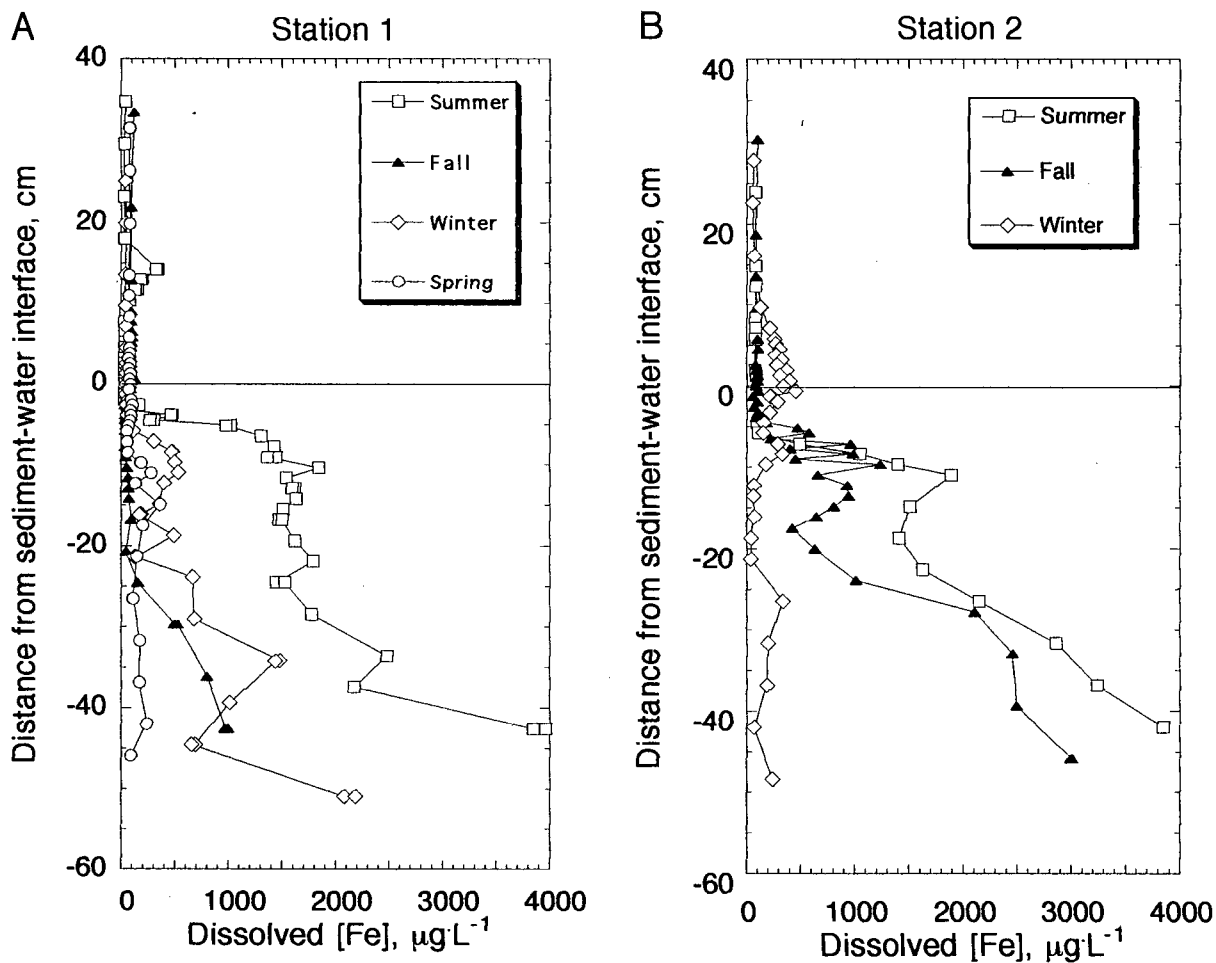


Fig. 5.5. Seasonal peeper profiles of dissolved Fe for stations 1 and 2 (A and B, respectively) in Balmer Lake. Replicate samples are represented by double symbols at specific single depths.

Winter Iron

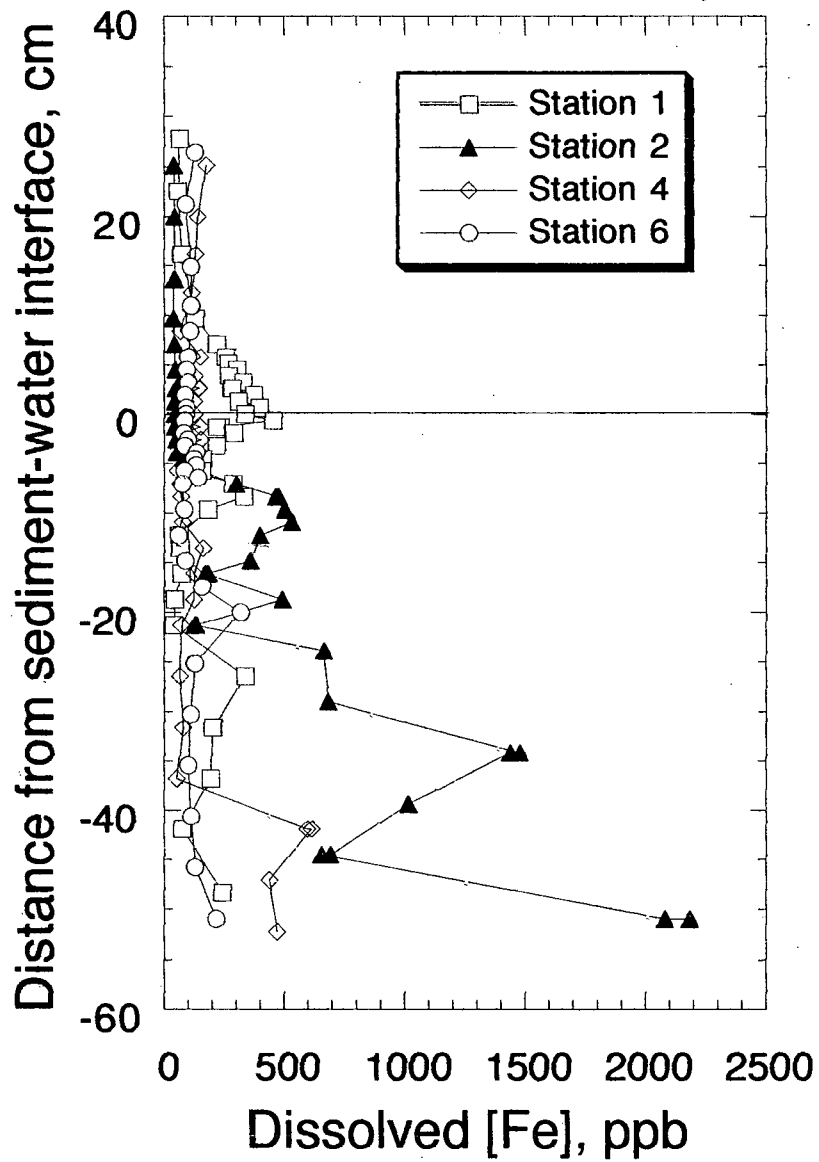


Fig. 5.6. Winter peeper profiles of dissolved Fe for stations 1, 2, 4 and 6 in Balmer Lake. Replicate samples are represented by double symbols at specific single depths.

unclear. The rapid oxygenation of Fe(II) in the presence of oxygen does make the sampling of reducing porewaters more susceptible to potential error.

The biological processes leading to sulphide mineral formation are generally characteristic of anoxic sediments where the bacterially-mediated oxidation of organic matter is accomplished via reduction of porewater sulphate and production of hydrogen sulphide (Berner, 1984). Under such conditions, metal ions remobilized by reductive dissolution of oxide minerals can react with H₂S and other sulphur compounds to form a variety of sulphide minerals. Due to the abundance and ubiquitous nature of Fe, these authigenic precipitates are often dominated by Fe-sulphides.

The major iron sulphide minerals found in lacustrine sediments are mackinawite (Fe_{0.995-1.023}S), greigite (Fe₃S₄), pyrite (FeS₂) and amorphous-FeS (Morse *et al.*, 1987). As an assemblage, amorphous-FeS, mackinawite and greigite are generally termed acid volatile sulphides (AVS) because they are readily decomposed by acids. In the presence of HS⁻ at concentrations above pyrite saturation, transformation of these metastable phases usually proceeds to pyrite, a more thermodynamically stable mineral (Berner 1984). However, pyrite can precipitate directly in environments where the more soluble monosulphides are undersaturated with respect to sulphide (Perry, 1993). The amount of pyrite that may form in sediments is controlled by the rates of supply of labile organic matter, reactive detrital iron minerals and dissolved sulphate (Berner, 1984). In most marine systems (those with oxygenated bottom waters), the amount and reactivity of organic matter buried in the sediment represent the primary control on pyrite formation because it is this organic supply which limits the rate of *in situ* sulphate reduction and thus hydrogen sulphide production (Berner, 1984; Calvert and Karlin, 1991). Such sediments deposited in oxygenated

environments generally show a linear relationship between total or pyritic sulphur and organic carbon (Raiswell and Berner, 1985).

In contrast to marine systems, pyrite formation in freshwater regimes is generally inhibited by low concentrations of dissolved sulphate (Berner, 1984). Therefore, much higher concentrations of pyrite typically form in organic-rich marine sediments; this has led to the use of C/S ratios to distinguish freshwater and marine sedimentary rocks (Davison *et al.*, 1985). Experimental data suggest that limitations on pyrite formation are not important at sulphate concentrations greater than $5 \text{ mmol}\cdot\text{L}^{-1}$ (in Berner, 1984, from Westrich, 1983). Concentrations of $\sim 3 \text{ mmol}\cdot\text{L}^{-1}$ in Balmer Lake deep waters during the summer and fall imply that authigenic sulphide formation may be somewhat limited by sulphate abundance. During the winter and spring periods, however, a plentiful supply of both organic matter and reducible sulphate (i.e., $> 6 \text{ mmol}\cdot\text{L}^{-1}$) suggest that the amount of reactive Fe-phases limits pyrite formation during these periods.

From the above discussion, it can be proposed that extensive precipitation of authigenic sulphides in Balmer Lake sediments is likely a relatively recent phenomenon, reflecting the current unnatural abundance of SO_4^{2-} in the lake waters. Recent sedimentary sulphide additions to S-polluted lakes in the Sudbury region of southern Ontario have similarly been attributed to anthropogenic sulphate loadings (Carignan and Tessier, 1988). Diagenetic sulphur accumulations in excess of 3 wt.% (i.e., greater than those enrichments observed in Balmer Lake) have been reported in such lakes. Since the potential SO_4^{2-} supply has exceeded the labile-Fe (i.e., non-silicate) supply in these lakes, S fixation as inorganic sulphides appears to be iron limited (Carignan and Tessier, 1985a; Nriagu and Soon, 1985).

Reports of trace metal sulphide phases generally make no clear distinctions between precipitation as the pure metal sulphide or co-precipitation

with Fe sulphide. Experimental investigations have revealed that adsorption and coprecipitation of many trace elements with mackinawite (FeS) and pyrite (FeS₂) are important processes in marine anoxic sediments (Huerta-Diaz and Morse, 1992; Arakaki and Morse, 1993; Morse and Arakaki, 1993). Furthermore, analyses of lacustrine iron sulphide particles collected from the anoxic bottom waters in a soft-water lake in the U.K. revealed Cu and Zn concentrations in excess of 4,000 and 6,000 mg·L⁻¹, respectively; such levels were higher than those observed in iron oxide precursors (Davison *et al.*, 1992).

Control by phases other than oxide and sulphide precipitates may be affecting the behaviour of Fe species in Balmer Lake, although this is difficult to constrain with the available data. Iron carbonate and phosphate minerals, for example, are potentially important authigenic components of lacustrine sediments. Iron carbonate phases form in anoxic environments, where the metabolic generation of inorganic C species leads to supersaturation, favouring the formation of siderite (FeCO₃) (Suess, 1979). Such solubility control has been invoked to account for Fe distributions in several lacustrine studies (Emerson, 1976; Matisoff *et al.*, 1980; Cook, 1984; Carignan and Nriagu, 1985). Although no definite conclusions can be drawn for Balmer Lake, the abundance of reducible sulphate suggest that dissolved Fe species in the anoxic porewaters would be scavenged by free sulphide.

The seasonal porewater Mn distributions at stations 1 and 2 suggests that non-steady-state inputs of Mn-rich water are contributing to the temporal variability (Fig. 5.7). The summer and fall profiles are consistent with diagenetic processes; i.e., remobilization in reducing porewaters and precipitation in the oxic surficial horizons. However, the large winter maximum at ~15 cm depth at station 1 cannot represent a post-depositional signature. The exhausted inventory of reducible Mn-oxides in the surface sediments in late autumn

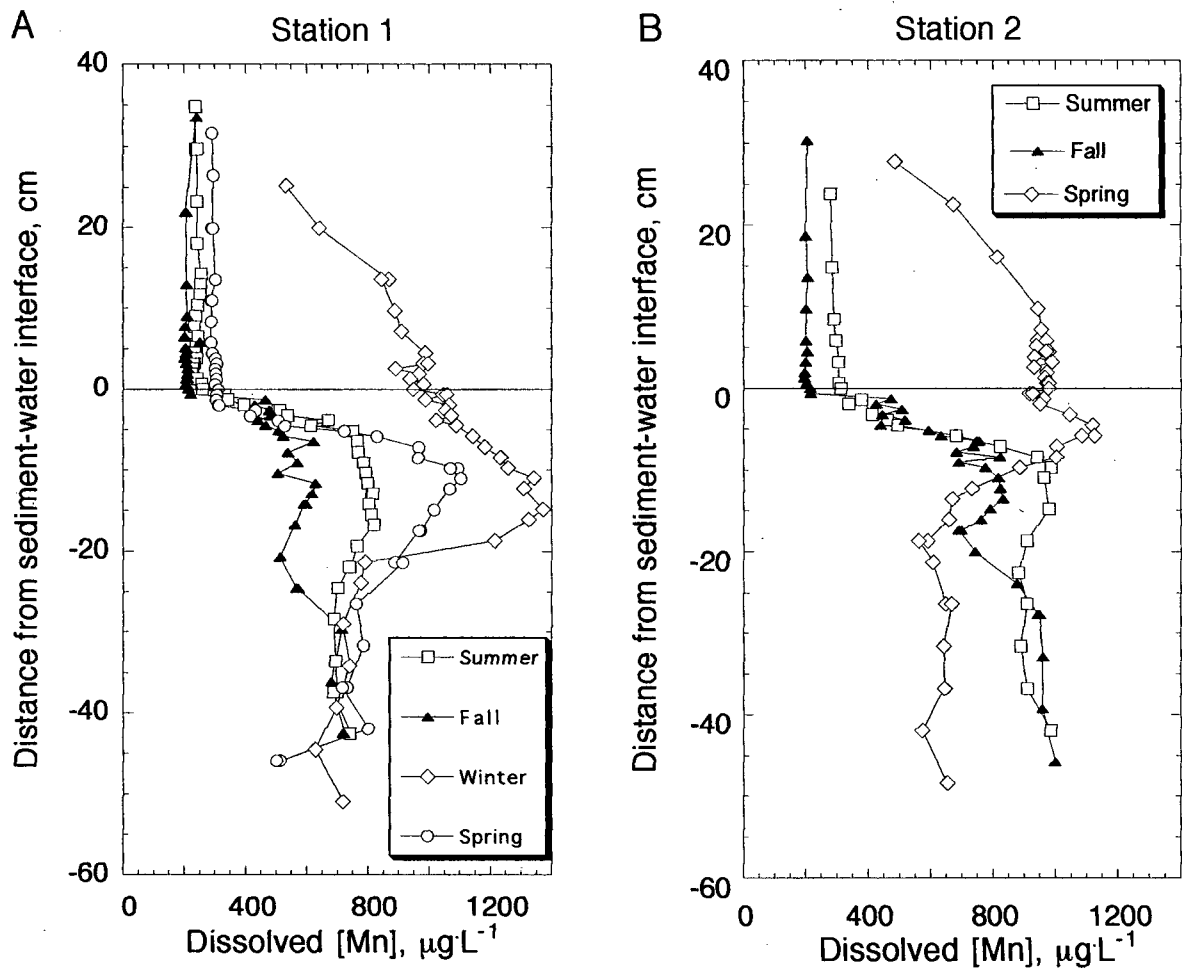


Fig. 5.7. Seasonal peeper profiles of dissolved Mn for stations 1 and 2 (A and B, respectively) in Balmer Lake. Replicate samples are represented by double symbols at specific single depths.

effectively excludes the dissolution of such phases as a potential source of the dissolved input. Furthermore, the depth of the dissolved maximum lies within the zone of postulated FeS precipitation, suggesting that labile Mn-oxides are not present at these depths. The above argument implies that an influx from the bottom waters is contributing to the observed winter profile (Fig. 5.7). Implicit in this argument is that at some point between the fall and winter sampling periods (Oct. to May), the sediments at station 1 were in contact with bottom waters hosting Mn concentrations in excess of $1400 \mu\text{g}\cdot\text{L}^{-1}$. The large mining-derived sedimentary accumulations of Mn in the upper facies (Fig. 4.35) do suggest that tailings pond effluents host abundant manganese.

Figure 5.8 illustrates the proposed temporal sequence. An instantaneous input of dissolved Mn to the fall bottom waters (5.8B), followed by diffusion of Mn into the sediments would foster increased concentrations in the upper porewaters (Fig. 5.8C). By late winter, the strength of the bottom water Mn source had decreased. However, due to the longer residence time of dissolved species in pore solution, evidence of the previous input persists (Fig. 5.8D). The high porewater concentrations support an efflux of Mn into the bottom waters during this period (Fig. 5.7). A similar deep porewater maximum was not evident for sulphate during winter sampling at stations 1 and 2 which may suggest that either: i) the consumption of sulphate in the interfacial horizons inhibits accumulation in the porewaters; or ii) the mining-related inputs of manganese and sulphate are temporally decoupled.

Dissolved Mn concentrations progressively decrease from the winter maximum through the spring, summer and fall (Fig. 5.7). The re-establishment of an interfacial Mn sink upon re-oxygenation of the water column in the spring suggests that the progressive consumption of the dissolved Mn near the

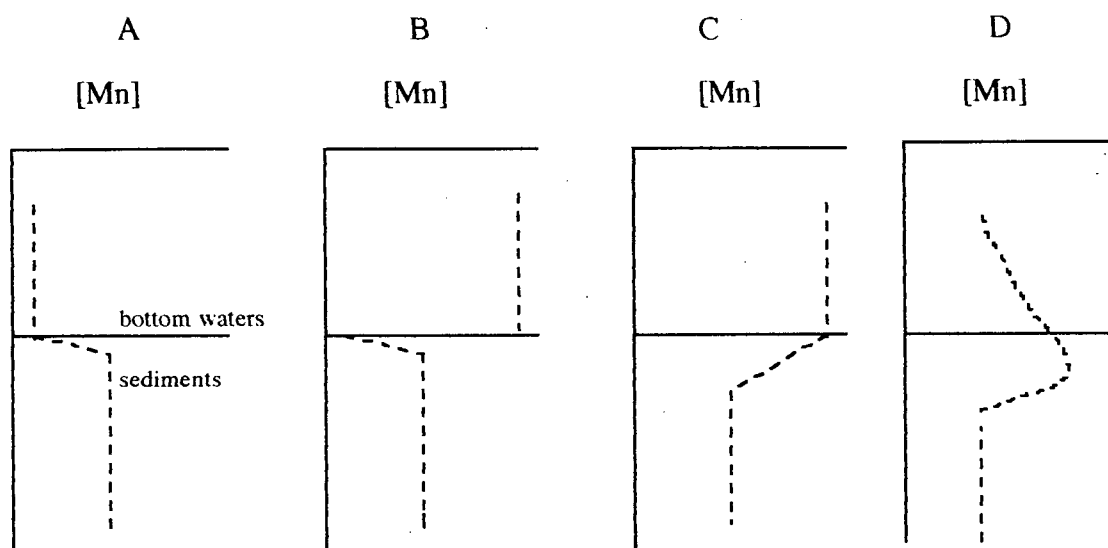


Figure 5.8. Time series of progressive bottom water and porewater profiles (A-D) over the fall-winter transition in Balmer Lake: A) fall profile, B) instantaneous input of Mn to bottom waters, C) profile after some time of equilibration, and D) late winter profile. Depth and concentration axes are in arbitrary units.

sediment-water interface, in conjunction with diffusional transport, are responsible for the declining values.

The minimal influence of mining-related bottom waters at station 4 make this site perhaps best suited to examine the winter Mn behaviour (Fig. 4.25B). The Mn-redoxcline has clearly migrated above the sediment surface at this site, and temporary diffusive equilibrium has been established across the sediment-water interface. The concave-upward profile between 8 and 25 cm above the lake floor is consistent with the oxidative precipitation and removal of upward diffusing Mn(II) species.

Upward diffusive effluxes determined for Mn ranged from 54-700 $\mu\text{g}\cdot\text{m}^{-2}\cdot\text{d}^{-1}$ (Appendix F). The low end represents fluxes calculated from the much shallower gradients observed during the late-winter period. This is consistent with the hypothesis that once the oxidative sink for dissolved Mn is removed

during winter anoxia, diffusional processes will cause a progressive decrease in the concentration gradient. Efflux estimates for the spring, summer, and fall exhibit reasonable consistency (Appendix F). Calculated effluxes were used to test the potential influence of such mechanisms on the bottom water composition. At station 4, for example, an excess of approximately $1 \times 10^5 \mu\text{g}$ has been added to the lower 0.5 m of the winter water column (Fig. 4.11). Calculations using a constant maximum gradient suggest that diffusive processes alone would take on the order of 140 days to account for such an accumulation. Similar calculations for hypolimnetic concentrations at station 1 ($\sim 2 \times 10^5 \mu\text{g}$ excess in the lower 0.5 m) and station 2 ($\sim 3.5 \times 10^5 \mu\text{g}$ excess in the lower 0.5 m), demonstrate that time scales on the order of 280 and 500 days, respectively, would be required. Since the maximum efflux of $700 \mu\text{g}\cdot\text{m}^{-2}\cdot\text{d}^{-1}$ was used in the above calculations, the estimated time periods most likely represent minimum values. The calculations suggest that mining-related inputs may have contributed to the bottom water enrichments at stations 1 and 2. Indeed, bottom water sulphate values are significantly higher at these two stations.

The contrasting dissolved Mn profiles observed in the winter at station 6, indicate that Mn is being consumed as opposed to being remobilized in the upper sediments at this site (Fig. 4.26B). Sulphide precipitation as MnS (Suess, 1979) and sorption with mackinawite (FeS) (Heurta-Diaz and Morse, 1992; Arakaki and Morse, 1993) have been suggested to control Mn distributions in marine sediments. The relatively soluble nature of MnS (alabandite, $\text{pK} = 0.40$) suggests that the latter is more favourable in Balmer Lake sediments. Laboratory investigations have demonstrated that adsorption of Mn(II) with fine-grained mackinawite is more important than coprecipitation, and has been attributed to a combination of the high specific surface area of FeS, and a small partition coefficient that limits Mn incorporation into the FeS lattice (Arakaki and Morse,

1993). The tailings-rich deposits at station 6 perhaps favour the removal of Mn from porewaters via such adsorption mechanisms.

The precipitation of Mn-carbonate phases has been suggested to govern the behaviour of Mn in the reducing porewaters of several lake sediments (Matisoff *et al.*, 1980; Carignan and Nriagu, 1985). Supersaturation with respect to carbonate minerals can be achieved in anoxic environments due to the pH-buffering effect by proteolytic formation of H₂S, other weak acids, and possibly H⁺-ion exchange (Suess, 1979). However, solubility considerations indicate that the porewaters at station 6 are likely undersaturated with respect to rhodochrosite.

5.3.4 Nickel

Peeper profiles suggest that two factors control the distribution of nickel in Balmer Lake porewaters: (1) release to solution from labile Ni-bearing phases at or near the sediment-water interface; and (2) the precipitation of authigenic Ni-bearing sulphide phases at depth. Each will be discussed in turn.

Surface or near-surface maxima of dissolved Ni can be observed throughout the year in almost all profiles collected from Balmer Lake sediments. Although the enrichments are generally small in relation to extent of removal at deeper depths, the peaks are well-constrained and appear to represent real signatures (Figs. 4.18-4.27). The magnitudes of these signals above the respective water column background concentrations average ~40 ppb and range from 30-200 ppb. Concentration profiles suggest that Ni is simultaneously diffusing from the interface to the sediments, and from the interface to the overlying water. The fact that these profiles exhibit reasonable seasonal consistency suggests that the spikes are representative of steady-state conditions.

Remobilization of trace metals at the sediment-water interface has been typically attributed to remineralization of organic matter and/or dissolution of Fe and Mn oxyhydroxides (Klinkhammer, 1980). In the case of Balmer Lake, the presence of dissolved Ni maxima 2 to 5 cm above the predicted horizon of Mn(IV) reduction during the summer sampling session suggests that Ni is released from the oxidation of organic matter, and not by dissolving oxides (Figs. 4.18D and 4.19D). Enrichments derived from organic matter oxidation would be expected to be observable at or near the sediment-water interface due to the higher rates of remineralization in the surface facies that stem largely from the greater reactivity of freshly deposited organic matter (Middleburg, 1989). In the fall period, the Mn and Fe redox horizons are immediately proximal to the sediment-water interface, and as such, a biogenic origin cannot be uniquely isolated (Figs. 4.13-4.14).

The cycling of organic matter has been invoked as a control on the distribution of Ni because the metal has a nutrient-like distribution in the oceans (Bruland, 1980). The principal mechanisms of incorporation into particles are active algal uptake and indiscriminant complexation by high-affinity surface ligands. It has been proposed that some non-essential constituents function as chemical analogues to those that are essential, and hence, are sequestered and transported in a similar manner (Morel and Hudson, 1985).

Although reports of Ni concentrations in porewaters are rare, the existing information sheds important light on the early diagenetic behaviour of the element. Westerlund *et al.* (1986), for example, used benthic flux chambers to assess trace metal transport across the sediment-water interface in Swedish coastal deposits. They showed that Cu, Ni, Zn and Cd, were released to the bottom waters in spite of the presence of abundant sulphide at shallow sediment depths. These trace metals were shown to be associated with phases from which

they were released via oxidation, rather than by reduction as was the case for Mn, Fe and Co. Similarly, Klinkhammer *et al.* (1980) and Tsunogai *et al.* (1979) attributed post depositional migration of Ni and Cu to release from labile organics during early diagenesis in pelagic sediments.

Interfacial enrichments on the order of ~ 10 ppb greater than immediately overlying water column values have been observed for some of the more biologically important elements (e.g., Zn; Morfett *et al.*, 1988). However, oxidative additions in excess of 30 ppb for elements having less strong associations with organic matter (e.g., Ni), have not been previously reported. It is proposed that the high concentrations of Ni in the water column of Balmer Lake (averaging >300 ppb) facilitates its sorption onto and/or incorporation with labile particulates in concentrations great enough to support interfacial releases of such large magnitude. Indeed, the particulate Ni concentrations observed in Balmer Lake (Section 4.1.4.2) are comparable to the highest ever reported (see Nriagu *et al.*, 1982).

In addition to its affiliation with organic matter, nickel has been shown to have a high sorptive affinity for oxide surfaces (Vuceta and Morgan, 1978; Young and Harvey, 1992), and is commonly associated with diagenetic Mn and Fe enrichments in lake sediments (Carignan and Nriagu, 1985; Cornwell, 1986). For these reasons, diagenetic accumulations of Fe and Mn in Balmer Lake sediments may be expected to liberate exchangeable Ni species at their respective reduction horizons. Indeed, the large shallow spike of dissolved Ni in the fall at station 1 (Fig. 4.20D) might reflect contributions from both organic and oxide sources. In addition, the slightly deeper Ni enrichments observed in the spring (at ~5-7 cm), correspond more closely with the apparent remobilization depths of Fe and Mn (Fig. 4.27D). Remobilized porewater Ni maxima in excess of 8 ppb have been reported in coastal marine sediments (Shaw *et al.*, 1990). Rapid sulphide

complexation/precipitation of liberated Ni may, however, prevent the formation of a dissolved Ni excess at deeper depths in the summer. Indeed, the reducing environment in Balmer Lake sediments suggests that the zones of trace metal remobilization (due to Mn(IV) and Fe(III) reduction) and sulphide precipitation almost overlap.

The downward concavity below ~5 cm seen in all profiles indicates that the sediments of Balmer Lake provide a sink for dissolved Ni throughout the year. Two observations support the precipitation of Ni-bearing sulphide phases as the most probable removal mechanism. First, the Ni removal zones in general correspond with SO_4^{2-} reduction horizons. Second, authigenic sulphide precipitation has been reported for Ni in several marine and lacustrine sediments (Morse and Arakaki, 1993; Green et al., 1989; Belzile and Morris, 1995), including reports from Canadian Shield lakes (Carignan and Nriagu, 1985).

Peeper profiles of dissolved Ni exhibit remarkable inter-site and inter-season consistency (Fig. 5.9). While sulphate distributions follow a seasonal pattern consistent with the development of anoxia in winter (i.e., reduction depths are shallowest in late winter and deeper in spring and fall), Ni removal profiles do not obey this sequence. In general, the predicted zones of Ni removal occur deeper in the winter than in the fall and summer. Reasons for this are not clear; however, a decoupling of Ni and sulphate during the winter months might be expected considering the variable rates of discharge and poorly constrained composition of mining inputs. Non-steady-state Ni profiles associated with variable mining discharges like those seen for NH_4^+ and Fe, are not easily discernible from the winter data. The predominantly uni-directional diffusive transport perhaps makes this element less susceptible to such influences.

Solubility calculations indicated that the porewaters in Canadian Shield lakes studied by Carignan and Nriagu (1985) were supersaturated with respect to

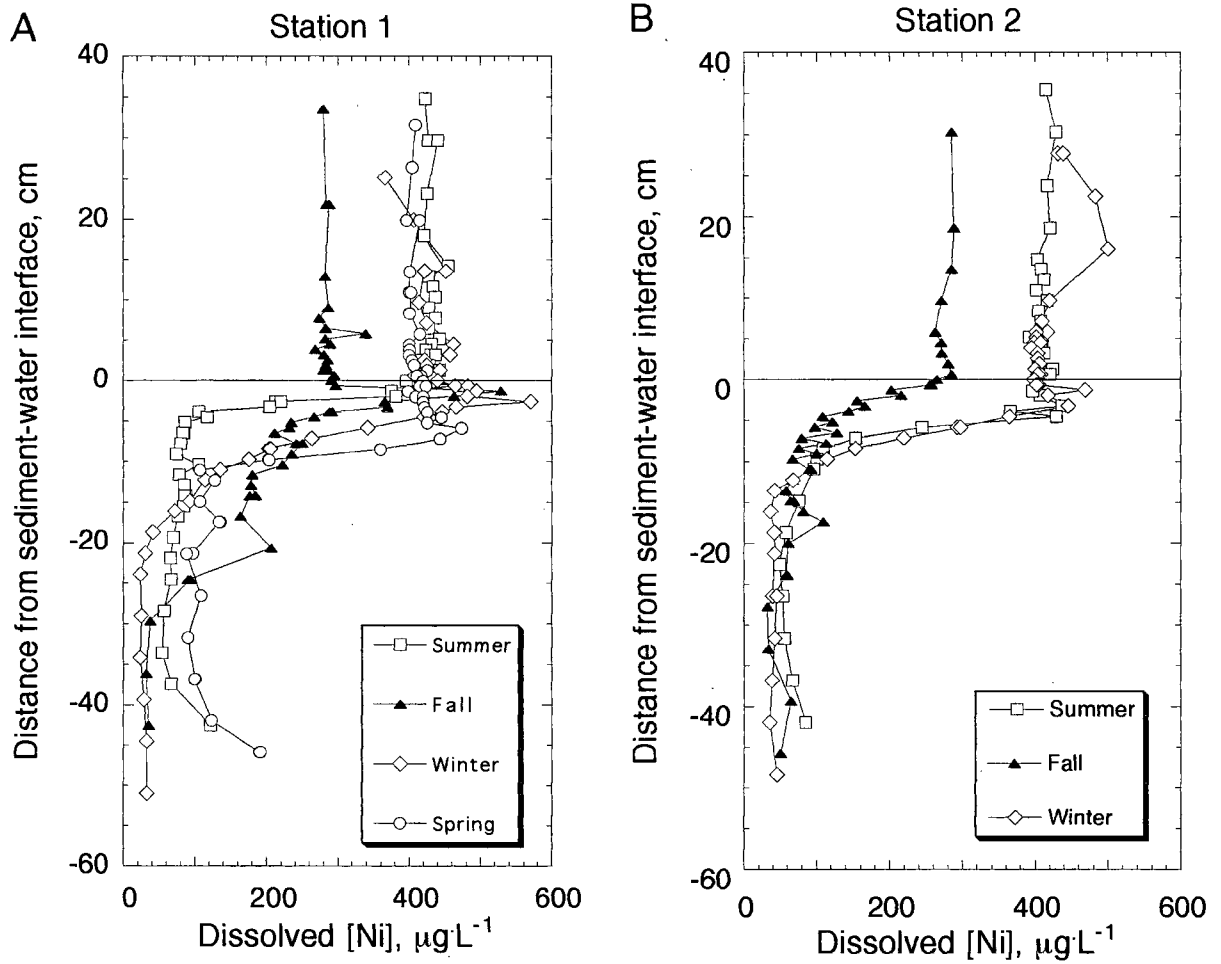


Fig. 5.9. Seasonal peeper profiles of dissolved Ni for stations 1 and 2 (A and B, respectively) in Balmer Lake. Replicate samples are represented by double symbols at specific single depths.

millerite (NiS). Diffusional influxes of Ni, which ranged from 10-51 $\mu\text{g}\cdot\text{cm}^{-2}\cdot\text{y}^{-1}$, represented 59-161 % of the calculated Ni accumulation rate. Similar influxes are calculated for Balmer Lake sediments: values range from 2.6-14.2 $\mu\text{g}\cdot\text{cm}^{-2}\cdot\text{y}^{-1}$ (Appendix F). On average, concentration gradients for nickel in Balmer Lake porewaters are steepest in the summer and fall; due to temperature-dependent diffusivities, this translates to the greatest diffusive influxes being observed in the summer. Assuming an average influx of 6 $\mu\text{g}\cdot\text{cm}^{-2}\cdot\text{y}^{-1}$ over the entire lake basin, a mean lake depth of 2.4 m, and an average water column concentration of 380 $\mu\text{g}\cdot\text{L}^{-1}$, it would take on the order of 15 years for the sediments to consume the whole-lake inventory of dissolved nickel. This corresponds to ~1% sediment retention of the total dissolved nickel burden with respect to a lake residence time of ~230 days, and suggests that sulphide precipitation has little effect on reducing the large burden of Ni in Balmer Lake. Furthermore, downward diffusion alone cannot account for the large sedimentary Ni accumulations. The accumulation rate, based on 0.3 wt.% Ni, a dry bulk sediment density of 0.35 $\text{g}\cdot\text{cm}^{-3}$, and a sedimentation rate of 0.3 $\text{cm}\cdot\text{y}^{-1}$, is estimated to be ~400 $\mu\text{g}\cdot\text{cm}^{-2}\cdot\text{y}^{-1}$ (Appendix G). Nevertheless, the gradients observed in the porewaters will support significant accumulation of Ni in periods when tailings over-flow is absent.

5.3.5 Copper

The general harmony between the porewater and bottom water distributions of Cu and Ni, suggest that their behaviours are influenced by similar controls (Figs. 4.18-4.27). Unlike Ni and Zn, however, dissolved Cu profiles exhibit no evidence of any interfacial remobilization above the depth of sulphide precipitation. For all seasons, the behaviour of Cu appears to be largely

dictated by authigenic sulphide precipitation at shallow sediment depths during the spring, summer and fall, and in the anoxic bottom waters during the winter period.

During the well-mixed periods of the spring, summer and fall, peeper profiles of dissolved Cu exhibit good inter-season and inter-site agreement (Figs. 4.18-4.22, 4.27). The minimal deviations reflect slightly different removal depths, bottom water concentrations and diffusive influxes. Because there is no evidence of any regeneration from labile solid phases in the upper sediment horizons during these three seasons implies that either particulate Cu is transported to the sediments in refractory phases that are not subject to remobilization, or Cu liberated to the shallow porewaters is rapidly precipitated. The biogeochemistry of Cu, and the conditions in Balmer Lake, suggest that the latter hypothesis is most tenable.

Copper is considered to be biologically more important than Ni with respect to algal metabolic requirements and is characterized by nutrient-like distributions in the oceans (Bruland, 1980; Sanders, 1983). Copper associated with labile organic matter appears to be released during early diagenesis in a wide range of sedimentary environments including lacustrine sediments (Morfett *et al.*, 1988; McKee *et al.*, 1989b; Reynolds and Hamilton-Taylor, 1992; Young and Harvey, 1992), coastal marine deposits (Elderfield, 1981; Westerlund *et al.*, 1986; Shaw *et al.*, 1994; Kerner and Geisler, 1995), pelagic sediments (Tsunogai *et al.*, 1979), suboxic hemipelagic sediments (Klinkhammer, 1980) and marine mine-tailings deposits (Pedersen, 1985). Examinations of Cu partitioning in various sedimentary phases have demonstrated that up to 80-90 % of the Cu burden may be organically bound (Elderfield, 1981; Young and Harvey, 1992).

The rapid scavenging of liberated species may account for the lack of dissolved Cu additions to pore and bottom waters at the sediment-water

interface. The extremely insoluble nature of CuS ($pK = 35.4$; Stumm and Morgan, 1981) as compared to NiS ($pK = 26.7$), may favour the preferential removal of Cu-sulphide phases in the interfacial sediments. This proposal is consistent with the geochemistry of Cu in the Balmer Lake water column. The chemical environment in the winter hypolimnion favours the removal of Cu presumably as sulphide precipitates; such a mechanism is not obvious for Ni.

A fundamental criticism of the previous argument is the fact that the postulated Cu removal is occurring at depths shallower than those predicted for sulphate reduction. However, sulphide precipitation has been implicated for trace element removal in sub-oxic sediments. The removal of porewater Cd at a suboxic front in abyssal Atlantic sediments, for example, was attributed to the precipitation of authigenic CdS (Rosenthal *et al.*, 1995). They suggested that the diffusion of free-sulphide from underlying anoxic sediments was sufficient to support sulphide formation. In addition, Sørensen and Jørgenson (1987) found that sulphate reduction can take place within the microenvironment of organic aggregates in the oxic zone. It is possible that the organic-rich sediments in Balmer Lake promote such development of heterogeneous redox conditions in the "oxic" horizons.

The tendency of a metal to form ligand complexes is usually explained in terms of ligand field crystal-stabilization theory (Stumm and Morgan, 1981). This led to the Irving-Williams order for complex stability of plus II cations, which increases in the order: $Mn^{2+} < Fe^{2+} < Co^{2+} < Zn^{2+} < Ni^{2+} < Cu^{2+}$. The sequence presented here reflects increases in the capability of the cation to take up electrons (i.e., increasing ionization potential of the metal). Complexation, steric hindrances, entropy effects and site specificity can distort this hierarchy (Benjamin and Leckie, 1981). Based on analyses of porewaters collected in Anderson Lake, Manitoba, Pedersen *et al.* (1993) suggested that the high sorptive

affinity of Cu for dissolved organic ligands, which would tend to keep Cu in solution, could account for Cu being removed at deeper depths than other metals such as Zn and Cd. This suggestion appears not to apply to the porewater Cu and Ni distributions in Balmer Lake, however, as the depth of Cu removal is always shallower than that for Ni.

The anoxic sediments in Balmer Lake clearly provide a permanent sink for dissolved Cu throughout the year. Comparisons of seasonal profiles for stations 1 and 2, for example, suggest active sulphide precipitation occurs at depths between 2-10 cm from spring through fall (Fig. 5.10). Unlike dissolved Ni, the seasonal migration in the depth of Cu removal is consistent with that of sulphate; precipitation zones migrate upwards over the summer-fall-winter transition and descend again in the spring.

Sulphide precipitation has been frequently proposed to limit Cu concentrations in marine and lacustrine porewaters (Elderfield, 1981; Pedersen, 1985; Gaillard *et al.*, 1986; Pedersen, 1988; Pedersen *et al.*, 1990; Hamilton-Taylor and Davison, 1994), including reports for shield lakes (Carignan and Nriagu, 1985; Pedersen *et al.*, 1993). Carignan and Nriagu (1985), for example, observed dramatic depletions of dissolved Cu at depths consistent with sulphide production in one acidic (pH ~ 4.5) and one slightly alkaline Canadian Shield lake (pH ~ 7.5); solubility calculations indicated that the porewaters were supersaturated with respect to covellite (CuS). Similarly, Pedersen and others (1993) attributed the precipitous decline of Cu in the shallow porewaters of contaminated Anderson Lake, Manitoba, to the precipitation of authigenic discrete or mixed metal sulphide phases. Indeed, framboidal pyrite was observed by these authors to be ubiquitous in the surface sediments.

Diffusional influxes clearly support significant accumulations of Cu in some lacustrine sediments. In the Shield lakes studied by Carignan and Nriagu

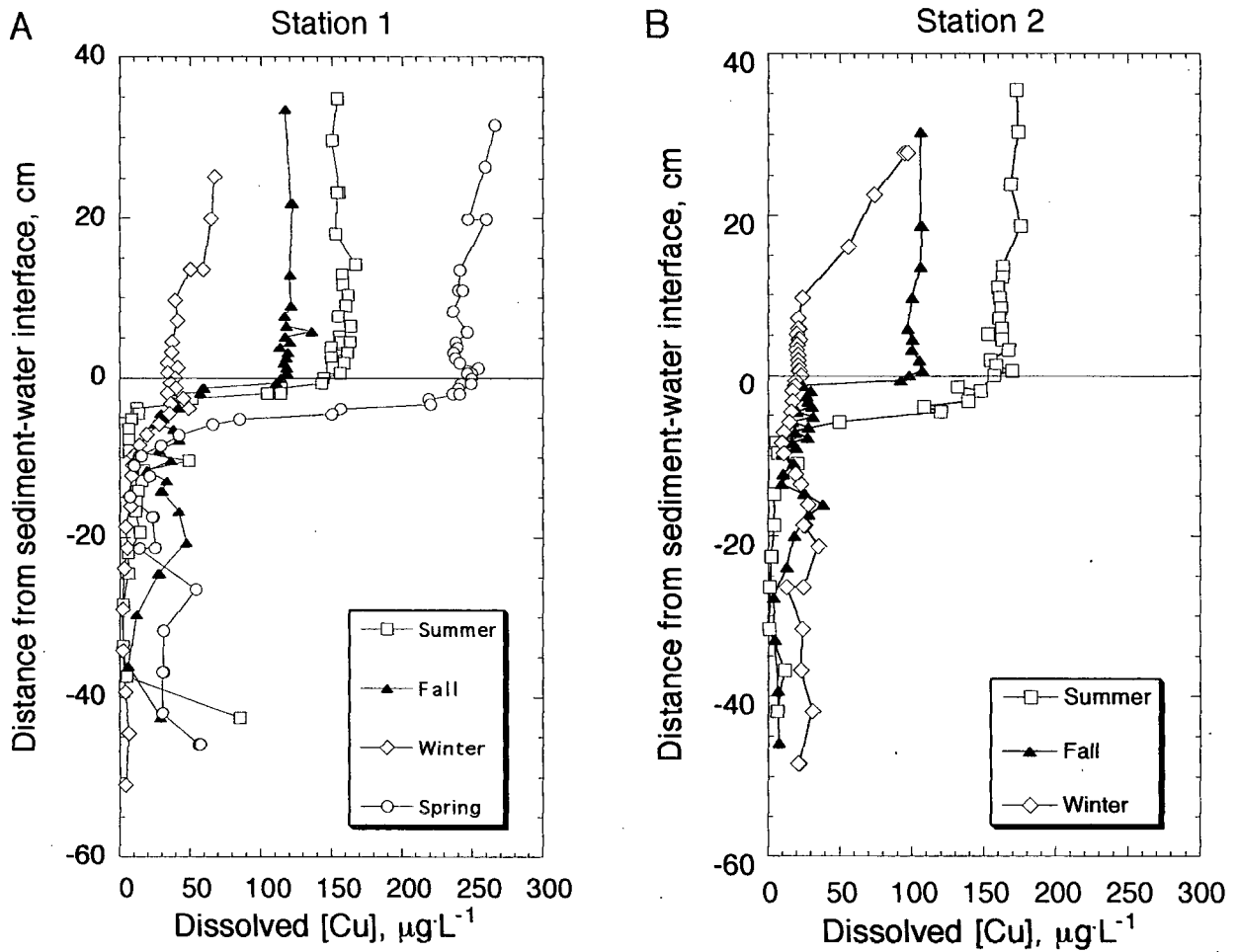


Fig. 5.10. Seasonal peeper profiles of dissolved Cu for stations 1 and 2 (A and B, respectively) in Balmer Lake. Replicate samples are represented by double symbols at specific single depths.

(1985), for example, diffusive influx estimates ranged from 0.5-5.1 $\mu\text{g}\cdot\text{cm}^{-2}\cdot\text{y}^{-1}$ and represented 1-52 % of the estimated Cu accumulation rate. In Balmer Lake, diffusive Cu influxes remained reasonably constant over the four seasons, with values ranging from 2.3-6.7 $\mu\text{g}\cdot\text{cm}^{-2}\cdot\text{y}^{-1}$ (Appendix F). In general, no obvious spatial or temporal trends are evident with respect to the inter-site and inter-season flux estimates. The rate of Cu removal by sediment influxes appears to have little effect on the total lake burden of dissolved Cu in Balmer Lake. Estimates assuming an average influx of 4 $\mu\text{g}\cdot\text{cm}^{-2}\cdot\text{y}^{-1}$, a mean lake depth of 2.4 m, and an average water column concentration of 200 $\mu\text{g}\cdot\text{L}^{-1}$, suggest that ~5% of the total dissolved Cu is fixed within the lake residence time of 230 days.

Downward diffusive fluxes of Cu in Balmer Lake do not appear to represent the principal depositional mechanism responsible for the large sediment concentrations. As suggested for Ni, the calculated rate of diffusion of dissolved Cu species from the bottom waters into the sediments is not sufficient to account for the bands of Cu-rich sediments (~1 wt.%) at station 1 (Fig. 4.35). The accumulation rate implied by the enriched horizons is estimated to be on the order of 1000 $\mu\text{g}\cdot\text{cm}^{-2}\cdot\text{y}^{-1}$ (Appendix G). However, since the last ephemeral episode of accidental tailings overflow (~1970), diffusional transport has most likely played a significant role in Cu accumulation. Indeed, the steep negative concentration gradients are comparable to the magnitudes observed in the cited previous studies in which the importance of such mechanisms has been stressed.

5.3.6 Zinc

The bottom water and porewater distributions of dissolved Zn in Balmer Lake appear to be controlled by two principal mechanisms: 1) intense remobilization from labile, Zn-rich sedimentary phases in the first 5 cm below

the interface; and 2) precipitation of Zn-bearing sulphide minerals at greater depths. Each will be described in turn.

Peepers profiles of Zn are characterized by shallow pronounced porewater maxima during all seasons (Figs. 4.18-4.27). Steep concentration gradients either side of the spike promote bi-diffusional transport away from the interfacial horizons. The concentrations of the surficial peaks average $75 \mu\text{g}\cdot\text{L}^{-1}$ greater than concentrations in the overlying bottom waters (Fig. 5.11). Typically, the largest interfacial spikes and gradients were observed during the fall period. Reasons for this are not fully clear, although the degree of enrichment will be related to the rate of supply and the rate of removal of dissolved Zn species. Specifically, such processes will be influenced by the supply of organic matter, rates of organic matter remineralization and rates of authigenic sulphide formation.

Diffusive effluxes, which ranged from $11\text{-}330 \mu\text{g}\cdot\text{m}^{-2}\cdot\text{d}^{-1}$, were computed in order to assess the potential contribution of remobilization on the Zn enrichment in the winter hypolimnion (Appendix F). The following discussion ignores potentially significant influences from advecting mining-flows. From water column profiles, bottom water enrichments in the lower metre of the water column at stations 1, 2 and 4, were estimated to be $\sim 5 \times 10^4$, 3.5×10^4 , and $1.5 \times 10^4 \mu\text{g}$, respectively. Assuming a constant efflux of $\sim 300 \mu\text{g}\cdot\text{m}^{-2}\cdot\text{d}^{-1}$ as seen in the fall, upward diffusion of Zn species at these stations would take ~ 170 , 120 and 50 days, respectively, to produce the concentrations observed in the bottom waters. These values represent minimum time estimates, as effluxes are expected to decrease as gradients lessen during ice-cover. They do, however, illustrate that benthic effluxes can have a significant impact on the metal content of the water column during the seasonally anoxic period.

The remobilization of Zn from the oxidation of organic matter is considered to be the most important source of labile Zn species in Balmer Lake

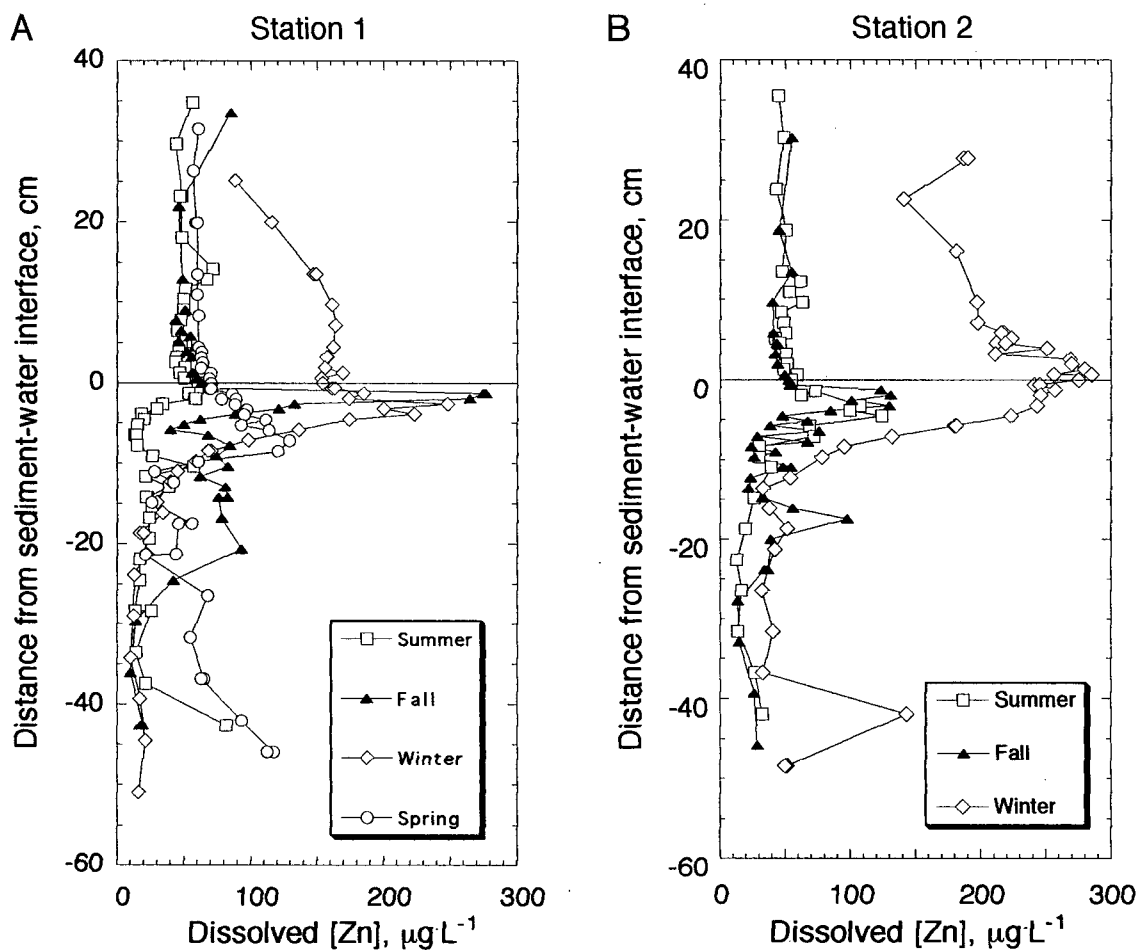


Fig. 5.11. Seasonal peeper profiles of dissolved Zn for stations 1 and 2 (A and B, respectively) in Balmer Lake. Replicate samples are represented by double symbols at specific single depths.

sediments. Four strands of evidence are offered to support this. First, zinc appears to be generated at shallower horizons than the respective remobilization depths of Fe and Mn during the summer period. The putative organic source is more difficult to distinguish in the more reducing fall sediments. Second, of the elements measured, zinc exhibits the best correlation with POM in water column particulates. Third, a pronounced surficial dissolved Zn spike was evident at station 1 during the winter at a time when Fe and Mn oxide sources should have been exhausted. And fourth, reports of strong Zn-organic associations abound in the literature. With respect to the latter point, compositional analyses of phytoplankton demonstrate that Zn is typically the most abundant trace metal in both marine and lacustrine algae; extensions of Redfield ratios to include micronutrients have revealed stoichiometries of $C_{113}N_{15}P_1Zn_{0.03-0.06}$ (Sigg, 1985; Reynolds and Hamilton-Taylor, 1992). However, porewater profiles that provide direct evidence of surficial enrichments derived from remobilized organic matter are scarce in the literature. Data from seasonally anoxic Esthwaite Water demonstrated that elevated dissolved Zn concentrations at the sediment surface were attributable to a remobilized source from decaying algal material (Morfett *et al.*, 1988). Transient interfacial Zn spikes coincided with large accumulations of organic material at the sediment surface, and were characterized by constant Zn:Cu ratios in a stoichiometry consistent with that of phytoplankton (Sigg, 1985; Reynolds and Hamilton-Taylor, 1992). Similarly, effluxes of Zn in Swedish coastal sediments were attributed to releases during the breakdown of labile organic matter at or near the sediment-water interface (Westerlund *et al.*, 1986).

Comparisons of the magnitudes of near-interface dissolved Zn contents between Balmer Lake and the studies cited above reveal considerable disparities. The greatest enrichments reported by Morfett and others (1988) and Westerlund (1986) were respectively ~ 12 and $20 \mu\text{gL}^{-1}$ above background water column

concentrations; those observed in this study ranged from 15-200 μgL^{-1} . It must be pointed out, however, that Balmer Lake is unique in that it hosts dissolved Zn concentrations over an order of magnitude higher than either Esthwaite Water or Swedish coastal waters. More importantly, particulate Zn concentrations are among the highest recorded anywhere (Table 4.6). Therefore, one can argue that potentially large burdens of labile, Zn-bearing particulates are deposited in Balmer Lake; the remobilization of such phases may facilitate the formation of the anomalously large Zn spikes in the surficial horizons. Due to the compressed redox depth scales in Balmer Lake, dissolved Zn contributed by near-interface reductive dissolution of Fe and Mn oxides is difficult to distinguish from Zn released during organic matter remineralization. A spatial decoupling of the two sources is evident only during the summer.

Previous studies which have assessed the partitioning of zinc between the water column and the sediments in lakes suggest that the binding of Zn by Fe and Mn oxides may be important in the seasonally oxic horizons in Balmer Lake (McKee *et al.*, 1989a; Tessier *et al.*, 1989; Williams, 1992; Young and Harvey, 1992). An examination of eight Canadian Shield lakes by Tessier *et al.* (1989) demonstrated a strong pH-dependence with respect to the distribution coefficients of Zn between particulates and solution phases (i.e., K_d increased with pH). Their results agree well with theoretical and experimental complexation models of cation sorption to oxide surfaces (Benjamin and Leckie, 1981). For the lakes assessed (pH values ranged from 4 to 8.4), the pH interval 5.5 to 6.5 defined a region of maximum potential change in % Zn sorbed to Fe oxyhydroxides; the results suggested that a large portion of the potentially available or mobile Zn present should be associated with the surficial sediments above pH 7, and be present in the water column below pH 5. A similar study of oxic lake sediments from seven other shield lakes examined the

sediment/porewater partitioning (i.e., K_d) of Zn together with the speciation of the bound fraction (Young and Harvey, 1992). Enhanced sorption between pH 5.0 and 6.5 was also observed in this work. Although Zn concentrations in Balmer Lake are complicated by mining inputs, the pH range of 7-7.4 (i.e., the upper end of the sorption edge) suggests that a significant portion of the sedimentary Zn inventory should be associated with Fe and/or Mn oxides in oxic sediment horizons. However, the role of these phases in the diagenetic cycling of Zn in the lake sediments is not clearly reflected in the porewater zinc profiles.

Below the horizons of near-interface remobilization, dissolved zinc species are rapidly consumed from Balmer Lake porewaters presumably by the precipitation of authigenic sulphides. The precipitation of Zn-sulphides is a widely recognized aspect of Zn behaviour in lacustrine systems (Pedersen, 1983; Carignan and Tessier, 1985b; Pedersen, 1988; Tessier *et al.*, 1989; Davison *et al.*, 1992; Williams, 1992; Pedersen *et al.*, 1993), and has been the subject of a fairly recent review (Hamilton-Taylor and Davison, 1994). For all seasons and sites, Zn and Ni are removed at very similar depths, which may reflect their relatively comparable solubility products with respect to sulphide. As for Ni, sulphide precipitation in the hypolimnion does not appear to present an important removal mechanism during winter.

During the summer, winter and spring periods, Zn concentrations in the interstitial waters are at least a factor of two lower than in the overlying bottom waters (Fig. 5.11), suggesting there is a net diffusive transport into the sediments. In the fall, however, diffusive equilibria between the sediments and water column are evident at stations 1 and 2 (Fig. 5.11). Diffusive influxes of dissolved Zn below the near-interface peaks exhibited little inter-season variability with seasonal averages ranging from 2.2-3.9 $\mu\text{g}\cdot\text{cm}^{-2}\cdot\text{y}^{-1}$. Except for the fall period,

concentration gradients associated with downward diffusion were greater than those corresponding to effluxes (Appendix F). Tessier *et al.* (1989) examined a large number of oligotrophic, shield lakes of varying pH and degrees of Zn contamination. In the more polluted lakes (pH<6), downward influxes driven by pronounced gradients ($0.39-1.7 \times 10^{-8} \text{ g}\cdot\text{cm}^{-4}$) suggested dissolved Zn species were being efficiently trapped as sulphide phases at depth; these gradients agree well with those seen in Balmer Lake deposits, which range from $2.2-5.3 \times 10^{-8} \text{ g}\cdot\text{cm}^{-4}$ (Appendix F). In lakes of pH>6, Tessier *et al.* (1989) observed that the vertical concentration gradients were generally much lower ($0.65-1.9 \times 10^{-9} \text{ g}\cdot\text{cm}^{-4}$). The greater Zn inputs to the acidic lakes in combination with more vigorous sulphide precipitation were suggested to contribute to the larger gradients.

In a related study, porewater Zn profiles were obtained by Carignan and Tessier (1985) in order to assess the relative importance of diffusion mechanisms in two acidic lakes. Loci of Zn removal at depths of 2 cm coincided with the presence of measurable porewater sulphide; in both sediments, the porewaters were slightly supersaturated with respect to sphalerite. Carignan and Tessier estimated that the diffusive influxes in the lakes ($1.0-1.7 \mu\text{g}\cdot\text{cm}^{-2}\cdot\text{y}^{-1}$) accounted for 76 and 52 % of the respective sedimentary Zn accumulations.

The importance of diffusive influxes to the overall Zn accumulation in Balmer Lake deposits cannot be established so rigorously given the significant seasonality in the porewater distributions. Nevertheless, the data collectively point to an important conclusion: early diagenetic reactions in Balmer Lake sediments render the deposits below 10 cm depth a significant and permanent sink for the metal. Calculations using an average influx of $3 \mu\text{g}\cdot\text{cm}^{-2}\cdot\text{y}^{-1}$ over the entire lake benthic area suggest that 13% of the total dissolved Zn inventory is retained with respect to the lake residence time of ~230 days.

5.4 Factors Controlling the Diagenetic Behaviour of As

The ubiquity of Fe and Mn oxyhydroxides, and their potential role in regulating trace element concentrations in natural waters, has stimulated numerous investigations on As behaviour in the presence of these substrates. The importance of Fe-bearing oxides has been repeatedly inferred to exert the principal control on the distribution and behaviour of As in marine and lacustrine systems (Crecelius, 1975; Edenborn *et al.*, 1986; Agett and Kriegman, 1988; Belzile and Tessier, 1990; De Vitre *et al.*, 1991; Widerlund and Ingri, 1995) while Mn has received relatively little attention (Takamatsu *et al.*, 1985; Anderson and Bruland, 1991). The apparent strong associations between As and Mn observed in Balmer Lake sediments imply that under certain conditions, manganese may also play a significant role in As geochemistry. The section below assesses the importance of Mn and Fe with respect to the diagenetic behaviour and mobility of As in sediments, and is presented within the contexts of experimental and theoretical considerations. The argument that is developed will be then applied to the seasonal geochemistry of As in Balmer Lake.

5.4.1 Experimental and Field Observations

Theoretical and experimental studies were reviewed in order to determine the geochemical influences of Fe and Mn on the diagenetic behaviour of As. A number of questions receive particular attention in the following paragraphs: 1) how do the sorptive properties of Fe and Mn oxide phases compare? 2) what are the As species predicted to be associated with these phases? and 3) what is the nature of the adsorption mechanism?

As discussed in sections 5.1.5.1 and 5.1.5.2, natural Fe and Mn oxides represent a diverse assemblage of phases that encompass a broad spectrum of sorptive characteristics. Due to variability in the chemical environment during their formation and their ability to incorporate foreign ions into their structures, significant natural heterogeneity can develop in oxides with respect to reactive surface areas, types of binding sites, site densities and steric effects. A comprehensive body of literature has been devoted to their sorptive properties. Although most experiments commonly use relatively pure Fe and Mn oxide phases, which may exhibit considerable compositional and morphological differences compared to natural particles, useful comparisons can be drawn.

Poorly ordered Mn and Fe oxides are typically characterized by loosely hydrated structures which are permeable to ions (Davison, 1993). The incorporation or adsorption of minor amounts of foreign ions in the formation of these phases appear to restrict crystal development, thus contributing to more random growth (Taylor, 1987). The permeability means that sorption reactions are not restricted to external sites as is the case for more crystalline solids. Thus, the reactive surface areas for the mostly amorphous phases can be large. BET analyses of synthetic MnO_2 and $\text{Fe}(\text{OH})_3$ suggest that they share similar specific surface areas. Estimates for the former range from $230\text{-}320 \text{ m}^2\text{g}^{-1}$ (Vuceta and Morgan, 1978), while those for amorphous Fe-oxide range from $182\text{-}600 \text{ m}^2\text{g}^{-1}$ (Davis and Leckie, 1978b; Davis and Leckie, 1978a; Benjamin and Leckie, 1982). Similarly, good agreement has been observed between Mn and Fe solid phases with respect to experimentally derived site densities and chemical free energies of adsorption for trace elements (Vuceta and Morgan, 1978).

More definitive contrasts between Fe and Mn oxide phases are evident upon comparison of the nature of their respective surface charges. The surfaces

of many oxides become relatively more negatively charged with increasing pH (and *vice versa*) due to variations in the adsorption of potential-determining ions (H_3O^+ and OH^-) (Stumm and Morgan, 1981). The pH at which the surface assumes a net zero surface charge (the point of zero charge, or pzc) can be used to estimate whether a surface is likely to be positively or negatively charged at a given pH (Kinniburgh, 1981). The pzc for goethite for example is 7.5-8.6 while that for birnessite is 1.5-2 (Kinniburgh, 1981); goethite ($\alpha\text{-FeOOH}$) and birnessite ($\delta\text{-MnO}_2$) represent two of the more abundant oxides of Fe and Mn in natural systems. Therefore, at neutral pH, Mn oxide is predicted to be strongly negatively charged and thus will repel anions. This argument has been proposed by several groups to support stronger associations of Fe oxides with arsenate (H_2AsO_4^-) at natural pH levels (De Vitre *et al.*, 1991).

To constrain further the diagenetic behaviour of As in sediments, it is necessary to define the chemical species involved and compare their behaviour. Thermodynamic arguments suggest that inorganic As in oxidized aquatic systems should be present as arsenate [As(V)] (Ferguson and Gavis, 1972); arsenic acid (H_3AsO_3 , $\text{pK}_{a1} = 2.2$, $\text{pK}_{a2} = 6.9$) is predicted to be largely dissociated at neutral pH's. Conversely, data in the literature show that arsenite [As(III)] typically predominates in anoxic interstitial waters (Edenborn *et al.*, 1986; Peterson and Carpenter, 1986; Agett and Kriegman, 1988); arsenous acid (H_3AsO_4 , $\text{pK}_{a1} = 9.2$) is expected to be predominantly neutrally charged in natural waters. For simplicity, organo-arsenicals will be ignored in the following discussion.

Both arsenite and arsenate are removed from solution in the presence of amorphous Fe-oxides, although As(V) is more readily sorbed than As(III) (Pierce and Moore, 1982; Bowell, 1994). The contrast has been attributed to charge

differences between the two complexes. Although accounts of solid-phase As speciation are rare, it is generally assumed that As(V) predominates in oxic sediments (Belzile and Tessier, 1990). Dissolution experiments using diagenetic Fe and As samples collected from 12 Canadian lakes, for example, demonstrated that only arsenate was present (De Vitre *et al.*, 1991). From the above discussion, it is apparent that the scavenging of As(III) by oxide surfaces involves an oxidation step. For example, As(III) removal from the porewaters in oxic horizons may involve oxidation to As(V) prior to adsorption. Alternatively, the oxidation of As(III) to As(V) may occur during or after its adsorption (Gulens *et al.*, 1979). Indeed, the sorption of As has been shown to occur simultaneously with the oxidation of As(III) to As(V) in several Saskatchewan lake sediments (Oscarson *et al.*, 1980).

Molecular O₂ and Fe and Mn oxyhydroxides are the most likely oxidants of arsenite in sedimentary porewaters. However, oxidation by molecular O₂ is kinetically slow, and thus is unlikely to be important (Cherry *et al.*, 1979). In contrast, Oscarson *et al.* (1980) observed that synthetic, poorly crystalline birnessite (δ -MnO₂) was very effective in oxidizing As(III). Microbial inhibition via the addition of HgCl₂ did not significantly retard the reaction, indicating that such oxidation was largely an abiotic process. Despite the thermodynamic favourability, a redox reaction between As(III) and Fe(III) oxide was not observed within three days in a similar experiment (Oscarson *et al.*, 1981a); the results were attributed to slow kinetics. However, in another study Fe oxyhydroxides (both natural and synthetic) were found to oxidize As quite rapidly; typically, 50-75% of spiked As(III) was oxidized with two days, irrespective of pH (De Vitre *et al.*, 1991). The apparent discrepancy between the two experiments may be explained by the much higher Fe:As ratios (3,400 vs. 10)

in the latter study. Thus, it appears that both Fe(III) and Mn(IV) serve as effective oxidants of As(III) given suitable conditions.

Experiments have shown that both coulombic attraction and specific adsorption are important in the uptake of arsenate by Fe-oxyhydroxides. In this context, specific adsorption refers to uptake that cannot be accounted for solely by electrostatic interactions, regardless of the sign of the surface charge (Stumm and Morgan, 1981). "Specific adsorption" which is a term equivalent to "ligand exchange", thus reflects the specificity in bonding of different ions due to their charge, size and polarizability (Taylor, 1987).

Several strands of evidence have been offered to support specific associations of arsenate with Fe-oxyhydroxides. First, the specific adsorption of anions induces a greater negative charge on oxide surfaces which results in a shift in the point of zero charge (pH_{pzc}) to a lower pH value. The amount of shift depends on the particular ion sorbed, its concentration, and the nature of the solid surface (Stumm and Morgan, 1981). Several groups have demonstrated pH_{pzc} shifts of several pH units for Fe-oxyhydroxide surfaces with sorbed arsenate, indicating specific interactions (Pierce and Moore, 1982; Fuller *et al.*, 1993; Bowell, 1994; Hsia *et al.*, 1994). Second, adsorption due to electrostatic processes is usually very rapid (i.e., seconds). Equilibration periods on the order of hours observed for As-Fe systems indicate formation of chemical bonds between the As species and the adsorbent (Oscarson *et al.*, 1980; Pierce and Moore, 1982; Fuller *et al.*, 1993). Additional evidence for direct coordination of arsenate has been derived from various other chemical and physical techniques including energy dispersive X-ray analysis (EDAX) and Fourier transform infrared (FTIR) methods (Hsia *et al.*, 1994).

Laboratory demonstrations which have established the importance of Fe in As cycling are consistent with other studies of marine and lacustrine

sediments. A very convincing data set of six Canadian lakes (pH between 4.0 and 8.4) demonstrated the importance of Fe on the behaviour of As (Belzile and Tessier, 1990). Tightly correlated porewater profiles for all lakes indicated that As was mobilized during the reduction and dissolution of Fe-oxyhydroxides. Moreover, binding constants derived from the field data compared well with those obtained in the laboratory for the adsorption of arsenate on amorphous Fe-oxides. Similar conclusions were drawn for comparable associations of dissolved Fe and As in a Canadian Shield lake (De Vitre *et al.*, 1991).

In general, field studies which have alluded to an As-dependence on Mn have not differentiated between Mn and Fe-oxide control. Lake Ohakuri in New Zealand, for example, is a seasonally anoxic lake that receives unusually high As inputs from geothermal sources. The accumulation of dissolved Fe, Mn and predominantly As(III) in the hypolimnion over the course of anoxia was attributed to sediment release via the reductive dissolution of Fe(III)- and perhaps Mn(IV) oxides (Agett and O'Brien, 1985; Aggett and Kriegman, 1988). Indeed, the large interfacial gradients supported sediment effluxes for all three elements.

Relatively fewer laboratory studies of arsenate sorption onto Mn-oxide phases exist in the literature. Oscarson *et al.* (1981) demonstrated that synthetically prepared birnessite could efficiently oxidize arsenite to arsenate; the reaction was accompanied by increases in the concentrations of remobilized Mn(II) and K^+ from the oxide lattice. However, while a significant portion of As(V) was removed from solution by Fe(III) oxide in an identical experiment, very little of the added As was sorbed by MnO_2 . Since the pzc of birnessite is close to pH 2 (Oscarson *et al.*, 1981b), it was assumed that the high negative charge density at experimental pH (pH=6.9-7.7) inhibited the sorption of the anionic arsenate species (largely $H_2AsO_4^-$ and $HAsO_4^{2-}$).

In a similar experiment with synthesized hydrous MnO_2 , Takamatsu *et al.* (1985) demonstrated that arsenate was not appreciably adsorbed in the pH range 6 to 8. However, in the presence of large concentrations ($20 \text{ mg}\cdot\text{L}^{-1}$) of a divalent cation, a substantial increase in the amount of adsorbed arsenate was observed; the percent adsorbed increased from <20% to 100 % at pH 6 with each of the added trace elements (Mn^{2+} , Sr^{2+} , Ba^{2+} and Ni^{2+}). The results were explained in terms of a shift in the surface charge of the Mn-oxide surface in the presence of abundant cations. Divalent cations such as Mn^{2+} and Ni^{2+} readily sorb to Mn-oxides, and in the process, displace protons to solution from the oxide surface (Stumm and Morgan, 1981). In this study, the amount of metal adsorbed relative to the extent of proton release was approximately 1:1 on a molar basis. Takamatsu and others (1985) suggested that since the ratio of charge equivalents released to charge equivalents adsorbed was <1, cation adsorption would increase the pzc of the oxide surface, and hence, enhance arsenate sorption.

In another experiment, a slurry of oxidized As-bearing surface sediment and seawater was incubated with added plankton material to simulate the sequential depletion of oxidants that occurs during early diagenesis (Edenborn *et al.*, 1986). The sequential release of reduced Mn and Fe species, as well as the timing of SO_4^{2-} reduction, were thermodynamically consistent with measured redox potentials. The release of As(III) to the porewaters occurred concomitantly with the release of Fe(II), suggesting strong Fe-As associations. It should also be noted that the As release came after the dissolution of almost all of the reducible Mn.

The thermodynamics of reductive dissolution of Fe and Mn oxyhydroxide phases has further implications with respect to their relative influences on the diagenetic chemistry of As. Theoretical examinations of organic matter diagenesis predict that Mn(IV) should be reduced at a higher redox potential

than Fe(III) (Froelich *et al.*, 1979). This implies that in reducing sediments, the addition of manganous ions to porewaters should occur at shallower sediment depths than corresponding ferrous ion inputs. In mildly reducing sediments where thermodynamic gradients are shallow (i.e., the redox horizons for the various interstitial metabolites extend over many centimetres), such spatial decoupling of Fe and Mn reduction can be observed (Edenborn, *et al.*, 1986). Therefore, even assuming As is associated with Mn oxyhydroxides, it is possible that any release of As to the porewaters upon Mn dissolution could be masked by re-adsorption onto Fe oxyhydroxide phases. Hence, the final expression of As release to the porewater would be more closely associated with increases of dissolved Fe²⁺. Such an argument was put forth by Peterson and Carpenter (1986) to account for strong associations observed between Mn and As solid phases in surface sediments, and the concomitant release of dissolved Fe and As in deeper horizons. Because intensely reducing sediments are less likely to foster a Fe/Mn redox decoupling, the mechanism of Fe control described above may be less important in such regimes.

In summary, contrasts in the surface charge characteristics of Fe and Mn oxide phases influence the sorption of charged species. The heterogeneity of these particulates makes comparisons of other parameters (e.g., specific surface areas, site densities, etc.) more difficult to assess. In addition, experimental data demonstrate a pH-dependence of arsenate sorption for which both coulombic and specific mechanisms are involved; however, the exact nature and variability of the chemi-sorptive processes are not completely understood. Speciation studies suggest that arsenate is the dominant species in oxic sediment horizons and that arsenite predominates in reducing interstitial waters; the removal of As(III) from solution appears to involve its oxidation by Mn(IV) and probably Fe(III) oxides. Finally, limited experimental data demonstrate weak associations

of As with Mn oxides; significant sorption has only been reported for high cationic-strength solutions in which the charge properties of the oxide surface have been modified. Conversely, similar studies offer conclusive evidence that Fe oxide phases exert significant control on the behaviour of As.

5.4.2 The Behaviour of As in Balmer Lake Sediments

Seasonal porewater profiles suggest that two principal controls are governing As distributions in Balmer Lake sediments. First, intense remobilization at shallow sediment depths indicate a redox-controlled release from labile, As-bearing particulates; and second, lower concentrations in the deeper horizons suggest the consumption of As as authigenic sulphide phases. Each of these processes will be described in turn.

During the well-oxygenated periods of the spring, summer and fall, porewater As profiles are characterized by steep gradients that begin just below the sediment surface (Figs. 4.18-4.22; 4.27). The depths of remobilization typically overlap with corresponding dissolved Mn production horizons. This suggests that a labile portion of As is associated with Mn-oxyhydroxide phases in the upper horizons, both of which follow a redox-pattern of dissolution in the suboxic zone, upward diffusion, and precipitation near the sediment-water interface. Where dissolved Fe gradients are clearly defined, corresponding As slopes are shallower (Fig. 5.12), suggesting that the dissolution Fe solid phases is not responsible for the porewater additions of dissolved As at sediment depths above than the Fe(III) redox boundary. The chemically analogous behaviours of phosphate and arsenate, and hence the potential for biological incorporation, might suggest that the remineralization of organic matter may contribute to the dissolved As enrichments; however, the decoupling between the oxidation of

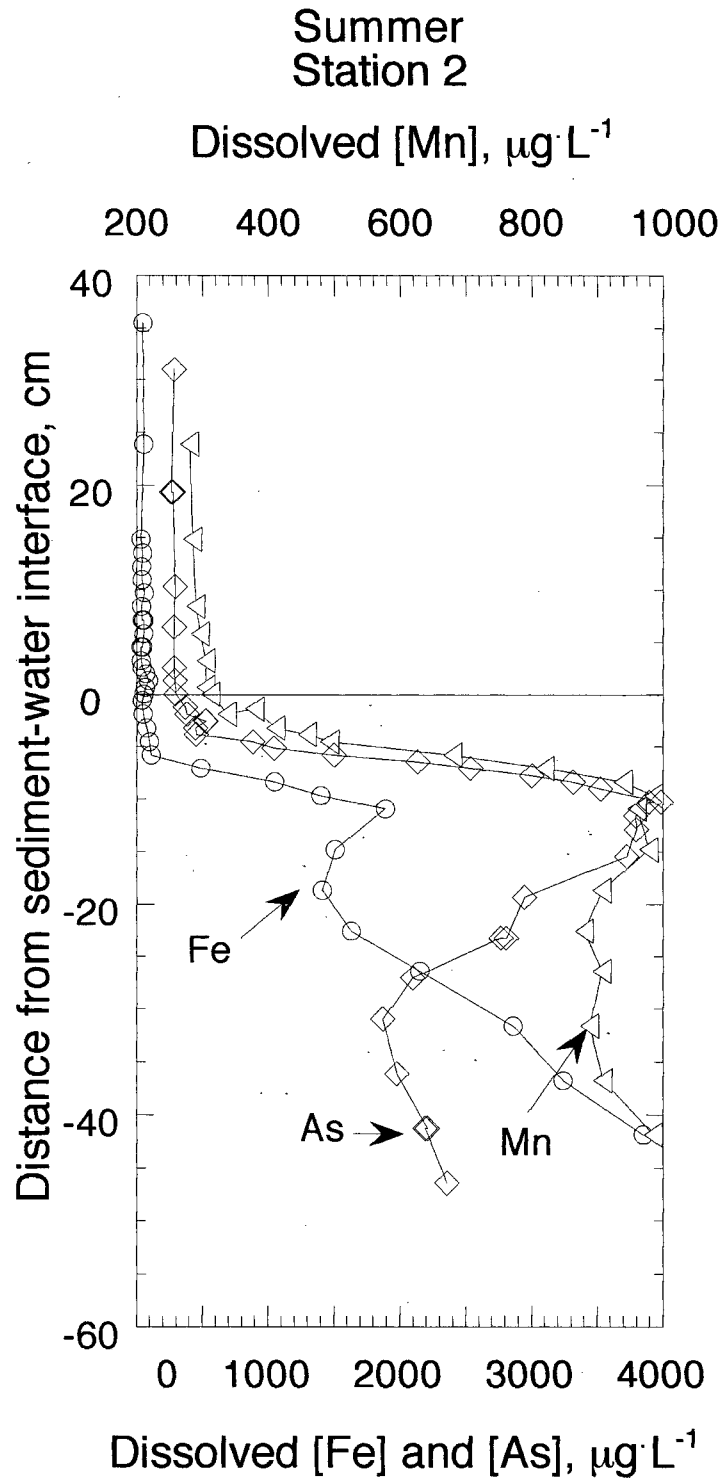


Fig. 5.12. Summer peeper profiles of dissolved Fe, Mn and As for station 2 in Balmer Lake. Replicate samples are represented by double symbols at specific single depths.

organic material and the dissolution of oxide phases as seen for Zn during the summer period is not clearly evident for As.

A linear regression was performed to assess further the dependence of As on the redox behaviour of Mn in Balmer Lake porewaters. Molar concentrations were compared at depths extending from the interfacial horizons to depths of ~20 cm in order to encompass the remobilization depth range (Fig. 5.13). Coefficients of determination (r^2) can be interpreted as the proportion of the variation in Y that is "accounted for" by linear regression of Y on X. In other words, an r^2 value of 0.9 means that 90% of the variation in porewater As concentrations can be accounted for by variations in Mn. The r^2 coefficients for the spring, summer and fall average 0.85 (0.70-0.96), indicating that the diagenetic cycling of Mn is significantly affecting the behaviour of As. Corresponding values for Fe and As over these periods are slightly lower (mean = 0.78(0.42-0.96)). The fact that the As/Mn slopes in Fig. 5.13 are not linear demonstrates that mechanisms other than the dissolution of Mn-oxide phases are involved; for each profile, uniform As/Mn ratios of <1 are evident to ~3-4 cm and then generally increase with depth to ~2 in the deeper horizons. The preferential removal of Mn from pore solution or the addition of As (e.g., via the dissolution of Fe-oxide phases) may account for the observed increases.

It should be stressed that the weaker correlations between As and Fe do not imply that Mn is exerting greater control on the distribution of As in Balmer Lake porewaters. Instead, the dearth of ferrous-Fe in the shallow porewaters may suggest that Fe is rapidly consumed as authigenic sulphide phases. Indeed, the zones of Fe(III) and SO_4^{2-} reduction are predicted almost to overlap. It is therefore possible that As is remobilized upon the reductive dissolution of Fe(III) oxides, but Fe consumption from porewaters hinders conclusive interpretations.

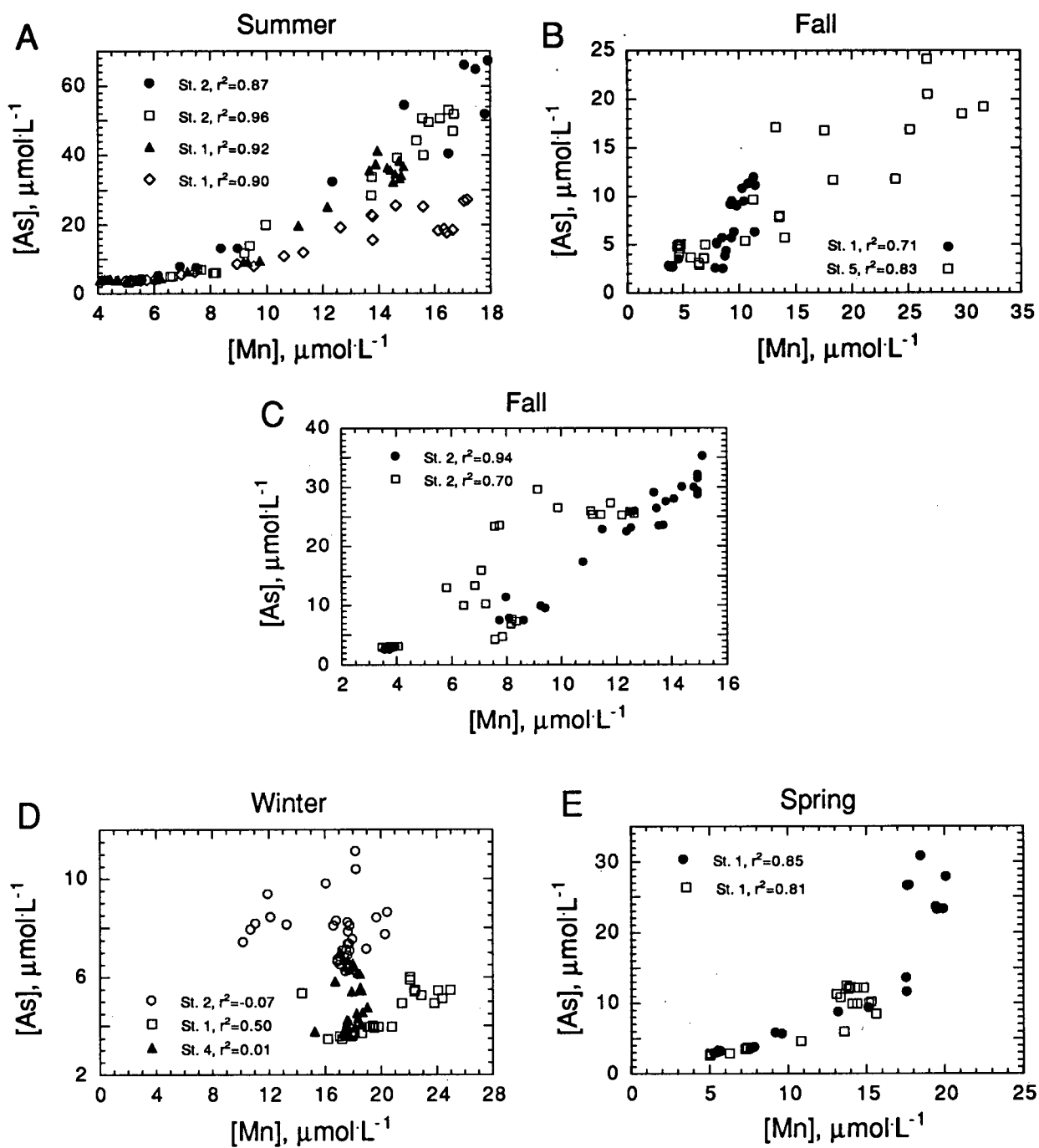


Fig. 5.13. X-Y scatter plot illustrating the dependence of dissolved As on the distribution of dissolved Mn. The values (molar concentrations) represent a depth interval spanning from ~ 3 cm above the sediment surface to ~ 20 cm below. Coefficients of determination (r^2) from linear regression analyses for the respective stations are included.

Similar correlative examinations performed for the winter period (r^2 values of -0.01-0.5) illustrate much weaker associations of As with Mn (5.12). This decoupling is consistent with the seasonal development of anoxia and the concomitant change in the redox chemistry at the sediment water interface. The sulphate reduction evident in the winter hypolimnion (section 5.3.2) implies that reactive Mn(IV)-oxides were absent in surface deposits during the time of sampling. Hence, the capacity of the surface sediments to sorb upward diffusing As species should have been greatly reduced. Under such conditions, the diagenetic cycle would have been interrupted; both As and Mn species would have diffused freely across the sediment-water interface.

Comparison of the porewater plots for Mn (Fig. 5.7) and As (Fig. 5.14) suggests that different mechanisms influence the seasonal distributions of the two elements. Mn porewater maxima, for example, progressively decrease from a winter maximum through the spring, summer and fall. The winter enrichments were suggested to stem from inputs of dissolved Mn to the porewaters from the overlying bottom waters (see section 5.3.3). Conversely, arsenic profiles decrease from maximum porewater values in the summer to minima in late winter (Fig. 5.14). The disparity implies that the non-steady-state inputs of Mn-rich water to the winter bottom waters did not host significantly elevated concentrations of dissolved As. Instead, the distribution of arsenic may reflect seasonal variability in the kinetics of remobilization and consumption of dissolved As in the porewaters. More specifically, variable rates of reductive dissolution of As-bearing oxides, consumption of dissolved As in the oxic horizons, and authigenic sulphide formation at depth, all contribute to the observed seasonality.

Large sub-surface porewater gradients in Balmer Lake sediments support year-round upward diffusion of dissolved As towards the sediment-water

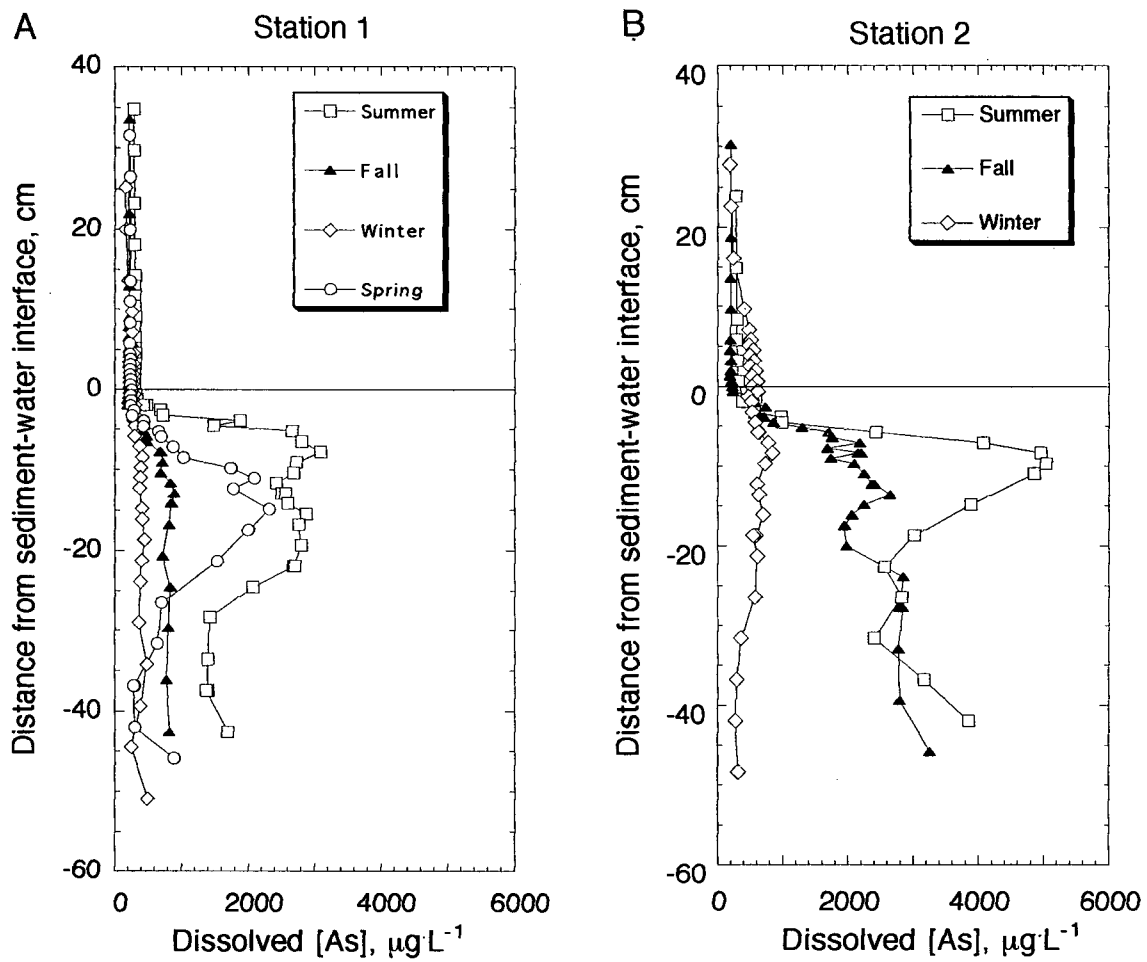


Fig. 5.14. Seasonal peeper profiles of dissolved As for stations 1 and 2 (A and B, respectively) in Balmer Lake. Replicate samples are represented by double symbols at specific single depths.

interface. Rates ranged from 5-175 $\mu\text{g}\cdot\text{cm}^{-2}\cdot\text{y}^{-1}$; the large gradients observed in the fall account for the upper limit of this range (Appendix F). These values are much greater than those reported for the Laurentian Trough (0.07-0.24 $\mu\text{g}\cdot\text{cm}^{-2}\cdot\text{y}^{-1}$; Belzile, 1988) a temperate estuary (2.2 $\mu\text{g}\cdot\text{cm}^{-2}\cdot\text{y}^{-1}$; Widerlund and Ingri, 1995) and various coastal and lake sediments (0.37-2.4 $\mu\text{g}\cdot\text{cm}^{-2}\cdot\text{y}^{-1}$; Peterson and Carpenter, 1986). The largely invariant concentrations of As across the sediment-water interface imply that upward migrating species are consumed by Mn and/or Fe oxides in the surface sediments (Figs. 4.18-4.27). However, the reduced sorptive capacity of the surface sediments during periods of bottom water anoxia might suggest that dissolved As species are periodically allowed to diffuse into the bottom waters. In addition, the uncertainty in the position of the sediment-water interface (± 2 cm), and the proximity of As gradients to the sediment surface, suggests that the upper gradient boundary at some sites may extend slightly into the bottom waters. By taking into account a maximum observed As gradient, and neglecting consumption mechanisms of upward migrating species, an upper measure of bottom water input can be estimated. For example, an efflux of 175 $\mu\text{g}\cdot\text{cm}^{-2}\cdot\text{y}^{-1}$, entering an average water column depth of ~ 3 m, would result in the addition of ~ 600 $\mu\text{g}\cdot\text{L}^{-1}$ in one year. Although this level represents a maximum, the result indicates that diffusive transport mechanisms have potential significance within the residence time-scale of Balmer Lake (~ 230 days).

The removal of porewater As below sediment depths of 20 cm at some sites in Balmer Lake is probably due to precipitation of As-bearing sulphide phases (Figs. 4.18-4.19; 4.27). Although the precipitation of As_2S_3 and mixed Fe-As sulphides have generally not been distinguished, incorporation of As into pyrite has been clearly shown to be an important removal mechanism in several anoxic marine sediments (Huerta-Diaz and Morse, 1992). Similarly, the precipitation of a mixed-sulphide phase was proposed by Peterson and

Carpenter (1986) to account for pronounced decreases in dissolved As below the sulphate redox transition in near-shore marine sediments.

In summary, the geochemical cycle of Fe has a dominant influence on the diagenetic behaviour of As in marine and lacustrine systems, but the influence of Mn on As behaviour is less clear. The lack of understanding partially stems from the dearth of appropriate data in addition to the inherently complex nature of natural systems. It must be realized that the high ionic strength of the polluted water column makes Balmer Lake unique in comparison to "pristine" water bodies. More specifically, the combined burdens of dissolved metal cations (Mn, Ni, Cu, Zn and Fe) exceed $2.5 \text{ mg}\cdot\text{L}^{-1}$ in near-interface oxic porewaters. Given such circumstances, sorption of the metals to Mn-oxide phases may shift the surface charge sufficiently to encourage the sorption of anionic As species (Takamatsu *et al.*, 1985).

VI. Summary and Conclusions

The distribution and behaviour of trace metals in Balmer Lake are influenced by both natural biogeochemical processes and inputs of mining-derived effluents. The formation of ice in early winter in conjunction with the high oxidant demand of the organic-rich sediments fosters the gradual development of stratification over the 5 month period of ice cover. Such seasonality results in spatial and temporal changes in the redox potential in the bottom waters and sediments. Non-steady-state inputs from the tailings circuits hosting elevated levels of trace elements, sulphate, cyanide and ammonium also contribute to the dynamic character of the system.

Dissolved and particulate metal concentrations in Balmer Lake are high, and compare with or surpass values reported for other polluted lacustrine environments. Homogenous distributions of all measured parameters evident during the summer, fall and spring are in marked contrast with the stratified water column conditions in late winter. The trace metal, nutrient and sulphate profiles during this period reflect the combined influences of redox-mediated reactions and inputs of dense mine-waters which migrate laterally across the lake bottom. Although the non-steady-state nature of the latter prevented definitive interpretations of the winter water column, it appears that variability with respect to the duration and intensity of reducing conditions in the bottom waters, and the proximity to effluent discharges contribute to the inter-station contrasts.

At sediment depths shallower than 10 cm, the deposits in Balmer Lake comprise contributions from both organic matter- and feldspar-rich natural detritus, and carbonate-, chlorite- and metal-rich tailings inputs. Enrichments of solid phase Cu, Ni and Zn at shallow depths were significantly lower immediately adjacent to the tailings discharge than at a site situated over 1 km

distant. The distribution likely reflects textural sorting of the tailings material, with the finer grain-size fractions hosting higher metal concentrations.

Both remobilization and scavenging mechanisms influence the behaviour of trace metals in the sediments and associated porewaters. Early diagenetic reactions in Balmer Lake sediments, for example, render the deposits below 5 cm depth a significant and permanent sink for dissolved Cu, Ni and Zn. Consumption horizons occur at depths consistent with zones of sulphate reduction, suggesting these elements are sequestered as sulphide precipitates. The extent of authigenic sulphide formation likely reflects the relatively recent addition of mining-derived sulphate to the lake waters.

Diffusive transport mechanisms have relatively little effect on the lake concentrations of Cu and Ni. Such processes can account for the removal of only 5 and 1% of their respective inventories with respect to a lake residence time of 230 days. The lake sediments provide a relatively greater diffusive sink for Zn; approximately 13% of the Zn inventory is consumed in this manner. Moreover, sulphide precipitation for these three elements contributes little to their overall accumulation rates. Episodic inputs of tailings material and the deposition of metal-rich particulates represent the principle contributors to the total benthic flux of these elements. Inputs of remobilized Zn and Ni from labile particulates result in pronounced spikes near the sediment-water interface. Since such peaks are shown to lie well above the Mn(IV) reduction horizon at some sites, it is suggested that the enrichments stem largely from the oxidation of labile organics, and not from the reduction of Fe and Mn oxides.

Contrary to most reports in the literature, the distribution of As appears to be largely dictated by the redox behaviour of Mn. In porewater profiles where the redox horizons for Fe(III) and Mn(IV) are clearly decoupled, dissolved As gradients closely match those of Mn. It is suggested that the large concentrations

of divalent cations in the shallow porewaters may significantly alter the surface charge properties of Mn oxides to encourage the sorption of anionic arsenic species. The largely invariant concentrations of As across the sediment-water interface during well-mixed periods imply that upward migrating species are consumed by presumably Mn oxides in the surface sediments. However, the reduced sorptive capacity of the surface sediments during periods of bottom water anoxia might suggest that dissolved As species are periodically allowed to diffuse into the bottom waters.

It is a reasonable expectation that once milling effluents are no longer discharged to Balmer Lake, concentrations of Cu and Ni should quickly diminish. This conclusion stems from the predominantly uni-directionally diffusive transport of these elements and the relatively short residence time of the basin. The same can be perhaps implied for Zn, although a fraction of the total benthic Zn-flux will continue to be regenerated back into the bottom waters. In addition, the settling of abundant organic and detrital particulates will continue to provide an effective transport mechanism of trace metals to bottom sediments. The apparent involvement of As in the redox cycling Mn has important ramifications with respect to the future water quality in the basin. The concomitant remobilization of As and Mn at shallow sediment depths produces large porewater gradients that will continue to support the upward migration of dissolved arsenic. However, the significance of potential effluxes to the lake waters and consumption mechanisms in the deeper porewaters remain unclear.

VII. Bibliography

Agett, J. and Kriegman, M. R. 1988. The extent of formation of arsenic(III) in sediment interstitial waters and its release to hypolimnetic waters in Lake Ohakuri. *Wat. Res.* **22**(4): 407-411.

Agett, J. and O'Brien, G. A. 1985. Detailed model for the mobility of arsenic in lacustrine sediments based on measurements in Lake Ohakuri. *Environ. Sci. Technol.* **19**: 231-238.

Almer, B., Dickson, W., Ekström, C. and Hörmström, E. 1978. Sulfur pollution and the aquatic ecosystem. In: *Sulfur in the Environment, Part 1*, pp. 271-311. Wiley-Interscience.

Anderson, L. C. D. and Bruland, K. W. 1991. Biogeochemistry of As in natural waters: the importance of methylated species. *Environ. Sci. Technol.* **25**(3): 420-427.

Andreae, M. O. 1979. Arsenic speciation in seawater and interstitial waters: The influence of biological-chemical interactions on the chemistry of a trace element. *Limnol. Oceanogr.* **24**: 440-452.

Arakaki, T. and Morse, J. W. 1993. Coprecipitation and adsorption of Mn(II) with mackinawite (FeS) under conditions similar to those found in anoxic sediments. *Geochim. Cosmochim. Acta* **57**: 9-14.

Baccini, P. 1984. Regulation of trace metal concentrations in freshwater systems. In: *Circulation of metals in the environment.*, pp. 239-288.

Balistreri, L. S. and Murray, J. W. 1992. The biogeochemical cycling of trace metals in the water column of Lake Sammamish, Washington: response to seasonally anoxic conditions. *Limnol. Oceanogr.* **37**(3): 529-548.

Belzile, N. and Tessier, A. 1990. Interactions between arsenic and iron oxyhydroxides in lacustrine sediments. *Geochim. Cosmochim. Acta.* **54**: 103-109.

Benjamin, M. M. and Leckie, J. O. 1981. Multiple site adsorption of Cd, Cu, Zn and Pb on amorphous iron oxyhydroxide. *J. Colloid Inter. Sci.* **79**: 209-221.

Benjamin, M. M. and Leckie, J. O. 1982. Effects of complexation by Cl^- , SO_4^{2-} , and $\text{S}_2\text{O}_3^{2-}$ on the adsorption behaviour of Cd on oxide surfaces. *Environ. Sci. Technol.* **16**(3): 162-170.

Berner, R. A. 1984. Sedimentary pyrite formation: un update. *Geochim. et Cosmochim. Acta* **48**: 1-42.

- Bischoff, J. L., Greer, R. E. and Luistro, A. O. 1970. Composition of interstitial waters of marine sediments: temperature and squeezing effects. *Science* **167**: 1245-1246.
- Bowell, R. J. 1994. Sorption of arsenic by iron oxides and oxyhydroxides in soils. *Appl. Geochem.* **9**: 279-286.
- Boyle, E. A. and Edmond, J. M. 1977. Determination of copper, nickel, and cadmium in seawater. *Anal. Chim. Acta.* **91**: 189-197.
- Brandl, H. and Hanselmann, K. W. 1991. Evaluation and application of dialysis porewater samplers for microbiological studies at sediment-water interfaces. *Aquatic Sci.* **53**(1): 55-73.
- Bruland, K. W. 1980. Oceanographic distributions of cadmium, zinc, nickel, and copper in the North Pacific. *Earth Planet. Sci. Lett.* **47**: 176-198.
- Bruland, K. W. 1983. Trace elements in seawater. In: *Chemical Oceanography*, pp. 157-220. Academic Press.
- Bruland, K. W. and Franks, R. P. 1983. Mn, Ni, Cu, Zn and Cd in the western North Atlantic. In: *Trace Metals in Seawater: NATO Conf. Series 4*, pp. 395-414.
- Bruland, K. W., Franks, R. P., Knauer, G. A. and Martin, J. H. 1979. Sampling and analytical methods for the determination of copper, cadmium, zinc and nickel at the nanogram per liter level in sea water. *Anal. Chim. Acta* **105**: 233-245.
- Bruland, K. W., Orians, K. J. and Cowen, J. P. 1994. Reactive trace metals in the stratified central North Pacific. *Geochim. Cosmochim. Acta* **58**(15): 3171-3182.
- Calvert, S. E. 1976. The mineralogy and geochemistry of near-shore sediments. In: *Chemical Oceanography* (ed. R. Chester) pp. 187-280, Academic Press.
- Calvert, S. E. and Karlin, R. E. 1991. Relationships between sulphur, organic carbon and iron in the modern sediments of the Black Sea. *Geochim. Cosmochim. Acta* **55**: 2483-2490.
- Campbell, P. G. C., Lewis, A. G., Chapman, P. M., Crowder, A. A., Fletcher, W. K., Imber, B., Luoma, S. N., Stokes, P. M. and Winfrey, M. 1988. *Biologically available metals in sediments*. National Research Council Canada. NRCC No. 27694.
- Carignan, R. 1984. Interstitial water sampling by dialysis: methodological notes. *Limnol. Oceanogr.* **29**(3): 667-670.

- Carignan, R. and Nriagu, J. O. 1985. Trace metal deposition and mobility in the sediments of two lakes near Sudbury, Ontario. *Geochim. Cosmochim. Acta* 49: 1753-1764.
- Carignan, R., Rapin, F. and Tessier, A. 1985. Sediment porewater sampling for metal analysis: A comparison of techniques. *Geochim. Cosmochim. Acta* 49(1): 2493-2498.
- Carignan, R., St-Pierre, S. and Gächter, R. 1994. Use of diffusion samplers in oligotrophic lake sediments: effects of free oxygen in sampler material. *Limnol. Oceanogr.* 39(2): 468-474.
- Carignan, R. and Tessier, A. 1985a. The co-diagenesis of sulphur and iron in acid lake sediments of southwestern Québec. *Geochim. Cosmochim. Acta.* 52: 1179-1188.
- Carignan, R. and Tessier, A. 1985b. Zinc deposition in acid lakes: The role of diffusion. *Science* 228: 1524-1526.
- Carignan, R. and Tessier, A. 1988. The co-diagenesis of sulphur and iron in acid lake sediments of southwest Quebec. *Geochim. Cosmochim. Acta* 52: 1179-1188.
- Cherry, J. A., Shaikh, A. U., Tallmann, D. E. and Nicolson, R. V. 1979. Arsenic species as an indication of redox conditions in groundwater. *J. Hydrol.* 43: 373-392.
- Chiswell, B. and Mokhtar, M. B. 1986. The speciation of manganese in freshwaters. *Talanta* 33(8): 669-677.
- Colley, S. and Thomson, J. 1984. Post-depositional migration of elements during diagenesis in brown clay and turbidite sequences in the North East Atlantic. *Geochim. Cosmochim. Acta.* 48: 1223-1235.
- Colvine, A. C., Andrews, A. J., Cherry, M. E., Durocher, P., Fyon, A. J., Lavigne, M. J., MacDonald, A. J., Poulsen, K. H., Springer, J. S. and Troop, D. G. 1984. *An integrated model for the origin of Archean lode gold deposits.* Ontario Geological Survey. Open-file report 5524.
- Conroy, N. and Keller, W. 1976. Geological factors affecting biological activity in precambrian shield lakes. *Canadian Mineralogist* 14: 62-72.
- Cook, R. B. 1984. Distributions of ferrous iron and sulfide in an anoxic hypolimnion. *Can. J. Fish. Aquat. Sci.* 41: 286-293.
- Corfu, F. and Andrews, A. J. 1987. Geochronological constraints on the timing and magmatism, deformation and gold mineralization in the Red Lake greenstone belt, northwestern Ontario. *Can. J. Earth Sci.* 24: 1302-1320.

- Corfu, F. and Wallace, H. 1986. U-Pb zircon ages for magma in the Red Lake greenstone belt, northwestern Ontario. *Can. J. Earth Sci.* **23**: 27-42.
- Cornwell, J. C. 1986. Diagenetic trace-metal profiles in Arctic lake sediments. *Environ. Sci. Tech.* **20**: 299-302.
- Crecelius, E. A. 1975. The geochemical cycling of arsenic in Lake Washington and its relation to other elements. *Limnol. Oceanogr.* **20**(3): 441-451.
- Cullen, W. R. and Reimer, K. J. 1989. Arsenic speciation in the environment. *Chem. Rev.* **89**: 713-764.
- Dai, M., Martin, J. and Cauwet, G. 1995. The significant role of colloids in the transport and transformation of organic carbon and associated trace metals (Cd, Cu and Ni) in the Rhone delta (France). *Mar. Chem.* **51**: 159-175.
- Davis, J. A. and Leckie, J. O. 1978a. Effect of adsorbed complexing ligands on trace metal uptake by hydrous oxides. *Environ. Sci. Technol.* **12**(12): 1309-1315.
- Davis, J. A. and Leckie, J. O. 1978b. Surface ionization and complexation at the oxide/water interface. II. Surface properties of amorphous iron oxyhydroxide and adsorption of metal ions. *J. Colloid Inter. Sci.* **67**(1): 90-107.
- Davison, W. 1993. Iron and manganese in lakes. *Earth-Sci. Rev.* **34**: 119-163.
- Davison, W., Grime, G. W. and Woof, C. 1992. Characterization of lacustrine iron sulphide particles with proton-induced X-Ray emission. *Limnol. Oceanogr.* **37**(8): 1770-1777.
- Davison, W., Lishman, J. P. and Hilton, J. 1985. Formation of pyrite in freshwater sediments: Implications for C/S ratios. *Geochim. et Cosmochim. Acta* **49**: 1615-1620.
- Davison, W. and Woof, C. 1984. A study of the cycling of manganese and other elements in a seasonally anoxic lake. *Water research* **18**(6): 727-734.
- Davison, W. and Woof, C. 1982. The dynamics of iron and manganese in a seasonally anoxic lake; direct measurement of fluxes using sediment traps. *Limnol. Oceanogr.* **27**(6): 987-1003.
- De Vitre, R., Belzile, N. and Tessier, A. 1991. Speciation and adsorption of arsenic on diagenetic iron oxyhydroxides. *Limnol. Oceanogr.* **36**(7): 1480-1485.
- De Vitre, R. and Davison, W. 1993. Manganese particles in fresh water. In: *Environmental Particles* (ed Lewis) pp. 440. Boca Raton.

- De Vitre, R. R., Buffle, J., Perret, D. and Baudat, R. 1988. A study of iron and manganese transformations at the O₂/S(-II) transition layer in a eutrophic lake (Lake Bret, Switzerland): A multimethod approach. *Geochem. Cosmochim. Acta.* 52: 1601-1613.
- Devuyt, E. A., Mosoiu, A. and Krause, E. 1982. Oxidizing properties and applications of the SO₂-air system. At Proc. 3rd Intl Symp. on Hydromet.
- Eadie, B. J. and Robbins, J. A. 1987. The role of particulate matter in the movement of contaminants in the Great Lakes. In: *Sources and Fates of Aquatic Pollutants*, pp. 319-364. American Chemical Society.
- Edenborn, H. M., Belzile, N., Mucci, A., Lebel, J. and Silverberg, N. 1986. Observations on the diagenetic behaviour of arsenic in a deep coastal sediment. *Biogeochemistry* 2: 359-376.
- EIG 1986. *Spring melt studies relating to the operation of an improved control structure for Balmer Lake*. Environmental Applications Group.
- Elderfield, H. 1981. Metal-organic associations in interstitial waters of Narragansett Bay sediments. *Amer. J. Sci.* 281: 1184-1196.
- Elinder, C. G. 1984. Metabolism and toxicity of metals. In: *Changing metal cycles and human health.*, pp. 265-274. Springer-Verlag.
- Emerson, S. 1976. Early diagenesis in anaerobic lake sediments: chemical equilibria in interstitial waters. *Geochim. Cosmochim. Acta* 40: 925-934.
- Ferguson, J. F. and Gavis, J. 1972. A review of the arsenic cycle in natural waters. *Wat. Res.* 6: 1259-1274.
- Florence, T. M. 1982. The speciation of trace elements in waters. *Talanta* 29: 345-364.
- Forel, F. A. 1892. *Le Léman: Monographie Limnologique. Tome I. Géographie, Hydrographie, Géologie, Climatologie, Hydrologie.*
- Forel, F. A. 1895. *Le Léman: Monographie Limnologique. Tome II. Mécanique, Hydraulique, Thermique, Optique, Acoustique, Chimie.*
- Forel, F. A. 1904. *Le Léman: Monographie Limnologique. Tome III. Biologie, Histoire, Navigation, Pêche.*
- Francois, R. 1990. Marine sedimentary humic substances: structure, genesis, and properties. *Reviews in aquatic sciences* 3(1): 41-80.

- Froelich, P. N., Klinkhammer, G. P., Bender, M. L., Luedtke, N. A., Heath, G. R., Cullen, D., Dauphin, P., Hammond, D. and Hartman, B. 1979. Early oxidation of organic matter in pelagic sediments of the eastern equatorial Atlantic: suboxic diagenesis. *Geochim. et Cosmochim. Acta.* 43: 1075-1090.
- Fuller, C. C., Davis, J. A. and Waychunas, G. A. 1993. Surface chemistry of ferrihydrite: Part 2. Kinetics of arsenate adsorption and coprecipitation. *Geochim. Cosmochim. Acta.* 57: 2271-2282.
- Gaillard, J. F., Jeandel, C., Michard, G., Nicolas, E. and Renard, D. 1986. Interstitial water chemistry of Villefranche Bay sediments: trace metal diagenesis. *Mar. Chem.* 18: 233-247.
- Green, W. J., Ferdman, T. G. and Canfield, D. E. 1989. Metal dynamics in Lake Vanda (Wright Valley, Antarctica). *Chem. Geol.* 76: 85-94.
- Grim, R. E. 1953. *Clay Mineralogy*. McGraw-Hill Book Company, Inc. pp. 384.
- Gulens, J., Champ, D. R. and Jackson, R. E. 1979. Influence of redox environments on the mobility of arsenic in ground water. In: *Chemical Modelling in Aqueous Systems.*, pp. 81-95. American Chemical Society.
- Gulson, B. L., Mizon, K. J. and Atkinson, B. T. 1993. Source and timing of gold and other mineralization in the Red Lake area, northwestern Ontario, based on lead-isotope investigations. *Can J. Earth Sci.* 30: 2366-2379.
- Hamilton-Taylor, J. and Davison, W. 1994. Redox-driven cycling of trace elements in lakes. In: *Lakes II*, pp. 129-152.
- Hamilton-Taylor, J. and Willis, M. 1990. A quantitative assessment of the sources and general dynamics of trace metals in a soft-water lake. *Limnol. Oceanogr.* 35(4): 840-851.
- Harrison, G. I. and Morel, F. M. M. 1983. Antagonism between Cd and Fe in the marine diatom *Thalassiosira weissflogii*. *J. Phycol.* 19: 495-507.
- Hesslein, R. H. 1976. An in situ sampler for close interval porewater studies. *Limnol. Oceanogr.* 21: 912-914.
- Heurta-Diaz, M. A. and Morse, J. W. 1992. Pyritization of trace metals in anoxic marine sediments. *Geochim. Cosmochim. Acta.* 56: 2681-2702.
- Higgs, T. W. 1979. *Factors affecting natural degradation of free and metal-complexed cyanides from gold mill effluents*. Report prepared for Fisheries and Environment Canada, Burlington, Ontario.

- Higgs, T. W. 1993. *Technical guide for the environmental management of cyanide in mining*. Mining Association of British Columbia.
- Hsia, T. H., Lo, S. L., Lin, C. F. and Lee, D. Y. 1994. Characterization of arsenate adsorption on hydrous iron oxide using chemical and physical methods. *Colloids and Surfaces*. 85: 1-7.
- Huerta-Diaz, M. and Morse, J. W. 1992. Pyritization of trace metals in anoxic marine sediments. *Geochim. Cosmochim. Acta*. 56: 2681-2702.
- Hutchinson, G. E. 1957. *A treatise on limnology I. Geography, Physics and Chemistry*. Wiley Inc. 1015.
- IEC 1979. *Factors affecting natural degradation of free and metal-cyanide complexed cyanides from gold mill effluent. Report prepared for Fisheries and Environment Canada*.
- Jackson, T. A. 1978. The biogeochemistry of heavy metals in polluted lakes and streams at Flin Flon, Canada, and a proposed method for limiting heavy-metal pollution of natural waters. *Environ. Geol.* 2(3): 173-189.
- Jackson, T. A. and Bistricki, T. 1995. Selective scavenging of Cu, Zn, Pb, and As by Fe and Mn oxyhydroxide coatings in lakes polluted with mine and smelter wastes: results of energy dispersive X-ray micro-analysis. *J. Geochem. Explor.* 52: 97-125.
- Jaworowski, Z., Bysiek, M. and Kownacka, L. 1981. Flow of metals into the global atmosphere. *Geochim. Cos. Acta*. 45: 2185-2199.
- Jenkins, M. C. and Kemp, W. M. 1984. The coupling of nitrification and denitrification in two estuarine sediments. *Limnol. Oceanogr.* 29: 609-619.
- Jenne, E. A. 1986. Chemical species in freshwater and terrestrial systems. In: *The importance of chemical "speciation" in environmental processes.*, pp. 121-148. Springer-Verlag.
- Jørgensen, B. B. 1977. The sulphur cycle of a coastal marine sediment (Limfjorden, Denmark). *Limnol. Oceanogr.* 22: 814-832.
- Kerner, M and Geisler, C. D. 1995. Dynamics of Cu release during early aerobic degradation in aggregated seston from the Elbe estuary. *Mar. Chem.* 51: 133-144.
- Kinniburgh, D. G. 1981. Cation adsorption by hydrous metal oxides and clay. In: *Adsorption of Inorganics at Solid-Liquid Interfaces*. pp. 91-160. Ann Arbor Science.

- Klinkhammer, G. P. 1980. Early diagenesis in sediments from the Eastern Equatorial Pacific, II. Pore water metal results. *Earth and Planetary Science Letters* 49: 81-101.
- Kubota, J., Mills, E. L. and Oglesby, R. T. 1974. Pb, Cd, Zn, Cu and Co in streams and lake waters of Cayuga Lake Basin, New York. *Environ. Sci. Technol.* 8: 243-248.
- Lantzy, R. J. and Mackenzie, F. T. 1979. Atmospheric trace metals: global cycles and an assessment of man's impact. *Geochim. Cosmochim. Acta.* 43(4): 511-525.
- Laxen, D. 1985. Trace metal adsorption/coprecipitation on hydrous ferric oxide under realistic conditions. *Water Res.* 19(10): 1229-1236.
- Laxen, D. and Chandler, I. M. 1983. Size distribution of iron and manganese species in freshwaters. *Geochim. Cosmochim. Acta.* 47: 731-741.
- LaZerte, B. D. and Burling, K. 1990. Manganese speciation in dilute waters of the precambrian shield, Canada. *Wat. Res.* 24(9): 1097-1101.
- Leckie, J. O. 1986. Adsorption and transformation of trace element species at sediment/water interfaces. In: *The importance of chemical "speciation" in environmental processes.* pp. 237-254. Springer-Verlag.
- Li, Y. H. and Gregory, S. 1974. Diffusion of ions in sea water and in deep-sea sediments. *Geochim. Cosmochim. Acta.* 38: 703-714.
- Manheim, F. T. 1970. The diffusion of ions in unconsolidated sediments. *Earth Planet. Sci. Lett.* 9: 307-309.
- Martens, C. S. and Klump, J. V. 1980. Biogeochemical cycling in an organic-rich coastal marine basin: 1. Methane sediment-water exchange processes. *Geochim. Cosmochim. Acta* 44: 471-490.
- Masala, C. 1995. Water and effluent management of Balmer Lake tailings management. M.Sc. Thesis, University of British Columbia.
- Matisoff, G., Lindsay, A. H., Matis, S. and Soster, F. M. 1980. Trace metal mineral equilibria in Lake Erie sediments. *J. Great Lakes Res.* 6(4): 353-366.
- Mayer, L. M. 1976. Chemical water sampling in lakes and sediments with dialysis bags. *Limnol. Oceanogr.* 21: 909-912.
- McKee, J. D., Wilson, T. P. and Long, D. T. 1989a. Geochemical partitioning of Pb, Zn, Cu, Fe and Mn across the sediment-water interface in large lakes. *J. Great Lakes Res.* 15(1): 46-58.

- McKee, J. D., Wilson, T. P. and Long, D. T. 1989b. Porewater profiles and early diagenesis of Mn, Cu, and Pb in sediments from large lakes. *J. Great Lakes Res.* 15(1): 68-83.
- McKelvey, B. A. 1994. The marine geochemistry of zirconium and hafnium. Ph.D. Thesis, University of British Columbia.
- Middleburg, J. J. 1989. A simple rate model for organic matter decomposition in marine sediments. *Geochim. et Cosmochim. Acta.* 53: 1577-1581.
- Morel, F. M. M. and Hudson, R. J. M. 1985. The geobiological cycle of trace elements in aquatic systems: Redfield revisited. In: *Chemical Processes in Lakes*. pp. 251-282. Wiley-Interscience.
- Morfett, K., Davison, W. and Hamilton-Taylor, J. 1988. Trace metal dynamics in a seasonally anoxic lake. *Environ. Geol. Water Sci.* 11(1): 107-114.
- Morse, J. W. and Arakaki, T. 1993. Adsorption and coprecipitation of divalent metals with mackinawite (FeS). *Geochim. Cosmochim. Acta.* 57: 3635-3640.
- Morse, J. W., Millero, F. J., Cornwell, J. C. and Rickard, D. 1987. The chemistry of hydrogen sulfide and iron sulfide systems in natural waters. *Earth-Science Reviews* 24: 1-42.
- Mortimer, C. H. 1941. The exchange of dissolved substances between mud and water in lakes. *J. Ecol.* 29: 280-329.
- Mortimer, C. H. 1942. The exchange of dissolved substances between mud and water in lakes (Parts III and IV, summary and references). *J. Ecol.* 30: 147-201.
- Mortimer, C. H. 1951. The use of models in the study of water movement in stratified lakes. *Verh. Int. Ver. Limnol.* 11: 254-260.
- Murray, J. W. 1987. Mechanisms controlling the distribution of trace elements in oceans and lakes. In: *Sources and Fates of Aquatic Pollutants*, pp. 91-130. American Chemical Society.
- Nriagu, J. O. 1989. A global assessment of natural sources of atmospheric trace metals. *Nature* 338: 47-49.
- Nriagu, J. O., Lawson, G., Wong, H. K. T. and Azcue, J. M. 1993. A protocol for minimizing contamination in the analysis of trace metals in Great Lakes waters. *J. Great Lakes Res.* 19(1): 175-182.

Nriagu, J. O. and Soon, Y. K. 1985. Distribution and isotopic composition of sulphur in lake sediments of northern Ontario. *Geochim. Cosmochim. Acta.* 49: 823-834.

Nriagu, J. O., Wong, H. K. T. and Coker, R. D. 1981. Particulate and dissolved trace metals in Lake Ontario. *Water Res.* 15: 91-96.

Nriagu, J. O., Wong, H. K. T. and Coker, R. D. 1982. Deposition and chemistry of pollutant metals in lakes around the smelters at Sudbury, Ontario. *Environ. Sci. Technol.* 16: 551-560.

Oscarson, D. W., Huang, P. M., Defosse, C. and Herbillon, A. 1981a. Oxidative power of Mn(IV) and Fe(III) oxides with respect to As(III) in terrestrial and aquatic environments. *Nature* 291: 50-51.

Oscarson, D. W., Huang, P. M. and Liaw, W. K. 1980. The oxidation of arsenite by aquatic sediments. *J. Environ. Qual.* 9(4): 700-703.

Oscarson, D. W., Huang, P. M. and Liaw, W. K. 1981b. Role of manganese in the oxidation of arsenite by freshwater lake sediments. *Clays Clay Minerals* 29: 219-225.

Papelis, C., Hayes, K. F. and Leckie, J. O. 1988. *HYDRAQL: A program for the computation of chemical equilibrium composition of aqueous batch systems including surface-complexation modeling of ion adsorption at the oxide/solution interface.* Stanford Univ. Dep. Civ. Eng. Tech. Rep. 306.

Parsons, T. R., Maita, Y. and Lalli, C. 1984. *A manual of chemical and biological methods for seawater analysis.* Pergamon Press. pp. 173.

PDI, 1986. *Spring melt studies relating to the operation of an improved control structure for Balmer Lake.* Environmental Applications Group Ltd.

PDI 1990. Balmer Lake Management program. Water quality and sediment coring results.

Pedersen, T. F. 1983. Dissolved heavy metals in a lacustrine mine tailings deposit, Buttle Lake, British Columbia. *Mar. Poll. Bull.* 14: 249-254.

Pedersen, T. F. 1985. Early diagenesis of copper and molybdenum in mine tailings and natural sediments in Rupert and Holberg Inlets, British Columbia. *Can. Jour. Earth. Sci.* 22: 1474-1484.

Pedersen, T. F., Malcolm, S. J. and Sholkovitz, E. R. 1985. A lightweight gravity corer for undisturbed sampling in soft sediments. *Can. J. Earth Sci.* 22: 133-135.

- Pedersen, T. F., Mueller, B. and McNee, J. J. 1993. The early diagenesis of submerged sulphide-rich mine tailings in Anderson Lake, Manitoba. *Can. J. Earth Sci.* 30: 1099-1109.
- Pedersen, T. F., Mueller, B. and Pelletier, C. A. 1990. On the reactivity of submerged mine tailings in fjords and a lake in British Columbia. At GAC/MAC Symposium on Acid Mine Waste, Vancouver, B.C.
- Pedersen, T.F. and Losher A. J. 1988. *Diagenetic processes in aquatic mine tailings deposits in British Columbia..* pp. 238-258. Springer-Verlag.
- Perry, K. A. 1993. The chemical limnology of two meromictic lakes with emphasis on pyrite formation. Ph.D. Thesis, University of British Columbia.
- Peterson, M. L. and Carpenter, R. 1986. Arsenic distributions in porewaters and sediments of Puget Sound, Lake Washington, the Washington coast and Saanich Inlet, B.C. *Geochim. Cosmochim. Acta.* 50: 353-369.
- Pierce, M. L. and Moore, C. B. 1982. Adsorption of arsenite and arsenate on amorphous iron hydroxide. *Water. Res.* 16: 1247-1253.
- Postma, D. and Jakobsen, R. 1996. Redox zonation: Equilibrium constraints on the Fe(III)/SO₄-reduction interface. *Geochim. Cosmochim. Acta* 60(17): 3169-3175.
- Raiswell, R. and Berner, R. A. 1985. Pyrite formation in euxinic and semi-euxinic sediments. *Amer. J. Sci.* 285: 710-724.
- Redfield, A. C. 1958. The biological control of chemical factors in the environment. *Amer. Sci.* 46: 206-226.
- Reimer, K. J. and Thompson, J. A. J. 1988. Arsenic speciation in marine interstitial water. The occurrence of organoarsenicals. *Biogeochemistry.* 6: 211-237.
- Reynolds, G. L. and Hamilton-Taylor, J. 1992. The role of planktonic algae in the cycling of Zn and Cu in a productive soft-water lake. *Limnol. Oceanogr.* 37(8): 1759-1769.
- Rosenthal, Yair, Lam, P. and Boyle, E. A. 1995. Authigenic cadmium enrichments in suboxic sediments: precipitation and post-depositional remobilization. *Earth Planet. Sci. Lett.* 132: 99-109.
- Rudd, J. W. M., Kelly, C. A. and Furutani, A. 1986. The role of sulphate reduction in the long term accumulation of organic and inorganic sulphur in lake sediments. *Limnol. Oceanogr.* 31(6): 1281-1291.

- Salomons, W. 1995. Environmental impact of metals derived from metal mining: processes, predictions, prevention. *J. Geochem. Explor.* **52**: 5-23.
- Sanders, J. G. 1983. Role of marine phytoplankton in determining the chemical speciation and biogeochemical cycling of arsenic. *Can. J. Fish. Aquat. Sci.* **40**(Suppl. 2): 192-196.
- Schaule, B. K. and Patterson, C. C. 1981. Lead concentration in the Northeast Pacific: evidence for global anthropogenic perturbations. *Earth Planet. Sci. Lett.* **54**: 97-116.
- Schindler, P. W. 1981. Surface complexes at oxide-water interfaces. In: *Adsorption of Inorganics at Solid-Liquid Interfaces*. pp. 1-50. Ann Arbor Science.
- Sclater, F. F., Boyle, E. and Edmond, J. M. 1976. On the marine geochemistry of nickel. *Earth Planet. Sci. Lett.* **31**: 119-128.
- Semkin, R. G. and Kramer, J. R. 1976. Sediment geochemistry of Sudbury-area lake. *Can. Mineral.* **14**: 73-90.
- Shaw, T. J., Gieskes, J. M. and Jahnke, R. A. 1990. Early diagenesis in differing depositional environments: the response of transition metals in pore water. *Geochim. Cosmochim. Acta* **54**: 1233-1246.
- Shaw, T. J., Sholkovitz, E. R. and Klinkhammer, G. 1994. Redox dynamics in the Chesapeake Bay: The effect on sediment/water uranium exchange. *Geochim. Cosmochim. Acta* **58**(14): 2985-2995.
- Sholkovitz, E. 1973. Interstitial water chemistry of the Santa Barbara Basin sediments. *Geochim. et Cosmochim. Acta* **37**: 2043-2073.
- Sholkovitz, E. R. 1979. Chemical and physical processes controlling the chemical composition of suspended material in the River Tay estuary. *Estuar. Coastal. Mar. Sci.* **8**: 523-545.
- Sholkovitz, E. R. 1985. Redox-related geochemistry in lakes: alkali metals, alkaline earth elements, and ^{137}Cs . In: *Chemical Processes in Lakes.*, pp. 119-142. Wiley-Interscience.
- Sigg, L. 1985. Metal transfer mechanisms in lakes: the role of settling particles. In: *Chemical Processes in Lakes.*, pp. 283-310. Wiley-Interscience.
- Sigg, L., Johnson, A. and Kuhn, A. 1991. Redox conditions and alkalinity generation in a seasonally anoxic lake (Lake Greifen). *Mar. Chem.* **36**: 9-26.

- Sigg, L., Sturm, M. and Kistler, D. 1987. Vertical transport of heavy metals by settling particles in Lake Zurich. *Limnol. Oceanogr.* **32**: 112-130.
- Sörenson, J. and Jörgensen, B. B. 1987. Early diagenesis in sediments from Danish coastal water: microbial activity and Mn-Fe-S geochemistry. *Geochim. Cosmochim. Acta.* **51**: 1583-1590.
- Stadelmann, P. 1971. Stickstoffkreislauf und Primärproduktion im mesotrophen Vierwaldstättersee (Hower Bucht) und im eutrophen Rotsee, mit besonderer Berücksichtigung des Nitrats als limitierenden Faktors. *Schweiz. Z. Hydrol.* **33**: 1-65.
- Stumm, W. and Morgan, J. J. 1981. *Aquatic Chemistry*. pp. 583. Wiley-Interscience.
- Stumm, W. and Sulzberger, B. 1992. The cycling of iron in natural environments: considerations based on laboratory studies of heterogeneous redox processes. *Geochim. Cosmochim. Acta.* **56**: 3233-3257.
- Suess, E. 1979. Mineral phases formed in anoxic sediments by microbial decomposition of organic matter. *Geochim. Cosmochim. Acta***43**: 339-352.
- Takamatsu, T., Kawashima, M. and Koyama, M. 1985. The role of manganous-rich hydrous Mn-oxide in the accumulation of arsenic in lake sediments. *Wat. Res.* **19**(8): 1029-1032.
- Taylor, R. M. 1987. Non-silicate oxides and hydroxides. In: *Chemistry of Clays and Clay Minerals*. pp. 129-202. Wiley-Interscience.
- Tessier, A. and Campbell, P. G. C. 1988. Partitioning of Trace Metals in Sediments. In: *Metal speciation: theory, analysis, and application.*, pp. 183-200. Lewis Publishers.
- Tessier, A., Carignan, R., Dubreuil, B. and Rapin, F. 1989. Partitioning of Zn between the water column and the oxic sediments in lakes. *Geochim. Cosmochim. Acta.* **53**: 1511-1522.
- Tessier, A., Fortin, D., Belzile, N., DeVitre, R. R. and Leppard, G. G. 1996. Metal sorption to diagenetic iron and manganese oxyhydroxides and associated organic matter: narrowing the gap between field and laboratory measurements. *Geochem. Cosmochim. Acta* **60**(3): 387-404.
- Tessier, A., Rapin, F. and Carignan, R. 1985. Trace metals in oxic lake sediments: possible adsorption onto iron oxyhydroxides. *Geochim. Cosmochim. Acta***49**: 183-194.

- Tipping, E. 1981. The adsorption of aquatic humic substances by iron oxides. *Geochim. Cosmochim. Acta* 45: 191-199.
- Tipping, E. and Cooke, D. 1982. The effect of adsorbed humic substances on the surface charge of goethite. *Geochim. Cosmochim. Acta.* 46: 75-80.
- Tipping, E., Woof, C. and Cook, D. 1981. Iron oxide from a seasonally anoxic lake. *Geochim. Cosmochim. Acta.* 45: 1411-1419.
- Tsunogai, S., Yonemaur, I. and Kusakabe, M. 1979. Post depositional migration of Cu, Zn, Ni, Co, Pb and Ba in deep sea sediments. *Geochim. J.* 13: 239-252.
- Turner, D. R. 1984. Relationships between biological availability and chemical measurements. In: *Circulation of metals in the environment.*, pp. 137-164.
- Van der Weijden, C. H. 1992. Early diagenesis and marine pore water. In: *Diagenesis III*, pp. 13-133. Elsevier.
- Vickell, G. A., Davies, D. T. and Gec, R. 1989. Hydrogen peroxide treatment of gold mill wastes. At Gold Mining Effluent Seminar Proceedings., Feb. 15-16, 1989, Vancouver, B. C.
- Vuceta, J and Morgan, J. J. 1978. Chemical modelling of trace metals in fresh waters: role of complexation and adsorption. *Environ. Sci. Technol.* 12(12): 1302-1308.
- Westerlund, S. F. G., Aderson, L. G., Hall, P. O. J. and Iverfeldt, A. 1986. Benthic fluxes of cadmium, copper, nickel, zinc and lead in the coastal environment. *Geochim. Cosmochim. Acta* 50: 1289-1296.
- Wetzel, R. G. 1975. *Limnology*. W. B. Saunders Company. pp. 741.
- Wetzel, R. G., Rich, P. H., Miller, M. C. and Allen, H. L. 1975. Wintergreen Lake: a study in hypereutrophy. *Arch. Hydrobiol.* 73: 31-56.
- Widerlund, A. and Ingri, J. 1995. Early diagenesis of arsenic in sediments of the Kalix River estuary, northern Sweden. *Chem. Geol.* 125: 185-196.
- Williams, T. M. 1992. Diagenetic metal profiles in recent sediments of a Scottish freshwater loch. *Environ. Geol. Water. Sci.* 20(2): 117-123.
- Wood, J. M. 1974. Biological cycles for toxic elements in the environment. *Science* 183: 1049-1052.

Young, B. L. and Harvey, H. H. 1992. The relative importance of manganese and iron oxides and organic matter in the sorption of trace metals by surficial lake sediments. *Geochim. Cosmochim. Acta* 56: 1175-1186.

Zoller, W. H. 1984. Anthropogenic perturbation of metal fluxes into the atmosphere. In: *Changing metal cycles and human health.*, pp. 27-42. Springer-Verlag.

VIII. APPENDICES

Appendix A. Typical ICP/MS operating conditions.

Parameter	Typical value
RF power (kW)	1.35
Argon gas flow rate (L/min):	
Cooling gas	13.83
Auxiliary	0.983
Nebulizer	1.032
Sampling Position (mm from load coil)	13
Sampler Cone (nickel) from orifice (mm)	1.0
Skimmer Cone (nickel) from orifice (mm)	0.8
Ion lens settings (volts):	
Extraction	-118
Collector	-2
L1	-2
L2	-45
L3	+5
L4	-45
Pole Bias	-3
Operating Pressure (mbar):	
Expansion	2.2
Interface	$\leq x 10^{-4}$
Analyzer	$2 x 10^{-6}$
Resolution:	
ΔM	5.3

Appendix B. Quality Assessment/Quality Control (QA/QC)

The QA/QC program included the analysis of quality assurance samples to assess the precision and accuracy of measurements of the various parameters. Several types of samples were included: laboratory blanks (DDW with added reagents), field process blanks, laboratory replicates and certified reference materials. Overall, the results for the QA/QC samples are indicative of good reproducibility, accuracy and contamination control.

I. Dissolved Trace Metals

Laboratory blanks for all trace metals were very low, and indicates good contamination control. Blank values were used to determine the detection limits which are reported as six times the standard deviation of the blank results.

Table A1. Detection limits and machine precision for trace metal determinations. Detection limits represent six standard deviations of 10 process blank values.

Element	Method	Detection Limit (ppb)	Precision (%)
Fe	GFAAS	1.8	2.0
Mn	ICP/MS	0.06	2.5
Ni	ICP/MS	0.10	2.7
Cu	ICP/MS	0.14	2.5
Zn	ICP/MS	0.84	2.6
As	ICP/MS	0.22	2.0
Pb	ICP/MS	0.50	2.0

Table A2. Analytical results for field blanks. Values represent the average of four samples.

	Fe	Mn	Ni	Cu	Zn	As	Pb
Water column filter blank	<1.8	<0.06	<0.1	<0.14	1.1	<0.22	<0.5
Core porewater blank	<1.8	<0.06	<0.1	<0.14	<0.84	<0.22	<0.5

Table A3. Expected (Exp) and Observed (Obs) values for standard reference materials supplied by the National Research Council (SLRS) and the National Water Research Institute (TM Series). Observed values correspond to the mean of 10 measurements. The error in the observed values represents two standard deviations.

Element	SLRS-2		TM-21		TM-02	
	Exp	Obs	Exp	Obs	Exp	Obs
Fe					50.0 ± 16	50.3 ± 2.0
Mn	10.1 ± 0.3	9.46 ± 0.38	6.2 ± 2.0	6.1 ± 0.14		
Ni	1.03 ± 0.10	1.17 ± 0.10	6.6 ± 2.4	6.47 ± 0.30		
Cu	2.76 ± 0.17	2.80 ± 0.16	7.6 ± 2.2	6.93 ± 0.28		
Zn	3.33 ± 0.15	3.63 ± 0.32	7.5 ± 2.2	7.80 ± 0.40		
As	0.77 ± 0.09	0.81 ± 0.14				
Pb	0.129 ± 0.01	0.148 ± 0.01	5.5 ± 1.6	5.20 ± 0.20		

II. Particulate Trace Metals

Table A4. Trace metal determinations of the sediment reference material BCSS. The analysis of seven replicates included digestion followed by ICP/MS (Mn, Ni, Cu, Zn, As and Pb) and GFAAS (Fe). The error in the observed values represents \pm two standard deviations.

Digestion	Fe	Mn	Ni	Cu	Zn	As	Pb
1	32,755	225	78	21	101	19	23
2	37,523	204	69	21	100	17	23
3	33,290	203	64	20	97	17	24
4		177	65	20	95	17	22
5		216	65	18	96	17	23
6	28,073	152	60	21	89	16	21
7	34,273	202	64	19	104	17	24
Mean	33,183 \pm 6,800	197 \pm 46	67 \pm 11	20 \pm 2	98 \pm 12	17 \pm 2	23 \pm 2
Expected	32,900 \pm 980	229 \pm 15	55 \pm 4	19 \pm 3	119 \pm 12	11 \pm 2	23 \pm 3

Table A5. Laboratory blanks for digested polycarbonate filters. All values are expressed as $\mu\text{g}\cdot\text{L}^{-1}$.

Digestion	Fe	Mn	Ni	Cu	Zn	As	Pb
1	0.02	0.02	0.01	0.01	0.25	0.04	0.00
2	0.02	0.01	0.01	0.00	0.52	0.00	0.00
3	0.07	0.03	0.06	0.00	1.13	0.13	0.03
4	0.06	0.02	0.01	0.00	4.85	0.09	0.00
5	0.06	0.02	0.02	0.00	3.92	0.10	0.01
6	0.07	0.02	0.09	0.08	0.68	0.10	0.23
7	0.02	0.03	0.06	0.09	2.42	0.10	0.01
Mean	0.05	0.02	0.04	0.03	1.97	0.08	0.04

III. Nitrate and Sulphate

Table A6. Detection limits and machine precision for nitrate and sulphate determinations. Detection limits represent six standard deviations of 10 process blank values.

Anion	Method	Detection Limit	Precision
NO ₃ ⁻	IC	0.1 μmol·L ⁻¹	1.0 %
SO ₄ ²⁻	IC	0.1 μmol·L ⁻¹	1.0 %

Table A7. Expected (Exp) and Observed (Obs) values for standard reference materials supplied by the National Research Council and the National Water Research Institute. Observed values correspond to the mean of 10 measurements. The error in the observed values represents two standard deviations.

	Ani-04		Ion-96		Dionex	
	Exp	Obs	Exp	Obs	Exp	Obs
NO ₃ ⁻	145 ± 43	141 ± 6	335 ± 38	347 ± 24	1629 ± 10	1665 ± 100
SO ₄ ²⁻	1170 ± 110	1126 ± 66	1044 ± 122	1084 ± 84	1550 ± 10	1626 ± 120

Appendix C. Porewater data

Porewater concentrations of dissolved Fe, Mn, Ni, Cu, Zn, As, Pb, NH_4^+ , NO_3^- and SO_4^{2-} in Balmer Lake for the summer, fall, winter and spring field seasons. All values are reported $\mu\text{g}\cdot\text{L}^{-1}$, except for NH_4^+ ($\mu\text{mol}\cdot\text{L}^{-1}$) NO_3^- ($\mu\text{mol}\cdot\text{L}^{-1}$) and SO_4^{2-} ($\text{mmol}\cdot\text{L}^{-1}$). Positive values for sampled horizons (cm) for both peepers and cores (C1, C2 and C3) refer to depths above the sediment-water interface. Note, that due an angled peeper insertion, the depth scales for the metal and nutrient data differ for the last spring peeper profile.

Appendix C cont.

Summer-Station 2

Depth (cm)	Mn μgL^{-1}	Fe μgL^{-1}	Ni μgL^{-1}	Cu μgL^{-1}	Zn μgL^{-1}	As μgL^{-1}	Pb μgL^{-1}	NH4 μmolL^{-1}	NO3 μmolL^{-1}	SO4 mmolL^{-1}
35.5		45	415	173	45		0.5	48	350	3.4
30.3			429	174	49		0.4			
23.9	281	57	417	169	43	279	0.2			
18.7			421	175	51		1.0	79	354	3.4
18.7									341	3.3
14.8	285	35	403			289	0.0	90	348	3.1
13.5		45	408	163	48		0.5			
12.3		37	413	163	62		0.4			
11.0		44	402	160	53		0.3	98	342	3.3
9.7		60	417	161	63		0.2			
8.4	290	39	405	162	47	297	0.3			
7.1		42	408	161	49		0.5	87	354	3.4
7.1		57							350	3.3
5.8	297	54	407	163	51	301	0.9			
5.2			392	153	42		0.2			
4.5		47	410	162	45		0.3			
4.5		33	408	163	46		0.2			
3.2	306	34	413	167	51	309	0.4	79	346	3.2
2.6		40						77	373	3.3
1.9		71	404	155	52		0.6	77	358	3.3
1.3		90	424	158	49		0.3	80		
0.6	306	66	421	169	59	320		73	433	3.3
0.0	313	57	402	157	55		0.3	70	371	3.2
0.0									374	3.3
-0.6		44						64	400	3.2
-1.3								72	381	3.3
-1.9	338	49	407	148	63	390	0.3	128	329	3.2
-1.4	380		396	132	73	591	0.4	209	194	
-3.2	412	75	437	139	107	567	0.2	269	180	3.1
-3.9	460		366	108	99	983	0.4	348	68	3.1
-4.5	494	100	429	120	124	992	0.4	354	92	3.0
-4.5									91	
-5.8	680	110	244	50	69	2430	0.8			
-7.1	820	490	154	15	72	4080	1.1	558	51	2.6
-8.4	940	1050	110	5	30	4960	0.5	574	77	2.6
-9.7	986	1400	101	7	30	5044	0.6	660	35	2.4
-11.0	961	1890	96	20	40	4862	1.9	618	41	2.2
-14.8	979	1510	76	4	26	3896	0.9	622	36	1.8
-18.7	908	1410	59	4	20	3028	1.0	642	15	1.2
-18.7									14	1.2
-22.6	881	1630	49	2	13	2561	0.6	655	23	1.0
-26.4	908	2150	54	1	17	2828	0.8	671	15	0.8
-31.6	888	2860	56	1	13	2405	1.0	647	14	0.6
-36.8	909	3240	67	11	27	3175	1.5	622	26	0.6
-36.8									27	0.6
-41.9	986	3850	86	6	33	3854	1.1	666	13	0.3

Summer-Station 2

Depth (cm)	Mn μgL^{-1}	Fe μgL^{-1}	Ni μgL^{-1}	Cu μgL^{-1}	Zn μgL^{-1}	As μgL^{-1}	Pb μgL^{-1}	NH4 μmolL^{-1}	NO3 μmolL^{-1}	SO4 mmolL^{-1}
31.0	289	65	421	164	47	285	0.5	72	344	3.3
27.1										
25.8		30						75		
24.5										
23.2										
21.9										
20.6										
19.4	288	26	415	161	45	266	0.4		366	3.3
19.4	285		414	154	42	278	0.4		341	3.3
18.1										
16.8										
15.5										
14.2								72		
10.3	298	60	430	171	52	296	0.3	78	343	3.2
9.7		42								
7.7		54								
7.1		33								
6.5	291	36	421	151	46	285	0.4	100	340	3.3
5.8		37								
5.2		35								
4.5		34								
3.9		48								
3.2		32								
2.6	287	40	423	160	48	286	0.4	105	343	3.3
1.3	299	56				293				
0.0	304	47	412	156	61	297	0.4	90		
-1.3	361	57	485	147	86	372	0.3	93	368	3.3
-1.9	366	38	460	143	125	384	0.4	95	360	3.3
-2.6	421	79	484	135	90	523	0.5	87	401	3.2
-2.6	414		489	131	88	530	0.5		385	3.1
-3.2	446	43	461	123	143	446	0.5	85	364	3.2
-3.9	451	58	427	112	88	451	0.4	85	327	3.1
-4.5	506	60	322	88	100	885	0.6	67	344	2.3
-5.2	517	78	295	81	52	1049	0.6	128	179	2.8
-5.8	549	197	218	51	60	1502	0.5	272	194	2.8
-6.5	756	381	209	28	34	2135	0.5	333	87	2.6
-7.1	757	744	171	18	45	2536	0.5	360	80	2.4
-7.7	858	837	167	13	28	3003	0.5	354	35	2.5
-8.4	844	1598	142	10	32	3319	0.4	456	71	2.3
-9.0	916	1457	123	6	41	3525	0.3	441	52	2.3
-10.3	908	1490	116	18	20	3985	0.2	439	56	2.0
-10.3	918		113			3995			54	2.0
-11.6	891	1677	111	7	23	3794	0.3	510	59	2.1
-12.9	855	1544	105	6	21	3798	0.1	580	54	1.9
-14.2								494	29	1.7
-15.5	869	1688	105	29	38	3725	0.2	609	30	1.7
-19.4	806	1460	79	7	22	2946	0.3	628	32	1.4
-23.2	800	2056	72	2	23	2808	0.5	636	10	1.0
-23.2	812					2767			14	1.0
-27.1	779	1464	72	1	26	2099	0.4	686	14	0.8
-31.0	764	1535	67	1	23	1870	0.3	650	9	0.6
-36.1	814	2923	59	1	16	1977	1.2	610	8	0.5
-41.3	845	3175	73	0	22	2208	0.2	588	9	0.4
-41.3	828		74			2192			8	0.4
-46.4	909	4230	129	12	79	2355	0.5	606	4	0.2

Appendix C cont.

Summer-Station 1

Depth (cm)	Mn μgL^{-1}	Ni μgL^{-1}	Cu μgL^{-1}	Zn μgL^{-1}	As μgL^{-1}	Pb μgL^{-1}	Fe μgL^{-1}	NO4 μmolL^{-1}	SO4 mmolL^{-1}	NH4 μmolL^{-1}
34.8	237	423	154	57	285	0.0	36	350	3.4	63
33.5										
32.3										
31.0										
29.7	237	427	150	44	287	0.0	31	360	3.5	77
29.7	243	441					28			
23.2	242	426	155	49	295	0.0	32		3.4	
23.2			154	47	292					
18.1	242	421	153	48	294	0.0	31	354	3.4	77
18.1							35			
14.2	256	455	167	72	316	0.1	342	401	3.4	85
14.2							330			
12.9	253	428	157	67	298	0.1	191			
12.9							178			
11.6	253	434	158	51	304	0.0	151			
11.6							134			
10.3	244	437	162	50	307	0.0	76			
9.0	237	428	160	50	310	0.0	41	390	3.5	91
9.0							37			
7.7	234	438	155	48	295	0.0	33			
7.7							31			
6.5	245	428	164	45	317	0.0	35	414	3.4	83
5.2	239	443	155	52	302	0.1	35			111
4.5	233	432	156	47	303		29			110
4.5			163	48	311	0.0				
3.9	240	424	149	46	301	0.0	31	447	3.3	115
3.2	234	431	161	45	313		29			108
3.2	230	438				0.0				
2.6	229	418	150	44	304	0.0	31	403	3.4	107
1.9	224	429	159	51	294	0.0	29			115
1.3	242	443	151	47	300	0.0	30			100
0.6	256	434	156	50	288	0.0	29	596	3.4	101
0.0	260	397	144	60	298	0.0	34	396	3.4	100
-0.6							34	406	3.4	87
-0.6	333	469	143	60	315	0.0		412	3.4	
-1.3	344	376	114	54	335	0.0	35	365	3.5	130
-1.3							356			
-1.9	395	382	114	58	481	0.0	31	360	3.5	185
-1.9			104	59	433	0.0	31			
-2.6	505	213			690	0.0		197	3.6	298
-2.6	513	220	51	34	689		162	199	3.5	
-3.2	537	205	42	30	718	0.0	75	149	3.6	397
-3.2							65			
-3.9	670	106	12	18	1875	0.0	475	53	3.4	450
-3.9							462			
-4.5	613	118	13	20	1481	0.1	300	44		447
-4.5							267		3.2	
-5.2	752	86	8	15	2663	0.0	1023	27	3.7	511
-5.2							980	27		
-6.5	765	85	6	13	2809	0.0	1307			611
-6.5		84	6	14		0.0				
-7.7	768	81	6	15	3086	0.1	1423	29	3.1	655
-9.0	787	75	7	26	2720	0.1	1445	13	3.6	624
-9.0							1365		3.6	
-10.3	793	106	49	57	2685	0.3	1845	15	3.4	682
-11.6	799	78	17	21	2419	0.2	1536	14	3.3	684
-12.9	812				2501	0.1	1620	31	3.2	660
-12.9	815	86	16	39	2561		1596	31		
-14.2	803	88	13	23	2598	0.1		32	3.0	642
-14.2		86	13	22		0.1	1633			
-15.5	810	84	12	26	2871	0.1	1510			570
-16.8	819	77	11	24	2757	0.1	1467	31	2.6	570
-19.4	764	70	14	24	2794	0.1	1619	33	2.2	646
-19.4									2.2	
-21.9	740				2673	0.1	1792			
-21.9	739	67	6	17	2705					
-23.2								28	1.8	565
-24.5	701	67	6	17	2066	0.1	1442			
-24.5							1523			
-28.4	688	56	2	14	1424	0.1	1775	28	1.2	567
-28.4		57	2	26		0.0				
-33.5	693	54	2	14	1391	0.1	2482	23	0.8	593
-37.4	699				1390	0.1	2173			
-37.4	687	67	5	21	1375					
-42.6	740	122	86	82	1694	0.6	3848	17	0.6	
-42.6							3963			553

Summer-Station 1

Depth (cm)	Mn μgL^{-1}	Ni μgL^{-1}	Cu μgL^{-1}	Zn μgL^{-1}	As μgL^{-1}	Pb μgL^{-1}	Fe μgL^{-1}	NO4 μmolL^{-1}	SO4 mmolL^{-1}	NH4 μmolL^{-1}
30.3	291	459	166	57	276	0.2	59			71
29.0	250	392				0.1	32	355		87
23.9			161	53	290	0.1				
22.6	276	428	159	47	281	0.6	44	392	3.3	
22.6	310	479	161	52	279					
17.4							32	349	3.3	89
17.4	272	420	159	48	284	0.2		364	3.5	
16.1										
14.8										
13.5	312	467	218	83	339	2.2		366	3.4	92
12.9										
12.3	288	448	162	48	285	0.2	43			
11.6										
11.0	296	447	154	46	278	0.2	32			
10.3										
9.7	270	426	162	49	288	0.2	36	352	3.4	93
8.4	305	472	169	49	287	0.2				
7.7	303	451	161	50	290		34			
7.7	322	463	159	47	275	0.2				
7.1	355	581	166	49	289	0.2	33			
6.5							32			
6.5	337	589	157	47	276	0.2				
5.8	355	602	165	49	281	0.2	32	365	3.4	97
5.2	329	489	163	49	283	1.6	43			
4.5	297	450	157	49	279	0.2	50			83
3.9	295	439	163	49	291	0.2	34			85
3.9	305	460	166	48	288					
3.2	279	412	162	49	294	0.4	93	389	3.4	95
2.6	364	514				0.8				97
2.6			170	50	279	0.8	87			
1.9	356	510	189	52	325	0.5	135	560	3.4	87
1.3	307	431	167	53	299	0.2	39			84
0.6	297	414	163	60	295	0.2	41	421	3.4	85
0.0	301	414	169	59	306	0.2	35	414	3.4	82
0.0								418	3.5	
-0.6	324	422	147	65	308	1.4	36	358	3.4	135
-1.3	397	511	152	80	344	0.6		321	3.4	190
-1.3	384	457	163	85	342					
-1.9	440	488	133	91	449	0.2	44	198	3.6	277
-2.6	443	394	129	113	494	0.2	40	115	3.6	355
-3.2	599	368	74	83	625	0.2		73	3.7	423
-3.9	637	304	67	77	610	0.2	79	34	3.7	459
-4.5	702	169	18	30	844	0.2	694	21	3.7	488
-5.2	712	176	16	36	942	5.4	541	29	3.7	542
-5.2									3.8	
-5.8	838	126	7	20	1469	0.3		18	3.7	580
-7.1	861	102	6	21	1731	0.2	1799	18	3.7	600
-7.1	861	105	7	20	1683		1726			
-8.4	890	88	7	40	1858	1.4	1826	19	3.7	529
-8.4	984		5			0.3	1689	18	3.5	646
-9.7		76	5	16	1962	0.3				
-9.7	1115	127	63	107	1115	5.7		27	3.3	641
-11.0										
-11.0	1017	79	15	31	1679	1.1	1650	35	3.2	649
-12.3							1628		3.2	
-12.3	1085	76	6	17	1415	0.3	1432	65	3.0	620
-13.5	1012	76	5	18	1415	0.3	1370	59	2.4	601
-14.8	1101	73	4	17	1381	0.2	1394	67	2.7	528
-16.1										
-16.1										626
-17.4										
-18.7	1106	77	4	18	1362	0.2	1311	71	2.4	558
-20.0								71		
-22.6	959				1835		1151	82	1.8	489
-23.9	1038	84	4	18	1742	0.3				
-27.7	987	60	4	14	1066	0.2	1499	80	1.4	545
-29.0									1.4	
-32.9							2092	73	1.1	510
-34.2	844	66	3	15	1096	0.3				
-38.1	975		5		1265	0.4	2615	68	0.9	505
-39.3		48	2	14		0.4				
-41.9		71	2	15		0.4	2437	68	0.9	503

Appendix C cont.

Fall-Station 2

Depth (cm)	Mn $\mu\text{g L}^{-1}$	Ni $\mu\text{g L}^{-1}$	Cu $\mu\text{g L}^{-1}$	Zn $\mu\text{g L}^{-1}$	As $\mu\text{g L}^{-1}$	Pb $\mu\text{g L}^{-1}$	Fe $\mu\text{g L}^{-1}$	NO3 $\mu\text{mol L}^{-1}$	SO4 mmol L^{-1}	NH4 $\mu\text{mol L}^{-1}$
30.3	205	285	106	55	202	0.3	102	304	3.6	58
18.7	200	288	106	45.8	209	0.2	90	301	3.7	62
18.7	202	289	107	45.2	212	0.2				
13.5	206	285	106	55.2	203	0.4	90	302	3.6	64
12.3										
11.0										
9.7	201	271	100	40.5	211	0.2	95	289	3.6	62
5.8	202	263	97	41.1	201	0.4	102	289	3.5	62
5.2										
4.5	205	271	100	43.5	195	0.3	109	268	3.2	62
4.5								275	3.2	
3.9										
3.2	201	272	100	42.3	206	0.3		293	3.6	63
2.6							86	285	3.4	63
1.9	198	281	105	44.6	205	0.3	93	291	3.6	60
1.3	196				194		103	295	3.6	61
0.6	203	285	107	49.7	215	0.6	100	292	3.6	60
0.0	215	265	98	52.7	222	0.5	93	294	3.6	62
0.0								288	3.5	
-0.6	217	256	92.5	53.7	233	0.9	112	287	3.5	57
-0.6		258	92.1	54.3		0.8				
-1.3	474	203	24.4	123.5	561	0.6	63	292	3.5	52
-1.9	426	216	29.9	131	565	1	103			
-2.6	508	156	27.1	101	745	0.6	75	162	3.0	85
-3.2	445	166	28	130	591	1.1	105	128	2.9	95
-3.9	517	144	30.2	84.5	714	0.8	91	39	2.6	139
-4.5	439	109	20.2	47.8	859	1.2	186	53	2.5	140
-4.5								2.6		
-5.2	594	122	31.5	67.2	1302	3	476	19	2.2	166
-5.8	632	98.2	16.6	38.5	1712	1.7	579	20	2.1	170
-5.8								20		
-6.5	754	128	28.2	76.1	1769	1.1	224	35	1.9	185
-6.5	745				1763					
-7.1	736	79.8	18.6	28.9	2183	2.5	959	20	1.9	204
-7.7	681	113	27.2	67	1689	2.1	404	23	1.7	225
-8.4	822	75.9	16.3	24.1	2202	2	986	25	1.8	220
-8.4	822				2153			1.8		
-9.0	689	101	19.7	42.3	1735	2.2	460	21	1.6	259
-9.7	775	67	10.2	26.6	2098	2.3	1237	29	1.7	262
-9.7								28		
-11.0	815	90.9	17.6	54.7	2250	1.1	662	18	1.6	332
-11.0		92.6	17.7	48.5		1.1				
-12.3	823	67.4	10.3	23.4	2364	1	931	16	1.5	364
-12.3	822				2410					
-13.5	832	58.4	9.6	21.7	2646	0.6	946	16	1.4	384
-14.8	791	64.5	24.7	32.8	2255	0.6	810	2	1.2	406
-14.8		69	26	33.7		0.7				
-16.1	759	82	38	56	2066	0.8	645	1	1.1	418
-17.4	697	110	28.6	97.5	1946	0.8	427	4	1.1	436
-17.4	690				1938			4		
-20.0	741	61.5	18.3	39.3	1983	1.1	632	2	0.9	458
-23.9	876	58.2	13	37	2848	1.1	1010	2	0.7	502
-23.9		60.2	13	34.2		1.1				
-27.7	943	32.3	3.8	13.5	2791	1.2	2108	2	0.6	513
-27.7	947				2840					
-32.9	957	34.5	4.6	14.5	2781	1.4	2455	13	0.6	491
-32.9									0.6	
-39.3	958	64.7	7.2	26.6	2797	0.8	2495	14	0.5	497
-45.8	999	51	7.4	29	3257	1.8	3009	8	0.3	
-45.8							2997	8	0.3	507

Fall-Station 2

Depth (cm)	Mn $\mu\text{g L}^{-1}$	Ni $\mu\text{g L}^{-1}$	Cu $\mu\text{g L}^{-1}$	Zn $\mu\text{g L}^{-1}$	As $\mu\text{g L}^{-1}$	Pb $\mu\text{g L}^{-1}$	Fe $\mu\text{g L}^{-1}$	NO3 $\mu\text{mol L}^{-1}$	SO4 mmol L^{-1}	NH4 $\mu\text{mol L}^{-1}$
30.3	202			65	238		92.4	311	3.5	67
18.7	206	295	116	56	235	0.4	94.9	312	3.6	66
18.7	198	290	117	71	238	0.4	93.7			
9.7	196	284	109	51	230	0.3	97.3	302	3.4	67
5.8	191	283	112	50	226	0.3	94.6	304	3.5	66
3.2	191	296	114	51	229	0.3	84.4	300	3.3	64
2.6	200	285	109	54	229	0.3	92.2	309	3.4	65
2.6								310	3.4	
1.9	207	289	111	55	240	0.3	91			63
1.3	223	308	109	80	239	0.3	78.9	310	3.4	60
0.6		280	106	56		0.4	106.9	313	3.4	62
0.6	198	274	107	55	218	0.4				
0.0								331	3.4	45
-0.6	416	326	63	203	320	0.5	50.7	335	3.6	34
-0.6							47.6			
-1.3	431	302	44	217	353	0.5	57.1	258	3.3	78
-1.3							50.3	255	3.2	
-1.9	459	223	49	170	546	0.5	42.2	230	2.9	79
-1.9	448				518					
-2.6	451	198	43	238	578	0.5	39.4	155	2.4	135
-3.2	398	135	38	77	767	0.6	51.9	126	2.5	142
-3.2		134	37	77		0.6				
-3.9	354	122	26	90	747	0.5	41.6	70	2.1	174
-4.5	376	106	29	48	1005	0.8	62.1	56	2.1	158
-5.2	319	84	19	37	975	1.1	92.5	27	1.9	185
-5.2								27	1.9	
-5.8	389	84	17	34	1197	0.7	67.4	25	1.9	181
-6.5		46	13	5	1595	0.1		18	1.7	213
-7.1	426	70	20	25	1768	0.9	119.6	15	1.7	219
-7.1	416				1757					
-7.7	502	55	15	20	2222	2.3	216.5	22	1.6	254
-7.7							212.1			
-8.4	543	62	17	29	1988	1	121.8	19	1.6	244
-8.4							123.9			
-9.0										
-9.7	648	97	29	63	2048	1.7	447.9	21	1.5	287
-9.7							423	20	1.5	
-11.0	629	98	80	63	1903	1.4	337.5	20	1.5	346
-11.0	612	100	81	64	1900	1.4				
-12.3	609	91	38	59	1950	1.3	421.2	16	1.4	356
-12.3		89	37	58		1.3				
-13.5								13	1.3	382
-14.8								6	1.1	421
-14.8				52		0.3				
-16.1	687	83	21	63	1941	1.1	453.9	6	1.1	445
-16.1	671	84	20	61	1893	1				
-17.4								7	0.8	463
-17.4								7	0.8	
-18.7										
-20.0	695	47	16	28	1912	0.9	650.7	11	0.9	489
-21.3										
-22.6										
-23.9	756	42	8	28	3287	0.8	919.2	8	0.7	537
-27.7	793	39	8	22	2049	1.7	1301	17	0.6	526
-32.9	830	23	1	10	2164	0.8	2417	14	0.5	547
-32.9	839	24	2.3	9	1749	0.9	3504	15	0.5	533
-39.3	823	24	2.5	11.5	1730	0.9			0.5	
-45.8	934	34	4	15	4082	1.8	3780	10	0.3	581
-45.8							3934	11	0.3	

Appendix C cont.

Fall-Station 1

Depth (cm)	Mn $\mu\text{g L}^{-1}$	Ni $\mu\text{g L}^{-1}$	Cu $\mu\text{g L}^{-1}$	Zn $\mu\text{g L}^{-1}$	As $\mu\text{g L}^{-1}$	Pb $\mu\text{g L}^{-1}$	Fe $\mu\text{g L}^{-1}$	NO3 $\mu\text{mol L}^{-1}$	SO4 mmol L^{-1}	NH4 $\mu\text{mol L}^{-1}$
33.5	240	280	117	85	214	0.17	119	357	3.8	63
21.9	203	284	121	46	214	0.48	93.7	352	3.7	63
21.9	207	288	122	46	218	0.53	92.8	350	3.7	
12.9	208	282	120	49	218	0.17	90.5	351	3.7	64
9.0	209	287	121	51	218	0.17	90.3	349	3.8	64
8.4										
7.7	204	274	117	44	216	0.23	94.8	350	3.8	63
7.1										
6.5	202	283	118	48	212	0.18	95.2	354	3.8	63
6.5							97			
5.8	251	339	136	55	264	0.18	99.8	355	3.8	62
5.2	204	282	117	46	211	0.17	96.2	355	3.7	59
5.2								349	3.7	
4.5	205	290	120	58	212	0.11	88.4	350	3.6	66
3.9	206				211		86.4	349	3.7	64
3.9	202	269	113	52	211	0.2				
3.2	207	281	119	56	205	0.2	91.7	357	3.7	65
2.6	213	286	118	64	214	0.17	91	355	3.7	65
1.9	210	283	116	62	205	0.26	94.5	353	3.7	64
1.3	207	280	118	57	212	0.16	94.9	358	3.8	63
1.3	210	286	118	56	215	0.16	93.3	350	3.7	
0.6	205	295	118	60	209	0.31	120.4	348	3.7	57
0.0	214	291	114	63	208	0.17	88.4	354	3.8	65
-0.6	221	297	111	71	204	0.17	86.9	330	3.7	56
-1.3	466	529	60	277	190	0.19	37.6	234	3.7	130
-1.3							0.2			
-1.9	431	463	57	265	195	0.26	34.4	147	3.3	126
-2.6	477	366	45	133	287	0.25	35.1	95	3.8	193
-2.6									3.7	
-3.2	482	370	39	121	327	0.37	45	70	2.9	173
-3.2								43.2	70	
-3.9	439	292	41	88	392	0.27	34.3	25	2.9	207
-3.9	439	288	42	89	383	0.3				
-4.5	465	267	29	62	431	0.41	37.96	30	2.7	232
-4.5								30		
-5.2	509	235	31	50	430	0.42	45.4		2.7	226
-5.8	523	232	25	40	476	0.53	40.1	19	2.5	275
-6.5	622	211	38	68	477	0.38	54.8	16	2.7	271
-6.5									2.6	
-7.7	536	242	42	84	676	0.36	38.9	13	2.4	290
-7.7	537	251	42	84	685	0.33	34.1			
-9.0	570	236	28	74	712	0.48	45.9	46	2.3	279
-10.3	505	223	36	83	686	0.4	51.3	23	2.1	290
-10.3								23		
-11.6	627	181	19	62	834	0.34	62.3	11	2.0	314
-12.9	617	179	33	81	894	0.24	70.44	8	2.0	329
-12.9							69.28			
-14.2	597	185	30	83	852	0.31	74.24	8	1.9	354
-14.2	590	177	29	76	845	0.24			1.8	
-15.5										
-16.8	561	164	42	78	811	0.4	93.24	19	1.9	388
-18.1										
-19.4										
-20.6	513	207	47	93	710	0.36	45.9	10	1.5	430
-20.6							46			
-24.5	564	90	27	42	829	0.58	152.8	10	1.4	404
-24.5	570	94	28	42	830	0.66	145.3	11		
-29.7	714	38	12	14	801	0.65	494.4	10	1.1	408
-29.7							530			
-36.1	680	32	5.8	10	775	0.31	803.1	11	0.8	398
-42.6	722	36	29	19	813	0.94	969	7	0.6	365
-42.6	719	36	29	17	816	1	1002	7	0.6	

Fall-Station 5

Depth (cm)	Mn $\mu\text{g L}^{-1}$	Ni $\mu\text{g L}^{-1}$	Cu $\mu\text{g L}^{-1}$	Zn $\mu\text{g L}^{-1}$	As $\mu\text{g L}^{-1}$	Pb $\mu\text{g L}^{-1}$	Fe $\mu\text{g L}^{-1}$	NO3 $\mu\text{mol L}^{-1}$	SO4 mmol L^{-1}	NH4 $\mu\text{mol L}^{-1}$
36.1	196	292	118	189	213	1.3	502	313	3.7	63
24.5	184	294	109	188	204	0.3	120	326	3.7	65
24.5	179	279	104	181	209	0.3				
19.4	188	296	110	89.7	215	0.3	98	313	3.7	67
15.5	192	298	110	73.7	223	0.4	96	323	3.7	67
11.6	204	307	110	57.5	255	0.3	97	313	3.6	75
11.6		300	107	55.6		0.3				
7.7	235	309	96	80.3	338	0.3	110	319	4.4	94
7.7							104	319	4.4	
7.1										
6.5	264	324	100	91	382	0.3	108	318	4.7	105
6.5	257				370					
5.8	254	323	96	117	369	0.3	99	319	4.7	106
5.2	259	323	94	79.5	376	0.3	112	320	5.1	110
4.5	254	324	92	75	376	0.1	112	318	5.1	109
4.5							100			
3.9	250	323	93	72	371	0.2	121	317	5.0	111
3.9	252	327	94	71	376	0.2				
3.2	244	321	91	67	359	0.2	103	317	5.1	109
3.2								317	5.1	
2.6	256	324	92	65	365	0.2	97	317	5.2	110
1.9	260	321	91	70	348	0.2	98	320	5.0	112
1.3	253	305	82	60	306	0.2	102	313	5.1	114
1.3	256	304	83	62	312	0.2	104			
0.6	310	307	57	37	277	0.1	77	312	5.0	114
0.6							74			
0.0	352	199	43	42	234	0.3	74	309	4.8	92
-0.6	353	125	21	19	220	0.3	66	295	4.7	107
-0.6								300	4.8	
-1.3	577	78	14	26	406	0.7	142	159	3.1	38
-1.3							146			
-1.9	377	60	9.7	12	266	0.4	69	146	3.3	58
-1.9	376	60	9.7	12	272	0.4	68			
-2.6										
-3.2	771	75	11.5	18	428	0.5	96			
-3.9	383	69	11.2	42	375	0.6	100	9	2.3	39
-5.2	744	79	13	25	590	1	9	2.3	50	
-5.2	747				598					
-6.5	619	69	13	43	725	0.9	209	5	2.1	52
-7.7	1008	91	17	35	873	1.1	191	5	1.9	55
-7.7									2.0	
-9.0	1312	106	20	31	886	1.2	210	4	2.3	51
-9.0								4		
-10.3	1384	112	22	32	1265	1.2	227	4	2.7	68
-10.3							222			
-11.6	1470	120	25	35	1539	1.1	206	3	2.1	92
-11.6										
-12.9	729	102	18	29	1285	1.1		2	2.4	125
-14.2	967	124	18	34	1258	1.2	211	2	2.3	129
-15.5										
-16.8	1639	151	24	44	1388	1.4	264	2	2.4	158
-16.8	1745				1441		257		2.4	
-18.1										
-18.1										
-19.4	1468	133	18	36	1808	1.1	203	2	2.8	218
-19.4								2		
-24.5	1784	84	23	20	3041	1	221	1	2.6	243
-29.7	904	43	5	9	2862	0.9	219	2	2.3	207
-29.7									2.3	
-34.8	683	40	5	15	2498	1.8	485	2	2.2	199
-34.8							449			
-40.0										
-40.0								2	2.4	187
-40.0									2.4	

Appendix C cont.

Winter-Station 2

Depth (cm)	Mn $\mu\text{g/L}^{-1}$	Ni $\mu\text{g/L}^{-1}$	Cu $\mu\text{g/L}^{-1}$	Zn $\mu\text{g/L}^{-1}$	As $\mu\text{g/L}^{-1}$	Pb $\mu\text{g/L}^{-1}$	Fe $\mu\text{g/L}^{-1}$	NO3 $\mu\text{mol/L}$	SO4 mmol/L	NH4 $\mu\text{mol/L}$
27.7	487	432	95	187	194	0.6	66	249	6.9	288
27.7	486	439	97	190	193	0.6				
22.6	671	483	74	141	209	0.5	57	193	9.0	284
16.1	812	501	56	181	238	0.3	71			
16.1							74			
14.8								34	10.1	393
14.8										389
9.7	942	420	24	197	414	0.2	132	7	10.3	457
9.7							129			
8.4										
7.1							218			
7.1	954	410	21	198	488	0.1	220	5	10.5	449
6.5										
5.8	941	417	22	218	512	0.2	259	6	10.3	401
5.8	970	402	21	216	516	0.1	8	9.8		
5.2	937	402	20	224	488	0.1	270	10	10.5	413
4.5	977	399	21	212	553	0.3	306	10	10.2	393
4.5	969	408	22	219	551	0.3				
3.9	930	395	20	251	497	0.1	268	7	10.0	413
3.2	988	404	20	211	565	0.1	329	14	9.3	433
2.6	930	404	21	269	504	0.2	281			
2.6							285			
1.9	972	406	21	270	589	0.2	374	11	9.2	
1.3	965	400	21	280	535	0.2	311	9	9.5	429
1.3								9	9.5	
0.6	970	408	21	256	618	0.1	398	7	8.9	413
0.6	978	404	22	285	606	0.2				
0.0	978	399	23	275	530	0.4	337	10	9.1	393
-0.6	915	405	19	241	606	0	455	9	8.6	377
-0.6	926	403	19	245	622	0				
-1.3	961	469	19	257	468	0.2	234	8	8.1	393
-1.3							219			
-1.9	949	418	17	246	532	0.1	286			
-1.9							291			
-2.6								8	7.8	417
-2.6										425
-3.2	1044	446	17	243	536	0.05	217	23	4.5	401
-3.2								24	4.5	
-3.9										
-4.5	1117	365	16	223	580	0.06	163	8	3.9	433
-5.2										
-5.8	1125	293	15	180	647	0.1	158	8	3.1	461
-5.8	1083	298	15	181	630	0.1				
-6.5										
-7.1	1003	220	11	132	780	0.1	287	6	2.8	453
-7.7										
-8.4	1001	154	9.7	95	835	0.4	333			
-8.4		154	9.5	95		0.3				
-9.0										
-9.7	885	115	11	78	736	0.3	182	11	2.2	489
-12.3	731	68	19	54	610	0.2	63	13	1.7	481
-12.3							65			
-13.5	668	43	23	33	632	0.2	66			
-13.5							67			
-14.8								10	1.5	477
-14.8								9	1.5	
-16.1	656	37	28	38	703	0.2	72			
-17.4								12	1.1	485
-17.4										473
-18.7	590	43	26	52	594	0.2	43			
-18.7	560	42	25	52	557	0.2				
-21.3	608	43	35	42	613	0.2	40	9	0.8	481
-25.2										485
-26.4	649	40	25	32	579	0.4	337	6	0.7	
-26.4	667	46	13			1.6				
-31.6	641	43	24	41	363	0.7	204	9	0.6	501
-31.6							201			
-36.8	644	39	23	33	300	1.1	192	8	0.4	501
-36.8	643	39	23	33	295	1.1	193			
-41.9	573	36	31	143	272	0.3	75	7	0.3	493
-48.4	651	46	22	52	314	0.9	241	5	0.3	497
-48.4	653	46	21	50	323	0.9				

Winter-Station 1

Depth (cm)	Mn $\mu\text{g/L}^{-1}$	Ni $\mu\text{g/L}^{-1}$	Cu $\mu\text{g/L}^{-1}$	Zn $\mu\text{g/L}^{-1}$	As $\mu\text{g/L}^{-1}$	Pb $\mu\text{g/L}^{-1}$	Fe $\mu\text{g/L}^{-1}$	NO3 $\mu\text{mol/L}$	SO4 mmol/L	NH4 $\mu\text{mol/L}$
25.2	531	367	67	88	159	0.27	41	256	10.3	437
20.0	641	407	65	116	172	0.23	42	259	11.3	487
13.5	868	452	59	147	198	0.51	46			
13.5	843	422	50	149	204	0.14	40			
12.3								132	13.0	524
12.3										528
9.7	887	414	39	161	255	0.15	39	52	12.8	582
8.4										
7.1	910	425	41	164	266	0.14	42	46	12.6	578
5.8										
4.5	986	462	37	162	275	0.14	46	48	12.1	536
4.5								49	12.3	
3.9										
3.2	981	457	37	158	280	0.25	71	51	12.1	549
3.2	996	458	37	157	283	0.22	68			
2.6	891	422			260		49	35	10.4	528
1.9	967	425	34	156	271	0.17	60	46	11.6	549
1.3	938	444	41	169	268	0.15	45	33	10.4	520
0.6	981	408	34	153	268	0.13	65	37	10.8	528
0.0	947	441	39	154	260	0.14	44	31	10.4	520
0.0								31	10.1	
-0.6	1046	465	36	161	298	0.11	66	27	10.4	528
-0.6	1058	483	36	163	298	0.11	65			
-1.3	989	495	40	185	269	0.12	45	25	9.9	520
-1.9	1067	482	34	174	301	0.12	72	24	8.3	495
-2.6	1055	571	45	248	297	0.13	49			
-3.2	1073	466	36	200	295	0.12	81	21	7.5	499
-3.9	1024	447	49	223	278	0.12	53	19	8.9	528
-4.5	1090	421	35	174	297	0.17	87			
-4.5							83			
-5.2								19	8.2	536
-5.2								19	8.2	532
-5.8										495
-5.8	1143	342	28	136	297	0.17	115	14	6.3	
-6.5										
-7.1	1182	264	19	98	369	0.2	300	12	5.5	499
-7.7										
-8.4	1234	204	14	70	411	0.22	477	20	4.7	507
-8.4	1232	206	14	68	405	0.22	467			
-9.0										
-9.7	1258	176	10	59	394	0.13	502	15	4.2	503
-10.3										
-11.0	1342	136	9	45	385	0.4	532			
-11.6										
-12.3	1309	115	8	40	369	0.23	400	16	3.4	507
-14.8	1372	93	7	30	410	0.21	359	15	2.7	495
-14.8								16	2.7	
-16.1	1325	72	7.4	34	408	0.11	183			
-16.1							171			
-17.4								7	2.7	495
-18.7	1214	41	4	17	441	0.27	493			
-18.7	1215	42	4.2	20	450	0.31				
-20.0								7	1.6	483
-20.0										491
-21.3	789	31	5	22	401	0.11	134			
-21.3							126			
-23.9	776	24	2.9	13	387	0.63	666	30	1.1	491
-27.7								8	0.9	478
-29.0	718	25	1.9	12.5	365	0.43	683			
-34.2	739	24	2.4	9.8	476	0.58	1476	5	0.7	474
-34.2							1438			
-39.3	697	29	4	17	386	0.53	1017	2	0.5	445
-39.3								2		
-44.5	628	33	6.3	21	250	0.59	692	5	0.4	416
-44.5							655			
-51.0	718	33	4	16	491	491	2081	3	0.2	404
-51.0							2186			

Appendix C cont.

Winter-Station 4

Depth (cm)	Mn $\mu\text{g L}^{-1}$	Ni $\mu\text{g L}^{-1}$	Cu $\mu\text{g L}^{-1}$	Zn $\mu\text{g L}^{-1}$	As $\mu\text{g L}^{-1}$	Pb $\mu\text{g L}^{-1}$	Fe $\mu\text{g L}^{-1}$	NO3 $\mu\text{mol L}^{-1}$	SO4 mmol L^{-1}	NH4 $\mu\text{mol L}^{-1}$
25.2	356	491	290	97	368	0.4	176	477	4.6	130
20.0	371	450	256	94	354	0.3	141	424	4.7	118
20.0	372	443	255	96	353	0.3				
16.1	454	441	209	121	330	0.3	132	364	4.9	142
12.3	556	425	145	138	315	0.3	115	290	5.5	171
12.3								283		
9.7								229	5.9	200
9.7										200
8.4	897	320	43	141	302	0.1	67			
5.8	966	315	39	151	305	0.3	151	55	6.8	
5.8	963	281	35	144	299	0.3		55	6.8	286
4.5	956	316	38	147	287	0.1	76	31	7.0	291
3.9	998	299	39		298	0.3	128	24	6.6	291
3.2	967	304	36	152	317	0.1	80	24	6.8	295
3.2	974				316					
2.6	950	274	41	157	277	0.3	147		6.4	274
2.6							144			
1.9							75	33	6.7	291
1.3	959	275	39	161	274	0.2	124	21	6.7	286
1.3							22	6.6		
0.6	1023	304	36	151	308	0.1	74	27	7.2	291
0.6	1009	306	36	153	324	0.1				
0.0	972	291	36	167	282	0.2	125	20	6.8	291
-0.6	1028	353	40	159	342	0.2	78	21	6.9	291
-1.3	1005	331	36	181	339	0.3	151	20	6.8	291
-1.9	1047	343	36	147	357	0.2	71			
-2.6	987	356	33	168	405	0.4	153	23	6.7	307
-3.2	1024	336	31	123	409	0.2	75	17	6.7	295
-3.2	1021	338	31	124	416	0.2	65	17	6.5	
-3.9	989	338	43	181	489	1.3	141	21	6.7	295
-4.5							13	5.7	295	
-5.2	957	280	24	98	501	0.3	77	17		315
-5.8	1009	257	26	94	463	0.2	55	12	5.9	
-5.8	1017	255	26	94	459	0.1				303
-6.5										
-7.1	988	211	27	81	480	0.3	64	11	5.3	299
-7.7										
-8.4	978	146	27	66	472	0.3	71	31	5.1	311
-8.4	991	141	27	64	491	0.3		30		
-9.0										
-9.7	958	107	15	44	481	0.2	79	12	4.5	303
-10.3										
-11.0	992	104	11	41	480	0.2	77			
-12.3								13	3.2	303
-13.5	972	79	4	32	502	0.3	162			
-14.8								15	2.5	344
-16.1	940	50	2	29	524	0.4	125			
-17.4								27	1.9	303
-18.7	921	45	3	25	436	0.2	125			
-18.7		47	3.1	26		0.2				
-20.0										
-21.3	841	45	7.2	32	283	0.2	71	25	1.6	299
-25.2								21	1.4	282
-25.2									1.4	
-26.4	684	70	14	65	191	0.2	64			
-30.3								3	1.0	254
-30.3										278
-31.6	729	53	7.2	43	211	0.2	80			
-31.6	726	55	7.5	45	206	0.2				
-35.5								4	0.8	237
-36.8	623	45	12	46	235	0.1	52			
-41.9	741	25	6.8	19	294	0.5	597			
-41.9							615			
-43.2								4	0.6	196
-47.1	705	26	7.1	20	134	0.5	436			
-47.1	696	26	7	19	131	0.5				
-51.0								4	0.4	155
-52.2	712	112	7.2	64	244	0.7	471			
-52.2	715	110	6.8	57	249	1.3				

Winter-Station 6

Depth (cm)	Mn $\mu\text{g L}^{-1}$	Ni $\mu\text{g L}^{-1}$	Cu $\mu\text{g L}^{-1}$	Zn $\mu\text{g L}^{-1}$	As $\mu\text{g L}^{-1}$	Pb $\mu\text{g L}^{-1}$	Fe $\mu\text{g L}^{-1}$	NO3 $\mu\text{mol L}^{-1}$	SO4 mmol L^{-1}	NH4 $\mu\text{mol L}^{-1}$
26.4	317	410	185	125	325	0.6	129	436	4.1	98
21.3	287	365	148	81	387	0.5	90	432	4.0	94
20.0										
18.7	325	418	185	85	382	0.5				
18.7	315	408	179	80	355	0.5				
17.4								473	4.8	98
14.8	313	414	182	83	375	0.5	112			
13.5								427	4.0	94
11.0	314	410	185	86	379	0.4	112			
11.0	284	376	163	81	365	0.5	112			
9.7								454	4.4	98
9.7										94
8.4	313	410	178	89	408	0.4	108			
7.1								439	4.1	90
7.1								434	4.2	
5.8	302	397	164	94	465	0.4	101	440	4.2	90
5.2	311	409	168	91	435	0.5		435	4.4	82
4.5	317	419	156	104	552	0.6	93	459	4.5	86
4.5	310	404	157	98	540	0.5	94			
3.9	332	435	170	94	458	0.5		463	4.5	78
3.2	314	415	157	112	612	0.5	99			42
2.6								453	4.4	66
2.6								457	4.2	
1.9	314	419	157	145	695	0.4	87	457	4.3	70
1.9	318	419	162	137	696	0.4				
1.3	321	426	163	114	545	0.6		465	4.5	58
0.6	311	409	162	118	732	0.5	91	475	4.4	54
0.0	314	413	154	122	613	1	90	464	4.4	50
-0.6	327	421	158	131	879	0.5	84			
-0.6	298	431	172	135	578	0.7	85			
-1.3	321	407	149	116	721	0.6		440	4.4	50
-1.9	324	409	157	144	952	0.4	83	426	3.9	46
-2.6	334	378	135	111	839	0.4	97	417	3.7	50
-3.2	324	422	148	126	1085	0.4	86	405	4.1	50
-3.2							151	128	0.4	84
-3.9	334	355	126	101	998	0.7	132	385	4.2	62
-4.5	327	376	138	186	1334	0.6	123	379	4.0	58
-5.2	343	341	126	147	1158	0.7	134			
-5.8	325	348	130	124	1468	0.6	84	312	3.6	66
-5.8							129	124	0.6	84
-6.5	378	313	97	82	1350	1	141			
-7.1	324	311	101	114	1714	0.6	75	221	3.3	86
-7.1								221	3.3	
-8.4	302	253	72	84	1974	1		236	4.0	82
-9.0										
-9.7	282	211	56	70	2264	1	81			
-11.0								191	3.6	98
-12.3	198	120	25	36	3028	0.7	60			
-13.5								108	3.1	113
-14.8	186	108	23	19	3507	1	88			
-14.8	155	103	26	19	3237		89			
-16.1								66	2.4	125
-16.1										129
-17.4	126	76	17	15	4875	1	158			
-18.7										
-20.0	95	61	14	7	6034	1	317	32	2.1	141
-23.9								20	1.9	149
-23.9								20	1.9	
-25.2	50	18	4	4	8536	0.5	127			
-25.2	50	18	4	3	8483	0.6	129			
-29.0								24	1.8	153
-29.0										161
-30.3	45	14	4	3	9314	0.5	108			
-34.2								7	1.9	165
-35.5	39	10	3	6	10160	0.3	101			
-40.6	36	10	3	2	10428	0.3	112			
-41.9								2	1.9	161
-45.8	36	12	4	2	11813	0.3	129			
-45.8					11478					
-49.7								5	2.1	173
-51.0	35	13	4	3	13909	0.6	216			

Appendix C cont.

Winter-Core 1

Depth (cm)	Mn μgL^{-1}	Ni μgL^{-1}	Cu μgL^{-1}	Zn μgL^{-1}	As μgL^{-1}	Pb μgL^{-1}	Fe μgL^{-1}	NO3 μmolL^{-1}	SO4 mmolL^{-1}
1.0	570	456	107	142	223	1.5	83	267	10.6
1.0	583	458	104	135	223	1.5	82	278	11.2
1.0							86		
-0.3	740	491	67	126	345	0.3	50	58	12.0
-1.3	839	621	25	122	419	0.1	31	6	11.0
-1.3	863	634	25	126	434	0.1			
-1.8	874	617	20	179	446	0.4	56	14	11.1
-1.8							57		
-2.5	1062	288	66	54	438	0.6	76	2	10.7
-2.5	1057	283	69	56	448	0.6		3	10.9
-3.5	986	121	12	23	1021	0.5	104	3	8.2
-4.5	1017	42	1.3	45	1343	0.1	387	7	7.6
-4.5							408		
-5.5	1033	13	1.3	4.6	1020	0.03	461	2	7.6
-5.5	1023	12	2	8.6	1035	0.08			
-7.0	990	9.4	1.1	3.3	709	0.05	252	2	6.0
-7.0								3	6.0
-9.0	989	6.6	1.1	3.8	533	0.02	222	2	5.8
-11.0	943	6.3	1.1	4.8	434	0.02	221	3	4.7
-11.0								2	4.6
-13.0	848	7	1	16	688	0.07	116	2	4.0
-13.0	873	6.5	0.8	12	685	0.02	116		
-15.5	848	4.8	0.6	6.9	423	0.02	436	3	3.2
-18.5	743	4.5	0.8	323	320	0.2	794	3	2.6
-18.5	737	4.5	0.9	318	321	0.2			2.5
-24.5	682	3.4	0.6	26	83	0.08	2411	2	1.1
-24.5							2469		
-30.5	650	2.9	0.6	20	17	0.2	3074	6	0.5
-30.5	743				17		2963	6	0.5

Winter-Core 2

Depth (cm)	Mn μgL^{-1}	Ni μgL^{-1}	Cu μgL^{-1}	Zn μgL^{-1}	As μgL^{-1}	Pb μgL^{-1}	Fe μgL^{-1}	NO3 μmolL^{-1}	SO4 mmolL^{-1}
1.0	755	561	129	145	234	1	102	272	10.3
1.0	692	561	163	141	237	1.4	104	308	8.9
-0.3	1083	663	71	129	386	0.4	44	54	12.5
-0.8	1020	676	68	142	374	0.4	44	19	12.3
-0.8	1071	694	70	154	383	0.4			
-1.3	1041	694	51	173	400	0.5	47	12	10.9
-1.3							49	11	
-1.8	1096	686	40	114	434	0.6	53	6	11.3
-1.8	1139	744	40	114	445	0.6			11.2
-2.5	1354	586	35	74	472	0.8	60	7	10.2
-2.5								7	
-3.5	1348	167	22	28	740	0.3	90	3	8.7
-3.5							91	3	
-4.5	1365	44	5	7.9	1020	0.2	469	3	8.1
-4.5									6.7
-5.5	1284	13	4	7.7	735	0.2	460	12	7.1
-7.0	1319	6	4	3.9	483	0.2	440	1	6.5
-7.0	1401	6	3.6	3.9	505	0.2			1
-9.0	1346	5	4	4.4	358	0.3	324	2	5.2
-9.0							331		5.3
-11.0	1216	8	5.5	4.1	309	0.2	291	1	4.9
-13.0	1103	4	3.5	4.1	268	0.2	316	1	3.9
-13.0	1039	6	4.8	4.2	254	0.2			
-15.5	897	4	3.9	3.9	271	0.2	390	1	3.1
-15.5							408		
-18.5	897	4	3.6	4	207	0.2	837	3	2.2
-18.5								3	
-24.5	722	2.7	4.4	5.4	44	0.3	2197	5	0.9
-24.5	735	3	4.6	5.7	44	0.3		5	
-30.5	897	3.3	4.2	4.3	9	0.3	3094	4	0.4
-30.5							3121	4	0.4

Appendix C cont.

Winter-Core 3

Depth (cm)	Mn μgL^{-1}	Ni μgL^{-1}	Cu μgL^{-1}	Zn μgL^{-1}	As μgL^{-1}	Pb μgL^{-1}	Fe μgL^{-1}	NO3 μmolL^{-1}	SO4 mmolL^{-1}
1.0	193	243	6	9	1888	0.5	56	340	4.5
1.0	190	252	3	7	1878	0.4	46	418	4.7
-0.3	281	321	95	37	2658	0.7	45		
-0.8	397	516	295	147	776	0.9	105	467	4.4
-0.8									
-1.3	364	395	147	88	1815	0.5	57	421	4.3
-1.3							55		
-1.8	264	300	47	23	3291	0.5	24		4.4
-1.8	259	301	46	25	3263	0.5			
-2.5	420	502	65	114	2151	1	83	365	4.1
-3.5	457	457	66	96	1289	0.8	80	318	3.9
-3.5	456	452	65	94	1290	0.9			
-4.5	451	276	41	49	1365	0.5	45	230	
-4.5								229	
-5.5	308	100	21	17	1780	0.4	31	124	3.4
-5.5							30	126	3.0
-7.0	186	54	11	8	2202	0.4	40	42	
-7.0	183				2212				
-9.0	72	13	2	73	5017	0.3	74	15	1.1
-9.0								13	2.8
-11.0	33	8.2	1	22	7553	0.3	82	21	2.8
-11.0							81		2.7
-13.0	32	6.9	1	4	7933	0.3	86	24	2.7
-15.5	32	6.3	0	2	9424	0.2	108	28	2.6
-15.5							27		
-18.5	27	5.1	1	2	9928	0.1	131	30	2.7
-18.5	27	4.9	1	3	10491	0.1			
-21.5					10142		118	25	2.7
-21.5	30	5.9	1	2		0.4			
-24.5	37	6.1	1	3	11649	0.4	109	28	
-24.5	35	5.9	1	2	11303	0.5	106		

Spring-Stallon 1

Depth (cm)	Fe μgL^{-1}	Mn μgL^{-1}	Ni μgL^{-1}	Cu μgL^{-1}	Zn μgL^{-1}	As μgL^{-1}	Pb μgL^{-1}	NO3 μmolL^{-1}	SO4 mmolL^{-1}	NH4 μmolL^{-1}
31.5	82	290	409	266	61	224	1.7	265	3.5	187
31.5	78									
26.4	77	295	405	259	57	233	1.8	263	3.5	185
19.9	82	290	397	247	59	228	1.5			
19.9		295	415	260	60	233	1.4			
18.6								269	3.6	191
18.6										187
13.5	75	301	401	241	60	231	1.3	262	3.6	185
12.2										
10.9	72	288	400	240	60	229	1.1			
10.9	72	290	403	243	60	227	1.1			
9.6								259	3.5	185
9.6								261	3.5	
8.3	73	287	401	236	61	226	1.1			
7.0								265	3.6	
5.7	72	288	415	246		222	0.96	256	3.4	189
4.5	73	291	400	238	61	222	0.97	260	3.4	185
3.8	80	302	401	239	63	230	0.12	255	3.5	187
3.2	68	307	400	237	63	233	1.3	268	3.6	185
2.5	82	302	404	238	64	228	1.3	259	3.4	191
1.9	68	303	407	241	63	227	1.1	260	3.6	185
1.9	70									
1.2	82	305	426	254	70	236	1.7	262	3.6	185
1.2								264	3.6	189
0.6	74	299	417	249		232	1.2	259	3.5	178
0.6		300	411	246	69	230	1.2			
-0.1	84	310	420	249	70	244	1.5	267	3.5	178
-0.7	74	309	415	242	69	237	1.5			178
-0.7		306	424	249	70	233	1.4			
-1.4		305	399	240	86	251	2.2	283	3.7	180
-2.0	91	312	409	236	78	241	1.1	268	3.7	185
-2.0		314	420	241	89	238	1.1	272	3.7	
-2.6	104	432	420	219	88	284	1.7	262	3.9	193
-3.3	85	415	421	220	97	260	1.3	175	4.2	230
-3.9	88	505	426	156	95	435	1.9	148	4.7	277
-4.6	79	528	446	150	111	424	1.6	118	5.0	331
-4.6	77									
-5.2	70	724	426	85	93	657	0.89			
-5.9	52	830	474	66	114	701	1.1	65	5.7	410
-5.9									5.7	
-7.2	54	966	444	42	129	877	1.4	30	5.9	453
-8.5	59	963	360	29	120	1022	1.2	20	6.0	485
-9.7	185	1094	203	14	61	1747	1.6	8	5.9	503
-9.7	189	1071	204	15	61	1743	1.5			
-11.0	277	1104	107	10	28	2090	0.75	10	5.5	511
-12.3	133	1067	128	21	42	1769	1.6	7	4.7	
-12.3	127									511
-14.9	366	1015	107	7.2	26	2316	0.87	8	3.9	
-14.9	366								4.0	503
-16.2										
-17.5	201	972	136	24	56	2001	3.3	2	3.4	515
-17.5		967	134	23	46	1995	3.2			
-20.1								11	2.9	511
-21.4	146	887	98	25	44	1532	2.7			
-21.4		913	89	14	21		1.7			
-22.6								9	2.6	498
-23.9										
-25.2								3	2.4	505
-25.2										498
-26.5	111	762	109	54	68	706	3.4			
-26.5	112									
-29.1								9	1.8	466
-29.1								9		
-31.7	175	785	90	31	55	637	2.2			
-34.3								11	1.3	440
-34.3									1.3	
-36.8	169	731	101	31	65	298	2.6			
-36.8		714	100	30	63	282	2.2			
-39.4								9	1.1	412
-42.0	239	800	124	30	93	298	2.7			
-42.0	238									
-44.6								4	1.1	397
-45.9	89	513	191	56	117	889	1.2			
-45.9		501	192	57	112	879	1.2			

Appendix C cont.

Spring-Station 1

Depth (cm)	Mn μg/L ⁻¹	Ni μg/L ⁻¹	Cu μg/L ⁻¹	Zn μg/L ⁻¹	As μg/L ⁻¹	Pb μg/L ⁻¹	Fe μg/L ⁻¹	pH	Depth (cm)	NO3 μmol/L	SO4 mmol/L	NH4 μmol/L
31.8	277	360	198	100	199	0.7	74		39.3	260	3.6	188
30.7								7.61	34.7	254	3.5	190
27.2	274	355	194	56	203	0.5	72		28.9	254	3.6	188
27.2	272	363	197	58	207	0.5			23.1	239	3.2	
26.0								7.77	23.1			185
21.4	272	335	180	53	200	0.4	74		17.3			181
21.4							76		15.0	254	3.5	185
20.3								7.81	14.4			
15.6	276	335	186		201	0.8	72		13.9	253	3.5	183
15.6	272	352	196	62	211	0.6			13.9	247	3.5	
14.5								7.80	13.3			
9.9	278	380	204	60	213	0.7	74		12.7	245	3.5	185
8.7								7.70	12.1			
4.7								7.78	11.6	252	3.6	185
4.1	280	363	199	64	215	0.8	72	7.95	11.0	248	3.5	185
3.5									10.4	253	3.5	188
2.9								8.02	9.8	251	3.6	185
1.8	275	352	200	66	203	0.9	69	7.99	9.8	243	3.5	
1.2									9.2	251	3.6	183
0.6	275	360	197	74	192	0.9	69	8.00	8.7	249	3.6	181
0.0									8.1	253	3.6	181
-0.5								7.80	7.5	250	3.6	179
-1.7	278	345	194	69	201	1	76		6.9	286	3.6	183
-2.3									6.4	253	3.6	179
-2.8	346	364	184	85	216	1	82		6.4	252	3.6	
-3.4								7.80	5.8	280	3.6	183
-4.0	401	396	173	85	262	0.9	79		5.2	251	3.5	177
-4.0							79		4.6	247	3.5	177
-5.2	402	373	173	77	266	1	83		4.0			
-5.2	409	379	176	87	277	1			3.5	244	3.5	173
-6.3	596	369	132	89	349	1	64	7.70	3.5			
-6.3									2.3	255	3.7	188
-7.5	747	339	97	81	448	0.8	50		2.3			
-7.5							47		1.2	265	3.8	192
-8.6	858	259	53	66	637	0.6	46	7.54	1.2	260	3.8	
-9.8	842	209	44	61	765	1.3	70		0.0	267	3.7	198
-9.8	834	209	44	62	747	0.14	70		0.0			
-10.9								7.53	-1.2			
-12.1	792	180	47	75	742	1.4	83		-2.3	186	4.7	296
-13.2	776	142	42	60	746	1.5	65	7.57	-2.3			
-14.4	792	112	27	40	916	0.9	74	7.54	-3.5			
-14.4	816	112	27	39	914	0.8			-4.6	57	5.9	437
-15.6	735	114	26	63	812	1.3	80		-5.8			
-15.6							75		-6.9			
-16.7	720	109	23	57	848	1.4	93		-6.9			
-17.9	755	96	19	55	939	1.3	92	7.46	-8.1	12		520
-19.0									-8.1			
-20.2	762	92	13	35	900	1	144	7.57	-9.2			
-20.2	767	93	13	37	917	0.9	138		-10.4			
-21.3								7.35	-11.6	5	5.2	529
-22.5	747	75	11	34	664	0.7	188		-12.7			
-22.5									-12.7			
-23.6								7.56	-13.9			
-24.8	699	67	6.3	42	562	1	311		-15.0	19	2.9	488
-26.0								7.41	-15.0		3.0	
-29.4	662	64	5.2	33	402	1.1	513		-16.2			
-30.6								7.32	-17.3			
-31.7									-19.6	23	2.0	458
-32.9	651	57	1.7	18	451	0.3	834		-24.3	78	1.4	392
-32.9	662	54	1.7	22	457	0.3	829		-28.9	17	1.4	439
-37.5	682	67	7.5	19	738	0.5	925	7.56	-28.9		1.4	

Appendix D. Sediment Data

Compositional sediment data arranged by sample depth for each core. Major elements, CaCO₃, Organic C and N are in wt.%; minor elements are in ppm.

Depth (cm)	CaCO ₃ (wt.%)	C _{org} (wt.%)	N (wt.%)	Si (wt.%)	Ti (wt.%)	Al (wt.%)	Fe (wt.%)	Ca (wt.%)	Mg (wt.%)	Na (wt.%)	K (wt.%)	P (wt.%)	S (wt.%)	As (ppm)
Core 1														
Station 1														
0.25	0.65	5.80	1.015	48.14	0.56	11.67	8.77	4.15	3.57	1.16	1.96	0.22	0.32	
0.75	0.96	6.85	1.595							0.75			0.43	
1.25	1.25	3.41	0.859	48.44	0.59	11.26	10.54	5.08	4.71	0.72	1.63	0.16	0.26	
1.75	0.98	2.28	0.739	50.19	0.63	13.05	11.87	5.05	4.95	0.60	1.63	0.15	0.28	4744
2.50	0.92	1.45	0.360	50.45	0.65	13.93	11.63	5.15	5.06	0.49	1.67	0.16	0.39	5029
3.50	0.82	2.97	0.630	48.54	0.58	13.28	10.77	4.45	4.47	0.58	1.73	0.19	1.20	4677
4.50	0.85	3.08	0.567	49.47	0.59	13.59	10.83	4.64	4.57	0.64	1.85	0.15	1.19	4450
5.50	0.49	4.29	0.730	48.89	0.56	13.65	10.16	3.84	3.81	0.76	1.87	0.17	1.43	4053
7.00	0.04	8.78	0.860	55.37	0.55	12.48	5.98	3.14	2.01	1.28	2.23	0.25	0.93	1272
9.00	0.01	8.84	0.787	46.79	0.51	9.80	5.09	2.84	1.59	1.37	2.02	0.22	0.57	318
11.00	0.00	8.64	0.755	55.96	0.54	12.34	4.30	2.94	1.84	1.41	2.15	0.26	0.47	173
13.00	0.00	8.59	0.740	53.40	0.54	11.56	4.27	2.88	1.77	1.42	2.16	0.23	0.43	115
15.50	0.00	8.48	0.725	53.27	0.55	11.86	4.46	2.89	1.77	1.46	2.16	0.26	0.39	74
18.50			0.687	54.57	0.57	12.55	4.46	2.81	1.87	1.53	2.33	0.25	0.29	25
24.50	0.00	7.75	0.676	54.72	0.59	13.00	5.44	2.70	2.00	1.61	2.35	0.23	0.20	0
30.50	0.00	7.54	0.663	55.62	0.59	13.17	4.61	2.70	1.76	1.62	2.36	0.24	0.16	0
Core 2														
Station 1														
0.25	0.67	5.93	1.059							1.15			0.37	
0.75	0.98	6.23	1.379	46.09	0.56	11.16	9.91	4.73	4.07	0.81	1.65	0.23	0.42	
1.25	1.18	3.66	0.956	47.94	0.58	11.24	10.62	4.95	4.73	0.75	1.66	0.16	0.24	4196
1.75	0.98	2.06	0.651	48.93	0.63	12.65	11.52	5.02	4.67	0.55	1.70	0.15	0.33	5014
2.50	0.93	1.53	0.370	50.38	0.65	13.81	11.71	5.13	5.00	0.56	1.68	0.18	0.42	5021
3.50	0.80	2.74	0.577							0.55			0.92	4751
4.50	0.76	3.04	0.593	49.43	0.58	13.65	10.69	4.44	4.33	0.59	1.87	0.15	1.23	4415
5.50	0.46	5.44	0.744	48.18	0.55	12.37	8.76	3.78	3.49	0.86	1.92	0.18	1.34	3505
7.00	0.05	8.55	0.774	53.13	0.54	12.25	5.13	2.98	2.06	1.32	2.04	0.23	0.67	751
9.00	0.01	8.81	0.754	52.78	0.53	11.55	4.41	2.88	1.75	1.36	2.08	0.23	0.48	265
11.00	0.01	8.78	0.750	55.14	0.54	12.30	4.50	2.90	1.96	1.37	2.07	0.25	0.45	181
13.00	0.01	8.68	0.730	51.67	0.53	11.15	4.32	2.85	1.73	1.40	2.05	0.22	0.42	114
15.50	0.00	8.43	0.697	51.73	0.54	11.34	4.31	2.85	1.77	1.48	2.24	0.23	0.35	54
18.50	0.00	8.09	0.672	49.22	0.54	10.95	4.45	2.76	1.65	1.54	2.34	0.22	0.36	30
24.50	0.00	7.86	0.658	51.78	0.57	12.11	4.65	2.68	1.85	1.58	2.44	0.21	0.20	0
30.50	0.00	7.89	0.685	53.33	0.58	12.60	4.52	2.62	2.07	1.55	2.30	0.23	0.15	0
Core 3														
Station 6														
0.25	2.44	1.43	0.150	51.02	0.51	9.15	10.26	8.02	6.32	0.43	1.08	0.07	0.32	2192
0.75	1.78	3.48	0.515	50.92	0.54	9.96	9.80	6.33	4.93	0.64	1.24	0.11	0.33	3756
1.25	2.13	2.91	0.388	49.81	0.57	10.32	10.75	7.23	5.95	0.44	1.23	0.10	0.19	
1.75	2.70	0.97	0.108	49.64	0.56	9.40	10.19	8.27	6.45	0.30	1.14	0.07	0.07	2527
2.50	2.36	1.14	0.170	50.32	0.57	9.93	10.88	7.53	6.37	0.40	1.15	0.08	0.09	3193
3.50	2.23	0.87	0.101	49.55	0.57	10.53	11.07	7.02	6.23	0.34	1.23	0.07	0.11	3570
4.50	2.41	0.64	0.050	48.94	0.58	10.56	10.99	7.50	6.66	0.31	1.28	0.07	0.11	3104
5.50	2.56	0.60	0.053	49.09	0.58	10.71	10.86	8.01	7.04	0.25	1.24	0.06	0.04	2813
7.00	2.64	0.56	0.037	47.39	0.56	10.06	10.88	8.22	6.98	0.20	1.24	0.06	0.14	2387
9.00	3.06	0.33	0.017	48.73	0.56	10.25	11.16	9.16	6.97	0.25	1.19	0.04	0.05	2022
11.00	3.18	0.35	0.019	42.62	0.52	8.28	10.41	9.08	5.68	0.26	1.18	0.05	0.07	1978
13.00	3.14	0.06	0.011	49.92	0.58	10.43	10.97	9.26	7.70	0.22	1.14	0.05	0.06	1976
15.50	3.20	0.05	0.007	48.88	0.57	9.50	10.36	9.22	7.20	0.23	1.05	0.06	0.06	1827
18.50	3.25	0.03	0.002	49.47	0.56	9.30	10.19	9.34	7.13	0.25	1.06	0.06	0.04	2072
21.50			0.018	52.23	0.59	10.46	11.64	9.05	7.45	0.23	1.16	0.07	0.14	2217
24.50			0.014	48.05	0.57	9.39	11.12	8.55	6.59	0.24	1.13	0.05	0.07	2451

Appendix D cont.

	Depth (cm)	Ba ppm	Co ppm	Cr ppm	Cu ppm	Mn ppm	Ni ppm	Pb ppm	Rb ppm	Sr ppm	V ppm	Y ppm	Zn ppm	Zr ppm
Core 1 Station 1	0.25	322	130	273	8280	1136	2177	132	68	158	167	22	2509	83
	0.75	209	310	372	6893	1457	4615	129	67	117	196	22	4781	62
	1.25	189	179	478	2687	1503	4105	105	45	119	220	27	2959	59
	1.75	154	98	399	1530	1600	2759	171	32	103	247	27	5856	57
	2.50	177	73	352	1412	1850	1748	196	28	99	277	31	2753	60
	3.50	200	317	334	18136	1645	4516	146	0	112	249	58	2222	64
	4.50	201	208	325	4060	1601	3302	159	0	114	253	56	1922	67
	5.50	237	203	285	3782	1391	2793	209	7	127	250	43	2902	76
	7.00	453	64	115	708	718	827	29	58	192	110	23	1013	111
	9.00	492	27	95	132	690	206	12	72	211	96	17	255	132
	11.00	522	24	90	58	683	127	12	78	220	94	15	184	142
	13.00	546	21	96	49	694	102	13	76	225	97	18	158	145
	15.50	533	18	91	39	654	86	16	74	224	95	18	145	143
	18.50	565	18	95	30	651	69	14	82	233	102	21	127	150
	24.50	585	17	96	22	624	52	15	83	228	105	19	129	148
	30.50	558	17	97	14	620	42	12	87	237	104	19	122	156
Core 2 Station 1	0.25	335	140	291	8539	1215	2413	122	68	162	177	26	2837	81
	0.75	239	253	393	6122	1438	4370	123	60	126	200	28	4095	64
	1.25	197	165	467	2928	1462	4045	118	42	116	217	24	3769	58
	1.75	150	91	378	1443	1705	2411	187	35	104	259	26	5596	59
	2.50	184	74	366	1128	1860	1775	205	23	99	275	25	2797	59
	3.50	198	226	336	11739	1694	3498	165	0	111	252	48	2101	62
	4.50	204	238	324	6433	1629	3780	174	0	113	264	56	2112	64
	5.50	280	170	257	2939	1261	2368	117	22	142	199	43	2610	83
	7.00	478	40	117	438	732	468	42	65	202	111	19	492	118
	9.00	525	26	95	122	681	200	24	72	213	96	19	225	130
	11.00	515	22	92	64	676	125	13	75	217	90	17	180	134
	13.00	547	25	93	44	684	93	18	71	216	92	17	152	140
	15.50	527	18	89	30	649	75	17	77	225	89	20	136	142
	18.50	549	21	93	23	644	64	14	84	223	96	17	131	146
	24.50	601	16	100	15	648	41	10	90	228	108	21	124	150
	30.50	575	19	97	17	627	43	8	84	229	100	17	123	145
Core 3 Station 6	0.25	89	66	609	1163	2060	406	90	12	99	205	19	428	37
	0.75	131	141	511	5160	1677	882	77	27	111	196	23	875	51
	1.25	110	111	586	3525	1922	780	107	12	99	221	24	770	42
	1.75	70	58	634	1041	2128	448	107	12	98	225	21	480	36
	2.50	74	52	599	1873	1901	764	126	13	88	220	22	994	40
	3.50	77	47	610	1097	1958	768	141	12	91	244	20	1145	41
	4.50	76	33	637	436	2124	549	161	12	90	256	22	822	38
	5.50	76	38	648	423	2166	420	159	14	91	247	21	727	40
	7.00	68	34	663	250	2212	313	162	13	90	246	22	534	38
	9.00	65	24	676	64	2313	196	154	8	89	249	20	319	34
	11.00	56	23	681	24	2255	176	153	14	91	231	25	282	32
	13.00	52	26	675	36	2315	194	131	9	93	238	24	305	37
	15.50	42	29	663	28	2354	178	115	8	89	228	20	276	36
	18.50	40	26	658	26	2289	174	117	4	89	222	19	260	31
	21.50	49	27	658	69	2240	204	144	11	93	237	21	359	37
	24.50	44	40	644	57	2169	237	124	4	96	234	22	373	34

Appendix E. Core Logs

Core BL-1 Notes:

- Collected 2 April 1994
- Clear skies, light breeze, -3°C
- Core collected with Pedersen corer through 1 m of ice
- Station 1, 4.0 m
- Core length 38 cm

Core Log:

Whole core: Very fine-grained, silty clay

Top 3 mm: Brownish floc, very fine-grained.

0 to 2 cm: Finely laminated alternating light/forest green; millimetre scale or less.

~0.9 cm: Distinct dark lamina.

~ 1 to 2.5 cm: Alternating light/dark fine laminations, cohesive clay.

2.5 to 4.0 cm: Homogeneous grey zone, less cohesive.

4.0 to 8.0 cm: Black layer, evidence of methane bubbles.

8.0 to bottom: Homogeneous, grayish/ chocolate brown.

Core BL-2 Notes:

- Collected 3 April 1994
- Overcast skies, 15 knot breeze, blowing snow, -5°C
- Core collected with Pedersen corer through 1 m of ice
- Station 1, 4.0 m
- Core length 41 cm

Core Log: Stratigraphy identical to Core BL-1

Core BL-3 Notes:

- Collected 3 April 1994
- Clear skies, 15 knot breeze, blowing snow, -5°C (-15 to -20 with wind chill)
- Core collected with Pedersen corer through 1 m of ice
- Station 6, 3.0 m
- Core length 54 cm

Core Log:

0 to 3 cm: Fine silty gray tailings material

1 to 1.5 cm: Separation plane 1 mm thick with ≤ 1 mm brownish layer on separation surface.

2.5 cm: Small separation 2-3 cm wide with thin brownish layer on planar separation surface. Myriad of tiny bubbles (≤ 1 mm) appeared progressively in the top several cm's of core during core logging (temperature effect?).

~3 to 4 cm: Very fine-grained irregular amber/ chocolate/ gray brown layer. Layer thickness unclear due to smearing down sides of core barrel.

4 to 25 cm: Very fine-grained light gray silt.

~26 cm: Separation plane ~ 1 mm thick, discontinuous laterally, water-filled.

~27 cm: Separation plane ≤ 1 mm, with ~ 1.5 cm thick dark gray layer (medium silt) immediately above (i.e., ~ 25 -27 cm).

27 to 41: Various gray-coloured medium silt to very fine silt tailings material. Irregular coarsening below 35 cm. Slight variations in colour but no obvious stratification.

Appendix F. Diffusive Fluxes

The diffusive flux (J_z) can be estimated using Fick's First Law (ignoring both bioturbation and advective transport):

$$J_z = \frac{D_j}{F} \phi \frac{dc}{dz}$$

where: J_z = flux

D_j = *in situ* diffusion coefficient (Li and Gregory, 1974)

F = formation factor ≈ 1.4 for silty clay (Manheim, 1970)

ϕ = porosity ≈ 0.87 , assuming an average particle density of $2.65 \text{ g}\cdot\text{cm}^{-3}$

$\frac{dc}{dz}$ = concentration gradient

The following data tables present diffusive influx estimates (positive values) for dissolved Zn, Cu, Ni, NO_3^- and SO_4^{2-} , and effluxes (negative values) for dissolved Zn, Ni, Mn, As and NH_4 . Diffusion coefficients were calculated from *in situ* surface sediment temperatures measured during the summer (17°C), fall (3°C), winter (3°C) and spring (10°C) sampling periods. For the sake of convenience, fluxes are expressed in both grams or moles per $\text{cm}^2\cdot\text{y}^{-1}$ (Flux 1) and grams or moles per $\text{m}^2\cdot\text{d}^{-1}$ (Flux 2).

Appendix F cont.

Downward Influxes

Season	Station	Element	Dj	Gradient g/cm ⁴	Flux 1 μg/cm ² /y	Flux 2 μg/m ² /d
Summer	2	Zn	5.98E-06	2.4E-08	2.8	77.4
	2	Zn	5.98E-06	3.3E-08	3.8	105.1
	1	Zn	5.98E-06	2.1E-08	2.5	67.4
	1	Zn	5.98E-06	2.3E-08	2.7	75.3
Fall	2	Zn	3.81E-06	2.4E-08	1.8	48.3
	2	Zn	3.81E-06	5.3E-08	3.9	108.0
	1	Zn	3.81E-06	1.1E-07	8.3	226.6
	5	Zn	3.81E-06	2.3E-08	1.7	46.3
Winter	2	Zn	3.81E-06	3.3E-08	2.4	66.9
	1	Zn	3.81E-06	3.3E-08	2.5	68.2
	4	Zn	3.81E-06	3.1E-08	2.3	63.9
	6	Zn	3.81E-06	2.6E-08	2.0	53.5
Spring	1	Zn	4.89E-06	3.7E-08	3.5	96.6
	1	Zn	4.89E-06	8.0E-09	0.8	21.0
Summer	2	Cu	5.74E-06	2.1E-08	2.3	63.3
	2	Cu	5.74E-06	2.7E-08	3.0	81.9
	1	Cu	5.74E-06	4.6E-08	5.2	141.8
	1	Cu	5.74E-06	5.9E-08	6.7	183.3
Fall	2	Cu	3.82E-06	5.7E-08	4.3	116.7
	2	Cu	3.82E-06	3.3E-08	2.5	68.0
	1	Cu	3.82E-06	3.5E-08	2.6	71.2
	5	Cu	3.82E-06	3.3E-08	2.4	66.9
Spring	1	Cu	4.78E-06	7.1E-08	6.7	182.4
	1	Cu	4.78E-06	3.6E-08	3.4	92.8
Summer	2	Ni	5.66E-06	7.3E-08	8.0	220.5
	2	Ni	5.66E-06	7.2E-08	8.0	218.2
	1	Ni	5.66E-06	1.3E-07	14.2	389.0
	1	Ni	5.66E-06	8.6E-08	9.5	261.0
Fall	2	Ni	3.56E-06	3.1E-08	2.2	59.9
	2	Ni	3.56E-06	7.4E-08	5.2	141.2
	1	Ni	3.56E-06	9.1E-08	6.4	174.2
	5	Ni	3.56E-06	1.2E-07	8.4	230.4
Winter	2	Ni	3.56E-06	5.8E-08	4.0	110.8
	1	Ni	3.56E-06	6.0E-08	4.2	115.4
	4	Ni	3.56E-06	3.7E-08	2.6	70.9
	6	Ni	3.56E-06	3.7E-08	2.6	71.6
Spring	1	Ni	4.61E-06	4.0E-08	3.6	97.8
	1	Ni	4.61E-06	5.7E-08	5.1	139.9

Appendix F cont.

				mol/cm ⁴	mmol/cm ² /y	mmol/m ² /d
Summer	2	NO3	1.57E-05	1.3E-07	0.04	1.1
	2	NO3	1.57E-05	1.3E-07	0.04	1.1
	1	NO3	1.57E-05	1.5E-07	0.05	1.3
	1	NO3	1.57E-05	1.3E-07	0.04	1.1
Fall	2	NO3	1.08E-05	9.8E-08	0.02	0.6
	2	NO3	1.08E-05	8.3E-08	0.02	0.5
	1	NO3	1.08E-05	8.9E-08	0.02	0.5
	5	NO3	1.08E-05	7.8E-08	0.02	0.5
Spring	1	NO3	1.33E-05	4.2E-08	0.01	0.3
	1	NO3	1.33E-05	5.6E-08	0.01	0.4
Summer	2	SO4	8.68E-06	1.3E-07	0.02	0.6
	2	SO4	8.68E-06	1.1E-07	0.02	0.5
	1	SO4	8.68E-06	1.2E-07	0.02	0.6
	1	SO4	8.68E-06	1.1E-07	0.02	0.5
Fall	2	SO4	5.65E-06	3.6E-07	0.04	1.1
	2	SO4	5.65E-06	4.7E-07	0.05	1.4
	1	SO4	5.65E-06	3.9E-07	0.04	1.2
	5	SO4	5.65E-06	7.8E-07	0.09	2.4
Winter	2	SO4	5.65E-06	3.3E-06	0.37	10.0
	1	SO4	5.65E-06	6.4E-07	0.07	1.9
	4	SO4	5.65E-06	4.2E-07	0.05	1.3
	6	SO4	5.65E-06	2.1E-07	0.02	0.6
Spring	1	SO4	7.17E-06	2.9E-07	0.04	1.1
	1	SO4	7.17E-06	2.9E-07	0.04	1.1

Upward Effluxes

	Station	Element	Dj	Gradient g/cm ⁴	Flux 1 μg/cm ² /y	Flux 2 μg/m ² /d
Summer	2	Zn	5.98E-06	-1.7E-08	-2.0	-53.5
	2	Zn	5.98E-06	-1.8E-08	-2.1	-56.2
	1	Zn	5.98E-06	-1.6E-08	-1.9	-51.8
Fall	2	Zn	3.81E-06	-4.1E-08	-3.1	-84.0
	2	Zn	3.81E-06	-7.8E-08	-5.8	-159.3
	1	Zn	3.81E-06	-1.6E-07	-12.0	-328.3
Winter	2	Zn	3.81E-06	-2.1E-08	-1.5	-42.0
	1	Zn	3.81E-06	-2.9E-08	-2.2	-60.3
	6	Zn	3.81E-06	-1.6E-08	-1.2	-33.0
Spring	1	Zn	4.89E-06	-8.2E-09	-0.8	-21.5
	1	Zn	4.89E-06	-4.3E-09	-0.4	-11.4
Fall	1	Ni	3.56E-06	-3.6E-07	-24.9	-682.2

Appendix F cont.

Summer	2	Mn	5.60E-06	-1.3E-07	-13.8	-377.0
	2	Mn	5.60E-06	-1.6E-07	-17.8	-487.4
	1	Mn	5.60E-06	-1.2E-07	-13.6	-372.4
	1	Mn	5.60E-06	-1.1E-07	-11.6	-318.0
Fall	2	Mn	3.50E-06	-2.0E-07	-13.6	-371.5
	2	Mn	3.50E-06	-1.4E-07	-9.3	-256.0
	1	Mn	3.50E-06	-3.8E-07	-25.9	-708.3
	5	Mn	3.50E-06	-1.4E-07	-9.5	-259.3
Winter	2	Mn	3.50E-06	-6.5E-08	-4.4	-121.4
	1	Mn	3.50E-06	-2.9E-08	-2.0	-54.0
Spring	1	Mn	4.55E-06	-1.7E-07	-15.0	-411.5
	1	Mn	4.55E-06	-1.3E-07	-12.0	-327.6
Summer	2	As	7.50E-06	-1.2E-06	-174.6	-4782.7
	2	As	7.50E-06	-7.8E-07	-115.0	-3151.5
	1	As	7.50E-06	-9.7E-07	-142.9	-3916.1
	1	As	7.50E-06	-4.2E-07	-61.0	-1672.2
Fall	2	As	4.79E-06	-5.1E-07	-47.8	-1309.6
	2	As	4.79E-06	-3.9E-07	-36.4	-998.3
	1	As	4.79E-06	-8.3E-08	-7.8	-213.3
	5	As	4.79E-06	-1.1E-07	-10.6	-289.3
Winter	2	As	4.79E-06	-5.2E-08	-4.9	-132.9
	1	As	4.79E-06	-4.4E-08	-4.1	-112.8
	4	As	4.79E-06	-4.2E-08	-4.0	-108.3
	6	As	4.79E-06	-2.4E-07	-23.0	-629.9
Spring	1	As	6.08E-06	-1.8E-07	-21.9	-599.6
	1	As	6.08E-06	-1.4E-07	-16.4	-449.9
				mol/cm ⁴	mmol/cm ² /y	mmol/m ² /d
Summer	2	NH4	1.64E-05	-8.8E-08	-0.03	-0.8
	2	NH4	1.64E-05	-1.3E-07	-0.04	-1.2
	1	NH4	1.64E-05	-1.1E-07	-0.03	-0.9
	1	NH4	1.64E-05	-1.1E-07	-0.03	-0.9
Fall	2	NH4	1.10E-05	-2.9E-08	-0.01	-0.2
	2	NH4	1.10E-05	-2.7E-08	-0.01	-0.2
	1	NH4	1.10E-05	-3.2E-08	-0.01	-0.2
	5	NH4	1.10E-05	-1.6E-08	0.00	-0.1
Spring	1	NH4	1.37E-05	-7.0E-08	-0.02	-0.5
	1	NH4	1.37E-05	-6.3E-08	-0.02	-0.5

Appendix G. Accumulation Rates

The following section provides very rough approximations of accumulate rate for various sedimentary components in Balmer Lake. The accumulation rate at a sediment depth Z (AR_Z), can be defined by:

$$AR_Z = \text{Wt.\% constituent} \times \text{Dry Bulk Density (DBD)} (g \cdot cm^{-3}) \times \text{Sedimentation Rate} (cm \cdot yr^{-1})$$

Where:

i) $DBD = (1 - \phi) \rho_{\text{sediment particles}}$

$\phi = \text{porosity} \cong 0.87$ assuming an average particle density of $2.65 g \cdot cm^{-3}$

ii) Sedimentation Rate approximated to be $\sim 0.3 cm \cdot yr^{-1}$

1) Sulphur

$$S_{AR} = 1.5 \text{ wt.\%} \times 0.35 g \cdot cm^{-3} \times 0.3 cm \cdot y^{-1} = 2 \times 10^{-3} g \cdot cm^{-2} \cdot y^{-1}$$

2) Nickel

$$Ni_{AR} = 0.4 \text{ wt.\%} \times 0.35 g \cdot cm^{-3} \times 0.3 cm \cdot y^{-1} = 4 \times 10^{-7} kg \cdot cm^{-2} \cdot y^{-1}$$

3) Copper

$$Cu_{AR} = 1 \text{ wt.\%} \times 0.35 g \cdot cm^{-3} \times 0.3 cm \cdot y^{-1} = 10 \times 10^{-7} kg \cdot cm^{-2} \cdot y^{-1}$$